

33 IGC excursion No 18, July 28 – August 4, 2008



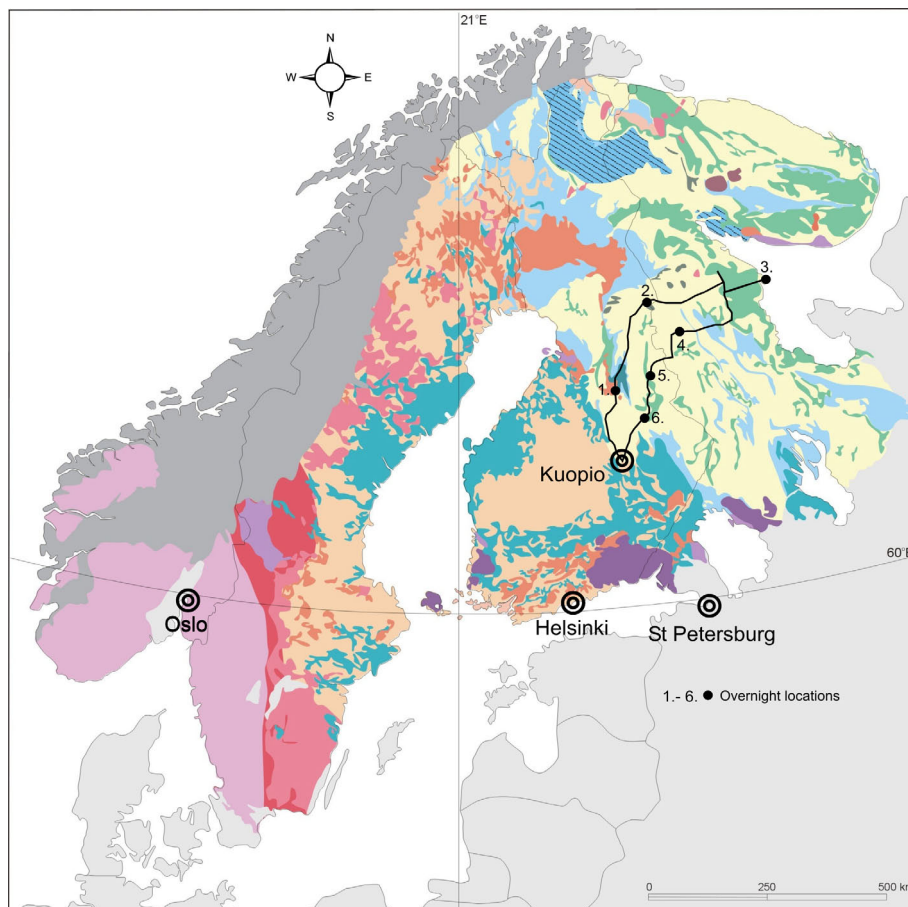
33 IGC, The Nordic Countries



Karelian Craton transect (Finland, Russia): Precambrian greenstone belts, ophiolites and eclogites

Organizers and editors of the field trip guide book

Petri Peltonen and Pentti Hölttä, Geological Survey of Finland, Espoo, Finland
Alexander Slabunov, Institute of Geology, Petrozavodsk, Russia



StatoilHydro




United Nations
Educational, Scientific and
Cultural Organization
Under the Patronage of UNESCO

TABLE OF CONTENTS

Abstract	3
Logistics	3
Day 1	4
Day 2.....	4
Day 3	31
Day 4	35
Day 5	53
Day 6	77
Day 7	98
Day 8	110
References	126

Abstract

Understanding when and why plate tectonics began is one of the most important unresolved problems in understanding Earth. The aim of this field trip is to demonstrate the recent discoveries made in Archean Karelian Craton that are relevant to the operation of modern-like accretion tectonic and seafloor spreading processes in the Meso- and Neoproterozoic times. We will examine in detail the Khizovaara structure, recently described as collage of a part of the Archean Iringora SSZ-ophiolite and an arc complex. Visit to Kostomuksha greenstone belt (interpreted as a remnant of Archean oceanic plateau + major economic BIF mine) and Kuhmo (Ni-Cu, Au showings) greenstone belts allow us to discuss the various geodynamic settings (mantle plume, spreading center, subduction) proposed for Archean volcanic successions. In the Gridino area on the White Sea we will examine spectacular Archean eclogites. They belong to a Neoproterozoic melange interpreted to have formed in subduction zone and exhumed due to a collisional orogeny. A full day will be devoted to the 1.95 Ga old complete Precambrian ophiolite: the Jormua Ophiolite Complex – recently reinterpreted as transitional passive-margin type ophiolite with truly unique Archean subcontinental mantle outcropping covering tens of square kilometers.

Logistics

Dates and location

Timing: From 28.07. 2008 – to 04.08. 2008
Start location: Kuopio, Finland (airport or railway station), evening of 28.07.
End location: Kuopio, Finland (airport or railway station), evening of 04.08.

Travel arrangements

Arrival of participants to Kuopio (Finland) in the afternoon/evening, but no later than by the 16:40-17:30 flight from Helsinki, or by the 14:12-18:43 (Kuopio)/20:36 (Kajaani) train from Helsinki (www.vr.fi, www.finnair.fi, www.blue1.fi). Bus will pick up participants either from the Kuopio airport or railway station. In the same evening drive to Kajaani (2 hrs), where introduction to the field trip, dinner and overnight.

Field trip ends to Kuopio 04.08 c. 17:20. Drop-off to Kuopio railway station (Helsinki trains 17:20-22:00, 19:51-00:36) or Kuopio airport (Blue 1 Kuopio-Helsinki 17:55-18:45) and hotels.

Accommodation

In hotels except 1 night in tents by the White Sea coast (camping gear provided). If you arrive 27.7. or leave 5.8. to/from Kuopio, please make your own hotel reservation for that night (e.g. hotel Puijonsarvi recommended)

Field logistics

Transportation by bus and by small boats to the White Sea islands and coastal areas, moderately demanding hiking.

Excursion Route and Road Log

Excursion Stops

Day 1, Monday 28.7. 2008

Arrival to Kuopio (Finland) in the afternoon/evening, but no later than by the 16:40-17:30 flight from Helsinki or 14:12-18:43 (Kuopio)/20:36 (Kajaani) train from Helsinki (www.vr.fi, www.finnair.fi, www.blue1.fi). Transportation to Kajaani (2 hrs), where introduction to the field trip, dinner and overnight (http://www.karolineburg.com/www/index_uk.htm)

Day 2, Tuesday 29.7. 2008

Possible arrivals in the morning to the Kajaani airport (6 am flight from Helsinki). Start of the field trip at 8:00 am (drive via airport). Jormua Ophiolite Complex – Palaeoproterozoic passive-margin type ophiolite with Archean subcontinental mantle outcrops (whole day), drive to Kuusamo, 3 h, where dinner, sauna and overnight.

(http://www.holidayclub.fi/portal/suomi/kylpylat/kuusamon_tropiikki).

The Jormua Ophiolite

Asko Kontinen and Petri Peltonen
Geological Survey of Finland

The 1.95 Ga Jormua Ophiolite Complex (Kontinen, 1987, Peltonen et al., 1996, 1998) is one of the only three presently known Palaeoproterozoic mafic-ultramafic complexes complying with the widely accepted Penrose Conference ophiolite definition (Anonymous, 1972). The other complexes besides Jormua are: (1) the 1.992 Ga Purtunig Ophiolite in northern Quebec, considered to represent a relatively mature open ocean or back-arc basin (Scott et al., 1992), and (2) the 1.83 Ga Payson Ophiolite in Arizona, thought to be of intra-arc origin (Dann, 1997). The Jormua complex differs from the two other Palaeoproterozoic ophiolites at least in two significant aspects. First, it comprises relatively large volumes of mantle tectonite peridotites which the other examples are completely lacking. Second, while the other ophiolites seem to have been generated in subduction-related settings (op cit.), the regional tectonic context, as well as pseudostratigraphical, trace element and isotope geochemical characteristics of the Jormua Ophiolite Complex (JOC) suggest it was formed in a Red-Sea type incipient ocean opening setting (Kontinen, 1987; Peltonen et al., 1996).

The agenda of the excursion is to visit all the main pseudostratigraphical units of the JOC. Emphasis is on outcrops that are critical for the ophiolite interpretation of the JOC and with regard to inferring its formative tectonic setting. In the following a brief introduction to the JOC and its regional geological setting is provided. For more and more detailed information on the JOC the reader is referred to Kontinen (1987), Peltonen et al. (1996, 1998), Peltonen et al. (2003), Peltonen and Kontinen (2004), and Peltonen (2005).

Geological setting

The JOC is the most completely preserved example of the many ophiolite fragments that occur within the narrowly interconnected North Karelia (NKSB) and Kainuu (KSB) schist belts

in eastern Finland (Fig. 2.1.). The two dominantly metasedimentary Palaeoproterozoic schist belts hosting the ophiolites are located 0-100 km to the east of the sharp contact, often referred to “collisional suture”, between their Archean basement complex and the c. 1.93-1.80 Ga old Svecofennian plutonic-metavolcanic-metasedimentary terrain to the west of them. The Svecofennian domain is usually interpreted as a collage of during 1.91-1.89 Ga accreted “microcontinents” and/or “island arcs” (e.g. Nironen, 1997; Lahtinen et al., 2005).

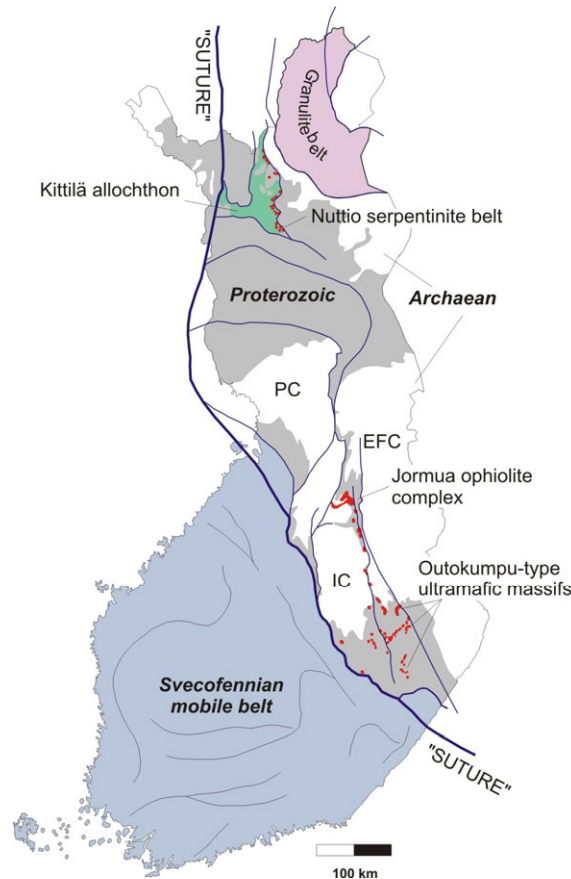


Fig. 2.1. Generalized geological map of the Kainuu Schist Belt (KSB). Major lithotectonic units of the belt are shown. Symbols not explained in the legend of the map: KaG=Kajaani Granite; UuG=Uura Granite; RiG=Ristijärvi Granite. Inset shows the location of the KSB in a geological map outlining the major lithotectonic units of the Southern Finland.

The JOC is found in the centre of the KSB, which comprises three main unconformity or thrust-separated tectonic-stratigraphic units, called to “tectofacies” by Laajoki (2005): (1) the autochthonous, cratonic to epicratonic Jatuli sequence (2.3-2.1 Ga) of predominantly fluvial to shallow marine, platformal feldspathic and quartz arenites; (2) the “Lower Kaleva” succession (2.1-1.95 Ga) of riftogenic conglomerates, quartz wackes, graywackes and pelites interleaved by P-Mn-C-chert-banded silicate-carbonate-sulphide iron formations and abundant, partly metal-rich black muds; and (3) the “Upper Kaleva” deep-marine turbiditic graywackes-shales and ophiolite fragments of the Jormua-Outokumpu Allochthon. The deposition of the Upper Kaleva turbidites in the Jormua-Outokumpu Allochthon (JOA) is bracketed by the youngest detrital zircon grains (Claesson et al. 1993) and assumed tectonic emplacement age of the JOA between about 1.92 Ga and 1.90 Ga. The ophiolite bodies, both in the KSB and NKSB, occur in tight association with, usually enclosed in the Upper Kaleva metaturbidites. The 1.95 Ga or older age of magmatic rocks in the Jormua-Outokumpu ophiolite fragments (Peltonen et al., 2008) emphasizes their nature as tectonically emplaced, fault-bounded massifs in the at least 20-30 Ma younger enclosing metasediments.

Other significant geological components of the central part of the KSB include: (1) the Central Puolanka Group (CPG) and its gneissic derivatives Kalpio and Kalhamajärvi gneiss complexes; (2) the 2.03-2.05 Ga old Otanmäki gneissic, peralkaline to peraluminous A-type granites; (3) the postkinematic, 1.859 ± 8 Ga old Ristijärvi and Uura granodiorite-granite stocks; and (4) the “post-orogenic”, about 1.80 Ga old, “minimum-melt” type Kajaani pegmatite granites and garnet-muscovite-biotite bearing leucogranites.

The Central Puolanka Group (CPG) along the western margin of the KSB contains a presumably 3.5 km thick succession of metasediments from deep-water turbidites through fluvial quartzites to shallow marine quartzites-pelites intercalated with minor mafic to felsic, typically pyroclastic metavolcanic rocks (Laajoki, 1991). Although a Palaeoproterozoic age of about 2.3 Ga is usually assumed (e.g. Laajoki, 2005), it has also been proposed that the CPG and the derivative gneiss complexes may in fact be of late Archean age (Kontinen et al. 1995). Either way, the CPG bears little significance for the JOC related problematics.

The 1.96 Ga Otanmäki granites occur in a narrow stripe along the southern margin of the Kajaani Complex to the south-southeast of the JOC, consisting mainly of Archean gneisses intruded abundantly by the Kajaani granite. The locally alkali-amfibole bearing Otanmäki granites are frequently strongly foliated and folded and thus are clearly pre-tectonic (Presvecofennian). Proposed estimations for their emplacement age vary from about 2.02 Ga (Hytönen and Hautala, 1985) to about 1.96 Ga (Peltonen et al., 1996, based on unpublished data). An age of at least 2.1 Ga is obvious noting that the granites are cutting Jatulian quartzites, dolomites and metavolcanic rocks at the Närhiniemi locality about 20 km to the south of Jormua (A. Kontinen, unpublished). Recently Kontinen and Huhma (in prep.) have obtained U-Pb zircon data that indicate magmatic emplacement between 2.03 and 2.05 Ga. A maximum age of about 2.06 Ga is set by that dykes of the Otanmäki type granite are cross-cutting the Otanmäki gabbros (M. Havola, pers comm. 1997) dated at about 2060 Ma (Talvitie & Paarma, 1980).

Chemically the Otanmäki granites are strikingly similar to A-type granites that formed during the early stages of the Red Sea opening about 30-20 Ma ago (e.g. Capaldi et al., 1987; Coleman et al., 1992). Based on this similarity, Peltonen et al. (1996) proposed that the Otanmäki granites were generated during the about 2.0 Ga break-up of the Karelian Craton, and that later, coinciding with the Outokumpu-Jormua ophiolite obduction, slices of the granite-intruded passive margin were thrust onto the Karelian craton. We agree upon the break-up association of the Otanmäki granites, but reserve the possibility these granites may after all represent a narrow stripe of fault-controlled intrusions still locating about at their original emplacement site. Anyway, the actual break-up, for which the Otanmäki granites signify, likely occurred significantly further to the west of the present “craton margin”. In the light of the newly sharpened understanding of the emplacement age of the Otanmäki granites, the Kalevian continental break-up process can now be assumed to have started at about 2.05 Ga ago.

The 1.859 ± 8 Ga Ristijärvi and Uura granites at the eastern margin of the KSB are practically taken undeformed, and clearly have emplaced subsequent to the main deformations in the surrounding Kalevian metasedimentary rocks. This situation is to some extent at variance with the fact that the 1.80 Ga Kajaani granites at the western margin of the KSB have been affected by profound, mylonite-zones producing deformation. Here it must be noted that the full ramifications of the 1.80 Ga shield-wide metamorphic-magmatic event, to which the Kajaani granite belongs, are currently poorly constrained; there may be more tectonic reworking of also the KSB related to the 1.80 Ga event than what is currently commonly perceived.

The Jormua and other ophiolitic bodies in the KSB and NKSJ were thrust onto the Karelian craton margin about 1.90 Ga ago, in an early stage of the Svecofennian orogeny, enclosed as tectonic fragments in Upper Kaleva metaturbidites. A remnant of the overthrust rocks including the JOC is preserved in the tectonically depressed middle part of the KSB. During the thrust transport and early regional deformation the JOC was dismembered into eventually four major fault-bounded “blocks” all representing different levels its original pseudostratigraphy (Peltonen et al. 1996, 1998). Strike-slip faulting along the KSB in a late stage of Svecokarelian tectonism (Kärki and Laajoki, 1995) was causing further disruption and deformation the main blocks, so that they presently show shapes of shear generated “mega-augens”.

The Svecofennian metamorphism in eastern Finland peaked under low P/T amphibolite facies conditions, probably sometime between 1.87 and 1.85 Ga, although the high-temperature conditions seem to have persisted relatively long, dropping below 500 °C not until about 1.80 Ga ago (Kontinen et al., 1992). The high-T metamorphism thus significantly outlasted the regional deformation that essentially ended already by 1.86 Ga (Tuisku, 1997). Vague evidence of pre-peak, medium-P metamorphism are provided e.g. by kyanite-bearing metasediments in the autochthon and some garnet+clinopyroxene bearing <2.0 Ga metadiabase dykes in the Archean basement complexes (Tuisku, 1997). The typical metamorphic mineral paragenesis in the metabasic rocks of the JOC is plagioclase(An_{>20})+actinolitic hornblende-hornblende±epidote±chlorite. The equilibrium metamorphic mineral paragenesis in the Jormua serpentinites is antigorite+Cr-magnetite±tremolite±olivine. These mineral assemblages indicate that the Svecofennian regional metamorphism at Jormua peaked at about 500±20 °C (Peltonen et al., 1996). The presence of olivine (all metamorphic) only in the serpentinites of the Hannusranta block suggest there is a slight westwards increase in the metamorphic grade within the JOC.

The main blocks

As explained above, the JOC presently consists of four main fault-bounded “blocks”, which are deformed by the late tectonic processes to large lens or augen shaped slivers:

The eastern Antinmäki block actually consists of several juxtaposed, fault-bounded blocks and slices of serpentinite, Mg-gabbro, Fe-gabbro, diorite, and plagiogranite (leucotonalite-thronjemitite), sheeted dykes and pillow lava. The main component are (serpentinized) mantle lherzolites-harzburgites and minor dunites intruded by abundant about 1.95 Ga old gabbro dykes and stocks and basaltic sheeted dyke complexes (Fig. 2.2.). The Antinmäki block is the only block of the JOC which is associated with significant volumes of extrusive rocks, these comprising three 50-400 m wide, 2-3 km long slices of metabasaltic, massive to pillowed lavas and minor pillow breccia (Fig. 2.6.). The gabbros, sheeted dykes and pillow lavas display all a clear E-MORB type chemical affinity and $\epsilon_{Nd}(1.95 \text{ Ga})$ around +2 (Peltonen et al., 1996). The pillow lavas in the Korteperä slice at the western margin of the Antinmäki block are overlain by banded amphibolites with calc-silicate-carbonate rich intercalations, interpreted as basic tuffs interbedded with sedimentary carbonate rocks. These metatuff-metacarbonate rocks are structurally overlain by typical upper Kaleva metaturbiditic black shales and graywackes.

The central Lehmivaara block consists of (now serpentinized) mantle lherzolites and harzburgites that with increasingly more doleritic-basaltic dyking, when moving from west to east over the block, give way to a spectacular sheeted dyke (dyke-in-dyke) complex (Fig. 2.6.) with only sporadic peridotite screens (septa). The dyke rocks do share similar E-MORB type chemical affinity and an $\epsilon_{Nd}(1.95 \text{ Ga})$ of +2 with the dykes and pillow lavas of the Antinmäki

block. The mantle peridotites of the Lehmivaara block contain a generation of ultramafic-mafic dykes not observed in the Antinmäki block. These “early” ultramafic-mafic dykes, presently oriented broadly N-S, are sharply cross-cut by the broadly E-W trending dolerite-basalt dykes. The “early dykes” have OIB characteristics with moderate to high (1.5-6%) TiO_2 , LREE and Nb, and $\epsilon_{\text{Nd}}(1.95 \text{ Ga})$ values of around +0 (Peltonen et al. 1996).

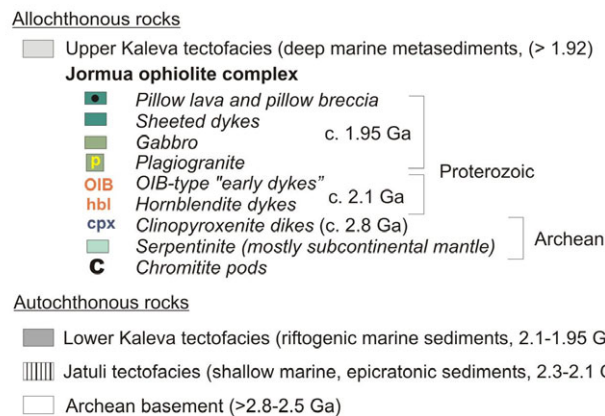
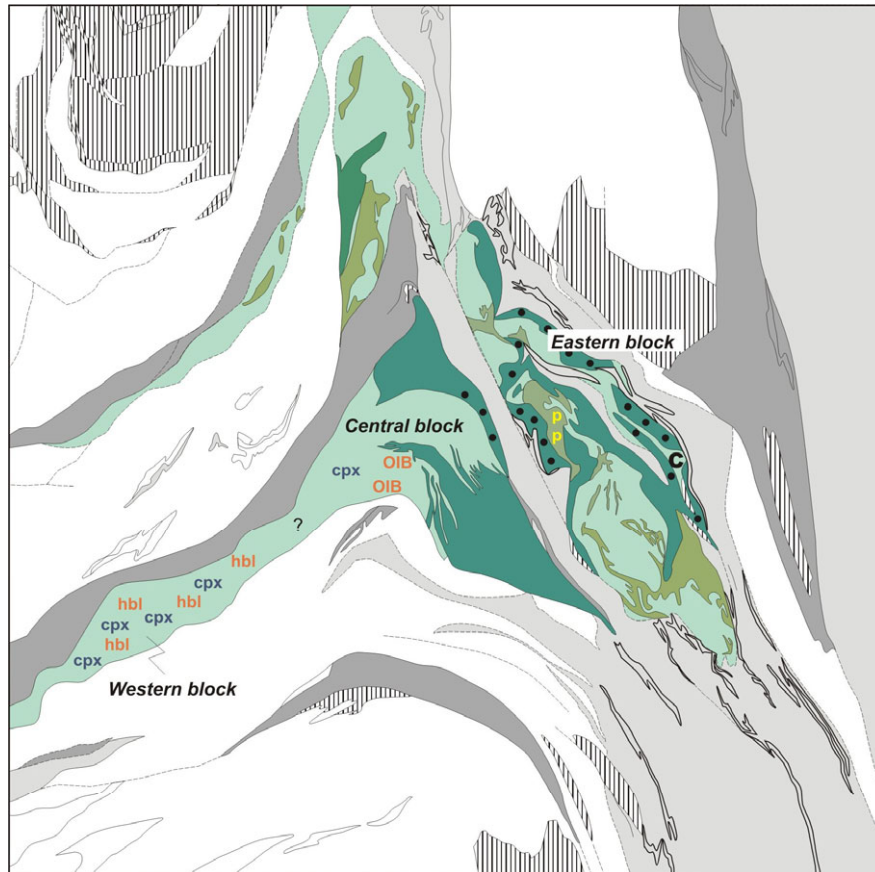


Fig. 2.2. Generalised geological map of the Jormua complex.

The western Hannusranta block differs significantly from the Antinmäki and Lehmivaara blocks in that the E-MORB type gabbros, basaltic dykes and pillow lavas are nearly entirely absent. The block consists of serpentinized lherzolitic-harzburgitic mantle peridotites extensively intruded by dykes and small, irregular plugs of coarse-grained clinopyroxene±amphibole and amphibole±garnet rocks obviously after igneous cumulates crystallized in magma channels in the enclosing upper mantle peridotites. Composition of preserved primary pyroxenes and amphiboles indicate these ultramafic-mafic cumulates precipitated from a parental melt of

alkali basalt composition. Whole rock and clinopyroxene Sm-Nd isotope data suggests that this alkaline melt may have been the same that produced the OIB dykes in the Lehmivaara block (Peltonen et al., 1998).

The northern Kannas block is the least exposed and studied of the Jormua blocks. Nevertheless, the presently available data suggest that this block is fairly similar to the Antinmäki block. Other than serpentinite, the main components exposed are gabbroic mantle dykes, some more voluminous gabbroic to dioritic intrusions and some massive metabasaltic amphibolites, probably of sheeted dyke origin.

Reconstructed structure

Despite strong tectonic disruption of the JOC, it still retains transitional contacts within its main blocks that, together with the chemical-isotopic evidence of obvious petrogenetic consanguinity of the main mafic lithologies, imply an originally contiguous sequence, in which peridotites and gabbros formed the basal, gabbros and sheeted dykes the middle and lavas the top part (Kontinen, 1987; Peltonen et al., 1996). A columnar reconstruction of the Jormua ophiolite (Fig. 2.3.) suggests that the mafic lid of the JOC unit was originally relatively thin and variable for its thickness and stratigraphy (200-2000 m), so that in places the lavas may even have extruded directly onto the mantle peridotites. By its structure the Jormua ophiolite shows clear similarities with oceanic crust generated at slow-spreading ridges or in small ocean basins (Nicolas, 1989). Ophiolites with similar pseudostratigraphy and inferred tectonic origin include the Western Alps and Ligurian ophiolites (e.g. Lemoine et al., 1987; Rampone and Picardo, 2001). Iberian margin (e.g. Chian et al., 1999; Cornen, 1999).

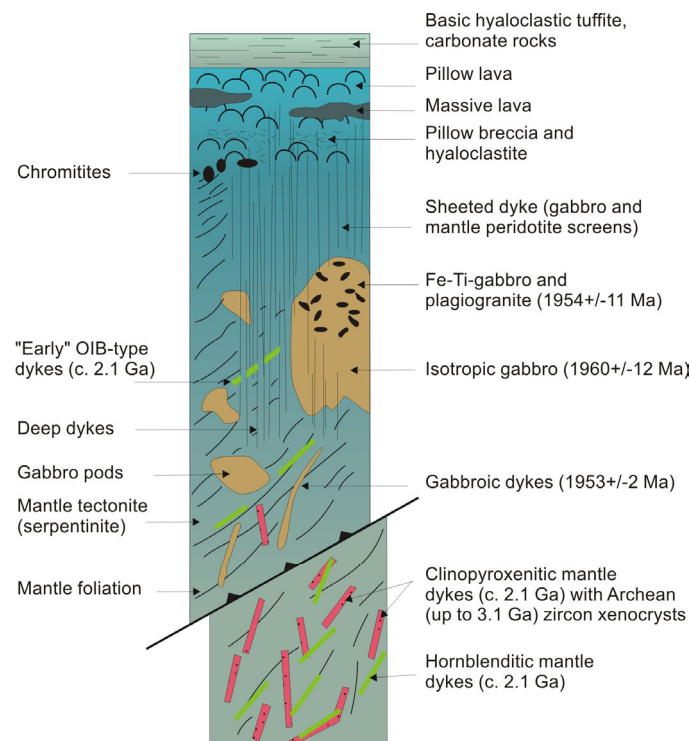


Fig. 2.3. Reconstructed cross-section of the original pseudostratigraphy of the Jormua complex. Note that the lower, fault-separated part of the column (Hannusranta block) likely represents a fragment from subcontinental mantle not directly related to the Jormua ophiolite proper. For this part the column reflects rather the present tectonostratigraphic situation than any original stratigraphy (Fig. 3 from Peltonen et al., 1996).

Mantle unit

The preservation of abundant mantle peridotites in the Jormua ophiolite makes it unique among the Precambrian ophiolites. In fact, about two thirds of the rock area, and probably also volume, of the Jormua ophiolite is mantle peridotite (Fig. 2.2. & 2.4.). Unfortunately, the mantle peridotites in the JOC have been thoroughly hydrated and metamorphosed to antigorite metaserpentinite during their obduction and subsequent lower amphibolite grade regional metamorphism. The only primary mineral phase preserved to some extent in the resultant antigorite metaserpentinites is chromite. The common presence of extensively metarodingitized minor gabbroic intrusions in the JOC serpentinites attest to possibly extensive low-T serpentinization of the protolith peridotites before the regional metamorphism and recrystallization to antigorite. This serpentinization may have occurred already in the seafloor stage of the JOC or/and during the obduction.

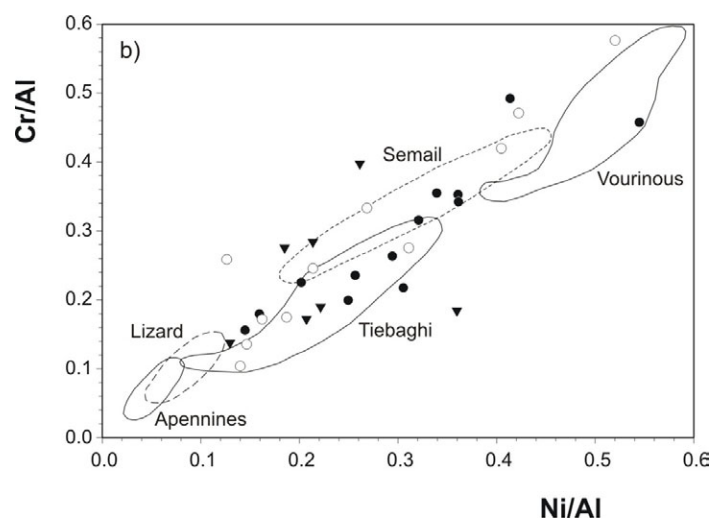


Fig. 2.4. Cr/Al vs. Ni/Al diagram illustrating the compositional variation of the Jormua mantle rocks. The trend from the Lizard-Apennine to the Semail-Vourinous peridotites represents is one produced by increasing degree of partial melting and accompanying change in residual material from lherzolites via harzburgites to dunites. Reference fields from Roberts and Neary (1993).

In terms of chemical composition the JOC serpentinites correspond mostly to depleted lherzolites and harzburgites, though minor dunites are also present. Despite of all the secondary alteration and recrystallization, locally the serpentinites still preserve pseudomorphic textures and structures typical of serpentinized mantle (residual) peridotites (Fig. 2.5a). Mantle tectonite origin of the serpentinites is supported especially by the fact that that they commonly show foliations/bandings defined by flattened chromite grains and pyroxene pseudomorphs, and which foliations/bandings, as being in several outcrops truncated by 1.95 Ga old basalt and or gabbro dykes, must be of pre-obduction, presumably mantle origin (Fig. 2.5b). The interpretation of mantle origin of the JOC peridotites is obvious also by that the peridotites calculated anhydrous yet display on Harker diagrams of the less mobile elements trends typical of variably melt depleted mantle peridotites.

Although the mantle origin of the JOC peridotites seems settled, less clear is what type of mantle these peridotites do represent. Peltonen et al. (1998) proposed that peridotites in Hannusanta blocks represented subcontinental lithospheric mantle, exposed to seafloor and attached to the JOC in the early stages of the break up of the Karelian Continent. The mantle units in the other blocks were considered of asthenospheric (convective mantle) origin. Later on Tsuru et al. (2000) published Re-Os isotope data on chromites that indicated that not only

Hannusranta but all JOC peridotites would represent subcontinental lithospheric mantle separated from the convective mantle already before 3.0 Ga. The presence of Archean xenocrystic zircon grains in Hannusranta pyroxenite and Lehmivaara Early (OIB) dykes is another reason to they would represent ancient lithospheric mantle, comprising felsic magma patches of Archean age or zircons from metasediments recycled in mantle already in Archean times.

Chromite is the only preserved primary mineral in the JOC peridotites. Most of the originally present 1-5 vol.% disseminated chromite in Jormua serpentinites has been altered to ferri-chromite and/or Cr-magnetite. Only occasionally there are grains still preserving cores of relict chromite. In these grains the boundary between the chromite core and surrounding ferri-chromite is sharp both optically and chemically, whereas towards the grain margin the ferri-chromite gradually grades to Cr-magnetite compositions. Electron microprobe analyses indicate that, in scale of hand samples, there is little variation in terms of Cr numbers between the cores of different grains or within individual cores, whereas in terms of Mg numbers there is a wide variation depending of core size and across the cores. Interiors of large cores are frequently more magnesian than interiors of small cores, and all cores are zoned towards less magnesian compositions towards their margins. Due to the alteration in divalent cations, Mg numbers of the JOC chromites tend to be lower than is typical of pristine chromites from nonmetamorphosed ophiolitic mantle peridotites. However, as there seems to be little alteration in terms of the trivalent cations, the variation in Cr numbers (45-70) of the chromite cores seem to record the variation in degree of melting/melt extraction in the host peridotites. Based on the Cr number data, most of the Jormua serpentinites appear to represent rather harzburgites than depleted lherzolites. Note that this conclusion does not necessarily apply to the peridotites of the Hannusranta block, which do not preserve relict chromite/spinel.

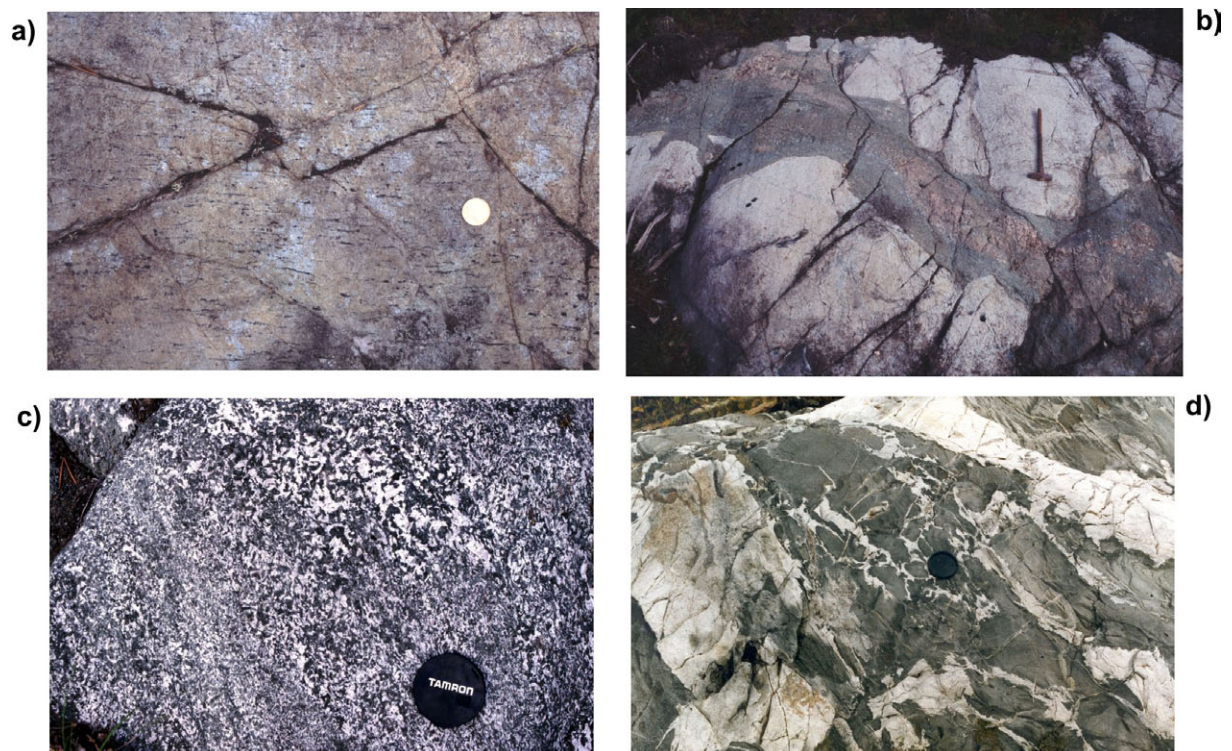


Fig. 2.5. A set of photographs of the typical rocks of the "lower level" lithological units in the Jormua complex: (a) serpentinite with pyroxene pseudomorphs (pale gray antigorite) in serpentine after olivine matrix (darker gray antigorite+magnetite dust), Mineraali; (b) gabbro dykes truncating foliated mantle peridotite (serpentinized harzburgite), Antinmäki; (c) varied-textured, ilmenite-rich Fe-gabbro, Sarvikangas; (d) leucotonalite (plagiogranite) dykes in fine-grained gabbro, Sarvikangas.

Magmatic suites

Main suite (gabbros, sheeted dykes and lavas)

The mafic suite of the JOC provides bulk of the crucial evidence of its nature as a rock complex and its formative tectonic setting. The presence of well preserved, voluminous bodies of sheeted dykes attest to an extensional setting of the mafic magmatism that formed the mafic lid of the JOC. The pillow lava units testify of a submerged, probably submarine origin of the complex. The obvious lack of terrigenous intercalations in the lavas indicate formation of the JOC in an environment that was located far away or were blocked for sediment streams from any continental domains. The Upper Kaleva turbidites, now enclosing the Jormua-Outokumpu zone ophiolites, seem to have rapidly covered the JOC after its formation, however.

The lavas and sheeted dykes of the JOC comprise a series of thoroughly metamorphosed doleritic-basaltic rocks, characterized by relatively high Mg numbers (73-59) likewise high Cr (700-240 ppm) and Ni (610-70 ppm). The dolerites-basalts thus do represent relatively little modified mantle melts. Trace element data suggest that the basalts represent a series of <5% to 25 % melt fractions of “enriched mantle”, modified by variable minor removal/accumulation in olivine and plagioclase (Peltonen et al., 1996; Peltonen, 2005). Mantle normalized trace element patterns of the basalts typically show slight positive rather than negative Nb anomalies and systematically lack enrichment in Th. Overall the JOC basalts lack any signatures of subduction or continental contamination in their composition. This all means that, compared to modern basalts, the JOC basalts closest resemble transitional to enriched MOR basalts (Kontinen 1987; Peltonen et al., 1996).

The mode of occurrence of gabbroic rocks in the JOC ranges from irregular dykes/dyke networks in the mantle unit to larger, up to km size bodies but that still seem to represent intrusions in the mantle unit. The gabbros in the larger bodies range in composition from high-Mg gabbros to ilmenite-rich ferrogabbros that locally show dioritic to leucotonalitic segregations and dykes. The gabbroic rocks are mostly thoroughly metamorphic but often preserve their primary structures and textures relatively well. The grain size of the gabbros is typically coarse, and irregular variations in grain size and modal composition over short distances is a prominent outcrop feature, whereas there rarely is any clear signs of modal layering. Based on pseudomorphic textures, the main primary constituents in Mg-gabbros were plagioclase and clinopyroxene added with some brown amphibole and abundant ilmenite in the Fe-gabbros. Rare plagioclase in Mg-gabbros and ilmenite and brown amphibole in the Fe-gabbros are the only primary major minerals preserved.

The variation in modal and chemical composition exhibited by the JOC gabbroic rocks does indicate profound differentiation (Fig. 2.7). In absence of modal layering, it seems that the differentiation was by cooling-diffusion controlled processes. The obvious sharp jump in outcrops and Harker diagrams from Mg-gabbro to Fe-gabbro compositions is puzzling. Maybe the differentiation process involved development of immiscible Mg and Fe rich melts? The origin of the Jormua plagiogranites occurring spatially close to Fe gabbros, has been addressed to filter pressing of felsic melt fraction from crystal mushes solidifying in a tectonically dynamic environment to the Fe-gabbros (Kontinen, 1987). However, magma mingling structures in outcrops of plagiogranite dykes suggests that melt immiscibility may have played a role also in the plagiogranite genesis.

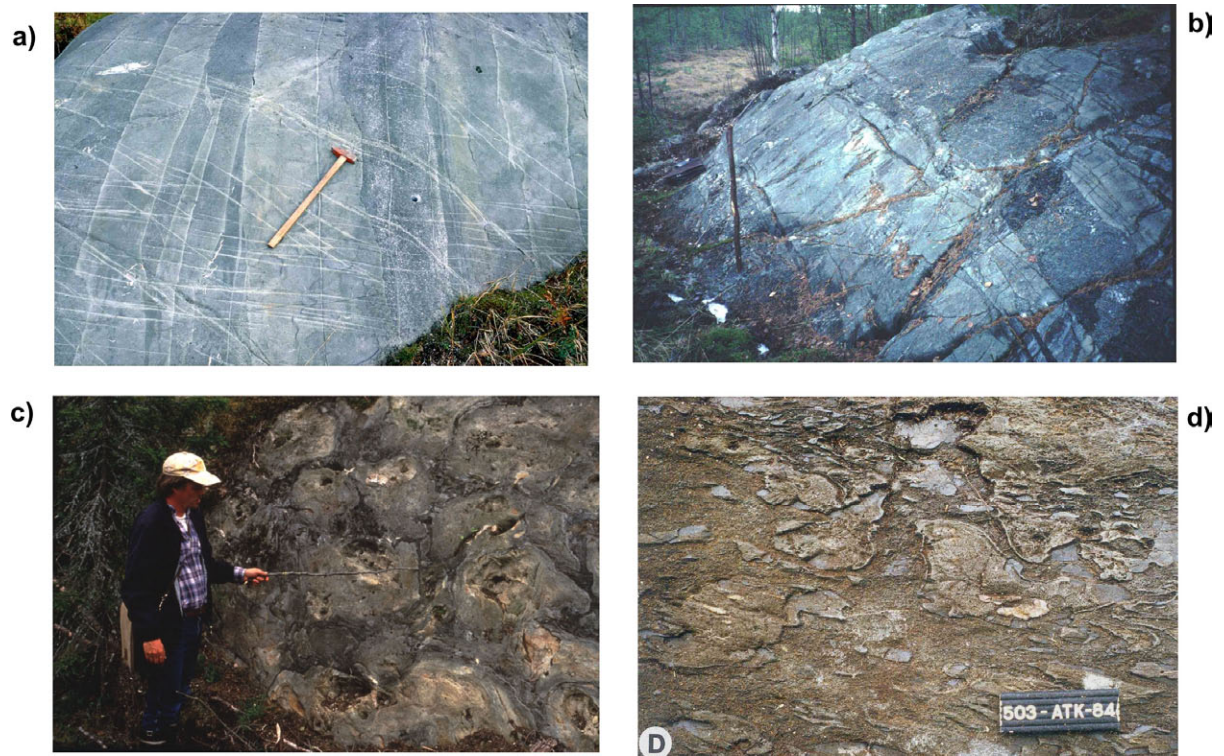


Fig. 2.6. A set of photographs illustrating the rocks of the “upper level” lithologic units in the Jormua complex: (a) sheeted dykes, Sammakkomäki; (b) sheeted dykes with gabbro screens, Sarvikangas; (c) pillow lava overlain by massive lava, Kylmä; (d) small pillows and pillow fragments in metahyaloclastic matrix, Kylmä.

The gabbro suite of the JOC defines it a high TiO_2 ophiolite in the terms of Serri (1981). In this respect similar ophiolites are e.g the Eastern Alps and Ligurian ophiolites in Italy. Also slow spreading oceanic ridges are known to be associated with Fe-gabbros and sodic plagiogranites. The high Y and Nb concentrations of the Sarvikangas diorites-leucotonalites place them in the within-plate granite field in the Nb vs. Y discrimination diagram of Pearce et al. (1984), which is consistent with the overall E-MORB character of the Jormua mafic rocks.

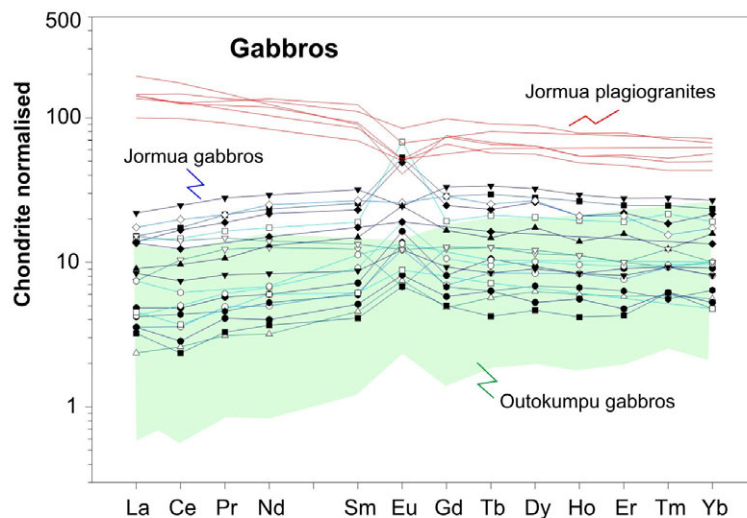


Fig. 2.7. Diagrams illustrating the compositional variation of the Jormua gabbros, ferrogabbros and plagiogranites, all samples come from the larger, upper level gabbro intrusions at Kivisuo and Sarvikangas.

The gabbros have yielded the most precise U-Pb zircon age so far from the JOC, namely 1953 ± 2 Ma (Peltonen et al. 1998) for a relatively Fe rich segregate from a gabbro dyke at Antinmäki. Closely similar, although somewhat less precise ages of 1960 ± 12 Ma and 1954 ± 11 Ma are obtained for another gabbro sample and a plagiogranite (leucotonalite) sample, respectively (Kontinen, 1987). The lavas and dykes, as well as gabbros and plagiogranites of the JOC yield all $\epsilon_{\text{Nd}}(1.95 \text{ Ga})$ values around +2 (Peltonen et al. 1996), which is providing strong evidence of the petrogenetic consanguinity of the rocks constituting the JOC mafic lid.

Early Suite (OIB dykes and Hannusranta dyke cumulates)

The OIB dykes in the Lehmivaara block and cumulate dykes in the Hannusranta were clearly emplaced before the main suite rocks. This is clear as both these lithologies are demonstrably cross-cut by main suite basalt dykes. Another important similarity between the Lehmivaara and Hannusranta dykes is that samples of both yield $\epsilon_{\text{Nd}}(1.95 \text{ Ga})$ values around +0. Furthermore, both lithologies contain Archean zircon grains interpreted to be inherited from the mantle unit of the JOC.

The early ultramafic-mafic dykes in Lehmivaara block are profoundly altered with possible primary minerals (mainly clinopyroxene) remaining only in one dyke. By their chemistry the dykes represent mafic rocks of ocean islands in several aspects showing LREE enriched strongly fractionated REE patterns and high Nb. Fractionated HREE and low Sc indicate generation of the melts in the OIB dykes by garnet stability field melting.

The Hannusranta dykes vary from “dry” clinopyroxenite to “wet” amphibole+clinopyroxene dykes. The sporadic presence of obvious magmatic garnet (pseudomorphic) in the latter implies, in comparison with P-T determinations from analogous rocks in orogenic lherzolites and mantle xenoliths, that the dykes crystallised at 30-50 km (8-15 kbar) and at 900-1000 °C (Peltonen, et al. 1998).

Formative setting

For deducting of the origin of the JOC the following aspects in its geology seem to be most critical. The obvious origin of its mantle unit as part of the subcontinental lithospheric mantle that once underlied the Karelian Craton was originally proposed by Peltonen et al. (1998) to the Hannusranta block only, but later on Re-Os data by Tsuru et al. has indicated that this would be the case for the major part of mantle rocks in the JOC. The high TiO₂ nature and the reconstructed structure of the JOC points out that it was formed in a slow spreading oceanic rift, possibly in early stages of ocean opening as is proposed in the case of the Western Alps and Ligurian ophiolites. Yet a true ensimatic, rather than ensialic, intracratonic rift setting is implied by the absence of terrigenous sedimentary intercalations within the pillow basalt sequence of the complex. Also, there are no indications of sialic assimilation in the trace element geochemistry of the JOC main suite mafic rocks.

Peltonen et al. (1998) proposed that the blocks of the Jormua Complex represent a sequence across an ancient ocean-continent transition recording the accretion of a mantle diapir to the subcontinental, probably Archean lithospheric mantle during the formation of an incipient oceanic basin c. 1950 Ma (Fig. 2.8). This event is likely connected to the major break-up of the Karelian continent perceived on other grounds to have occurred about 2 Ga ago. Rupture of the subcontinental lithosphere was preceded by OIB-type magmatism and coeval em-

placement of garnetiferous pyroxenite-hornblendite mantle dykes at depths of 30-50 km, and of peralkaline granites in continental crust flanking the opening ocean basin. This was immediately followed by uplift of parts of the recently accreted suboceanic mantle diapir and intrusion by gabbroic mantle dykes, upper level gabbros-ferrogabbros-plagiogranites and sheeted dyke complexes parts of which were feeding pillow lavas - all petrogenetically related and expressions of progressively shallower ocean-crust-forming magmatism. Some 30-50 Ma later this ocean crust was covered by upper Kaleva turbidites representing oceanward prograding passive margin turbidite fans.

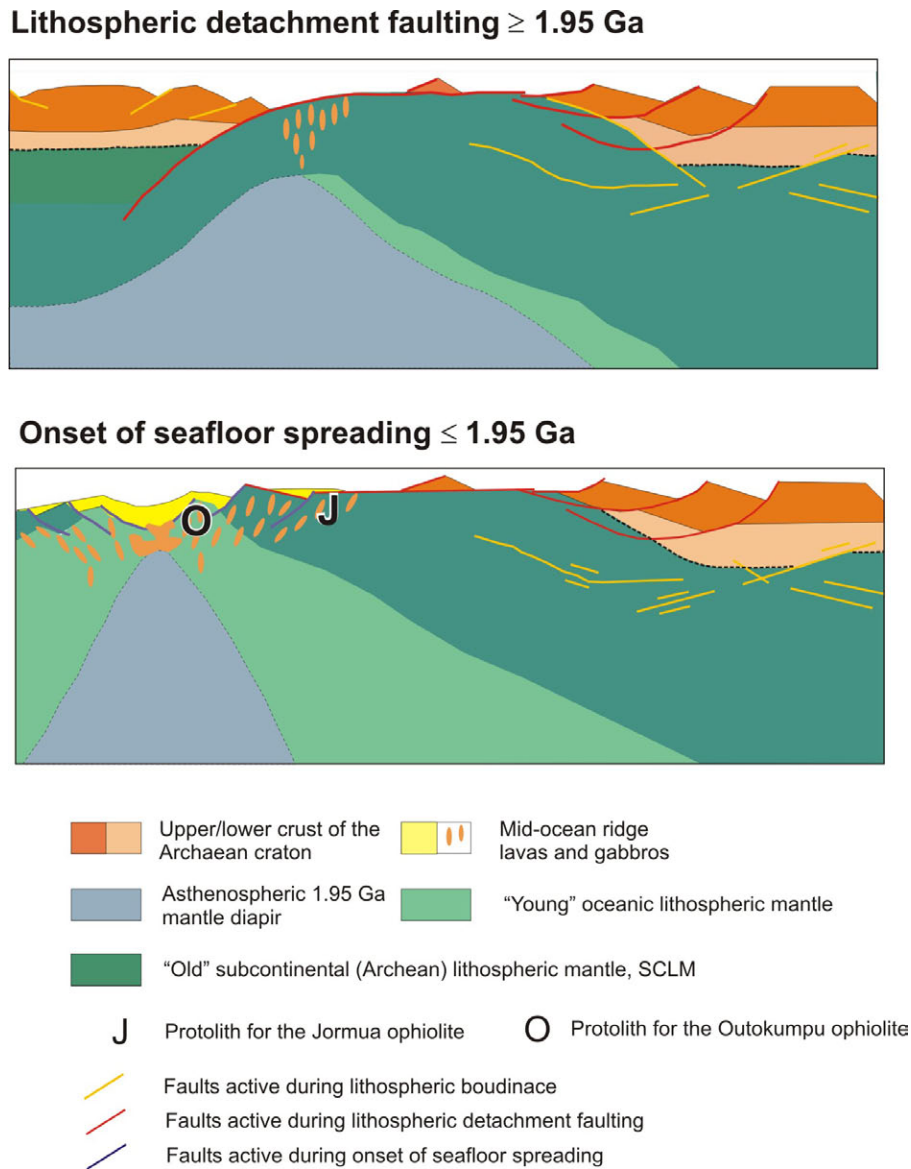


Fig. 2.8. A lithospheric-scale model illustrating a possible tectonic setting for the Jormua and Outokumpu ophiolites within a magma-poor passive margin at c. 1.95 Ga. After Peltonen (2005).

The tectonic setting of the Jormua ophiolite proposed above is based on its structural and geochemical features and its relation to the KSB. Nevertheless, its geotectonic significance can be fully understood only within the context of the other ophiolite occurrences along the western margin of the Karelian Craton. These include the c. 1.96 Ga sister ophiolite fragments in the Outokumpu area in the southern part of the Jormua-Outokumpu Allochthon (Koistinen 1981; Peltonen et al., 2008). Russian geologists have presented evidence for possible ophiolitic rocks in the north Ladoga area some 100 km southeast of Outokumpu (Ivanikov and

Philippov 1997). Hanski (1997) has argued that rocks with ophiolitic affinities exist along the NE margin of the Kittilä Allochthon in Finnish Lapland some 400 km north of Jormua.

The Kaavi-Outokumpu ophiolite fragments vary from small, sole serpentinite bodies to kilometre wide – several kilometer long serpentinite bodies with a variable component (5-25 vol.%) of intrusive gabbros and basaltic dykes and (at one locality) minor pillow lavas (Park, 1983, 1988; Rehtijärvi and Saastamoinen, 1985 ; Peltonen et al., in press). Despite of the about similar age of the mafic components and location in the same allochthon, there are some differences between the Kaavi-Outokumpu and Jormua cases, e.g. mafic rocks in the Outokumpu area ophiolite fragments are instead of E-MORB type basalts typical to the Jormua Complex, rather low-Ti basalts with high Mg-numbers and low incompatible element concentrations (Rehtijärvi and Saastamoinen 1985, Park 1983, 1988, Peltonen, 2005) The Kirjavalhti metalavas in the north Ladoga area include pillow lavas with N-MORB affinity. The Kittilä greenstone complex comprises a diversity of metavolcanic rocks showing mainly within-plate basalt or MORB, but also apparent island-arc basalt affinities (Hanski, 1997). Whether these, and other differences between the various ophiolites on the western margin of the Karelian craton can be explained in terms of one collision, for example, or whether they require more complex tectonic explanations, remains to be evaluated in further studies.

Part of the answers related to the tectonic origin/significance of the ophiolites along the Karelian margin will come through improving our understanding of the nature of the west lying Svecofennian domain and the contact zone, often referred to collisional “suture”, between it and the Karelian craton. Although the present paradigm for Svecofennia is that of a collage of (buried) microcontinents and island arcs accreted to the Karelian margin, there is lot of reason to be skeptical about. For example, an analysis of the published maps of the Svecofennian domain (in Finland) indicates that only about 5 % of its area (probably far less of the whole crustal volume) is actually comprising volcanic rocks (including first cycle volcanic-clastic rocks), while obvious multicycle turbidite metasediments (frequently with mixed Archean – Proterozoic zircon grain populations) make about 32 %, the rest consisting mainly of what are usually referred to syn, late and postorogenic granites. Further, more “diagnostic” island arc rocks, such as low-K tholeiites seem to make only less than one percent of the total rock area. One key question is the relationship of the upper Kaleva turbidites hosting the Jormua-Outokumpu ophiolites and the turbidites in the Svecofennian domain. Overall, the formative tectonic environment of the Svecofennian dominant supracrustal component, its huge piles of possibly “cogenetic” metaturbidites.

Finally, one factor complicating tectonic interpretation of the JOC, as well as other Precambrian ophiolites, is the potential differences between Precambrian and modern plate tectonic and related magma generating processes. The main reason to doubt such differences have existed would be the higher radiogenic heat production of the Precambrian Earth. The relative rarity of ophiolites in the Precambrian terrains suggests that there indeed were differences in that how the Precambrian Earth did and how the Phanerozoic-present Earth did/does work. Thus, for example, discrimination based solely on chemical criteria of rocks may potentially be misleading and yield faulty interpretations of the formative tectonic settings. This means that for true resolving of the messages that the rare Proterozoic ophiolites bring on the Precambrian tectonics, study of their rocks, structures, alteration histories and tectonic situations from as many perspectives as possible is a *sine qua non*.

Location of the excursion stops on a geological map and the reconstructed structure of the JOC

Remarks on the Jormua area and field conditions there in August time

The JOC is located on the eastern bank of the fifth largest lake in Finland, the Oulujärvi Lake. In the past, the 29 km wide, 70 km long and on average 7 m deep lake was a central part an important water way from Kainuu to the Oulu harbor at the coast of the Bothnian Bay of the Baltic Sea. Nowadays the economic importance of the lake is mainly in its role as the main water reservoir for the 8 hydroelectric power stations built along the Oulujoki River flowing from the Oulujärvi Lake to the Bothnian Bay of the Baltic Sea. Before the built of the power plants, Salmo Salar used to return in a big way from the Baltic Sea via Oulujoki to Oulujärvi, and further in the rivers from the east. Now the native, pure Baltic Salmon is at the verge of extinction, meaning that, even building the much anticipated fish steps would not necessarily bring the original Baltic Salmon back in the Oulujärvi Lake.

The surrounding sparsely populated province, characterized by vast pine and spruce forests, quartzite hills, sandy plains and boglands crossed by slow-moving rivers and plotted by a few big lakes, is called Kainuu. The area was long known as one of the poorest parts in Finland, being often called as “the land of hunger” (“Nälkämaa”). During the nineteenth century the living standard in Kainuu started to slowly rise, partly because of incomes from wood tar exports, mainly to Great Britain. Tar was for centuries vital as preservative of wood and rigging of sail ships and in their waterproofing. The Oulujärvi Lake is part of the lakes and rivers chain that was used for floating of the tar, packed in wooden barrels, from Kainuu to the Oulu harbour sited on the Gulf of Bothnia at the mouth of the Oulujoki River that originates from the Oulujärvi Lake. Nowadays the Kainuu province is about as other mainly rural areas in Finland, also in that respect that the area is slowly running out of people. The migration away has, however, considerably slowed since its climax during the 1960-1970s.

Jormua is an age old village being populated at least since the Stone Age. The meaning of the word Jormua is not known but probably it is of Saamian origin, as many other locality names in Finland, which was populated mainly by Saami people before the start of the immigration of “Finns” about 1000 year ago. The nearest city to Jormua is Kajaani located about 20 km to the south of it. Kajaani is the administrative and commercial center for the surrounding province, and also a site of paper industry, hydroelectric power generation and nowadays also electronic industry. The city is connected to the rest of Finland by the Highway 5, the Helsinki-Oulu railway, and there are also daily domestic flights from the Kainuu airport at Paltaniemi to Helsinki and back. Several high quality hotels and hostels are available for the traveler in Kajaani.

Kajaani was founded 1651 by Per Brahe the Younger, the famous Governor General in Finland, well remembered from the many blessings for Finland by his wise and provident rule (Note Finland was under Swedish rule until 1809, and then an autonomous Grand Duchy of Russia until 1917). Still today the expression “Kreivin aikaan” (“at Count's Time”) in the Finnish language means “at the correct/good time”. There is a statue for Per Brahe at the marketplace in the centre of the city. It could be mentioned that the folklorist and medical doctor Elias Lönnrot began many of his travels from Kajaani to collect material in Karelia for his famous “Kalevala”, which is the national epic of Finland and has provided inspiration for many famous composers, painters and writers, including e.g. Jean Sibelius, Akseli Callen-Kallela and J.R.R. Tolkien. One interesting historical monument in Kajaani are the ruins of the Kajaani Castle, located on the River Kajaani in the centre of the city. The castle was origi-

nally built in 1604 and completed in 1619. The castle served as an administrative centre, prison, military base and a refuge for the citizens.

Early August tends to be the driest and often also warmest period of the summer in Finland. The Finnish name for August “Elokuu” has the meaning: “the month of crop ripening and harvesting”. However, as a rainy, cold day is always a high possibility in the Finnish summer, being prepared to it with a raincoat (or at least an umbrella) and water resistant boots is always a sensible precautionary measure. With one modest exception (Stop 2, Lehmivaara), most of the stops are physically fairly easy. Note that the terrain in the field may yet be in places a bit rough, bushy and wet. The viper is the most “dangerous” animal one is likely to face in the Jormua area, where it is rather common. The viper is moderately venomous, but aggressive only when frightened. Mosquitoes are generally not a big problem in August. If you are sensitive to their bites, even in a warm day, try to use more covering cloths than just shorts and a T-shirt. Or you may use repellants, such as the traditional liquid-form “Johnson Off”. This stuff containing 45 vol. % dinitrotoluamide, verifiably keeps the mosquitoes at a distance, but it also seems to solute and migrate in about anything, according some studies maybe even into your brain. Up to mosquitoes, moose flies may also occur in August. If they abound, some people are likely to find them really nasty. For the annoyance caused by these tiny biting evils, there is no truly working salvation, you just have to grin and bear it. Tight-fitting, demure clothes may help a bit though.

Stop 2.1. Hannusranta: Early suite cumulate dykes in serpentinite

The Hannusranta stop is located in the western part of the JOC, about 6 km to the east of the Paltaniemi village about 20 km N of the Kajaani town. The Paltaniemi village is well-known due to the Hövelö House, the birth place of Eino Leino, one of the most important poets in Finland. Paltaniemi is famous also of its Picture Church, a small wooden church built in 1726 and decorated for its ceilings and walls with impressive paintings of biblical subjects by Emanuel Granberg in 1778-81. Visiting the Hannusranta stop requires about 1.5 km walking, in part along a clear forest path, in part in a bushy terrain with humpy outcrops and intervening small depressions with water drains. Sturdy, water-resistant boots are recommended.

The Hannusranta stop is to the western main block of the JOC, interpreted to represent the lowermost unit in the original pseudostratigraphy of the Jormua Complex, The “block” comprises a thin (0.5-1.5 km) but long (over 10 km) sliver of serpentinitized mantle peridotites in fault contacts with the Palaeoproterozoic (Lower Kaleva) metasediments and Archean granitoid-gneissic rocks in the north and south, respectively. Characteristic for the Hannusranta block is the abundance of mantle cumulate dykes intrusive in and sharply truncating the serpentinitized mantle peridotites (Fig. 2.5a,b).

WESTERN BLOCK

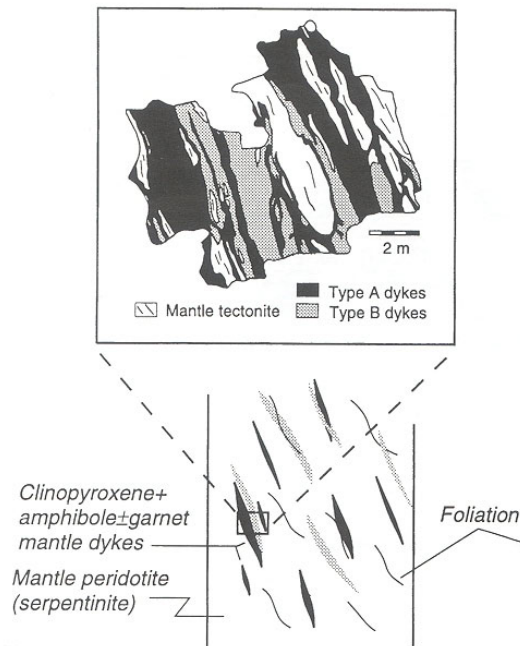


Fig. 2.9. Field sketch illustrating the field relationships of the early facies pyroxenite, late facies hornblende cumulate dykes and serpentinized mantle peridotite at Hannusranta. In this outcrop the mantle peridotite is present just as narrow screens between the broadly subparallel cumulate dykes. After Peltonen et al. (1998).

The Hannusranta serpentinites are massive to schistose antigorite serpentinites lacking any pseudomorphic primary peridotite textures or structures except for locally preserved chromite (altered) banding that seems to be of mantle tectonic origin. Porphyroblasts of metamorphic olivine and tremolite, the former variably replaced by retrograde lizardite, are locally common. The stable coexistence of olivine-tremolite antigorite suggests metamorphic peak was attained at temperatures of c. 520±20 C, obviously in a relatively late stage of the Svecofenian orogeny. Chemically the Hannusranta serpentinites comply to Iherzolites-harzburgites variably depleted in basaltic components such as Al_2O_3 and TiO_2 , but variably enriched in such elements as Zr and LREE, the latter feature probably due to mantle metasomatism in association with the emplacement of the mafic dykes (Peltonen et al., 1998).

The first outcrops (Northing: 7136132; Easting: 3537932) visited at Stop 2.1 show peridotite abundant in the mafic cumulate dykes typical of the Hannusranta block. It is seen that the dykes occur in two succeeding generations; the first generation comprises clinopyroxene±amphibole (mainly magnesio-hornblende) dykes and the second one amphibole (mainly magnesio-hastingsite)±garnet dykes. The latter dykes in places grade to very coarse-grained, amphibole-rich (pargasitic hornblende±edenite) pegmatoid rocks. The clinopyroxene (diopside) in the first generation dykes is replaced more or less completely by retrograde fibrous amphibole (tremolite-actinolite). Some of the second generation dykes show obvious garnet pseudomorphs. A garnet origin of the pseudomorphs is supported by the variable garnet effect seen in normalized REE patterns of samples from the second generation dykes (Fig. 2.10).

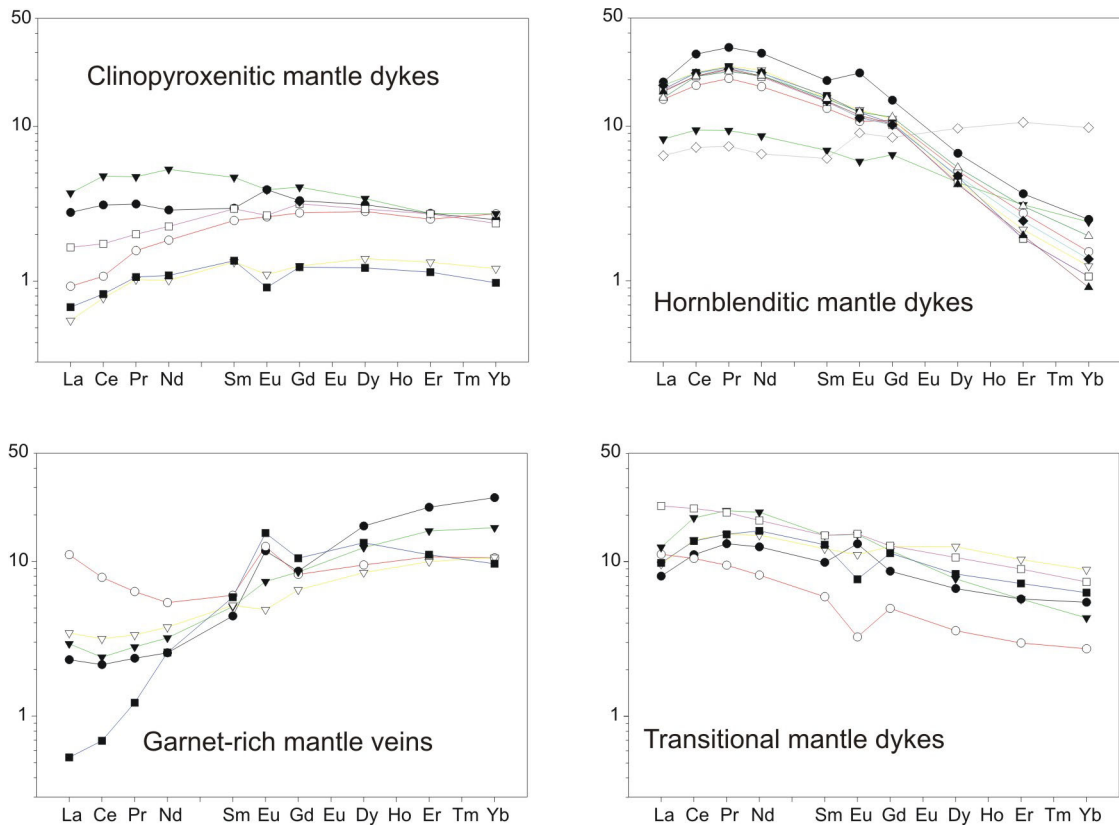


Fig. 2.10. REE spiders of the pyroxenitic and hornblenditic mantle dikes of the Jormua Ophiolite Complex.

The second outcrop visited (Northing: 7136132; Easting: 3537932) shows one of the rare first generation “dry” clinopyroxenite dykes still preserving abundant, obviously primary clinopyroxene. Based on SIMS analyses the diopside in this dyke is relatively LREE enriched. Melt calculated to be in equilibrium with the diopside has similar REE concentration and chondrite-normalized pattern than the early OIB type dykes in the Lehmivaara block (Peltonen et al. 1998; the Lehmivaara OIB dykes will be seen at Stop 2.2). Although rather low in the element zircon, the clinopyroxenite dyke comprises some zircon grains. Zircon grains separated from the dyke are intriguing for their age distribution.

Whole rock samples and pyroxene separates from the Hannusranta dykes plot on the Sm-Nd isochron diagram along a line with an age indication of 1968 \pm 58 Ma and $\epsilon_{Nd1950\text{ Ma}}$ -0.1 (Peltonen et al. 1998). This means that the enrichment of the dykes in LREE, and therefore probably also their magmatic emplacement must be of Proterozoic age. The Archean zircons in the dykes thus most likely are xenocrysts crabbled in the magmas from their wall mantle rocks. The precise origin of the zircon grains remains obscure, however. One explanation would be they derive from Archean intermediate-felsic dykes in the Hannusranta (or relatively deeper) mantle. An alternatively the zircons could be detrital grains introduced in the perioditites at late Archean subduction zones.

It is worth to mention here that, in addition to the clinopyroxenite and amphibolite dykes, also carbonatite-like veins seem to occur in the Hannusranta sliver. So far the evidence is only by three boulders in clacial drift on Hannusranta sliver found to contain such dykes. However, as the boulders are of angular shapes and contain antigorite serpentinite, it is most likely that they are of local derivation from the Hannusranta sliver. One of these boulders consists mainly of carbonate, amphibole, chlorite and magnetite, while the other two, dominantly ser-

pentinite boulders comprise cm to dm wide dykes composed of mainly calcite with some apatite, magnetite-ilmenite and amphibole.

The third outcrop (Northing: 7136146; Easting 3537932) shows a narrow (c. 20 cm) basalt dyke sharply cutting clinopyroxenite and serpentinitized peridotite. A chemical analysis for this dyke reveals that it has a perfectly similar whole rock composition as is typical of the main suite E-MORB dykes and lavas. The presence of this dyke, and another similar dyke in a nearby outcrop, are important evidence of two relationships. First, the basalt dykes, although rare, tie the Hannusranta block with the other main blocks of the JOC. Second, the dykes demonstrate emplacement of the Hannusranta dykes, similar as the Lehmivaara OIB dykes, before the main suite magmas.

The fourth outcrop of Stop 2.1 (Northing: 7136232; Easting: 3537907) shows coarse grained, 10-30 cm wide, partly sharply bound, obviously primarily garnet bearing dykes or segregations in a hornblende rich host rock. A comb layering like structure characterizes some of the more garnet-rich dykes. Apart shapes, also chemical composition supports a garnet origin of the supposedly garnet pseudomorphs. Chemical compositions of two samples of the pseudomorphs are compatible with their origin from relatively pyrope-rich garnet (e.g. 112A: Alm27.2Prp48.1Sps0.4Grs24.3, Peltonen et al. 1998).

Stop 2.2. Lehmivaara: Early suite ultramafic (OIB) and main suite (EMORB) dykes in serpentinite

The Lehmivaara stop is to the central main block of the JOC, the Lehmivaara block (Fig. 2.2). Visiting the stop includes c. 3 km walking, partly along forest road and partly in open-cut to young pine forest. Sturdy boots or jogging shoes are recommended. Given fair weather, climbing high on the Lehmivaara hill should reward by a nice view over the easternmost part of the Oulujärvi Lake.

The central part of the Lehmivaara block visited at the Stop 2.2 is characterized by extensive dyking of mantle peridotites by metagabbroic to metabasaltic dykes, these dykes being similar in their field appearance and chemical composition to the dykes in the main sheeted dyke and pillow basalt units of the JOC. Considering the Lehmivaara block as a whole, there is a clear gradation from serpentinite dominated outcrops in its western part to nearly 100% dyke outcrops in the Sammakkolampi sheeted dyke “complex” (visited at Stop 2.3) in its eastern part. It is believed that the western part of the Hannusranta block originally located relatively deep in the original pseudostratigraphy of the JOC, representing a “root zone” to the Sammakkolampi sheeted dykes. In addition to the ubiquitous E-MORB dykes, rare, mostly pervasively chloritized mafic-ultramafic dykes of OIB chemical affinity are also present at Lehmivaara. So far a dozen of such dykes, ranging from less than 10 cm to 1.5 m in thickness, have been observed. Based on field evidence the OIB dykes are older than the main suite dykes, therefore they have been termed also as “early dykes”.

In the first Stop 2.2 outcrop visited high on the Lehmivaara hill (Northing: 7139059; Easting: 3544.298) one of the thickest and best preserved of the presently known Lehmivaara OIB dykes is seen. The c. 1.2 m wide dyke shows sharp contacts against the wall metaserpentinite. The dyke consist mainly of coarse amphibole, but there are clinopyroxene dominant patches in its middle parts. Minor mineral constituents in the latter domains include magnetite intergrown with ilmenite, chlorite, some apatite, zircon and trace sulphides. The second outcrop visited at Stop 2.2 (Northing: 7139273; Easting: 3543887) illustrates the emplacement relationships of the early OIB dykes and the main suite metabasalt dykes. It is seen in this outcrop

that an SW-NE oriented OIB dyke is sharply cross-cut by E-W trending main suite metabasalt dykes. This is concrete evidence of that the OIB suite dykes must be at least slightly older than the main suite dykes. OIB dykes at Lehmivaara are characterized by strongly LREE-enriched chondrite-normalized REE patterns and variably high TiO₂ and Zr concentrations. Though alkalis are low in the present composition of the dykes, it is possible that this is merely by alteration, and that the protoliths yet were Mg-rich alkali basalt or ultramafic lamprophyre-like rocks.

Stop 2.3. Sammakkolampi: sheeted dykes

The Stop 2.3 is to the largest single occurrence of sheeted dyke type lithology within the JOC, the Lehmilampi dyke complex in the eastern part of the Lehmivaara block. This Stop takes altogether about 0.5 km walking, mostly along a gravel road. Note that a private summer villa is located quite near to the outcrops of Stop 2.3. Thus, please do not throw any trash in the field or along the road. Also, all hammering and any further stripping of moss at Stop 6 and in the surrounding area are strictly forbidden, by demand of the land/villa owner. Other good outcrops of sheeted dykes of the Lehmilampi dyke unit are present in the area to the south of the nearby Särkijärvi Lake (at Northing: 7137880; Easting: 3546290, for example).

The Lehmilampi dyke complex consists nearly 100 % of subparallel, typically 20 cm to 1.2 m wide metadolerite and metabasalt dykes (Fig. 3a). The total area of this sort of lithology in the Lehmilampi unit is about 3.5 km². Although nearly 100% of dykes, even in the easternmost part of the Lehmilampi unit, there occur occasional, usually less than 1 m wide, but locally up to 20 m wide serpentinite and gabbro screens between the dykes. And, as we described above, the Lehmilampi complex shows increasingly more serpentinite (peridotite) screens towards the west and middle part of the Lehmivaara block. The presence of mantle peridotite+gabbro screens in all the sheeted dyke occurrences of the JOC attests to their origination by extensive extension and related mafic dyking in the mantle unit. It is obvious that the starting point for the development of the mafic lid in the JOC was a dominantly mantle peridotitic lithosphere. A general scenario seems to be that by extension the ultramafic lithosphere was first intruded by gabbro dykes and stocks, and that by further extension by doleritic-basaltic dykes locally feeding pillow lavas. The lavas provide proof of that at least in the later stages of this progression the system was forming part of seafloor. It is quite possible that part of the lavas may have been deposited directly of the wider screens of mantle peridotite that may have been remaining between more extensive/coherent mantle plus gabbro screened dyke-in-dyke zones.

The Stop 2.3 consist of several outcrops between coordinate points Northing: 7136933; Easting: 3546295 and Northing: 7136971; Easting 3546258. A well exposed section about 100 m wide of the sheeted dyke unit is seen in these outcrops. Besides one minuscule screen (septa) of tremolitized peridotite, all that is seen in these outcrops are fine-grained metadoleritic to metabasaltic dykes in dykes. The dykes clearly have been intruding as many successive dyke-in-dyke generations; up to 6 generations can easily be discerned in a typical outcrop. The dykes of the older generations seem to have been wider and somewhat coarser grained than the dykes of the younger generations. The younger dykes, mostly 20-80 cm wide, distinctly intrude and split the older dykes that have been transformed to interdyke screens of “half” (or “one-way chilled”) and “marginless” dykes. Most of the dykes appear aphyric to sparsely plagioclase phyric, some contain abundant plagioclase, sometimes distinctly concentrated in the dyke interiors, obviously by synemplacement magmatic flow. Dyke contacts are sharp and show well distinguishable, very-fine grained recrystallized chill margins. Branching of the dykes and apophyses along dyke margins are common features. Most of the dykes appear

subparallel, but due to the slight attitude-orientation variations, the older, split dykes are often truncated at low angles by the younger dykes and are hence seen to usually taper off rather rapidly. And there are locally also more complex, breccia-like intrusive relationships present.

Stop 2.4. Antinmäki: gabbro dykes in serpentinitized mantle peridotites

The Stop 2.4 is to present typical features of the gabbro dykes and small stocks that are distinctive of the largest of the main blocks in the JOC, the central Antinmäki block. These are dykes that were referred to gabbroic mantle dykes by Peltonen et al. (1998). Visting the two separate outcrop groups that will be examined takes about 1 km walking, about all this along passable forest roads/paths.

The first outcrops (Northing: 7138568; Easting: 3548514) high up on the Antinmäki hill show a network of gabbro dykes in serpentinitized peridotite, a characteristic feature of the whole Antinmäki serpentinite hill (Fig. 2.5.b). The gabbro dykes in the Stop 2.4 and surrounding outcrops vary from a few dm to a few metres wide, multiply branching solitary or networked dykes of fine to very coarse-grained gabbro. At their usually sharp contacts the intruding gabbroic magma is sometimes seen to have broken blocks from the wall peridotite to “float” as usually somewhat rounded inclusions in the dykes. In many Antinmäki outcrops bands defined by pseudomorphic pyroxene and altered chromite in the serpentinite, and that probably are of mantle tectonic/flow origin, are sharply truncated by the gabbro dyke margins. All these features, indicative of that the gabbro dykes intruded in a mantle peridotite that was concurrently deforming in a semi-brittle way, are well illustrated in an outcrop (Fig. 2.11).

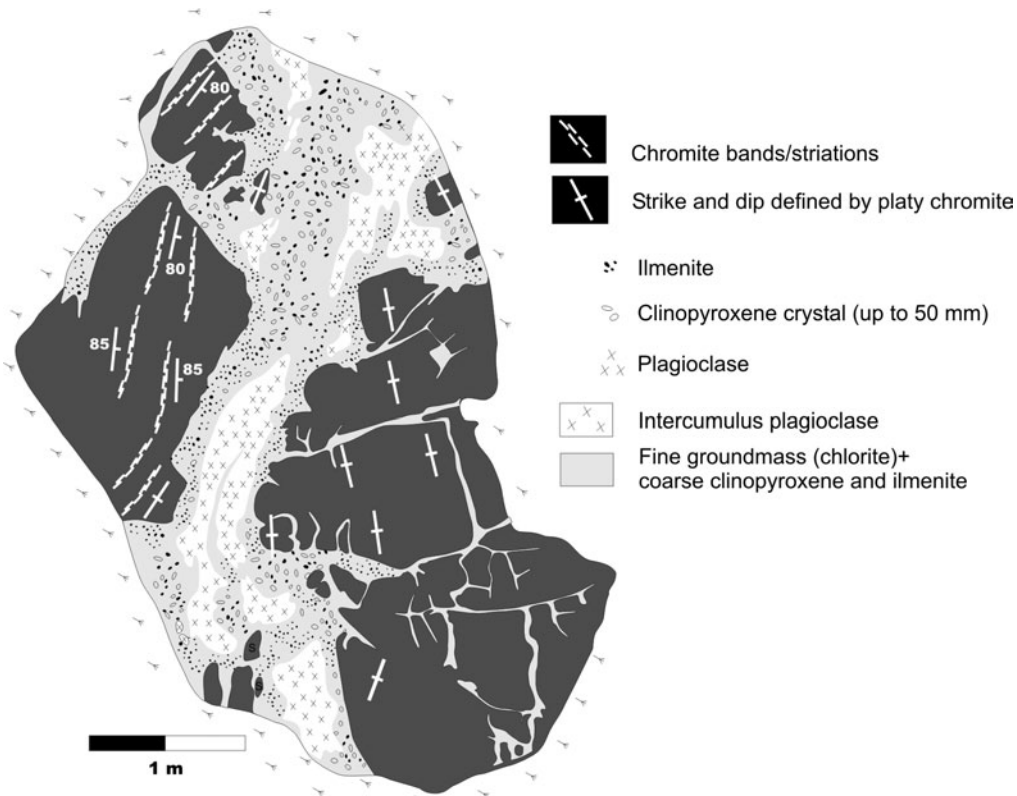


Fig. 2.11. A gabbroic feeder dike cross-cutting mantle tectonites.

In many cases of the Antinmäki gabbro dykes, the margins of the dykes consist of 5-20 cm of fine-grained chloritized material (chilled basalt?), sometimes with coarse-grained clinopyroxene crystals (phenocrysts/xenocrysts?), but whose primary composition is largely obscured by

intense post-emplacement alteration to chlorite related to across the dyke-peridotite interfaces. In some cases the enclosed clinopyroxene crystals exhibit features suggesting internal plastic deformation. This indicates that the clinopyroxene crystals were xenocrysts recording deformation either in the source regions of the gabbro magma, or alternatively in the host dyke during periods of low amount of interstitial magma due to varying amounts of tectonic compaction and related filter pressing. For their central parts the dykes are often coarse grained to pegmatoid, and consist of clinopyroxene±amphibole±plagioclase with variable amounts of titaniferous magnetite and ilmenite. The plagioclase is extensively replaced by epidote+grossularite garnet and ilmenite by sphene and rutile. The secondary mineralogy is indicative of premetamorphic, possibly already in the seafloor stage or perhaps early obduction stage rodingitization of the the gabbro dykes. An early origin for the rodingitic alteration is likely as it is a process known to be restricted to minor mafic bodies enclosed in ultramafic rocks that have undergone low-T (< 200°C) serpentinization. The early removal of sodium by the rodingitic alteration facilitated preservation of clinopyroxene through the subsequent low amphibolite facies regional metamorphism.

The other target at Antinmäki (Northing: 7138940 Easting: 3548289) is representing a somewhat larger, and possibly somewhat higher level gabbro dyke than those visited first higher on the Antinmäki hill. A serpentinite outcrop is located near the road to the gabbro outcrop, providing an easy view on the wall serpentinites. The wider Antinmäki gabbro dykes as here probably acted as feeders for even larger *in-situ* differentiated Mg-gabbro-ferrogabbro-plagiogranite intrusions still higher up in the ophiolite pseudostratigraphy. The gabbro varies medium to coarse-grained and is thoroughly metamorphic for its mineralogy consisting mainly of hornblende and oligoclase-andesine. In a difference to the smaller gabbro dykes the more voluminous gabbro dykes do show evidence for metaroddingitization only locally for their very margins and narrow apophyses. Lacking the rodingitic alteration and associated sodium loss, the common low-amphibolite facies reaction of clinopyroxene with plagioclase to eventually produce hornblende+sodic plagioclase was possible and pervasive.

Stop 2.5. Kivisuo: Mg-gabbros

The Kivisuo outcrops are visited to see Mg-metagabbros typical of the larger dominantly gabbroic bodies in the JOC. The outcrops locate about 100-200 m off a local gravel road. Beware of bypassing cars when leaving/getting back to the buss — the local people are sometimes overtaken by their rally racer alter ego.

According to mapping and geophysical data, the Kivisuo outcrops belong to a gabbro body that is at least 1 km² in its surface area. Field observations at contact outcrops and geophysical maps show that the Kivisuo gabbro is intrusive with twisty contacts in the surrounding peridotites of the Antinmäki block. The gabbro is variably coarse to pegmatoid in its grain size. As in the case of the JOC gabbros in general, there are little evidence for magmatic layering. The gabbros sampled at the Kivisuo stop are among the most magnesian (MgO 9-11 wt.%) so far observed from of the JOC, yet the compatible trace element concentrations are low, lower than in most JOC basalts. This together with low incompatible element abundances is attesting the gabbro was of “cumulate” origin. The original mineral composition was probably clinopyroxene+plagioclase±olivine. Of these minerals only plagioclase is occasionally partially preserved. Olivine and clinopyroxene have totally been replaced by mainly chlorite and uralitic amphibole, respectively.

Some ophiolites, especially those supposed to have originated above subduction zones, have noticed to bear some PGE potential, e.g. in their gabbro units. PGE analyses for a set of sam-

ples of the Kivisuo and other Jormua gabbros performed a few years ago indicated that they are not associated with any PGE enrichments. The low PGE all over the JOC could be considered one more feature supporting a subduction unrelated origin of this ophiolite.

Zircon grains separated from a pegmatoid variety of the Kivisuo gabbro have yielded, based on multigrain fractions an TIMS U-Pb age of 1.96 ± 0.12 Ga.

Stop 2.6. Shell Kontiomäki: serpentinitized harzburgitic mantle peridotite

At stop 2.4. some examples of serpentinites typical of the Antinmäki block were seen. The Stop 2.6 shows one more outcrop of relatively little strained metaserpentinized harzburgite, and which is thus showing some fairly well preserved (pseudomorphic) primary textures and structures. Also in this outcrop a dyke of metaroddingized, coarse-grained gabbro is seen to cut the peridotite. The Stop 6 locates (Northing: 7135914; Easting 3550586) immediately to the S of the parking place of the Kontiomäki Shell service station-restaurant-shopping centre, which is providing a casual visitor of the JOC an easy option for a meal or refreshments, and refilling also the car's tank.

The weathering surface of the Shell serpentinite is patterned by pale gray, slightly elevated "knobs" that obviously are pseudomorphs after orthopyroxene (bastite recrystallized to antigorite). The knobs occur in a slightly darker grey "groundmass" of felty, fine-grained antigorite, stained darker by relatively abundant magnetite dust. This material obviously is mainly after olivine. Besides serpentine after pyroxene and olivine the Shell serpentinite contains 1-2 vol.% of 1-5 mm altered chromite grains, which now consist predominantly of ferritchromite surrounded by Cr-magnetite but with occasional chromite cores. The oxide grains define a weak foliation of probable mantle origin. Also a vague dm scale banding is seen in the serpentinite, this banding being defined by variations in modal abundance of the pseudomorphic orthopyroxene and olivine.

Although the dominant serpentinite phase in the Shell serpentinite, and JOC serpentinites in general, is peak metamorphic antigorite, sporadic patches of serpentine with magnetite dust mesh typical of low-T serpentine generations (lizardite-chrysotile) are preserved in the domains after olivine. This together with the metaroddingitic nature of many of the gabbro dykes in the Antinmäki block suggest that the Jormua metaserpentinities most probably have experienced extensive low-T serpentinization before their prograde recrystallisation to the present antigorite dominated assemblages. Whether this premetamorphic low-T serpentinization took place in the oceanic stage of the JOC, or later, as during the obduction of the ophiolite, is not known.

Chromite preserved in cores of the coarser oxide grains of the Shell serpentinite has Cr and Mg numbers around 75 and 50, respectively (samples 76B and 76N in Table 1). These are similar values as are typical of chromites in the Jormua chromitites (Stop 2.7). The relatively high Cr number is in unison with the low Al₂O₃ content of the serpentinite, indicating a depleted harzburgite parentage, too. Samples from the Shell serpentinite are among the strongest depleted mantle samples analysed from the JOC.

Chromite cores of the Shell site serpentinite are surprisingly high in ZnO (up to 3.25 wt.%), revealing that divalent cations have been affected by secondary alteration, this involving Zn addition. Elevated ZnO (0.50-2.50 wt.%) and MnO (0.50-1.0 wt.%) contents are a typical feature of chromites in JOC serpentinites, being an ubiquitous feature also of other ophiolitic serpentinites in eastern Finland. It may be noted that Zn content in one representative whole

rock sample of Shell serpentinite is 86 ppm. As this is a somewhat high value for mantle peridotite, there may be in this case some minor Zn addition from outer sources (black schists around JOC are relatively rich in Zn). In general, however, the whole rock Zn concentrations in samples of JOC serpentinites, also in samples comprising Zn-rich chromites, are lower, averaging to 52 ppm compared to 55 ppm Zn in primitive mantle. This suggests that the Zn mobility related to the Zn-enrichment in the JOC chromites was usually restricted within the hand sample scale.

Even much higher ZnO and MnO concentrations than in the Shell serpentinite chromites, exceeding 10 wt.% and 5 wt.%, respectively, are found in hydrothermally recrystallized chromites in “Outokumpu type” quartz rocks commonly found in association with talc-carbonate altered and/or carbonatized serpentinites and derived metaperidotites of the Jormua-Outokumpu belt. In Jormua such chromites are found from one quartz rock occurrence at the western margin of the Antinmäki serpentinite. The hydrothermally modified chromites in this occurrence are very distinct from the chromites in the adjacent serpentinites in being very low in Al and ferric iron, and very high in Cr. The highly zincian-manganous and sometimes also vanadian chromites are a typical feature especially of the Outokumpu type Ni-Co-Zn-Cu sulphide ore environments, found at the ore margins, both in the ore and in the typically hosting quartz rocks. Considering that the quartz rocks represent silicified mantle peridotites (Kontinen, 1998; Säntti et al., ; Peltonen et al., 2008), it is most likely that also their chromites, including the Zn+Mn±V rich chromites, are ultimately of mantle origin. It may be that the addition of Zn+Mn±V in these chromites occurred concurrent with the passage of the ore-forming fluids; however, as well the high concentrations could be after later metamorphic equilibration with the Zn+Mn±V enriched sulphidic host rocks. In any case, Zn-rich spinels are not providing a truly useful prospecting tool for Outokumpu type sulphide mineralizations. As the background Cu and Zn concentrations in the typical host rocks of the Outokumpu type mineralizations are constantly very low, presence of even traces of chalcopyrite and sphalerite in these rocks provides a far less ambiguous indicator of possible near-locating mineralizations.

Stop 2.7. Pitkänperä: chromitite pod

Chromitites are a feature of many ophiolites, typically found in their upper mantle to mantle-crust transition parts. At Stop 2.7 (Northing: 7139132; Easting: 3550211) one of the rare chromitite pods so far found in the peridotites of the JOC will be seen. This target locates about 100 m off the road.

In the JOC peridotites chromitite bodies are rare indeed, being presently known only in the 100-400 m wide, about 3 km long Matokallio peridotite slice between the Pitkänperä and Kylmä pillow lava slices. The Matokallio slice is presently by far the economically most important component of the Jormua ophiolite, albeit not due to the chromitites but as comprising a resource of over 20 Mt of talc-ore-grade talc-carbonate rock. There has been test mining from three open pits in the southern part of the Matokallio slice, and plans for a 20 year 500 000 tons per year mining operation, by Mondo Minerals. The company runs the biggest single talc production facility in the world (400,000 tons per year), utilizing a talc-carbonated ophiolitic peridotite lens at Lahnaslampi about 22 km to the south of Jormua.

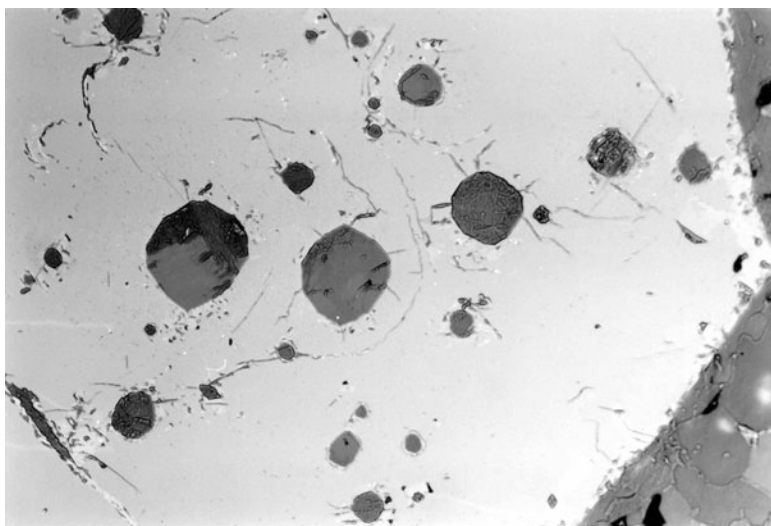


Fig. 2.12. Microphotograph of amphibole inclusions in a chromite grain from the chromitite lens at Stop 8. Microanalyses of the two largest inclusions and the enclosing chromite are given in Table 4. The diameter of the largest inclusion is about 0.08 mm.

The talc resource of Mondo Minerals occurs mainly along the western margin of the southern end of the Matokallio slice in a 80 to 150 m wide, about 1 km long zone of mostly pervasively sheared, schistose talc-carbonate rock. The opposite margin of the Matokallio slice is showing a 40-60 m wide, about 600 m long zone of tremolite “skarn”, carbonate rock and quartz rocks. These rocks are a typical example of the “Outokumpu association”, representing, like the talc-carbonate rocks, metamorphic-hydrothermal alteration of the peridotites of the Matokallio slice (Säntti et al., 2006; Peltonen et al., in press). The skarns, carbonate rocks as well quartz rocks comprise all chromite and have Cr and Ni concentrations about as high as the protolith serpentinites.

Chromitite pods and peridotites rich in disseminated chromite are sporadically occurring along the eastern margin of the Matokallio slice in an about 700 m long zone. For most part of the chromitite-bearing zone contains only small (cm to dm size) chromitite fragments often in a brecciated serpentinite/peridotite matrix. The largest of the known chromitite pods is, however, about 1 m thick (max) and at least 5 m long.

The elongated, folded chromitite pod at Stop 2.7 is situated in a heavily carbonated serpentinite. Margins of the chromitite pod comprise strongly fractured chromite, being along the fractures extensively replaced by carbonate and chlorite. In a contrast, the core parts of the body consist of surprisingly fresh, coarse-grained chromite. The fresh chromite in the pod interior has a moderately aluminous composition with Mg and Cr numbers averaging around 75 and 55, respectively, and a TiO_2 content around 0.24 wt.%. Small, roundish inclusions, generally filled by secondary chlorite and/or carbonate are common in the chromites. A few of the inclusions comprise about only tshermakitic hornblende relatively high in pargasite-edenite component (Fig. 2.12). Compositionally this amphibole is close to the pargasitic amphibole inclusions found in chromites of some oceanic and ophiolitic peridotites and chromitites, and which inclusions are thought to be after melts whose percolation through and reaction with the enclosing peridotites produced the chromitites. This same interpretation may be true also for the amphibole-filled inclusions in the Pitkänperä chromites.

It is worth to note that the chromite in the Pitkänperä chromitite pod is of nearly similar composition as the chromite in the Vasarakangas chromitites in the Kylylahti serpentinite massif

in the Outokumpu area. This could be taken as an indication of similar origin and tectonic affinity of the Jormua and Kylylahti massifs. An interesting comparison would be between the primary melt inclusions in the Jormua and Kylylahti chromites, but such have not yet been reported from the latter, although they are rich in (altered) inclusions.

Stop 2.8. Sarvikangas: gabbros, ferrogabbros and plagiogranites

Stop 2.8 is included to present the more evolved gabbros, diorites and associated plagiogranites (leucotonalites-thronjemitites) of the JOC. This stop involves about 1 km walking in a partly bushy forest.

The eastern part of the Sarvikangas area comprises a 300 m wide zone of metadolerite-basalt dyke-in-dyke lithology with some 20-50 % screens of coarse-grained gabbro and sporadic serpentinite. The dyke zone is in the east in sharp contact to serpentinite and in the west to a body of Fe-gabbros with inclusions of sheeted dykes and serpentinite. Although the dyke unit is in contact against mainly serpentinite and Fe-gabbros, the interdyke gabbro screens are mostly of Mg-gabbros both in their outcrop appearance and chemical composition similar to the Mg-gabbros at Stop 5 at Kivisuo. The “cumulate” nature of the gabbros in the screens is evident, as incompatible elements such as Ti and Zr are present in concentrations much lower than in the splitting dolerite-basalt dykes or in the Jormua lavas and dykes in general. Also compatible elements such as Cr and Ni are in most samples present in significantly lower concentrations than is typical of the JOC main suite lavas and dykes.

The western part of the Sarvikangas area, which will be our target, comprises a 100-400 m wide, about 1.5 km long body of dominantly Fe-gabbro with a 150-200 m patch of more evolved, dioritic to thronjemitic (plagiogranitic) rocks at its northern end. The latter are in a sharp contact against an about 400 m to 1 km body of mainly Mg-gabbro further in the north. In the west the Sarvikangas Fe-gabbro is in sharp, presumably faulted contact against the 100-300 m wide and at least 3 km long Korteperä slice consisting mostly of pillow lavas. The Sarvikangas Fe-gabbro encloses a 50 x 100 m inclusion of sheeted dykes in its middle part, and there is a 50-100 m wide, 700 m long tongue of serpentinite between the Fe-gabbro body and the sheeted dyke unit to the east of it. The Fe-gabbro has clear intrusive contact against this serpentinite.

The Fe-gabbro is mainly of varied textured nature, the grain size is ranging irregularly from fine grained to pegmatitic. Metamorphic re-equilibration has been almost thorough. Primary pyroxene, presumably augite has been converted to hornblende and plagioclase to granoblastic mass of oligoclase-andesine. The Sarvikangas gabbros do not contain any magnetite but the dominant oxide phase is ilmenite altered variably to sphene and rutile. Some samples comprise brown amphibole interstitial and marginal to large uralite pseudomorphs of clinopyroxene. The ilmenite and brown amphibole are the only obviously primary major phases preserved in these gabbros.

Some of the best outcrops of the plagiogranites are presently in rather poor condition because of extensive lichen cover developed during the years after their stripping from the moss. Nevertheless, the excursion outcrops (around coordinate point Northing:7140305; Easting 3547338) will show a plethora of dioritic to leucotonalitic segregations and dykes and their immediate host rocks: Fe gabbros, Fe-diorites and diorites. The type of plagiogranite occurrence varies from solitary, sharply bound dykes (<5 cm-6 m thick) to irregular networks of cm to dm thick, branching and cross-cutting dykes. Although most of the plagiogranite seems to occur in sharply cross-cutting dykes and dyke networks, there are several outcrops in which

there are evidence for coeval emplacement of gabbroic-dioritic and granitic magmas and their mingling. In some outcrops main suite basalt dykes are seen to cross-cut sharply the diorites-plagiogranites.

The Sarvikangas Fe-gabbros are very rich in iron (FeO_T 14-20 wt.%) and titanium (TiO_2 2.6-6.8 wt.%), as is typical of gabbros produced by extreme tholeiitic fractionation. Emphazing their evolved nature, compared to the Mg-gabbros, the Fe-gabbros are a significantly higher also in REE-Y, Zr and Nb. The plagiogranitic rocks range 56-73 wt.% in SiO_2 , are distinctly rich in Na_2O (5.4-7.4 wt.%) but very poor in K_2O (<0.27 wt.%) and Rb as is typical of modern ocean ridge granites. Chondrite-normalized REE patterns are slightly fractionated at a relatively high level of REE and show negative Eu anomalies (Fig. 11). Ga, Nb, Y and Zr concentrations are high, and consequently the granitic samples plot as A-type on the discriminant diagrams of Whalen et al. (1987) and in the within-plate granite field in the Nb vs. Y discrimination diagram of Pearce et al. (1984).

Zircon from one several metres thick leucotonalite dyke (Northing: 7140321; Easting: 3547392) yields a somewhat imprecise U-Pb age of 1.954 ± 0.12 Ga. $\epsilon_{\text{Nd}}(1.95 \text{ Ga})$ obtained for this same sample is +1.6, which is close to the average $\epsilon_{\text{Nd}}(1.95 \text{ Ga})$ of +2 yielded by samples from the main suite lavas and dykes.

Stop 2.9. Kylmä: pillow lavas

The stop 2.9 is to visit the best exposed occurrence of pillow lavas of the JOC. The outcrops examined at the Kylmä stop (around Northing: 7140440; Easting: 3549265) are located near to a privately maintained road going to summer houses and cottages situated along the strand of the nearby Pitkänperä bay of the Oulunjärvi Lake. A note for casual visitors of the JOC, and who is maybe using this excursion guide: In principle, for legit car riding on this local road, a permission is needed from the organ of the local people maintaining the road. You may walk on the road freely, however.

Most of the extrusive metavolcanic rocks of the JOC occur within the Antinmäki block, in three up to 400 m thick and 2-3 km long fault-bound tectonic slices. The about 2 km long and up to 400 m thick Kylmä slice is the second largest and best exposed of these slices. The Kylmä slice has its upper (SW) contact against a narrow slice of serpentinites and talc-carbonate rocks (Matokallio slice), and its footwall (NE) contact against a several hundreds metres thick nappe slice of upper Kalevian black schists and metagraywackes.

Most of the outcrops in the Kylmä sheet show metres thick pillow lava flows topped/intercalated with thin, discontinuous layers of pillow and hyaloclastite breccia. Some of the thicker flows show massive lower parts. In its footwall part of the Kylmä sheet is intruded by a about 20 m thick gabbro-pyroxenite sill that can be traced for some 200 m. In this environment there are also metadolerite-basalt dykes cutting the pillow lavas. Although carefully sought for during the fieldwork, no examples of even thin intercalations of any terrigenous sedimentary material have been yet found in the Kylmä or other JOC lava occurrences. Nor are there observations for interbeds of any sort of chemically precipitated sediments.

The pillow lavas in the Kylmä sliver are least strained in sections perpendicular to the tectonic elongation plunging 40-60 degrees towards SW. In such outcrop sections the primary lava structures are often remarkably well preserved. The pillows in the Kylmä outcrops are usually rather tightly packed but yet with some variable component of interpillow hyaloclastic breccia. Originally probably microcrystalline to classy chill margins are typical of most of the

well preserved pillows. The pillows are mostly nearly non-vesicular, suggesting extrusion depth of 1 km at least. In some flows there are many pillows that seem to have been gas-charged/gas-channels for their core parts, however.

The Kylmä lavas are of clear EMORB like basalt origin as the JOC sheeted dykes and lavas in general (above). Although the JOC basalts in general have preserved their original chemical compositions rather well, there are deviations to this pattern. The Kylmä lavas e.g. register sporadic depletion in LREE and related disturbance in Sm-Nd isotope systematics. Most of this alteration seems to be related with infiltration of CO₂-rich metamorphic fluids that caused talc-carbonate alteration in the nearby mantle peridotites. Sm-Nd isotope data suggest this alteration took place at a relatively late stage of the Svecofennian metamorphism, after 1.8 Ga (Peltonen et al., 1996).

Chill margins of the pillows have been sampled and studied by Furnes et al. (2005) for evidence of microbially-mediated alteration. Although textural evidence for microbial alteration in the JOC basalt chill margins is destroyed by their lower amphibolite facies regional metamorphism, robust biosignature was found in the generally depleted $\delta^{13}\text{C}$ values of disseminated carbonate extracted from the originally glassy pillow fringes, relative to crystalline samples. The same distribution of $\delta^{13}\text{C}$ values is well documented in samples of recent oceanic crust as well as Phanerozoic ophiolites, and is commonly interpreted to result from microbe-induced fractionation during oxidation of organic matter. Thus it seems likely that microbes were colonizing the JOC basalts subsequent their eruptions, and were utilizing the class in the pillow chill margins in their metabolism.

Stop 2.10. Hollihaka: Upper Kaleva metaturbidites

The rocks seen at Stop 2.10 are not rocks of the JOC proper but yet are of crucial importance for speculations of its tectonic origin. After all, Upper Kaleva metaturbidites as in the Hollihaka outcrop make over 90 % of the Jormua-Outokumpu Allochthon. The Hollihaka outcrop (Northing: 7139225; Easting: 3550955) may not be the most spectacular example of the UK metaturbidites, but nevertheless one at an easy to reach place to have a discussion on the Upper Kaleva and its tectonic messages.

The Hollihaka turbidite is relatively fine-grained, thinly bedded variant of the Upper Kaleva metaturbidites that usually are medium to fine-grained, medium-bedded. There are no chemical data available for the Hollihaka metaturbidites but in general the Upper Kaleva turbidites are very homogenous for their whole rock and isotope compositions as well as detrital zircon grain age populations. The chemical variation from outcrop to regional scale is largely a function of hydraulic sorting (Kontinen and Sorjonen-Ward, 1991; Lahtinen, 2000). Claesson et al. (1993) have published data that indicate the major part of the detrital zircon grains (60 %) in the UK turbidites were 1.98-1.92 Ga Proterozoic and 2.8-2.7 Ga Archean grains (30 %), and that up to this there were only a minor population of grains with ages in the 2.5-2.0 Ga range.

It is clear that the large volume of very well mixed but clearly multisource Kaleva turbidites must have been deposited in a large scale basin that received its material from voluminous, already well mixed middle store reservoirs (most probably large deltaic complexes at mouths of very large river systems). This points to a continental margin environment. Furthermore, morphological characters of the zircon grains (fairly coarse, distinctly oscillatory zoned, unrounded) combined with whole rock Sm-Nd data imply that this source must have comprised a large component of dominantly juvenile felsic-intermediate plutonic rocks. Thus the evi-

dence on the depositional setting of the Upper Kaleva is pointing to a passive margin of rather narrow continent with an orogenic magmatic zone in its hinterlands, that is, to something like the eastern, trailing edge of the present South American continent.

One enigmatic point with the Upper Kaleva is the question about where did the dominant 1.98-1.92 Ga zircon grains/material come from? As pointed above, morphological characters of the zircon grains combined with whole rock Sm-Nd data imply this source comprised mainly juvenile felsic-intermediate plutonic rocks. There are currently only guesses about location of this critical source component, maybe it was in the Lapland-Kola granulite belt as proposed by Kontinen and Sorjonen-Ward (1991) or maybe in the Ukrainian Shield where plutonic-volcanic rocks about suitable age and isotopic juvenility are known to be present (e.g. Claesson et al., 2001). The Svecofennian domain is a poor candidate as it seems to comprise only very minor volumes of suitable 1.98-1.92 Ga old plutonic rocks.

Day 3, Wednesday 30.7. 2008

Wake-up at 7:00 am, breakfast, start at 8:00 am. Across the Finnish-Russian border at Suoperä, drive to Gridina (c. 300 km, Pjaozerskii, Kestenga, Louhi, Gridino), roadside geology stops of Archean geology of the Karelian Craton: e.g. sanukitoids of Northern Karelian batholith. Arrival to Gridino at the White Sea coast in the late afternoon, overnight in a field camp (tents and sleeping bags provided).

North Karelian dioritic-plagiogranitic (sanukitoid) massif in the Central Karelian Terrain of the Karelian Craton

A.I. Slabunov¹, A.V. Samsonov² and A.A. Shchipansky³

¹*Institute of Geology, Karelian Research Centre, RAS (Petrozavodsk)*

²*Institute of Ore Geology, Petrography, Mineralogy and Geochemistry (IGEM), RAS (Moscow)*

³*Geological Institute (GIN), RAS (Moscow)*

The goal of the Day 3 is to see the largest sanukitoid massif in the Archean Karelian craton. Sanukitoids are quite common in the Central Karelian terrain, which is the youngest terrain in the Neoproterozoic Karelian craton (Slabunov et al., 2006). The North Karelian Tavajärvi or Pjozero dioritic-plagiogranitic (sanukitoid) massif (Bibikova et al., 1997; Konshin, 1995; Larionova et al., 2007) is the largest massif of this type in the region. It is located in the northern part of the terrain, in close proximity to the North Karelian system of greenstone belts of the Belomorian province (Fig. 3.1) The North Karelian massif (batholith) covers an area of ca. 5000 km²; in plan view, it has the shape of an ellipse split into blocks. Its long axis, oriented near-E-W, is about 120 km in size, and its short axis is ca. 85 km (Fig. 3.1).

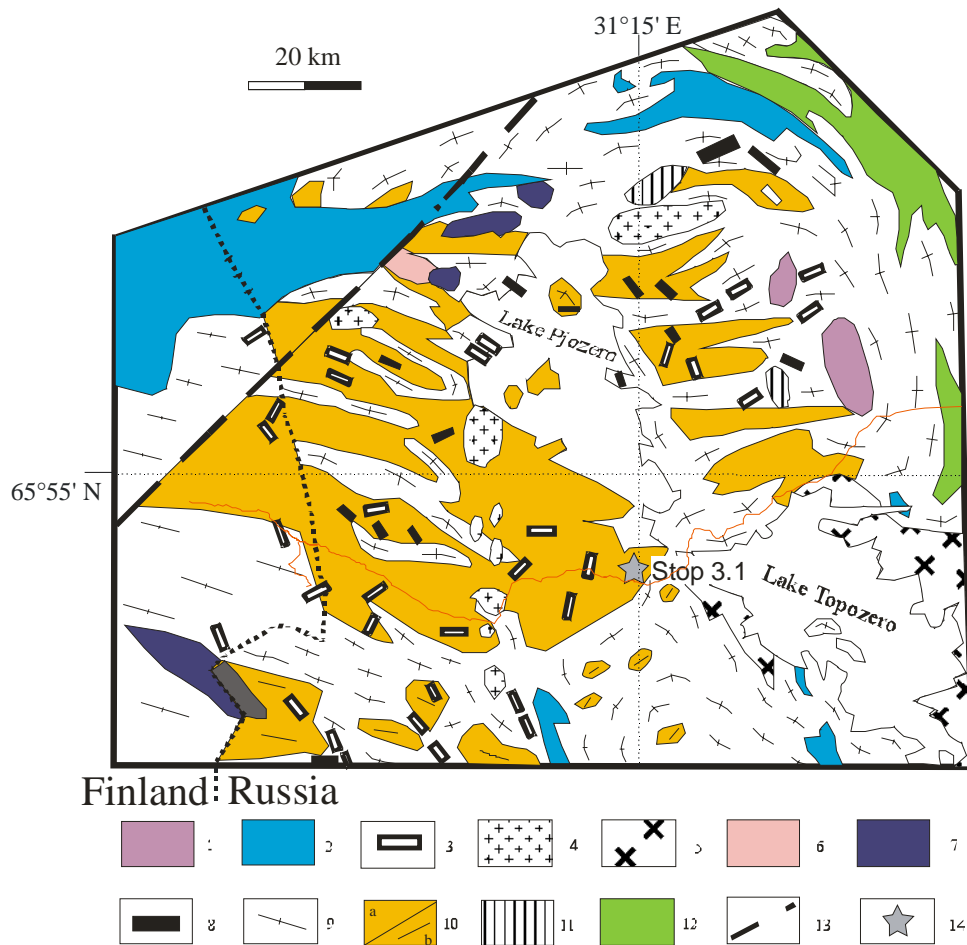


Figure 3.1. Scheme showing the geological structure of the North Karelian dioritic-plagiogranitic massif in the Lake Pyaozero area, North Karelia (Bibikova et al., 1997 with supplements). 1 = Elet'ozero alkaline complex (1.7–1.8 Ga); 2 = Paleoproterozoic (2.5–1.92 Ga) sedimentary and volcanogenic rocks; 3 = gabbro-diabase dykes (2.1–2 Ga); 4 = Nuorunen-type microcline granites (2.45 Ga); 5 = Topozero-type intrusive charnockites and metacharnockites (ca. 2.45 Ga); 6 = granophyres; 7 = Olanga Group layered intrusions (2.44–2.36 Ga); 8 = gabbro-diorite dykes (2.446 Ga); 9 = Neoproterozoic plagiomicrocline gneissose granites; 10 = Neoproterozoic (2.72 Ga) diorites, quartz diorites, granodiorites and plagiogranites: a) massive and moderately gneissose and b) highly gneissose; 11 = Kundozero-type subalkaline gabbro-diorites; 12 = Meso- and Neoproterozoic greenstone complexes; 13 = Sokolozero fault zone; 14 = stop

Furthermore, south of its main distribution area some bodies, 4–20 km in size, similar in composition but more intensely gneissose, have been encountered over a distance of about 40 km, and similar diorites occur northwards in a basement scarp in Paleoproterozoic rocks of the Pana-Kuolajärvi structure and at its northern flank. Rocks, older than the diorite-plagiogranites of the batholith, have preserved in it as xenoliths. These amphibolites, schists and metaultrabasic rocks are similar in composition to volcanics of greenstone belts (Slabunov & Stepanov, 1993). In addition, the batholith shows structures, unique for the Archean, that are extremely similar to mingling-structures in Phanerozoic orogenic systems. This proves that mantle (basic) and crustal (monzonitic and granomonzonitic) magmas intruded and mixed mechanically almost simultaneously. It should be noted that in two-dimensional cavities of exposures mingling-structures look like an abundance of pillow-like basic xenoliths in monzogranitoids (Fig. 3.2), whereas in three-dimensional exposures one can clearly see evidence for the dyke intrusion of both basic rocks and granitoids. Mingling-structures are often understood as an indicator of orogenic collapse (e.g. Weibe, 1973; Vogel & Wilband, 1978; Snyder et al., 1997).



Figure 3.2. Pillow-like metabasite bodies within the sanukitoids of the North Karelian batholith. Western shore of Lake Pyaozero. (by A.A. Shchipansky)

The batholith is cut by bodies of Neoproterozoic plagiomicrocline granites. Granitoids of the same type rim the batholith on the south, west and east. The northern flank of the batholith is truncated by the Proterozoic Pana-Kuolajärvi structure. There are not found contact sanukitoids with host rocks. Neoproterozoic granitoids (Buiko et al., 1995) and paleoproterozoic dykes of at least three generations cut the massif (Stepanov, 1994; Mertanen et al., 1999; Vuollo et al., 1996).

The North Karelian sanukitoid massif (batholith) was formed in Neoproterozoic time. The U-Pb age of zircon from these rocks is 2724.4 ± 7.8 Ma and shows the time of a magmatic stage in massif formation, whereas the age of sphene, 2700 Ma, shows the time of late magmatic processes in it (Bibikova et al., 1997). Sm-Nd isotopic data (Bibikova et al., 1999; Larionova et al., 2006; Slabunov et al., 2000), obtained for massif rocks ($\epsilon_{Nd}(2,7) = +1.24$ to $+2.2$), suggest that the crustal prehistory of the rocks was not long. It should be noted that the Sm-Nd isochrone for massif rocks agrees with the line 2725 Ma (Larionova et al., 2006). The fairly approximate U-Pb age of zircons from the plagiomicrocline granites that cut the diorite-plagiogranites of the batholith is 2702 ± 84 Ma (Buiko et al., 1995).

Table 3.1. Composition of rocks The North Karelian sanukitoid massif (batholith). ** - Bibikova et al., 1997; Larionova et al., 2007

Rock type	Q diorite	Q diorite	diorite	gabbro	granodiorite	trondhjemite	syenite	syenite	lamprophire
Sample	2421/1**	K-41-1*	1020/1	PY-703/5*	K-44-5*	B-254	K-27*	K-32-1*	K-41-2*
Stop	Stop 3.1								
SiO ₂	61.30	63.30	56.87	48.40	66.11	69.99	57.81	54.29	57.35
TiO ₂	0.52	0.57	0.66	1.37	0.51	0.34	0.81	0.83	0.90
Al ₂ O ₃	16.22	16.05	17.10	16.82	15.39	14.42	18.08	17.85	18.11
Fe ₂ O ₃	6.01	5.42	7.33	11.46	4.86	3.29	6.01	8.43	7.20
MnO	0.11	0.15	0.11	0.17	0.14	0.03	0.16	0.17	0.15
MgO	2.88	2.94	3.76	6.34	2.40	0.98	2.31	4.48	2.59
CaO	4.58	4.16	5.16	8.34	3.96	3.18	4.71	7.00	4.76
Na ₂ O	4.96	4.30	4.79	3.83	3.97	3.92	5.98	4.63	4.95
K ₂ O	1.60	2.89	2.38	2.58	2.46	2.26	3.53	1.94	3.30
P ₂ O ₅	0.23	0.21	0.40	0.69	0.19	0.11	0.59	0.37	0.69
LOI	1.04	99.95	1.26	99.99	99.94	0.38	99.98	99.94	99.95
Mg #	48.69	51.79	50.39	52.28	49.44	37.10	43.22	51.28	41.60
Cr	152	113	134	105	108	260	23	92	31
Ni	64	54	25	60	47	14	24	47	21
Co	17	16	20	33	14	8	13	25	15
V	90	102	124	171	93	37	78	148	93
Cu	39	11	15	18	3	7	27	40	24
Pb	9	15	4	6	13	19	22	9	19
Zn	132	74	73	117	66	44	102	91	96
W	0.51	0.27	0.81	0.06	0.23	0.31	0.25	0.26	0.40
Mo	1.26	0.57	0.41	0.35	0.48	0.55	0.61	0.58	0.30
Rb	46	116	66	68	92	81	86	52	87
Ba	872	989	1079	1330	1278	554	1484	721	1613
Sr	861	701	856	1185	693	193	1318	1057	933
Ta	0.20	0.41	0.41	0.02	0.25	0.12	0.61	0.54	0.70
Nb	3.5	8.1	4.8	1.6	4.7	4.6	12.7	10.7	16.4
Hf	3.98	4.56	3.85	3.45	4.97	6.52	3.47	4.78	7.89
Zr	162	180	154	146	199	240	145	191	379
Y	9	17	13	24	13	6	12	21	18
Th	1.60	4.44	4.38	1.71	6.69	36.99	4.10	3.92	13.83
U	0.44	1.00	0.80	0.29	0.67	0.91	1.01	1.47	2.27
La	15.95	34.67	32.09	87.44	42.14	35.25	60.90	50.58	85.30
Ce	37.71	72.73	74.15	212.90	78.28	66.13	140.50	111.00	200.10
Pr	5.00	9.11	9.05	26.34	8.74	5.49	16.38	13.28	23.79
Nd	21.22	34.82	35.98	99.81	32.13	16.99	60.50	49.77	90.51
Sm	3.98	5.92	6.23	14.69	5.26	2.69	9.02	8.28	13.90
Eu	1.27	1.20	1.78	3.28	1.25	0.84	2.37	2.18	3.35
Gd	3.15	4.26	4.76	8.41	3.70	2.05	5.05	5.43	7.89
Tb	0.35	0.54	0.55	1.01	0.45	0.28	0.58	0.69	0.86
Dy	2.10	2.84	2.62	4.73	2.28	1.16	2.61	3.50	3.69
Ho	0.33	0.55	0.51	0.83	0.42	0.23	0.44	0.68	0.59
Er	0.84	1.49	1.34	1.98	1.12	0.54	1.10	1.83	1.43
Tm	0.12	0.22	0.17	0.27	0.16	0.07	0.15	0.26	0.18
Yb	0.84	1.43	1.03	1.55	0.97	0.41	0.88	1.77	1.05
Lu	0.12	0.22	0.15	0.22	0.16	0.08	0.13	0.27	0.16

The main rock types that make up the batholith are quartz diorites, diorites, granodiorites and plagiogranites; syenites and subalkaline gabbroids are less abundant (Bibikova et al., 1997; Larionova et al., 2007; Stepanov, 1994). The petrographic characteristics of these rocks are described in detail by Konshin (1990, 1994) and Stepanov (1994) and isotopic-geochemical characteristics by Bibikova et al. (1997) and Larionova et al. (2007).

Slightly altered varieties have a massive structure and a hypidiomorphic-granular texture, often with coarse (up to 2 cm) idiomorphic plagioclase grains. Blastocataclastic structures are also common. In satellite blocks south of the main body of the batholite, rocks of the complex are represented by lepidonematoblastic-structured gneisses.

The main mineral phases of the rocks are plagioclase that varies in composition from 60% An to 5–10% An, quartz which is present in varieties more felsic than diorite and K-feldspar. Dark-coloured minerals are usually represented by biotite and epidote, orthopyroxene and diopside being less common. Apatite, sphene and zircon are present as accessories and ore minerals are represented by magnetite and sulphides (Konshin, 1994).

The rocks of the batholith vary in composition from gabbroids to leucogranites, although quartz diorites and granodiorites dominate. On binary variation diagrams one can clearly see that the rocks of the massif form a continuous sequence of compositions from gabbro to granites. They are more basic than rocks of the TTG- association and are richer in MgO, CaO, Ni, Cr and Sr. Diorites of the massif typically have a high Mg content, high percentages of Cr, Ni, Co, alkalies, Ba, Sr, LREE and P and low percentages of Ti and Nb (Bibikova et al., 1997; Larionova et al. 2007). They also display highly fractionated REE spectra ((La/Yb)_N – 18-44). The compositions of syenites, lamprophyres and gabbroids of the massif are shown in Table 3.1.

They are comparable in petrogeochemical characteristics to Archean sanukitoid series rocks from the Superior Province, Canadian Shield (Shirey & Hanson, 1984; Stern, Hanson, 1991; Stern et al., 1989), the Pilbara craton on the West Australian Shield (Smithies & Champion, 2000) and other parts of the Karelian craton, where two different-aged (2740 and 2710 Ma, respectively) groups of these rocks were identified (Petrova et al., 2003; Samsonov et al., 2001; Chekulaev, 1996; Bibikova et al., 2003; Halla, 2000; Käpyaho et al., 2006; Lobach-Zhuchenko et al., 2003; Samsonov et al., 2003). Like those on other cratons, they postdate the most common rocks of the TTG-association. The North Karelian sanukitoid massif is the largest intrusive of this series on the Karelian craton.

Stop 3.1: Lake Tungzero

Massive and gneissic quartz diorites with porphyries of plagioclase. The age of the massif was estimated at 2720 Ma. The quartz diorites are cut by metagabbro dykes and consist of inclusions of basic rocks. The quartz diorites and metagabbro correspond in petrochemical characteristics to sanukitoid-series rocks (Table 3.1).

Day 4, Thursday 31.7. 2008

Wake-up at 7:30, breakfast, start boat trip approximately at 8:30 (depending on weather). Visit islands in Gridino area, Archean eclogites as part of metamorphosed melange, Proterozoic mafic dikes, eclogitisation processes.

Lunch in the island. Return to Gridino at 3 p.m. and start driving to Louhi (80 km), arrival to Louhi at 8 p.m., dinner and overnight at hotel.

Archean eclogites and Paleoproterozoic eclogitized gabbroids, Gridino area, White Sea

A.I. Slabunov, O.I. Volodichev, A.V. Stepanova, O.S. Sibelev, V.S. Stepanov, I.I. Babarina

The Neoproterozoic eclogite-bearing complex (Volodichev et al., 2004) to be visited is located in the eastern Belomorian province (Fig. 4.1 A). It forms a tectonic slice which dips gently ENE (Slabunov et al., 2006). Its outcrops are now known as the Gridino zone which is ca. 50 km long and 6–7 km wide (Fig. 4.1.B).

The complex is correlatable texturally with highly migmatized and deformed mélangé - metamélangé. It consists of a groundmass (metamatrix) and fragments. The groundmass of the metamélangé is made up of variably migmatized gneisses, gneissose granites and metaenderbites (Sibelev et al., 2004). The former are probably the early highly reworked matrix of mélangé formed by destruction of all the rocks that make up a fragments. The gneissose granites and metaenderbites were formed at later stages in the evolution of the complex and could have been produced by melting of its rocks. The fragmental component of the mélangé is formed by numerous unevenly distributed lenticular and less common irregular-shaped bodies. The fragments vary in size from tens of centimeters across to tens of metres (Slabunov et al., 2007b). The concentration of fragments in the Gridino complex also varies considerably, making up locally 25–30% of its total volume. Special studies have shown that fragments in the Gridino mélangé are distributed unevenly: lens-shaped NW-trending, ca. 200-300 m thick fragments -enriched bodies were identified (Fig. 4.1 C). The compositions of the fragments are diverse, but mafic rocks, such as variably altered eclogites, garnet-, garnet-clinopyroxene and feldspathic amphibolites and metamorphosed gabbroids, predominate. Furthermore, fragments, composed of metaultramafics, zoisitic and amphibole-zoisitic blastoliths, kyanite-garnet-biotite gneisses are encountered. A great variety of rocks in the fragments that differ in composition, degree of deformation and metamorphic grade provides a strong argument in favour of the assumption that eclogite-bearing complex is a metamélangé formed in the subduction zone.

Eclogites are a rare but very important constituent of a metamélangé. Six sites, where Archean eclogites occur, were located and studied in the Gridino tectonic slab. In spite of considerable multiple alterations, the eclogites have retained zones of bimineral garnet-omphacite composition and an equigranular structure with homogeneous, nonzonal minerals that contain practically no inclusions. Here, omphacite contains 27 to 31% jadeite (average 30%; Volodichev et al., 2004). Garnet is relatively poor in pyrope (20–22% Prp), but is rich in Ca (28–31% Grs). A typical and dominant accessory mineral is rutile. Eclogite was generated at a pressure of 14–17.5 kbar and at a temperature of 740–865° C (Volodichev et al., 2004).

The U-Pb zircon age of eclogite is estimated as Neoproterozoic, 2720 ± 8 Ma (Volodichev et al., 2004). Based on geological and geochronological data (Table 4.1) the upper age limit of eclogite-bearing mixite was estimated accurately: it is not younger than plagiogranites, whose postkinematic vein cuts it on Stolbikha Island. Accessory zircon from the vein is dated at 2701.3 ± 8.1 Ma (Volodichev et al., 2004).

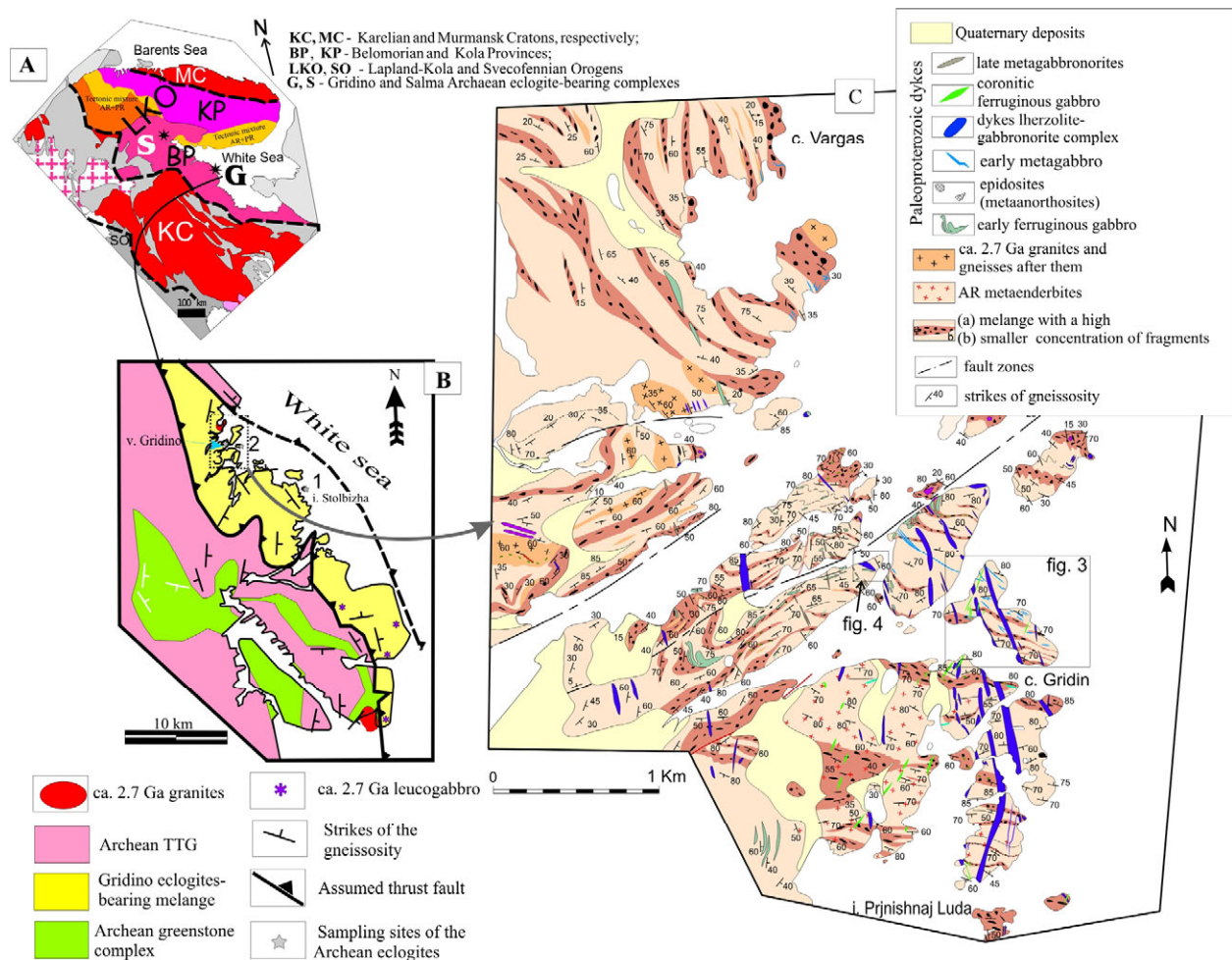


Fig. 4.1. Tectonic scheme of the eastern Fennoscandian shield (Slabunov et al., 2006) (A); Distribution of the eclogite-bearing complex in the Gridino area (Slabunov, 2005) (B); Geological map of the Cape Vargas-i. Prynishnaya Luda area, White Sea (Slabunov et al., 2007a).

The eclogites from the Belomorian mobile belt are the world's first well-proven finding of Neoproterozoic crustal eclogites (Volodichev et al., 2004). Eclogites and their weakly amphibolitized varieties correspond compositionally (Table 4.1) to tholeiite-series mafic rocks, and most of them are considered to be MgO-rich tholeiites. The REE content of Neoproterozoic eclogites is chiefly 2–12 times that of chondrites, and their distribution spectrum is either “flat” or poorly differentiated ($LaN/SmN = 0.99–1.8$; $GdN/YbN = 0.77–1.17$). Unlike mid-oceanic ridge basalts (MORB), they are slightly enriched in HREE and HFSE (Zr, Hf, Y and Ti), but have the same Nb concentration. Compositionally similar tholeiites occur commonly among oceanic-plateau mafic rocks; they have also been encountered among oceanic basic rocks in the Central Belomorian greenstone belt.

Eclogites, formed 2720 Ma ago at pressures of 14.0–17.5 kbar (i.e. at depths of up to 60–65 km) and temperatures of 740–865°C, suggest that in Neoproterozoic time crustal rocks were subducted and then exhumed from considerable depths. Eclogites are part of the clastic constituent of Neoproterozoic migmatized mixtite (mélange). The latter makes up the tectonic slice.

Table 4.1. Chemical composition of rocks from the Neoproterozoic eclogite-bearing complex, Stolbikha Island .

rock type	eclogites			trond-hjemite	meta-pyroxenite	zoisitite*	plagiogneissose granite			amphibolite
<i>m\samp</i>	1\2913-11	2\2913-12	3\2913-5	4\2913-6	5\2913-7	6\2913-20	7\2913-10	8\St-126	9\St-136	10\St110
stop	4/1.1	4/1.1	4/1.1	4/1.2	4/1.2	4/1.3	4/1.2	4/1.1	4/1.4	4/1.4
SiO ₂	50.30	49.02	49.93	72.62	52.40	39.56	69.28	61.24	64.02	49.12
TiO ₂	0.93	0.51	0.97	0.29	0.32	0.74	0.36	0.69	0.47	0.68
Al ₂ O ₃	15.64	12.25	14.60	14.50	6.10	31.51	15.23	15.05	15.45	15.27
Fe ₂ O ₃	2.97	3.11	2.45	0.72	2.78	2.69	0.65	2.49	1.75	3.21
FeO	7.18	7.61	8.22	1.58	5.89	0.50	2.15	4.17	3.74	7.18
MnO	0.206	0.200	0.178	0.03	0.21	0.03	0.04	0.10	0.08	0.17
MgO	6.55	9.83	7.81	1.04	12.29	0.21	1.64	4.32	3.08	9.77
CaO	12.24	13.38	11.08	2.98	16.09	22.78	3.41	4.86	4.58	10.08
Na ₂ O	2.33	2.93	2.83	4.15	1.23	0.39	4.59	3.66	3.64	2.36
K ₂ O	0.37	0.05	0.49	1.19	1.02	0.20	1.55	1.46	1.68	0.16
P ₂ O ₅	0.11	0.08	0.07	0.08	0.06	0.10	-	0.09	0.13	0.12
H ₂ O	0.16	0.30	0.15	0.11	0.38	0.01	0.06	0.10	0.06	0.10
Loi	0.81	0.54	1.10	0.54	0.88	1.38	1.02	1.46	1.12	1.34
Cr	452	1383	405	90	93	72	46	150	144	509
Ni	293	266	95	18	32	7	32	29	21	50
Co	64	64	38	4	30	2	9	33	23	64
V	296	241	263	20	169	74	43	106	100	257
Cu	165	236	35	8	-	4	14	28	30	71
Pb	16	6	1	7	13	3	7	4	8	2
Zn	112	108	71	35	0	16	43	72	42	79
Rb	5	1	19	39	34	3	47	66	74	5
Ba	48	16	106	453	300	22	550	442	531	33
Sr	189	50	45	337	72	1267	338	315	440	74
Ta	0.69	0.32	0.27	0.27	-	1.94	0.22	1.96	0.46	7.68
Nb	10.0	4.8	4.4	4.5	3.0	6.0	4.9	7.8	5.2	5.9
Hf	1.26	0.75	1.10	3.16	-	1.12	8.75	1.99	2.35	1.04
Zr	42	23	39	123	30	35	356	72	80	28
Y	24	17	23	2	6	7	3	13	13	22
Th	0.26	1.17	0.26	2.13	-	2.55	4.19	3.70	6.82	1.04
U	0.37	0.50	0.12	0.13	-	0.19	0.22	0.16	1.62	0.26
La	4.01	4.15	2.17	18.52	-	29.79	30.99	15.94	27.42	6.16
Ce	10.52	11.47	5.77	36.90	-	50.90	55.86	39.32	56.40	14.00
Pr	1.54	1.65	0.85	3.60	-	4.96	5.38	4.83	6.56	2.00
Nd	7.50	7.39	4.28	12.08	-	16.28	16.69	19.09	24.65	8.60
Sm	2.45	2.18	1.34	1.67	-	2.24	1.87	4.22	4.41	2.38
Eu	0.85	0.63	0.43	0.46	-	1.08	0.56	0.97	1.18	0.83
Gd	3.10	2.48	1.92	0.95	-	1.88	0.97	3.25	2.84	2.60
Tb	0.56	0.43	0.42	0.11	-	0.25	0.11	0.44	0.47	0.50
Dy	3.74	2.76	3.33	0.48	-	1.32	0.45	2.53	2.64	3.35
Ho	0.82	0.57	0.78	0.08	-	0.26	0.09	0.48	0.47	0.75
Er	2.30	1.55	2.09	0.19	-	0.67	0.22	1.24	1.20	2.09
Tm	0.35	0.22	0.31	0.03	-	0.10	0.03	0.18	0.18	0.32
Yb	2.26	1.40	1.98	0.16	-	0.66	0.24	1.00	1.11	2.07
Lu	0.34	0.20	0.29	0.02	-	0.10	0.05	0.15	0.17	0.30

* percentages of elements in zoisitite from sample 2919-1 (island near Izbnya Luda Island).

Table 4.2. Paleoproterozoic gabbroids and eclogitized gabbroids from the Vorotnaya Luda Island (1-5) and Gridino area (6-9)

nn	1	2	3	4	5	6	7	8	9
Sample	C-2407-3	C-2407-20	C-2407-21	C-2407-41	C-2407-64	B-30	B-16/67	B-35	B-53
SiO ₂	51.02	50.50	49.13	50.44	48.83	48.1	48.7	48.08	47.74
TiO ₂	0.6	0.73	1.05	1.08	0.99	0.57	0.53	1.27	1.15
Al ₂ O ₃	10.56	11.60	14.20	10.39	14.66	8.82	12	14.9	15.25
Fe ₂ O ₃	3.26	1.20	4.30	2.54	3.4	1.1	2.46	3.3	2.56
FeO	8.76	9.33	8.74	10.49	9.76	9.4	7.8	11.25	10.9
MnO	0.18	0.238	0.240	0.18	0.22	0.19	0.17	0.23	0.21
MgO	14.48	13.66	7.50	9.83	7.32	20.9	15.3	7.22	7.46
CaO	8	8.40	11.00	9.25	11.02	8.22	8.98	9.53	9.52
Na ₂ O	1.68	2.00	2.24	2.95	1.96	1.2	1.85	2.22	2.67
K ₂ O	0.51	0.61	0.04	0.79	0.03	0.32	0.44	0.4	0.67
P ₂ O ₅	0.08	0.17	0.15	0.16	0.09	0.07	0.08	0.18	0.14
H ₂ O	0.17	0.16	0.26	0.15	0.05	0.07	0.31	0.13	0.21
Loi	0.75	1.04	1.19	1.43	1.14	0.93	1	1.09	1.46
Cr	1813	810	151	404	96	3913	1862	170	127
Ni	521	213	126	423	164	1627	850	217	126
Co	102	-	79	87	59	101	69	62	47
V	224	-	358	140	179	203	195	348	236
Rb	16	-	6	19	-	9	10	14	-
Cs	0	-	-	3.76	0.01	0.15	0.26	0.28	-
Ba	183	-	20	234	7	108	181	202	559
Sr	145	-	47	368	53	116	220	124	112
Ta	0.03	-	-	0.78	0.2	0.17	0.18	0.43	-
Nb	3	-	4	10.7	4.7	2.7	2.4	6.5	7
Hf	0	-	-	2.8	0.71	1.02	1.27	1.91	-
Zr	67	-	47	110	23	38	49	70	69
Y	13	-	17	17	21	12	15	34	28
Th	1.4	-	0.02	2.33	0.5	1	0.99	1.37	-
La	5.2	-	-	20.39	3.71	5.64	4.61	9	-
Ce	12	-	-	44.19	9.49	13.12	11.32	21.87	-
Pr	1.55	-	-	6.09	1.41	1.71	1.59	2.96	-
Nd	8	-	-	25.27	6.62	7.22	7.27	13.78	-
Sm	1.95	-	-	5.53	2.07	1.67	1.8	3.54	-
Eu	0.5	-	-	1.38	0.62	0.51	0.62	1.09	-
Gd	2.05	-	-	4.37	2.43	1.73	1.9	4.05	-
Tb	0.27	-	-	0.63	0.44	0.29	0.32	0.72	-
Dy	2.3	-	-	3.48	3.27	1.91	1.98	4.99	-
Ho	0.34	-	-	0.71	0.78	0.43	0.43	1.11	-
Er	1.25	-	-	1.85	2.48	1.21	1.2	3.35	-
Tm	0.14	-	-	0.27	0.39	0.17	0.18	0.52	-
Yb	1.18	-	-	1.69	2.51	1.14	1.1	3.27	-
Lu	0.15	-	-	0.25	0.39	0.18	0.16	0.49	-

1, 2 – olivine gabbronorites, 3 – tholeiitic dyke; 4 – early Mg-tholeiites, 5 – tholeiitic dyke, 6, 7- eclogitized gabbronorites 8, 9, 7 – eclogitized Fe-tholeiitic gabbro

Paleoproterozoic eclogitized gabbroids (Dokukina, Konilov, 2005; Kozlovsky, Apanovich, 2007; Travin, Kozlova, 2005; Volodichev, 1990) are associated with occurrences of a 2.45 Ga intrusive lherzolite-gabbro-norite complex common in BMB (Stepanov, 1981; 1990) and also known as a drusitic complex. Eclogitization in the complexes, seen as garnet-clinopyroxene associations in coronary structures, usually ceases at this stage. However, in some dykes, occurring in the Gridino area, different stages in its progressive evolution and even signs of regression in the form of scarce symplectites are observed. Like elsewhere in the region (Volodichev, 1990), eclogitization is autonomous in magmatic chambers that commonly have chill zones in undisturbed bedding and clearly occupy a cross-cutting position relative to the Archean eclogite-gneiss complex. In the dyke at the eastern end of Gridino there are two generations of eclogites: one was formed at the subsolidus-metamorphic stage transition (Gr_t48-49 - Om_p30-41, Gr_t48-51 - Om_p38-48 - corundum. T = 930-765 °C, P = 15-19 kbar) and the other at the metamorphic stage proper (Gr_t44-48 - Om_p19-24 - Opx, T = 785-715 °C, P = 12.5-14.0 kbar).

For isotopic dating of this group of eclogites zircons from kyanite-bearing eclogite-like rocks from Vysoky Island in Velikaya Bay of the White Sea were sampled. Accessory zircons were present in very small quantities. Their isotopic age was estimated by E.V. Bibikova at 2416.1±1.3 Ma. This age agrees with the age of the magmatic stage in the evolution of the rock (Slabunov et al., 2003). Data on the Nd-isotopy of eclogite-like rocks are in good agreement with the results of U-Pb dating. The Nd-systematics ($\epsilon_{\text{Nd}}(2400) = -1.8$, $t_{\text{DM}} = 2760$ Ma) of these eclogites shows that their protolith is contaminated by relatively old crustal matter. The same behavioral pattern of Nd isotopes is characteristic for Paleoproterozoic (2.43-2.45 Ga) gabbroids of the lherzolite-gabbro-norite complex (Lobach-Zhuchenko et al., 1993, 1998).

As mafic dykes near Gridino are abundant, the area was called the Gridino dyke field (Stepanov & Stepanova, 2006). Lherzolite-gabbro-norite dykes prevail (Stepanov, 1981). They are oriented dominantly NW and seem to be a fragment of a large dyke swarm. Furthermore, there are many dykes in the area that have different orientation and mineralogical composition. Direct geological correlations, established between dykes in some magmatic zones (Stepanov, 1990), and recent evidence suggest that there are at least seven mineralogical-age groups of dykes in the area that seem to differ in rank. Some are magmatic complexes that evolved on an areal scale in the BMB, others are interpreted tentatively as magmatic phases of the former or prototypes of new, poorly understood complexes.

Stop 4.1. S-SE part of Stolbikha Island (Fig. 4.3)

Stolbikha Island. This small (ca. 350 by 250 m) island (Fig. 4.2) with a well exposed shoreline is an excellent geological locality, where the complex internal structure of the mélangé (Fig. 4.3) and the formation and alteration of its rocks can be demonstrated. The eclogites found on Stolbikha Island (Volodichev, 1977, 1990; Volodichev et al., 2004, 2005) are well-preserved, which is a rare case. The area was mapped geologically in detail, and the structural, petrographic and geothermobarometric study of some rock varieties was carried out (Sibelev et al., 2004).



Fig. 4.2. The central part of Stolbikha Island (a) The low-tide outcrops in the SE part of Stolbikha Island (b)

At the observation point, visitors will see an basic rock inclusion (clast), 5 by 6 m in size, among highly gneissose and folded tonalite-trondhjemite-series amphibole-biotite orthogneisses and granitoids. Eclogites make up the eastern part of the clast; common in its western part are banded symplectitic amphibolitic eclogites and garnet-clinopyroxene amphibolites thrown into isoclinal folds. All the varieties are similar in chemical composition (Table 4.1, nn 1-3). In the southern part of the clast they are cut by a 20 cm thick pegmatite vein with a well-defined endocontact amphibolization zone. Zircons from symplectitic apoeclgites and from the monomineral omphacite fraction of eclogites were sampled from this exposure for radiological age determination. As a result, an Archean age of 2720 ± 8 Ma was obtained in both cases.

The least altered eclogites consist of garnet and omphacite (Gr_t22 Om_p27-31) with a small quantity of later minerals such as amphibole and plagioclase (Fig. 4.4). In transitional varieties, omphacite persists as patches, but in most cases symplectitic diopside-plagioclase intergrowths that mark a stage of transition to symplectitic apoeclgites are formed after it. Garnet, which occurs here as porphyroblastic grains with apatite, ore mineral, quartz and plagioclase inclusions, is also recrystallized. In some associations of symplectitic apoeclgites (Gr_t24-25 - Di₈ - Pl₂₄ and Gr_t28-33 - Di₆₋₉ - Pl₃₈₋₄₉) the composition of plagioclase is common for symplectitic eclogites of this area (24% An), in others it is abnormal (38-49% An). The latter have mafic plagioclase (85% An), which is a relic of a magmatically generated protolith.

Amphibole is formed in small quantities simultaneously with the formation of symplectites, chiefly at the stage, where symplectitic apoeclgites are altered to garnet-clinopyroxene amphibolites. The eclogitization stage took place at temperatures of 740-750 °C and a pressure of 14.2 kbar, and the retrograde alteration stage at temperatures of 710-750 °C and pressures of 8.5-10.5 kbar.

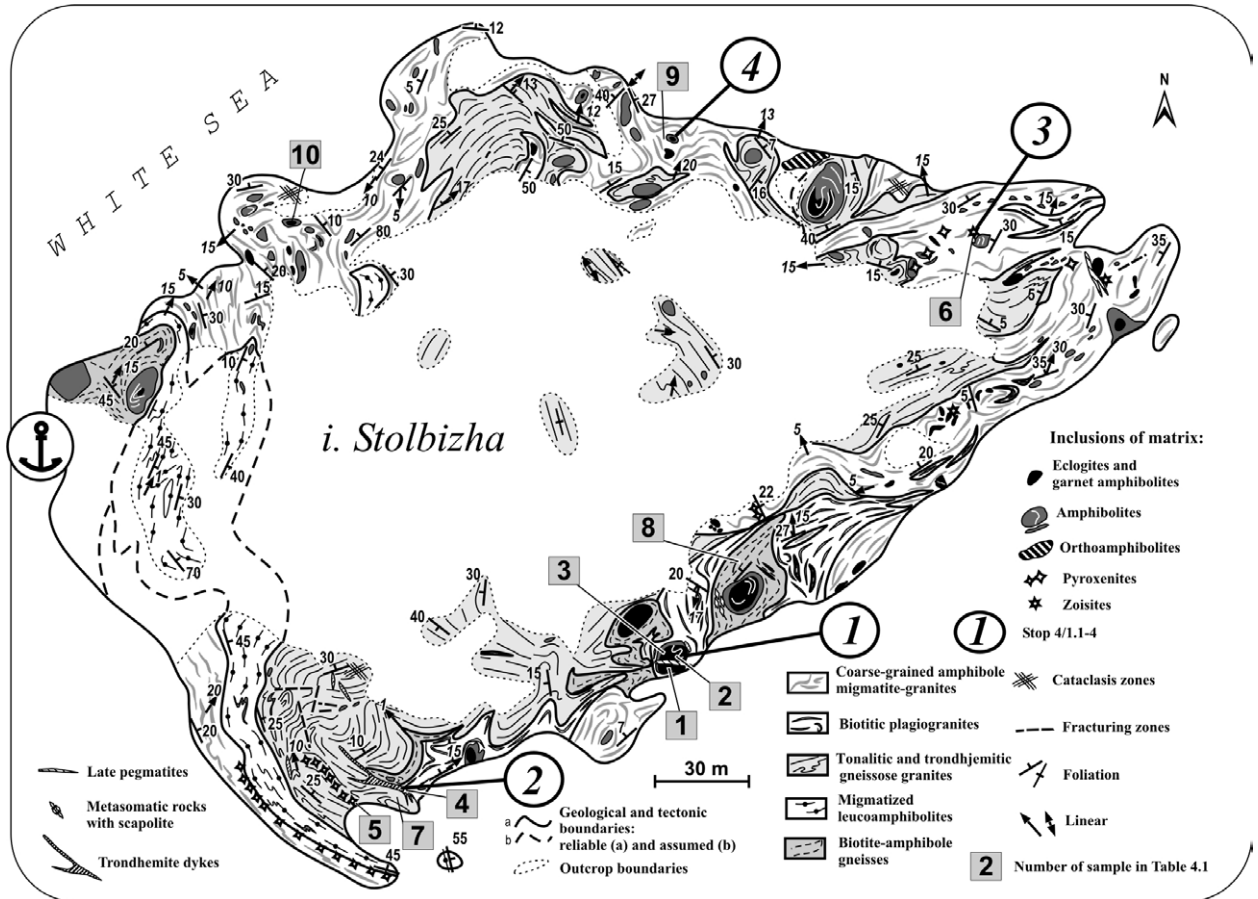


Fig. 4.3. Geological scheme of the eclogite-bearing complex on Stolbizha Island (Sibelev et al., 2004).

Stop 4.2. The S part of Stolbikha Island

A late kinematic ca. 1-1.5 m thick trondhjemite vein (Fig. 4.5; for chemical composition, see Table 4.1, nn 4), which cross-cuts gneissosity in gneissose granites (Ms + Bt + Pl + Qz) and amphibole-biotite granite-gneisses (Gt_{20.5-24.3} + Bt_{41.5-45.3} + Hbl_{1.7-1.8} ± Ksp + Pl_{26.6-32.0} + Qz) and contacts between them, was revealed here (Fig. 4.5). There are host rock inclusions in the vein. Its U-Pb zircon age is 2701.3±8.1 Ma (Volodichev et al., 2004).

Gneissose plagiogranites of the complex are homogeneous, poorly migmatized and poorly gneissose, dominantly fine-grained, granoblastic- and lepidogranoblastic-structured rocks. The mineral composition of the gneissose granites (Mu + Bt + Pl + Qz) is stable. Accessory minerals are represented by epidote, apatite, orthite and carbonates.

Where the rocks have no big inclusions, compressed flat-lying isoclinal folds, thrown, in turn, into open gently sloping folds, occur. The slopes of such folds are often disrupted. In the exposure south of the vein one can see that the contact between amphibole gneisses and plagiogranite-gneisses is subconcordant with gneissosity inside the body but exhibits a distinct shear pattern.

Encountered among mixtite inclusions are metapyroxenites (± Opx ± Gt + Cpx + Pl + Hbl, ± Bt, Cb, Table 4.1. nn 6) that make up chains restricted in space to the contacts of different type of gneisses.

Stop 4.3. NE part of Stolbizha Island

In this stop there is a small (ca. 0.3 by 0.5 m) zoisite inclusion in amphibole migmatite-granites. Zoisites are light, yellowish-green, medium- to coarse-grained, massive rocks. Major minerals are ± Qz + Pl + Zo; they occur occasionally together with secondary minerals such as Scp, Mu and Kfs. Accessories are represented by Sph. Zoisite grains (Ep, Czo), even within one thin section, differ markedly from each other in relief, shade of colour and birefringence, suggesting that their chemical compositions are variable. The chemical composition of the rocks is shown in Table 4.1. no 6.

Amphibole migmatite-granites that host the zoisite inclusion are banded, medium- to coarse-grained, inequigranular rocks showing granoblastic and partly glomeroblastic and reticulate structures. In outcrops, it is often hard to distinguish them from plagiogranite-gneisses because they pass gradually into each other, but their mineral composition and structural and textural characteristics are clearly different. In spite of their diverse appearance and structural and textural heterogeneities, migmatite-granites have a persistent mineral composition: Czo_{12.6-12.7} + Bt_{40.6-52.3} + Hbl_{2.1-2.3} + Pl_{23.5-28.7} + Qz, (± Cb, Ap, Hem, Ilm). Unlike other types of granitoids, common on the island, amphibole migmatite-granites contain no muscovite or microcline but host an abundance of large, well-developed epidote (Czo) grains, epidote acting here as a main mineral.

The PT-parameters of metamorphism of the amphibole migmatite-granite samples analysed, like those of other amphibole-bearing gneisses of the mélange matrix, are within high temperature amphibolite facies (T 650-770°C, P 7.4-8.2 kbar).

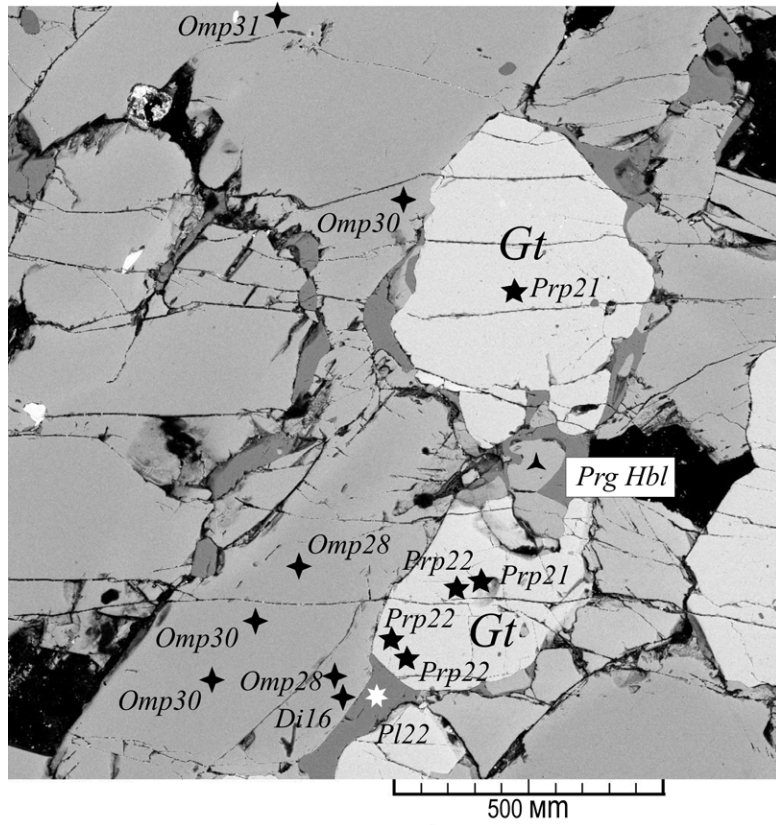


Fig. 4.4. A microphotograph of eclogite (Volodichev et al., 2004)



Fig. 4.5. 2.7 Ga trondhjemite vein, which cross-cuts gneissosity in metamelange

Stop 4.4. The northern part of Stolbizha Island

Visitors will see a series of metaeclogite and amphibolite inclusions that have their own internal structure, different from the matrix structure. The early planar elements of the inclusions form ductile flow structures – small (up to several metres in amplitude), irregular, asymmetrical and less common isoclinal folds, whose axial surfaces are sometimes discordant with each other, even within one inclusion. The metamorphic and migmatitic banding of the inclusions is either truncated by or is turned under the contact plane. The matrix structure adapts itself to the irregular-lenticular shape of disintegrated metaeclogitic rock bodies, forming centric (rotational) structures. Formed in the matrix are compressed isoclinal folds, whose axial planes and lineations, like the general structure, are curved concordantly with inclusion boundaries.

Vorotnaya Luda Island (Figs. 4.1 C, 4.6, 4.7). A Paleoproterozoic gabbroid dyke swarm that cuts an eclogite-bearing metamelange and eclogitized gabbronorite dykes of a lherzolite-gabbronorite complex (Stepanov & Stepanova, 2007; Volodichev et al, 2005)

Vorotnaya Luda Island is located in the Gridino dyke field (GDF), where mafic dykes are abundant. Paleoproterozoic dykes in the GDF cross-cut the rocks of the Gridino eclogite-bearing complex.

Based on the studies carried out in the past few years, the dykes exposed in the GDF were split up into six groups distinguished geologically, mineralogically, petrologically and geochemically. Exposed on Vorotnaya Luda Island are three groups of mafic dykes: early Mg-tholeiites, olivine gabbronorites and late tholeiites.

Dykes of early Mg-tholeiites are the oldest in the GDF. They have been highly deformed under enclosing rock plastic flow conditions and seldom retain the primary dyke morphology. Early Mg-tholeiites form a near-E-W-trending swarm and are traced from the western end to the central Vorotnaya Luda Island. The bodies are typically long, vary considerably in thickness (most bodies are not more than 1 m thick) and display sharp, cross-cutting contacts. Apophyses and branching are common, and fold-like forms are occasionally encountered. The rocks of early dykes have been highly altered and have largely lost the primary structural and mineral composition. Analysis has shown no magmatic minerals in early Mg-tholeiites. The association Cpx (6-13% Jd, F=13-15) + Pl (15-16%An) ±Grt (21-22% Prp, 13-14% Grs) ±Opx (F=44-46) + Hbl (Ed Hbl and Hbl), characteristic of the least deformed dykes, is heterogeneous in mineral composition, suggesting that primary rocks have been altered to varying degrees. They typically host symplectitic Cpx and Pl intergrowths that seem to have replaced earlier Cpx enriched in jadeitic mineral. The latest Cpx of these rocks correspond to diopside. Relics of gabbroic and drusitic structures suggest that plagioclase was an essential constituent of primary rocks and that olivine was also present.

The chemical composition of early Mg-tholeiites in the GDF is fairly persistent, as shown by representative analyses in Table 4.2. Metagabbro is classified as a tholeiite-series-, normal-series rock with mixed Ti – Cr geochemical specialization, differentiated REE distribution and LREE enrichment.

Dykes of olivine gabbronorites are the most common dykes in the GDF. They belong to a lherzolite-gabbronorite complex (Stepanov, 1981), dated at ca. 2.43 Ga (Yefimov & Kaulina, 1997; Slabunov et al.2001), and make up a NW-trending swarm in the GDF. The dykes vary in thickness from a few centimeters to 100 m. One petrographic characteristic of the rocks is

that the Opx-Cpx association is common in coronitic structures. The olivine gabbronorites correspond chemically to the SHMB series (Sun, 1989).

Occurring on Vorotnaya Luda Island are three relatively large (over 50 m thick) dykes and a series of small dykes of olivine gabbronorites that extend in a northwestern direction across the entire island and continue outside. The dyke contacts are steep, vertical to near-vertical and typically intrusive: they exhibit a cross-cutting pattern with well-defined chill zones, numerous apophyses and host rock xenoliths. The internal structure of the dykes is simple, and differentiation is only observed as minor variations in the chemical composition of the rocks and in the occurrence of small gabbro-pegmatite schlieren. The gabbronorites have largely retained the primary mineral paragenesis, Opx+ Cpx+ Pl±Ol, and magmatic hypidiomorphic-granular textures.



Fig. 4.6. The outcrops in the Vorotnaya Luda Island. Gabbronorite dyke are in the foreground (photo by V.S. Stepanov).

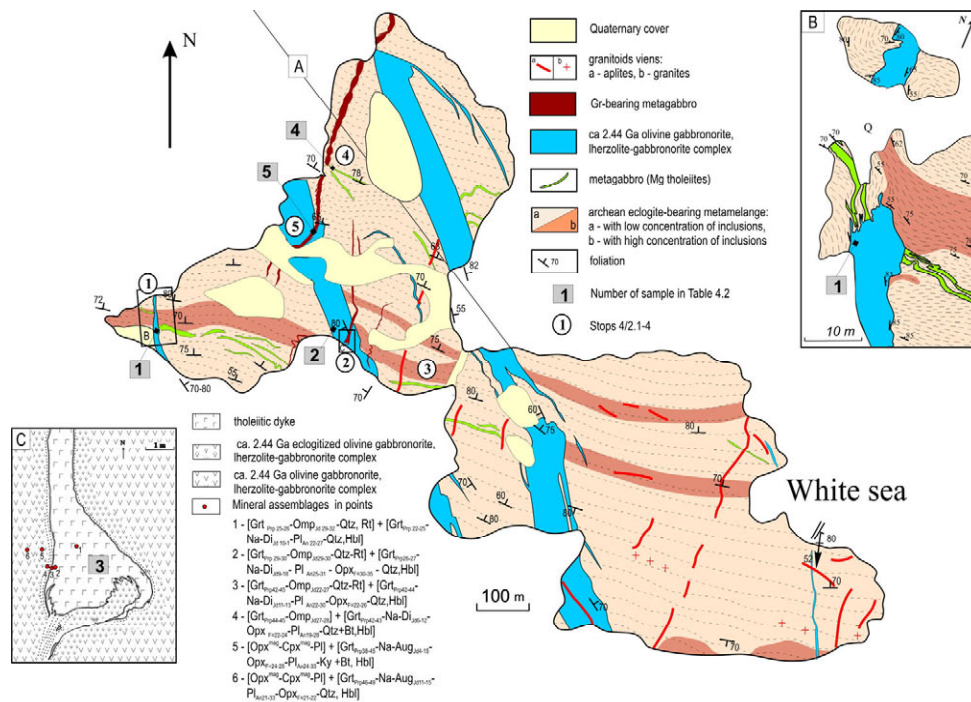


Fig. 4.7. Geological scheme of the Vorotnaya Luda Island (Stepanov, Stepanova, 2007)

The original magmatic melt, presumably similar in composition to chilled dyke rocks (Table 4.2), was crystallized in the stability field of the Ol – Pl association ($P < 8$ kbar). Bipyroxene drusitic (coronitic) structures were generated more recently at higher pressures ($P > 8$ kbar). Their formation was triggered by a total bimetasomatic reaction between Ol and Pl in the rocks of the complex. Subsequent alteration of the structure and mineral composition of the gabbronorites is displayed locally in tectonic and contact zones. At this stage, the Grt – Cpx rims of coronitic structures formed over a wide range of pressures and temperatures and, judging by the compositions of the minerals (Table 4.2), reached eclogite facies. The Grt – Cpx association with a high percentage of jadeite in Cpx was identified in metamorphosed gabbronorites at the contacts with the dykes of coronitic gabbro that cut across them. Amphibolization is usually the latest process common in the rocks of the complex. On Vorotnaya Luda Island, amphibolization seems to occur on two time levels. The earlier level, seen as a 2 – 3 cm thick streak at the contact zone of the dykes, is much earlier than the late one. The fact that amphibolization zones have also been located at contacts with xenoliths of gneissose granites suggests that their formation was close in time to the generation of the dykes. The gabbronorites of the dykes are rich in Mg ($Mg = 0.7$), Cr (over 900 ppm) and SiO₂ and show a differentiated REE distribution pattern. Therefore, they are considered a typical representative of SHMB complexes.

Dykes of tholeiite composition, younger than those of olivine gabbronorites, form a NE-trending swarm. Their rock constituents do not retain primary minerals and structures and consist of Grt, Cpx and Pl. The rocks of this group are classified chemically as tholeiites similar in the distribution pattern of incompatible elements to N-MORB. Their bodies are persistent along the strike and clearly cut across the banding of host rocks. At the same time, in the ca. 20 – 30 cm thick contact zone the early structural elements of gneissose granites are completely lost, and the newly-formed elements clearly agree with the configuration of the dyke contacts and disagree with the early banding of the enclosing rocks.

Petrographically, metagabbros are garnet–plagioclase-clinopyroxene (high pressure granulite facies) and garnet-clinopyroxene (eclogite facies) rocks. The latter rock consists of Grt (25-

26% Prp) and Omp (29-32% Jd) with quartz and rutile. The rocks have been subjected to moderate retrograde alterations that gave rise to both clinopyroxene-plagioclase symplectites and monocrystals of clinopyroxene with reverse zoning from omphacite to diopside and intergranular aggregates of plagioclase.

There are garnet- and clinopyroxene-omphacite- enriched zones at the contacts of the dykes. Retrograde alteration in the zones are more intense, especially in the external zone, where biotitization and amphibolization processes, associated with deformations, are common. Host rocks (Fig. 4.7 C, points 5 and 6) are represented by gabbronorites with drusitic structures that suggest a low degree of their eclogitization in this zone.

The chemical composition of these rocks is illustrated by a representative analysis (Table 4.2). They typically contain low percentages of Ti and mg# of 0.52 – 0.53. N-MORB is most similar in trace element distribution to Vorotnaya Luda coronitic gabbro.

Stop 4.5. The western part of the Vorotnaya Luda Island (Fig. 4.7 a)

This locality is characteristic of a geological relationship between an olivine melanogabbro-norite dyke and early Mg-tholeiite dykes. Here gabbronorites are represented by a small NW-trending dyke. On the island, it occurs as two fragments connected obviously by a thin conductor. The dyke has chilled cross-cutting contacts with host rocks and cuts across symplectitic metagabbro dykes (Fig. 4.7a). The intersecting dykes differ in the orientation and mineralogical composition of rocks (Table 4.2). Their geological interrelations are unambiguous: the gabbronorite dykes and younger than the metagabbro dykes.

On the way from Stop 4/2.1 to Stop 4/2.2 the group will be shown the morphology of metagabbro dykes, a mélangé complex with varying degrees of inclusions saturation and intensity of multiple deformations and a dyke showing tholeiite composition. The morphology of the dyke in the southern part differs markedly from that in the northern part, which is in good agreement with the composition of its host rocks. In gneissose granites the dyke is rectilinear, and in the clast-saturated zone it is deformed. Such a pattern is also characteristic of other dykes of this group.

Stop 4.6. The western part of the Vorotnaya Luda Island (Fig. 4.7 A)

Located near the western contact of an olivine melanogabbro-norite dyke (Fig. 4.7). The group will also see the cross-cutting pattern of the contact between a late tholeiite dyke and an olivine gabbro-norite dyke (Fig. 4.7 B, C).

Petrographically, tholeiite metagabbros are garnet-plagioclase-clinopyroxene (high pressure granulite facies) and garnet-clinopyroxene (eclogite facies) rocks. The latter rock consists of GrtPrp 25-26 and OmpJd 29-32 with quartz and rutile (Fig. 4.7 C, point 1). The rocks have been subjected to moderate retrograde alterations that gave rise to both clinopyroxene-plagioclase symplectites and monocrystals of clinopyroxene with reverse zoning from omphacite to diopside and intergranular aggregates of plagioclase. There are garnet- and clinopyroxene-omphacite- enriched zones at the contacts of the tholeiitic dyke (Fig. 4.7 C, points 2-4). Retrograde alteration in the zones are more intense, especially in the external zone, where biotitization and amphibolization processes, associated with deformations, are common. Host rocks (Fig. 4.7 C, points 5 and 6) are represented by gabbro-norites with drusitic textures that suggest a low degree of their eclogitization in this zone.



Fig. 4.8. Dyke of metagabbro (Mg tholeiites). Vorotnaya Luda island (Made by V.S. Stepanov).

Stop 4.7. The NW part of the Vorotnaya Luda Island (Fig. 4.7 A)

The group will stop here to see a late tholeiite dyke and its relationship with host rocks and early Mg-tholeiite dykes. Stop 4/2.5 The NW part of the Vorotnaya Luda Island (Fig. 4.7 A). This intersection, together with those discussed earlier (Stop 2), shows clearly that the tholeiite dykes (Fig. 4.9) are younger than the gabbro-norite dykes. A tholeiite dyke, up to 2 – 3 m in thickness, has been traced for over 400 m in a northeastern direction. It extends outside the island, and in its southern part the dyke falls into a series of lens-shaped bodies spaced widely apart. As the dyke has been deformed, its contacts are undulating, and numerous contractions that show an interboudin habit.



Fig. 4.9. NE trend dykes of Gr-bearing metagabbro (MORB-type tholeiites). Vorotnaya Luda Island. (photo by V.S. Stepanov)

Gridino village area (Figs. 4.1 B, C; 4.10). At the eastern end of Gridino, a Neoproterozoic eclogite-bearing mélangé is cut by Paleoproterozoic gabbroid dykes and dyke-like bodies, some of which are eclogitized.

Stop 4.8. The eastern end of Gridino village (Fig. 4.1C)

An eclogitized olivine gabbronorite dyke on a mainland point (Fig. 4.11, Table 4.2). The central part of the dyke is made up of coronitic (drusitic) eclogites – medium-grained rocks, whose mineral composition and structural and textural pattern of the protolith are best preserved (Zone 1). These magmatic-metamorphic units consist of magmatic cumulus minerals, such as olivines, orthopyroxenes and clinopyroxenes, and completely metamorphosed intercumulus ingredients represented, together with thin omphacitic rims of ortho- and clinopyroxenes, by the eclogitic associations Grt48-49-Omp30-41, Grt48-51-Omp38-48-corundum formed at temperatures of 765-930 °C and pressures of 15-19 kbar. The isotopic age of magmatic zircons from this zone is 2393 ± 13 Ma (Volodichev, Slabunov, 2007).



Fig. 4.10. The Gridino village on the White sea coast. Outcrops of Neoproterozoic eclogite-bearing metamélange. (photo by P. Azimov).

Clinopyroxene in gabbro cumulus occurs as diopside (chrome-diopside with percentages of jadeite uncommon for magmatic rocks: 12% in the grain centre to 26% on the grain margin). The clinopyroxene contains many orthopyroxene-enstatite intergrowths and abundant suboriented lamellar amphibole-edenitic hornblende intergrowths not observed in the rim of this crystal composed of omphacite that contains up to 41% Jd. A similar pattern has formed in an altered orthopyroxene crystal whose central, unaltered portion contains a lot of very small, suboriented spinel inclusions and intergrowths with clinopyroxene, similar in composition to omphacite (19% Jd). Evolving after the orthopyroxene is diopside that contains 17% Jd, inclusions or relics of orthopyroxene and, like in the crystal described earlier, abundant suboriented, elongate lenticles (lamellae), in this case paragonitic hornblende which does not occur in the marginal omphacitic rim. Interestingly, the above Jd-bearing diopsides are typically rich in Cr_2O_3 (0.63-1.24%) and are, in fact, chrome-diopsides correlatable with those from peridotites, garnet lherzolites and plagioclase peridotites, the percentage of Cr_2O_3 in the rim omphacites decreasing considerably.

The above evidence suggests that as early as the subsolidus stage gabbro cumulates were crystallized at increasingly high pressures with involvement of fluids (amphibole lamellae). Crystallization was followed by a metamorphic stage in rock eclogitization.

The intermediate zone (2) consists of medium-grained “granulated” eclogites that have already become a largely metamorphic rock composed of garnet, orthopyroxene and omphacite. It contains varying quantities of unequally altered magmatic minerals such as orthopyroxenes and smaller amounts of clinopyroxenes in the form of omphacite-rimmed porphyroblasts that contain, 19-22% Jd, as do granulated mass omphacites. The associations Grt44-48-Omp19-22-Opx show that they were generated at temperatures of 715-785 °C and pressures of 12.5-

14.0 kbar. Amphibole (edenitic or pargasitic hornblende) and biotite are already present constantly in these rocks.

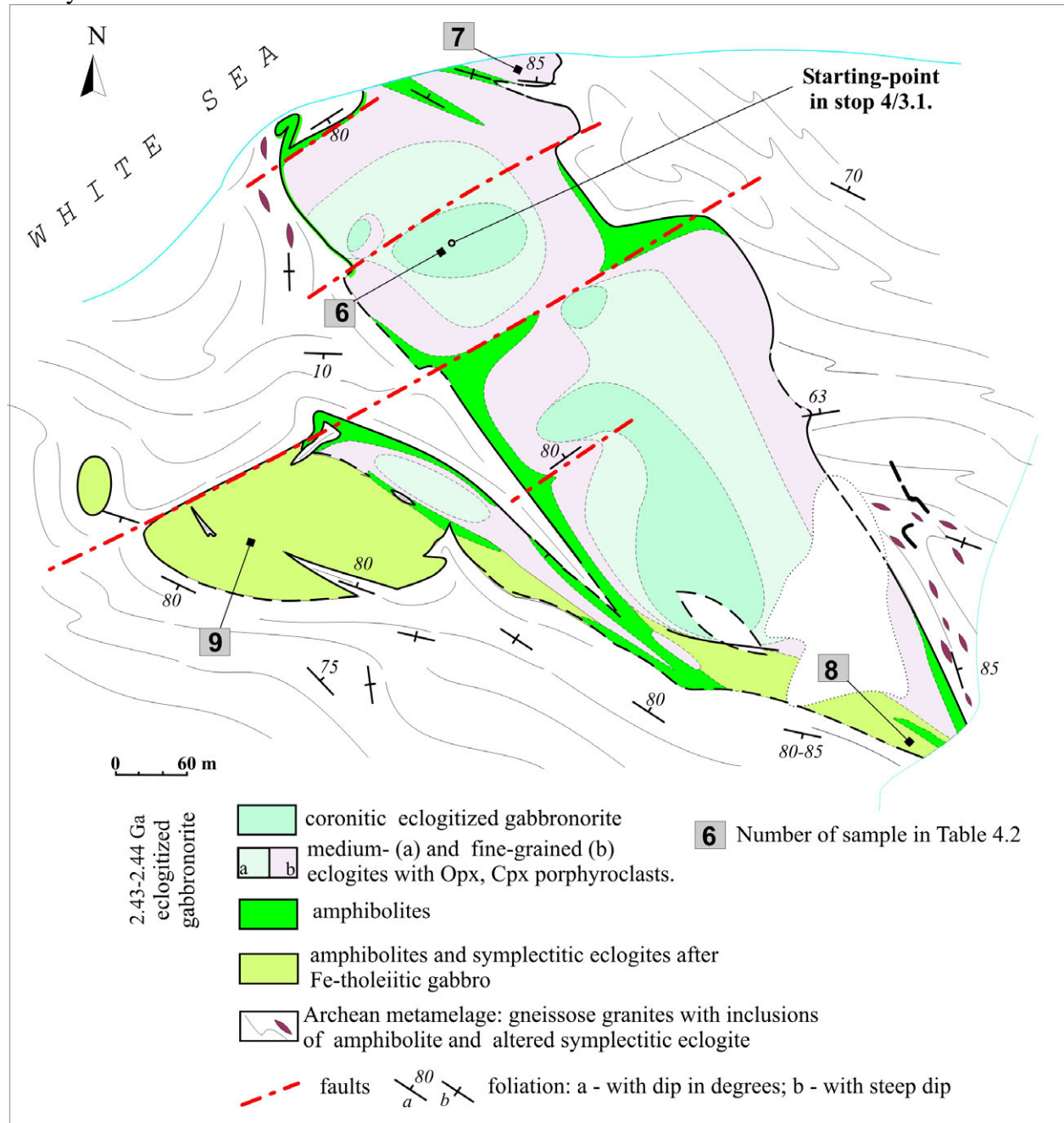


Fig. 4.11. Geological scheme of an eclogitized gabbronorite dyke of the 2.43-2.44 Ga lherzolite-gabbronorite complex at the eastern end of Gridino. By O.S. Sibelev and O.I. Volodichev.

The marginal zone (3) (Fig. 4.11) is built by fine-grained, equigranular eclogites with scarce, dominantly orthopyroxene, porphyroclasts. The rock consists of garnet (42-46% Prp), omphacite (18-24% Jd) and orthopyroxene. Amphibole, which occurs as common, actinolitic and pargasitic hornblende, is present in varying quantities (up to 20-25%). These rocks have suffered marked retrograde alteration such as a decrease in the percentage of Prp on garnet grain margins, the emergence of zonal clinopyroxenes with an omphacitic core and a diopside (6-7% Jd) margin and the formation of plagioclase (29-34% An) at the garnet-omphacite boundary, commonly together with pargasitic hornblende, which evolves along the edges of actinolitic and common hornblende crystals.

Retrograde alteration is most distinct in sample C-16/67 (Table 4.2), where, on one hand, the eclogitic associations (Grt37-Omp24, $T = 800-810\text{ }^{\circ}\text{C}$ and $P = 14.5\text{ kbar}$) are fairly well preserved; on the other, gradual transitions of omphacite to intergrowths of symplectitic diopside (7% Jd) with plagioclase (20% An), associated with orthopyroxene are encountered. The Py content of the garnet declines slightly from the centre toward the margin. The retrograde alteration occurred at temperatures of $700-710\text{ }^{\circ}\text{C}$ and pressures of $9-9.5\text{ kbar}$.

Stop 4.9. Central part of Gridino Village

A fragment of an eclogite-bearing mélangé with a high concentration of clasts (Fig. 4.12). The clasts are dominated by amphibolites, but amphibolitized symplectitic eclogites are also encountered.



Fig. 4.12. The eclogite-bearing mélangé.

Day 5, Friday 1.8. 2008

Wake up at 7:00, breakfast. Part 1: visit to Khizovaara (Archean greenstone belt supracrustals with boninites and inferred oceanic origin of the complex). Part 2: drive to Kalevala, road-side geology stops of Archean geology at the boundary between Karelian Craton (lamprophyre dikes) and Belomorian mobile belt (metavolcanites of Keret greenstone belt). Overnight and dinner at Kalevala.

Neoarchean Khizovaara greenstone complex in the lake Verkhneye area

V.N. Kozhevnikov¹, A.N. Shchipansky²

¹ *Institute of Geology, Karelian Research Centre, RAS (Petrozavodsk)*

² *Geological Institute (GIN), RAS (Moscow)*

The goal of the field trip is to show a Neoarchean greenstone complex in the Khizovaara structure, which includes fragments of subduction ophiolites, island-arc volcanogenic, sedimentary and sedimentary-volcanic rocks and surrounding granitoids. The Khizovaara structure is located on the shore of Lake Verzhnye (Fig. 5.1) which belongs to the lake system of Keret Lake. Khizovaara is a part of the North Karelian greenstone belt located in the zone

affected by Neoproterozoic and Paleoproterozoic collision processes that manifest themselves in the Belomorian mobile belt.

The Khizovaara structure is an asymmetrical, structurally complex synform with a southward-plunging axial surface made up of volcanics and sediments and surrounded by granitoids (Kozhevnikov, 1992, 2000). The results of its integrated study have shown that it is a tectonic collage of several stratotectonic associations (STA) of volcanic, sedimentary-volcanic and sedimentary nature (Fig. 5.2) formed in different paleogeographic and paleogeodynamic environments at the convergent micro-ocean-microcontinent boundary (Kozhevnikov, 1992, 2000; Kozhevnikov et al., 2006).

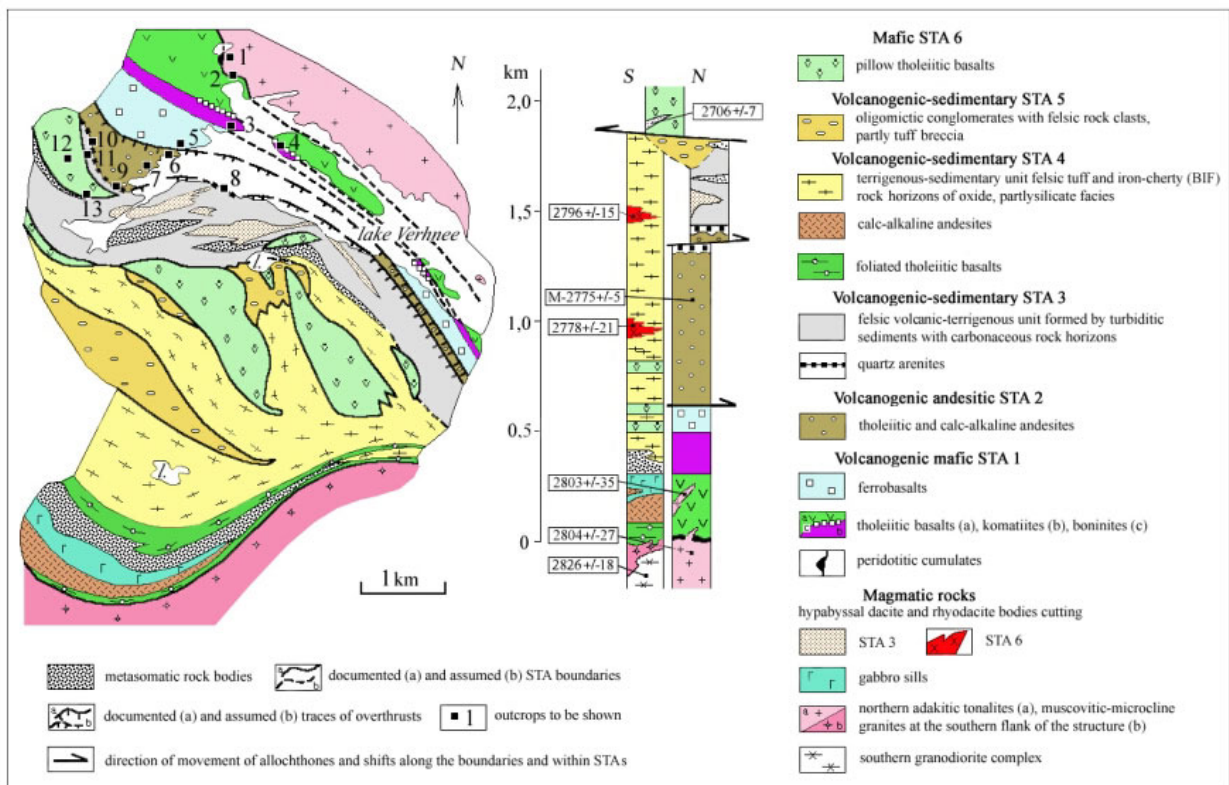


Fig. 5.1. Geological map of the Khizovaara structure (revised, simplified version after Kozhevnikov, 2000) and the STA column (revised after Bibikova et al., 2003; reference zircon ages are given in Ma; M = metamorphic age).

The lower volcanogenic STA1 is a rock sequence, whose lower part contains fragments of peridotitic cumulates (serpentine + anthophyllite ± chlorite + ore) overlain by three petrogenetic groups of orthoamphibolites (from the base upwards): 1) a moderately titaniferous group (0.8-1.3% TiO₂), corresponding geochemically to island-arc metabasalts (hornblende + plagioclase ± epidote ± cummingtonite ± garnet); 2) basaltic to peridotitic komatiites (anthophyllite + tremolite + talc + carbonate ± chlorite) with a horizon formed by low-Ti (0.3-0.45% TiO₂) quartz-bearing amphibolites that exhibit the geochemical characteristics of boninites; and 3) a group of Ti-rich (1.2-2.5% TiO₂) amphibolites interpreted as metamorphosed ferrobasalts (hornblende + plagioclase ± ore).

The lower volcanogenic STA1 is a rock sequence, whose lower part contains fragments of peridotitic cumulates (serpentine + anthophyllite ± chlorite + ore) overlain by three petrogenetic groups of orthoamphibolites (from the base upwards): 1) a moderately titaniferous group (0.8-1.3% TiO₂), corresponding geochemically to island-arc metabasalts (hornblende + plagioclase ± epidote ± cummingtonite ± garnet); 2) basaltic to peridotitic komatiites (anthophyllite + tremolite + talc + carbonate ± chlorite) with a horizon formed of low-Ti (0.3-0.45% TiO₂) quartz-bearing amphibolites that exhibit the geochemical characteristics of boninites; and 3) a group of Ti-rich (1.2-2.5% TiO₂) amphibolites interpreted as metamorphosed ferrobasalts (hornblende + plagioclase ± ore). Such a succession of basaltic series, differing in the percentage of TiO₂, is characteristic of many suprasubduction ophiolite complexes such as the Troodos massif on Cyprus and Koch ophiolites in New Caledonia (see Shchipansky et al., 1999 for references).

Metaboninites occur as 0.5-1.0 m thick, highly deformed, sheeted quartz amphibolite bodies among less cherty varieties of orthoamphibolites. It is hard to visually distinguish between the metaboninites and associated Mg-rich metatholeiites. The only distinctive character in outcrops is that the metaboninites are more massive than less cherty rocks referred to in the literature as primitive Mg-rich lava, low-Ti ophiolitic basalts or island-arc picrites (see Shchipansky et al., 1999 for references).

This sequence is 100 to 650 m thick. Characteristic for it are massive textures (pillow textures are scarce), thin hyaloclastite and bedded tuff seams and the absence of felsic terrigenous sediments between flows, suggesting that the mafic association was formed in a non-intracontinental setting. In the north, the base of the sequence is cut by trondhjemites that display the geochemical characteristics of adakites and are dated at 2804±27 Ma (Bibikova et al., 2003). The age of the felsic dykes that cut the association is estimated at 2803±35 Ma (Kozhevnikov, 1992). Observed in the upper part, near the contact, are intense carbonatization, schistosity and pencil structures – evidence for the tectonic nature of the upper contact of the sequence. STA1 is understood as a complex of suprasubduction ophiolitoids formed in an intraoceanic environment (Shchipansky et al., 1999) or in a continental margin spreading setting (Kozhevnikov, 2000).

The next volcanogenic STA2 varies in thickness from 100 to 700 m and consists of andesites. Their amygdaloidal, homogeneous, dark-grey (plagioclase + hornblende ± biotite ± epidote), amygdaloidal varieties with signs of primitive pillow textures, glomeroporphyric and coarse pyroclastic varieties occur in the thickest unit from the base upwards (Fig. 5.2). Near the lower contact in amygdaloidal lava quartz, quartz-plagioclase and chlorite-carbonate-quartz amygdales are elongated along A-lineation, the ratio of three axes being 20:3:1. A thin glomeroporphyric andesite horizon, traced for several kilometers, is overlain through a crust of weathering by a terrigenous quartzite-quartz arenite horizon. The age of the zircons from the andesite unit, estimated at 2775±5 Ma, is interpreted as the age of early metamorphism (Bibikova et al., 2003).



Fig. 5.2. The amygdaloidal andesite unit (andesites-1) consists of biotite-quartz-amphibole-plagioclase schists.

The third sedimentary association, STA3, is represented by a sequence of sedimentary and volcanic-sedimentary rocks. Its base is formed by terrigenous quartzites and quartz gravelstones with quartz conglomerates in its lower part that rest on glomeroporphyric andesites with or without a crust of weathering thereon (Fig. 5.3). Analysis of detrital zircons from these rocks has shown that they originated from several sources dated at 3152 ± 4.6 Ma, 2832 ± 6 - 2811 ± 7 Ma, 2747 ± 5 - 2705 ± 10 Ma and 2687 ± 11 - 2651 ± 3.5 Ma (Kozhevnikov et al., 2006).



Fig. 5.3. Direct contact of andesites from STA 2 and quartz arenites

Resting on the quartz arenites is a unit built by graded turbidites with indications of Bouma cycle elements, with felsic lava and ash flow lenses and horizons that show complex lateral relations, and chemically precipitated rocks such as cherty, alumino-cherty, alumino-iron-cherty and iron-cherty rocks (Thurston, Kozhevnikov, 2000). Part of the unit is made up of carbonaceous and fuchsite schists. All of these low-Ca rocks consist of various mineral associations formed by quartz, kyanite, staurolite, garnet, feldspar, amphibole, muscovite, biotite, fuchsite, magnetite, graphite and other minerals. Rhythms of different order of magnitude vary in thickness from 1 cm to tens and probably hundreds of metres. In the upper parts of each rhythm the percentage of alumina increases. The top of this unit is composed of felsic lava and agglomerate tuffs that form fairly thick lenses. An intrusive facies is represented by felsic veins, dykes and stocks, with which autohydrothermal processes are associated, accompanied by a rise in Pb, Zn, Ag, Au and Bi concentrations. The age of galena is ca. 2.67 Ga (analysed by G.V. Ovchinnikova, Institute of Precambrian Geology and Geochronology, RAS), and the Pb-Pb ages of tourmaline from hydrothermal aureoles is 2718 ± 55 Ma and from quartz-muscovite metasomatites is 1794 ± 130 Ma (analysed by N.M. Kudryashov, Geological Institute, Kola Science Centre, RAS).

STA4 in the southern part of the structure is *similar in age to STA1 and 2*. It consists of terrigenous sediments that alternate in the lower part of the unit with mafic volcanics such as pillow basalts and mafic, intermediate and less common felsic tuffs. Thin horizons and lenses, formed of chemically precipitated BIF rocks, are encountered in the sedimentary part of the unit and in association with basalts. The lower boundary of this association extends along a tectonized intrusive contact with granitoids of the southern margin. A large part of its upper boundary is in tectonic contact with dominantly volcanic-sedimentary part of STA3 and is overlain by rocks higher in the section. Where it is not overlain, the boundary is traced by lenticular metasomatic and felsic hypabyssal intrusive bodies. Two other STA rest unconformably on sediments of STA3 and the upper part of the southern, dominantly sedimentary STA4.

Coarse clastic rocks of STA5 form two wide fields in the centre of the structure with signs of discordance. They are in contact with both underlying and overlying complexes. Fragments have a persistent dacite-rhyolite composition, more felsic than the matrix, and the rocks occur as oligomictic and volcanic conglomerates with a scoured tuff matrix. At some localities the latter are closely associated with felsic lava breccia. This association is interpreted as a preserved part of a pull-apart basin traced as fragments northwards in the Vincha, Iringora and Vichany structures (Kozhevnikov, 2003).

The composition of the matrix and clasts in the oligomictic conglomerates was studied. Most fragments exhibit a persistent dacite-rhyolite composition, more felsic than the matrix. Fragments of epidotes, metasomatic rocks that provide evidence for metamorphism that preceded the deposition of coarse clastic sediments, are encountered. The matrix of the conglomerates differs in chemical composition from graywackes of STA3, containing more MgO and CaO. It is very similar in trace element geochemistry with distal rhythmites. Two samples of clasts are geochemically similar to matrix rocks in spite of their different nature. The age of clastic zircons from these conglomerates varies from 2838 ± 25 to 2747 ± 14 Ma (NORDSIM, Stockholm, pers. comm. with Pentti Hölta).

The upper mafic STA6 is represented by a unit formed by pillow tholeiitic basalts (hornblende + plagioclase) (Fig. 5.4). Encountered in its lower part are thin sills of basaltic, pyroxenitic and less abundant peridotitic (anthophyllite, anthophyllite \pm scarce plagioclase grains) komatiites contaminated with continental-crustal material. They differ considerably geo-

chemically from komatiites in STA1. Thick (>100 m) flows with a lower gabbroid and an upper top zone, formed by basalts with a primitive pillow jointing were reported. Toward the metasomatic rocks in shear zones in the pillow parts of the flows the rocks are more intensely deformed, and their metasomatic reworking is accompanied by alteration of initial basalts first to andesite composition and then to garnet-kyanite-plagioclase-quartz rocks, in which green chill zones persist as shadows. The isotopic age of this STA has not been determined. It overlies with structural unconformity all the associations, presumably except STA1, and is cut by rhyodacite and granodiorite dykes (Fig. 5.5), whose isotopic age is estimated at 2706 ± 7 Ma (Shchipansky et al., 1999).

The structure of Khizovaara was affected by three deformation stages (Kozhevnikov, 1992, 2000).



Fig. 5.4. Pillow holeitic basalts-basalts of STA6 (photo by V.N. Kozhevnikov).



Fig. 5.5. Rhyodacite dyke cutting upper pillow-basalts of STA6 (photo by V.N. Kozhevnikov).

Stage D¹ deformations are observed in two early stratotectonic associations STA1 and STA2. The earliest structures formed at this stage occur as upthrusts documented by intense (800-1400%) deformation of andesites assessed by 3D measurement of amygdales. Minor folds, into which the andesite flows are thrown, also belong to this generation.

Stage D² includes deformations superimposed on the products of volcanism and sedimentation that began with the deposition of quartz arenites and ended with rhyodacitic volcanism and the deposition of oligomictic conglomerates. At *D²*-stage, near-E-W-trending folds with gently dipping hinges and steep axial surfaces were formed. Major folds, produced at this stage, are documented by a structural discordance overlain by mafic volcanics of STA 6.

Stage D³ comprises four generations of *3F¹-3F⁴*- folds. Some are responsible for the formation of shear-sliding zones, which controlled metasomatic processes, and fracturing that controlled late dacite dykes and veins in the upper basalts of STA6. The deformations that occurred at this stage are superposed on the entire Khizovaara structure and on surrounding tonalites, but in rocks of the upper mafic associations they occur in pure form unaffected by earlier structures.

Metamorphic processes in the Khizovaara structure were studied in detail by S.M. Bushmin (Bushmin, 1978; Glebovitsky & Bushmin, 1983). The metamorphic regime was as follows: T°C = 580-640°, P = 6.5-7.5 kbar. As temperatures decreased to 300-550° and partial water pressure in the fluid rose to a maximum at the retrograde stage, acid leaching was invigorated.

Stop 5.1. Lake Verzhneye, 400 m to north from lakeside (Fig. 5.6)

Exposures of peridotitic cumulates that make up the basal unit of mafic STA1. Aphanitic serpentinites, “augen” amphibolized and chloritized serpentinites with anthophyllite and chlorite (Table 5.1) and lenticular-banded and foliated serpentinites are recognized here.

These rocks contain extremely high percentages of MgO (up to 41.27%) and Ni (up to 2350 ppm) and low percentages of Al₂O₃, TiO₂, alkalis, HFSE and REE. Some samples have abnormally small quantities of Cr (as small as 44 ppm), the quantities of Cr in the main batch varying from 1806 to 3082 ppm. Their REE distribution pattern shows impoverishment in light (La/Sm)_N = 0.51 and heavy -(Gd/Yb)_N = 1.10 lanthanoids and a negative Eu-anomaly - Eu/Eu* = 0.7. In addition, a positive Zr-anomaly and a negative Ti-anomaly are observed (Table 5.1, Fig. 5.7a).



Fig. 5.6. Cape in NW part of the Lake Verzhneye.

Table 5.1. Average and representative compositions of major rock types from mafic STA1 and STA6 and late komatiite sills.

No.	1	2	3	4	5	6	7	8	9	10
sample	022-3	675-2	576-6	656-2	N=4	N=4	H-321	H-334/1	N=3	585a-1
SiO ₂	44.90	46.41	50.87	50.48	50.76	51.93	56.77	60.14	49.55	50.46
TiO ₂	0.18	0.38	0.53	0.64	0.84	1.07	0.42	0.36	1.98	1.96
Al ₂ O ₃	3.30	8.64	13.03	11.43	15.13	14.54	11.73	10.05	14.03	15.32
Fe ₂ O ₃	10.64	10.84	11.30	11.37	12.15	13.69	10.86	10.02	16.93	16.60
MnO	0.18	0.07	0.24	0.17	0.18	0.20	0.17	0.16	0.20	0.17
MgO	35.67	22.68	10.13	19.24	8.62	7.46	9.13	9.16	5.75	3.98
CaO	3.23	8.90	13.67	7.63	10.83	9.47	10.15	9.31	9.08	8.16
Na ₂ O	0.09	0.52	0.66	2.95	1.12	1.23	0.55	0.66	2.10	4.39
K ₂ O	0.01	0.03	0.26	0.20	0.29	0.27	0.16	0.07	0.18	0.05
P ₂ O ₅	-	0.04	-	0.09	0.08	0.13	0.05	0.07	0.19	0.31
Li	-	-	-	-	20.2	18.8	23.30	30.4	19	-
Sc	-	-	-	-	41.90	41.3	36.3	46.4	28.2	-
Ti	480	2158	3057	3837	5023	5812	2500	2186	11882	11391
V	120	165	383	279	206	299	104	223	285	207
Cr	2574	3569	697	1486	269	290	762	919	154	133
Co	95	101	62	58	48.4	50	77.6	62.3	48.3	37.0
Ni	1769	657	172	267	112	112	306	191	46.0	48.0
Cu	-	-	-	-	73.58	27	49.8	27.3	86.7	51.0
Zn	-	-	-	-	80.0	99	86.7	65.3	105	62.0
Ga	-	-	-	-	14.5	18	11.5	9.56	19.3	19.0
Rb	0.85	0.74	6.82	9.02	10.1	7.48	2.25	0.74	2.05	1.00
Sr	3.9	36.58	98.26	87.48	99	97	82.5	73.5	248	86
Y	3.64	7.49	12.06	13.5	23.0	23.5	11	14.5	30.4	17.0
Zr	18.48	16.73	25.32	72.69	14.2	52.2	20.0	26.5	111	127
Nb	0.27	0.57	0.92	3.03	2.29	2.81	0.754	0.865	10.3	5.0
Cs	0.31	0.1	0.36	6.00	0.48	0.14	0.123	0.053	0.083	-
Ba	-	-	-	-	42	106	59.2	31.5	47	30
La	0.29	0.65	0.91	7.12	3.45	2.67	1.04	1.34	13.3	2.73
Ce	1.00	1.91	2.7	17.39	9.12	7.45	2.84	3.59	32.7	12.17
Pr	0.18	0.34	0.47	2.34	1.40	1.27	0.425	0.54	4.69	1.74
Nd	0.92	1.67	2.62	9.92	7.03	6.90	2.38	2.95	21.2	9.83
Sm	0.37	0.63	0.98	2.36	2.41	2.30	0.9	1.06	5.35	2.89
Eu	0.10	0.26	0.41	0.74	0.75	0.72	0.402	0.372	1.59	0.95
Gd	0.52	1.07	1.68	2.44	2.98	3.09	1.27	1.54	5.94	2.42
Tb	0.09	0.19	0.31	0.38	0.52	0.53	0.27	0.28	0.93	-
Dy	0.58	1.21	2.02	2.4	3.70	3.77	1.83	2.2	5.77	2.3
Ho	0.14	0.28	0.45	0.52	0.81	0.86	0.433	0.5	1.19	-
Er	0.44	0.77	1.35	1.51	2.38	2.46	1.2	1.42	3.2	1.22
Tm	0.06	0.12	0.19	0.22	0.34	0.37	0.194	0.216	0.44	-
Yb	0.39	0.81	1.29	1.38	2.22	2.32	1.22	1.48	2.65	1.34
Lu	0.07	0.126	0.194	0.212	0.33	0.35	0.174	0.259	0.38	0.24
Hf	0.56	0.52	0.74	1.92	0.61	1.63	0.62	0.75	2.90	2.73
Ta	-	-	-	-	0.13	0.61	0.188	0.056	0.63	-
Pb	-	-	-	-	1.72	1.75	3.07	0.896	2.22	-
Th	0.05	0.07	0.1	1.17	0.29	0.27	0.082	0.065	1.09	3.04
U	0.05	0.02	0.03	0.22	0.06	0.07	0.038	0.008	0.23	0.48
La/Yb _N	0.53	0.57	0.51	3.70	1.07	0.79	0.58	0.61	3.05	1.46
La/Sm _N	0.51	0.66	0.60	1.95	0.92	0.74	0.73	0.80	1.40	0.61
Gd/Yb _N	1.10	1.09	1.08	1.46	1.09	1.10	0.84	0.84	1.72	1.49
Eu/Eu*	0.70	0.97	0.98	0.94	0.86	0.83	1.15	0.89	0.88	0.91

Note. Recalculated to 100% on a volatile-free basis.

1 = peridotitic cumulate, 2 = komatiite, 3 = komatiitic-series metabasalt, 4 = pyroxenitic komatiite from sills among sedimentary rocks of STA3, 5 and 6 = average compositions of tholeiitic metabasalts from the northern

and southern parts of the structure, 7 = boninitic-series metavolcanics; 8 = Ti-ferrobasalt.; 9 – average compositions of Fe-Ti metabasalts; 10- Fe- metabasalt with Nb anomaly at the ratios $(Th < Nb < La)_{PM}$ in this indicator triad.

The cumulate body is cut by thin potassic-sodic granite-porphyry dykes that contain abnormal quantities of Rb, Zr and Nb. The isotopic age of these intraplate A-type granites is Svecofenian and is estimated at 1840 ± 10 Ma (N.G. Berezhnaya, pers.com).

Stop 5.2. Lake Verzhneye, 150 m to north from lakeside (Fig. 5.7).

A direct magmatic contact between northern trondhjemites and massive tholeiitic basalts (Table 5.1). The trondhjemites, dated at 2804 ± 27 Ma (Bibikova et al., 2003), have the geochemical characteristics of adakites (Samsonov, 2004). The basalts host granitoid veins, and migmatization in volcanics is not apparent. Indications of primitive pillow jointing are observed in the basalts.

Granitoids on the northern margin of the structure and subvolcanic rhyodacites (Stop 5.3) among mafic rocks show similar petrogeochemical characteristics and correspond to calc-alkaline alumina-rich trondhjemites with high percentages of Sr, low percentages of Y and HREE, highly fractionated lanthanoid spectra: $(La/Sm)_N = 4.6-5.3$, $(Gd/Yb)_N = 3.6-3.8$, minor Eu anomalies ($Eu/Eu^* = 0.94-1.03$) and pronounced negative Nb anomalies.

Stop 5.3. Cape in Northern part of the Lake Verzhneye

A unit consisting of peridotitic (Table 5.1), pyroxenitic, basaltic komatiites that fall into massive, lava-breccia and hyaloclastic varieties and thin boninite horizon (Table 5.2). The unit is cut by thin rhyodacite-rhyolite dykes dated at 2803 ± 35 Ma (measured by O.A. Levchenkov, in Kozhevnikov, 1992).

Stop 5.4. Dlinnyy Island on the Lake Verzhneye (Fig. 5.1).

Exposures of tholeiitic and komatiitic basalts, similar to the rocks at Stop 5.3 that host a thin boninite horizon (Table 5.2, Fig. 5.7a) at the northwestern end of the island. The rocks are cut by thin folded rhyodacite dykes.

Resting on the cumulates is a tholeiitic basalt unit. The basalts contain moderate percentages of TiO_2 and show flat or more complex REE distribution pattern and weak variable-sign Nb and Zr anomalies (Fig. 5.8). The tholeiitic basalts pass gradually into MgO-rich rocks that correspond to komatiitic and boninitic ($MgO > 8\%$, $SiO_2 > 52\%$ and $TiO_2 < 0.5\%$) series. Komatiitic-series rocks contain more MgO (up to 29%), TiO_2 (MgO content being the same), Al_2O_3 , CaO, V, Cs and less SiO_2 (42.8-50.3%) and total REE than boninitic-series rocks (Table 5.2). The REE distribution pattern and spidergrams for rocks of both series are similar (Fig. 5.8).

Table 5.2. Representative compositions of metaboninites and associated Mg-metabasalts

nn	1	2	3	4	5	6	7	8	9	10
sample	H-333	H-325	X-126/1	X-130	H-320	H-325/1	H-326	H-334/1	H-332	H-335
SiO ₂	47.13	48.78	59.84	55.12	58.68	54.1	53	59.36	65.69	62.66
TiO ₂	0.41	0.42	0.37	0.4	0.34	0.42	0.43	0.36	0.33	0.35
Al ₂ O ₃	10.08	12.31	9.67	11.02	9.86	12.19	11.92	9.92	10.45	9.32
Fe ₂ O ₃ *	12.93	11.87	10.12	11.17	9.26	11.1	10.76	9.89	10.15	9.98
MnO	0.18	0.2	0.18	0.17	0.16	0.17	0.17	0.16	0.16	0.15
MgO	16.59	12.66	8.22	10.34	8.56	9.21	10.13	9.04	8.31	7.95
CaO	10.48	10.91	9.43	10.01	9.98	10.02	10.89	9.19	3.34	7.67
Na ₂ O	0.49	0.46	0.38	0.7	0.31	0.42	0.69	0.65	0.61	0.18
K ₂ O	0.06	0.49	0.08	0.09	0.09	0.42	0.17	0.07	0.13	0.16
P ₂ O ₅	0.05	0.07	0.12	0.13	0.05	0.05	0.07	0.07	0.04	0.06
loi	1.62	1.84	1.74	0.93	2.77	2.02	1.83	1.43	0.79	1.73
Sum	100.02	100.01	100.15	100.08	100.06	100.12	100.06	100.14	100	100.21
Mg#	74.9	71.2	65.3	68.1	68.3	66.4	68.6	67.9	65.5	65
Cr	1412	939	1003	1067	1519	996	912	919	977	1603
Ni	325	223	201	220	415	215	219	191	226	342
Co	72.2	63.4	62.6	64	78.7	67.5	66.8	62.3	66.7	77.9
Sc	40.9	42.9	43.1	45.8	41.1	52.3	47.9	46.4	48	45.7
V	167	244	265	265	251	277	254	223	228	179
Pb	1.11	1.33	2.51	0.61	1.92	3.21	1.71	0.896	1.17	0.752
Ba	8.77	103	28.9	24.5	45.3	342	23.8	31.5	45.1	37.6
Rb	0.01	24.7	2.23	1.43	2.15	42.4	2.66	0.737	7.38	6.84
Sr	25.5	73.2	61.3	45.3	104	85.3	127	73.5	37.2	55.2
Ta	0.047	0.076	0.084	0.054	0.047	0.094	0.049	0.056	0.057	0.054
Nb	0.821	0.948	1.04	0.91	0.787	0.986	0.971	0.865	1.1	0.818
Hf	0.381	0.354	0.357	0.486	0.31	0.278	0.498	0.411	0.375	0.292
Zr	25.26	24.03	27.7	32.97	20.96	21.33	35.21	26.53	27.78	21.23
Y	12.8	13.8	12.9	14.1	12.4	13.1	14.8	14.5	13.5	13.6
Th	0.121	0.097	0.174	0.155	0.098	0.153	0.122	0.065	0.137	0.113
U	0.027	0.021	0.04	0.028	0.03	0.045	0.041	0.008	0.019	0.026
La	1.17	1.25	1.12	1.15	1.33	1.16	1.4	1.34	1.99	1.44
Ce	3.02	3.21	2.65	3.33	3.39	2.94	3.58	3.59	4.82	3.51
Pr	0.496	0.524	0.465	0.575	0.578	0.46	0.599	0.54	0.712	0.587
Nd	2.58	2.84	2.79	2.85	2.62	2.45	2.96	2.95	3.26	2.4
Sm	0.983	0.988	1.14	1.06	1.07	0.941	1.07	1.06	1.12	0.987
Eu	0.373	0.407	0.401	0.328	0.468	0.388	0.45	0.372	0.182	0.261
Gd	1.22	1.5	1.35	1.52	1.31	1.31	1.51	1.54	1.46	1.42
Tb	0.225	0.283	0.274	0.274	0.261	0.242	0.298	0.271	0.267	0.274
Dy	1.87	2.1	2.16	2.2	1.91	1.9	2.06	2.2	1.8	1.9
Ho	0.387	0.453	0.434	0.513	0.404	0.45	0.473	0.5	0.491	0.469
Er	1.3	1.39	1.15	1.37	1.42	1.25	1.56	1.42	1.45	1.39
Yb	1.02	1.35	1.37	1.44	1.27	1.36	1.68	1.48	1.34	1.13

Note: recalculated to 100% on a volatile-free basis,
 1-2 – HMg- primitive metabasalts, 3-10 – metaboninites,

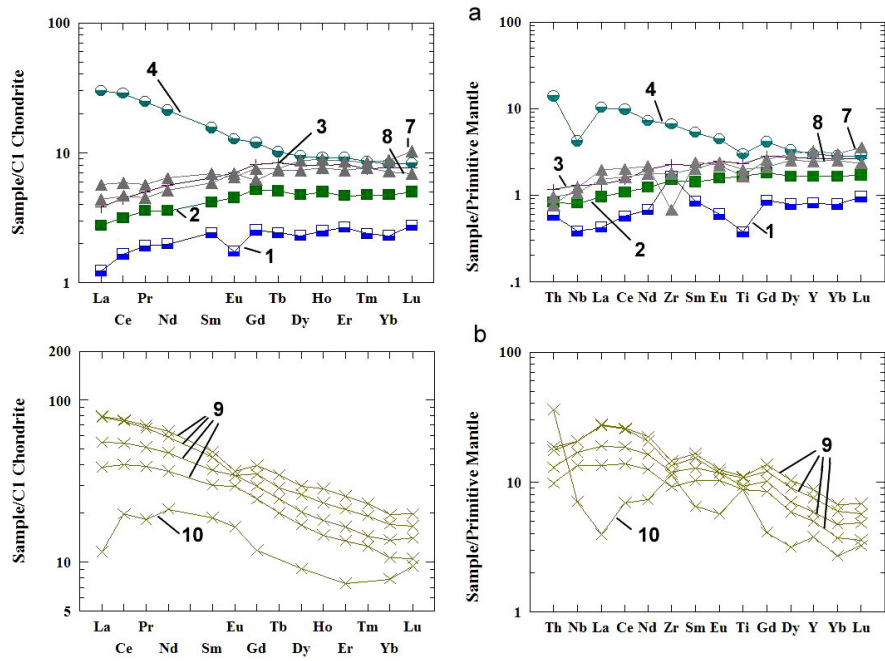


Fig. 5.7. Chondrite-normalized REE distribution and PM-normalized spidergrammes in mafic and Mg-rich rocks. Numbers on Figs in Table 5/1.

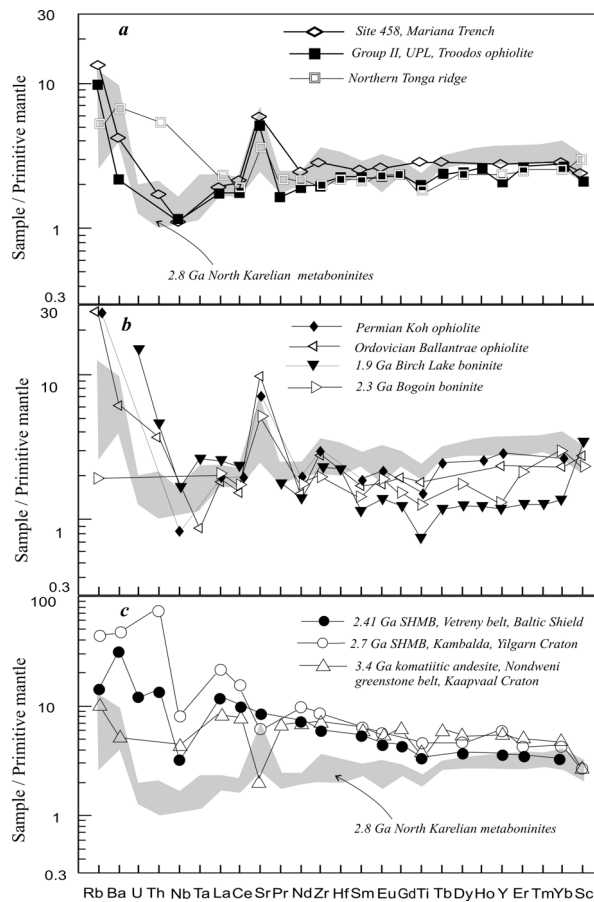


Fig. 5.8. PM-normalized spidergrammes in North Karelian boninites and modern (a), Paleozoic and Paleoproterozoic high-Ca boninites (b) and crust-contaminated komatiitic lavas (c) (Shchipansky et al., 2004). PM by Hofmann, 1988.

Isotopic-geochemical data show boninites and less cherty, low-Ti metatholeiites form one petrogenetic series similar (Table 5.2, Fig. 5.8) to well-known volcanics of groups I and II of upper pillow lava of Troodos suprasubduction ophiolites recognized as a standard used to identify Ca-rich boninites (references see on Shchipansky et al., 2004). Boninites from the North Karelian GSB are also similar geochemically to younger boninitic series from different regions of the Earth and differ clearly from crust-contaminated MgO-rich melts known as highly siliceous MgO-rich basalts (HSMB) (Fig. 5.8). This geochemical similarity of boninitic series that differ so greatly in age (Late Archean and Late Mesozoic) is probably due only to similarity of their petrogenetic and geodynamic settings. Boninitic series can melt out in an intraoceanic environment if several requirements are met, the most essential being: 1) spreading above an ensimatic subduction zone; 2) the occurrence of a mantle wedge, whose rocks were preliminarily and, as a rule, repeatedly depleted; and 3) high temperatures and shallow depth of melting of such a refractory mantle wedge. Available evidence suggests that such conditions were responsible for the formation of boninitic-series rocks in the subduction complex of the North Karelian GSB ca. 2.8 Ga ago.

Stop 5.5. Cape in W part of the Lake Verzhneye (Fig. 5.1)

A fragment of a Ti-rich ferrobasalt unit with a high percentage of Zr and complex REE profiles (Table 5.1, no.8; Fig. 5.7b). The unit being structurally homogeneous, some horizons with scarce small quartz amygdales are encountered.

The ferrobasalts ($\text{Fe}_2\text{O}_3 > 15\%$) are rich in TiO_2 (up to 3%), Na_2O , P_2O_5 , REE, Zr, Nb, Th and U. Most ferrobasalt samples typically show fractionated REE distribution over the entire range, negative Ti- and Zr-anomalies and a weak variable-sign Nb anomaly at the ratios $(\text{Th} < \text{Nb} < \text{La})_{\text{PM}}$ in this indicator triad. However, some samples exhibit a flatter, complex REE distribution that reflects impoverishment in LREE $(\text{La}/\text{Sm})_{\text{N}} = 0.61$ and the presence of a positive Ce-anomaly, high Th and U content and intense positive Th-, Zr- and Ti-anomalies, the scheme in the indicator triad $(\text{Th} >> \text{Nb} > \text{La})_{\text{PM}}$ being very uncommon for magmatic rocks. Such geochemical characteristics suggest that subducted sediments are involved, produced by destruction of felsic rocks enriched in lithophile and HFSE elements (Kozhevnikov, 2000).

Regardless of whether the geodynamic setting in which STA1 was formed was a back-arc basin (Kozhevnikov, 2000) or an intraoceanic environment (Shchipansky et al., 2004), it should be emphasized that such a complex combination of three different petrogenetic series, including boninites in one unit is direct evidence for subduction, and the occurrence of peridotitic komatiites, superhigh-temperature melts, suggests that the most probable geodynamic setting in which STA1 was generated was interaction between a mantle plume and a gently dipping subduction zone (Kozhevnikov, 2003).

Stop 5.6. South part of Cape in W part of the Lake Verzhneye (Fig. 5.1)

The first rocks to be shown here are intermediate metavolcanics (STA-2). They correspond in composition to low-alumina high-Fe sodic andesite-basalts and andesites (53-64% SiO_2) of both calc-alkaline and tholeiitic series. Based on their petrogeochemical characteristics, the andesites fall into three groups (Table 5.3, Fig. 5.9 A-C). The amygdaloidal andesite unit (andesites-1) consists of biotite-quartz-amphibole-plagioclase schists in which horizons with mafic fragments are distinguished. The unit is highly deformed by axial flow along the dip line of the rocks marked clearly by pencil-like elongation of amygdales and mineral lineation

along the A_c -axis. The degree of deformation, estimated by 3D-measurement of the amygdals, is as high as 800-1400%. Also belonging to this generation of structures are small folds into which andesite flows are thrown. The amygdaloidal andesites have low HFSE and REE levels with poorly fractionated spectra of LREE and HREE, negative Eu anomalies: $(La/Sm)_N = 0.79-1.9$, $(Gd/Yb)_N = 1.5-1.9$, $Eu/Eu^* = 0.82-0.94$ and minor negative Nb- and Ti-anomalies (Fig. 5.9).

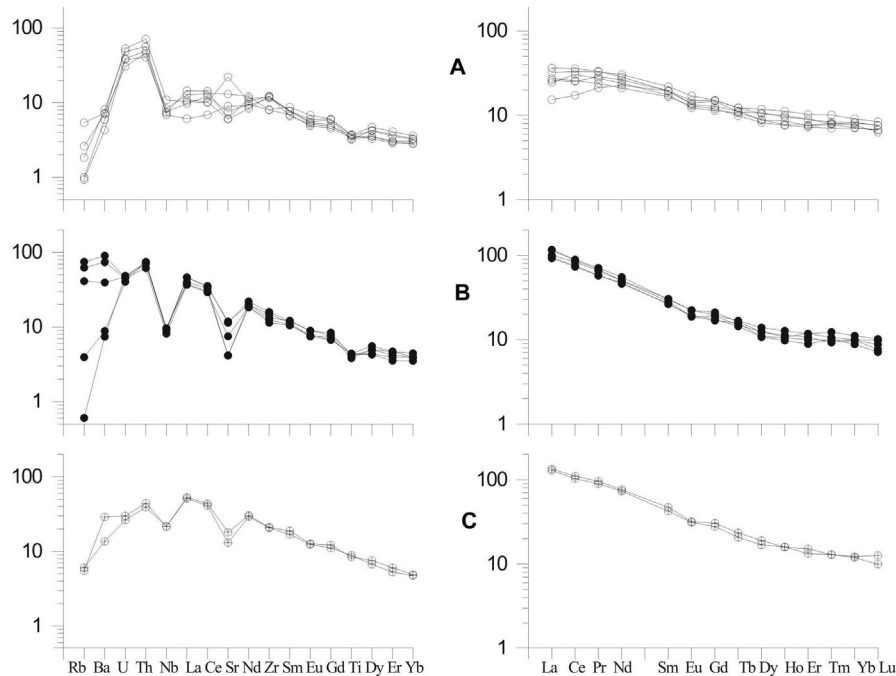


Fig. 5.9. PM-normalized spidergrammes and chondrite-normalized REE distribution in andesites. Numbers on Figs. in Table 5.3.

Stop 5.7. Lake Verzhnee, western part of lakeside (Fig. 5.1)

A fragment of a unit formed by high-Na, low-K, massive, homogeneous andesites of group 2 (Table 5.3). Andesites 2, showing dominantly homogeneous-banded textures, occur in bands that vary in thickness at the northern and southern flanks of the andesite unit. Unlike “primitive” andesites, they contain similar quantities of petrogenic elements, are highly enriched in light lanthanoids: $(La/Sm)_N = 3.3-4.1$, $(Gd/Yb)_N = 1.7-2.1$, $Eu/Eu^* = 0.81-0.92$, have slightly higher percentages of HREE and HFSE and clearly show negative Nb- and Ti- anomalies (Fig. 5.9 C).

Andesites 3, showing well-defined glomeroporphyrpic structures, constitute a thin horizon in the southern part of the andesite unit and have high Fe_2O_3 , TiO_2 , Zr and Nb content, low MgO content and high REE concentrations with moderately fractionated spectra of light and heavy lanthanoids: $(La/Sm)_N = 2.8-3.0$, $(Gd/Yb)_N = 2.3-2.5$, $Eu/Eu^* = 0.84-0.91$ and an indistinct negative Nb-anomaly.

Table 5.3. Representative compositions of main types of andesites on STA 2.

No. sample	1 X-7/96	2 X-27-2/96	3 X-28/96	4 K-78/97
SiO ₂	53.31	62.70	57.60	57.27
TiO ₂	0.85	0.86	0.63	1.62
Al ₂ O ₃	15.60	13.51	14.40	14.05
Fe ₂ O ₃	14.17	10.08	10.24	13.17
MnO	0.16	0.15	0.17	0.18
MgO	6.19	3.40	5.18	3.18
CaO	4.95	4.60	5.78	5.39
Na ₂ O	4.44	4.45	5.70	4.69
K ₂ O	0.13	0.09	0.09	0.21
P ₂ O ₅	0.19	0.15	0.21	0.23
Li	20.1	8.21	9.72	14.8
Sc	22.7	22.5	26.4	17.1
Ti	4770	4800	3505	9147
V	214	205	161	138
Cr	27.6	8.62	91.5	34.5
Co	40.9	28.6	40.7	47.3
Ni	47.6	23.4	52.3	65.9
Cu	69.2	87.2	12.2	158
Zn	131	127	69.6	152
Ga	21.7	19	18.8	20.3
Rb	2.11	0	1.39	2.95
Sr	76	76	164	329
Y	16	18	17.9	24.6
Zr	133	134	105	155
Nb	6	6	4.24	13.3
Cs	0	0	0	0
Ba	54	45	42.8	175
La	23.3	24.6	3.75	32.8
Ce	48.1	53.3	11.0	70.3
Pr	5.61	6.33	2.04	9.23
Nd	21.8	23.8	10.8	36.10
Sm	4.14	4.71	2.98	7.28
Eu	1.09	1.30	0.804	1.85
Gd	3.45	4.00	3.02	6.24
Tb	0.589	0.629	0.410	0.881
Dy	2.78	3.54	2.72	4.84
Ho	0.597	0.723	0.543	0.900
Er	1.66	1.95		2.52
Tm	0.252	0.316	0.214	0.332
Yb	1.62	1.84	1.37	2.03
Lu	0.196	0.259	0.192	0.322
Hf	2.85	3.34	2.84	5.18
Ta	0.368	0.408	0.196	0.750
Pb	5.08	7.04	4.97	5.08
Th	6.08	6.02	3.76	3.60
U	0.821	0.989	0.622	0.610
La/Yb _N	9.71	9.02	1.85	10.91
La/Sm _N	3.54	3.29	0.79	2.84
Gd/Yb _N	1.72	1.76	1.78	2.48
Eu/Eu*	0.88	0.92	0.82	0.84

Note: recalculated to 100% on a volatile-free basis.

1-2 -andesites 1; 3- andesites 2; 4 - andesites 3.

Stop 5.8. Lake Verzhnee, South part of lakeside (Figs. 5.1 and 5.10)

A detailed site on the southern shore of Lake Verkhneye, where two andesite horizons (A1 and A2) and two quartz arenite horizons (Q1 and Q2) occur.

Resting on disintegrated weathered glomeroporphyric andesite A1 is a paleoregolith with a fractionated REE distribution pattern and negative Ce-anomaly and a ca. 20 cm thick quartz conglomerate bed that passes gradually into fine-pebble arenites with poorly rounded white quartz pebbles. The matrix is formed by grey quartzite, consisting of quartz grains with plagioclase and biotite impurities, which suggests a low textural and mineralogical maturity of the rock. Distinguished in andesite unit A2 are two flows; their massive lower part passes upwards into pyroclastic breccia. On the massive part of flow 3 is a second 7 m thick quartzite horizon. The second Q2-horizon rests with a sharp contact on weathered andesites A2. Its rocks typically show a yellowish colour produced by the presence of finely dispersed iron sulphides; - thin parallel lamination deformed locally to produce small-scale corrugation; - a dominantly sand and finer size of quartz grains and scarce 10-15 cm thick horizons that contain fine (<1 cm) quartz pebbles; - and ca.10-15 cm thick muscovite-enriched horizons responsible for the rhythmic structure of the horizon. On quartz rocks Q2 there is a carbonaceous kyanite-mica shale seam.

Active overthrusting that caused the twinning of the andesite-quartz arenite unit at this point is documented by schistosity and mineral and aggregate A-lineation zones with a well-defined kinematic indicator – quartz pebbles, elongated along lineation, in gravelstones.

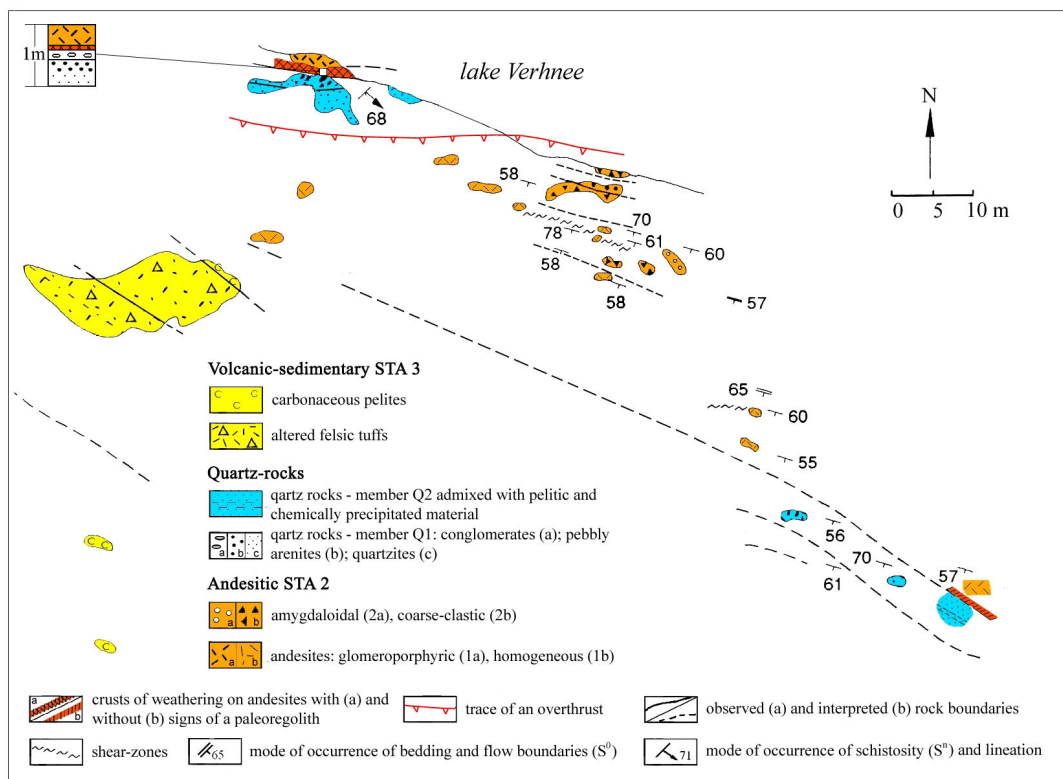


Fig. 5.10. Structure of the transition zone of andesitic STA2 and volcanic-sedimentary STA3 at Stop5.8.

Geochemistry of the quartz arenites. The percentages of petrogenic and rare elements in the sand- and pebble-sized quartz arenites from two parts of quartite unit Q are shown in Tables 5.4 and 5.5.

Table 5.4. Average chemical composition of quartz arenites from the Khizovaara structure in comparison with similar rocks from some other Archean regions.

No	1	2	3	4	5	6	7	8
Sample	X-10	X-4	X-9	X-1	X-22	X-3	X-8	X-49
SiO ₂	94.4	94.5	92.13	95.97	87.02	88.65	92.11	93.45
TiO ₂	0.04	.05	0.06	0.02	0.1	0.26	0.07	0.04
Al ₂ O ₃	2.21	2.44	4.34	2.24	4.47	7.71	4.58	4.07
Fe ₂ O ₃	1.58	1.4	1.07	0.79	1.95	0.7	1.09	0.55
MnO	0.02	0.02	0.01	0.01	0/08	0	0.01	0.02
MgO	0.42	0.35	0.31	0.2	2.47	0.44	0.88	0.27
CaO	0.43	0.26	0.26	0.07	2.98	0.1	0.09	0.14
Na ₂ O	0.76	0.46	0.98	0.04	0.07	0.36	0.24	0.17
K ₂ O	0.15	0.42	0.83	0.65	0.83	1.76	1.01	1.24
P ₂ O ₅	0.02	0.05	0.02	<0.01	0.02	0.01	0.01	0.03
SiO ₂ /Al ₂ O ₃	42.7	38.8	21.2	42.8	19.5	11.5	20.1	23
K ₂ O/Na ₂ O	0.2	0.9	0.8	16.2	11.9	4.9	4.21	7.3
Al ₂ O ₃ /Na ₂ O	2.9	5.3	4.2	56	63.9	21.4	19.1	23.9
CIA	52	63	62	71	n.d.	74	73	69

Recalculated on an anhydrous basis, *N* = number of analyses.

1-4 = Khizovaara quartz rocks: quartzites of members Q1 (1) and Q2 (2); pebbly quartz arenites, members Q1 (3) and Q2 (4); 5-8 = quartz arenites from the Keewaywin (5) and Keeyask Lake Formations (6) in the Sandy Lake greenstone belt, Sachigo subprovince, Superior craton; Pongola Supergroup (7), Kaapvaal craton; Yavannahalli greenstone belt, Dharwar craton, India (references see on Thurston & Kozhevnikov, 2001).

The percentages of some major constituents, such as SiO₂, Al₂O₃, Fe₂O₃, FeO, CaO, Na₂O and K₂O, vary considerably. The percentages of TiO₂ and MgO are less variable. Khizovaara quartzites are richer in SiO₂, CaO, and Na₂O and poorer in Al₂O₃ and K₂O than quartzites

Table 5.5. Trace element geochemistry (ppm) of of quartz-rich rocks from Khisovaara.

No	1	2	3	4	5	6	7	8
La	1.12	1.96	0.70	7.53	4.31	8.17	6.14	21.11
Ce	2.59	4.35	1.67	15.48	9.50	13.95	11.21	43.54
Pr	0.33	0.52	0.22	1.84	1.06	1.93	1.28	5.04
Nd	1.25	1.96	0.90	6.67	3.73	6.74	4.72	18.02
Sm	0.27	0.40	0.22	1.17	0.68	1.12	0.85	2.99
Eu	0.06	0.08	0.05	0.21	0.16	0.16	0.19	0.69
Gd	0.22	0.33	0.19	0.91	0.55	0.89	0.74	2.21
Tb	0.03	0.04	0.02	0.13	0.07	0.11	0.11	0.30
Dy	0.18	0.22	0.13	0.61	0.34	0.56	0.58	1.30
Ho	0.03	0.04	0.03	0.12	0.06	0.11	0.11	0.22
Er	0.11	0.13	0.10	0.33	0.18	0.32	0.37	0.58
Tm	0.02	0.02	0.02	0.04	0.02	0.04	0.06	0.08
Yb	0.17	0.15	0.17	0.34	0.25	0.39	0.50	0.58

Lu	0.03	0.03	0.04	0.06	0.04	0.06	0.08	0.10
ΣREE	6.41	10.23	0.46	35.44	20.95	34.55	26.94	96.76
La_N/Yb_N	4.32	8.82	2.78	14.95	11.64	14.11	8.29	24.57
La_N/Sm_N	2.61	3.09	2.00	4.05	4.00	4.60	4.55	4.44
Gd_N/Yb_N	1.02	1.78	0.90	2.16	1.78	1.84	1.20	3.08
Eu/Eu*	0.75	0.67	0.75	0.62	0.80	0.49	0.73	0.82
Th	4.38	2.84	3.32	9.33	8.46	10.62	6.35	9.82
U	1.24	0.71	1.12	1.78	1.78	2.22	1.64	2.69
Th/U	3.5	4.0	3.0	5.2	4.8	4.8	3.9	3.7
Zr	60	62	112	82	57	56	206	110
Cr	41	58	65	37	59	59	74	74

from other Archean regions. They show higher $\text{SiO}_2/\text{Al}_2\text{O}_3$ ratio and lower $\text{K}_2\text{O}/\text{Na}_2\text{O}$ ratio. Their chemical index of alteration, CIA, is markedly lower than that of rocks from other Archean regions. All this shows that Khizovaara quartz rocks are less mature chemically. Such an unusual combination of the chemical immaturity of rocks with a very high percentage of SiO_2 is largely responsible for their trace element geochemistry. Khizovaara rocks exhibit low ΣREE content, varying fractionated LREE distribution, the V-shaped profile of HREE and a negative Eu-anomaly ($\text{Eu}/\text{Eu}^* = 0.49\text{--}0.82$) typical of post-Archean sedimentary rocks that have a lower Eu/Eu^* value (0.67) than the Archean Eu/Eu^* value (≥ 0.85) (Mc Lennan et al., 1984, 1990; Taylor, 1979). Th and U distribution seems to be controlled largely by heavy minerals, primarily zircon. For example, one sample contains abnormal quantities of some trace elements: Zr = 933 ppm, Th = 338 ppm, Y = 57 ppm and Pb = 72 ppm. The rocks generally have small quantities of Zr (56–101 ppm, aver. = 75 ppm, n = 12) and Y (4–11 ppm, aver. = 6.5 ppm, n = 12) and varying amounts of Cr (42–581 ppm, aver. = 235 ppm). This, together with V-shaped HREE distribution, shows that the matrix of the quartz arenites contains impurities produced by destruction of ultramafic rocks (Fig. 5. 11).

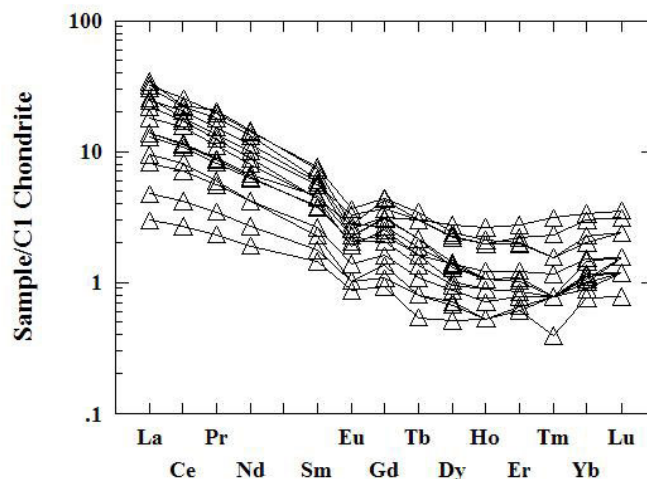


Fig. 5.11. Chondrite-normalized REE distribution in quartz arenites.

The study of detrital zircons from these rocks has shown that they originated from several sources dated at $3152 \pm 4.6\text{Ma}$, $2832 \pm 6 - 2811 \pm 7\text{Ma}$, $2747 \pm 5 - 2705 \pm 10\text{Ma}$ and $2687 \pm 11 - 2651 \pm 3.5\text{Ma}$ (Kozhevnikov et al., 2006). In addition, hydrothermal high-U zircon grains, dated at $2486 \pm 6 - 2435 \pm 8\text{Ma}$, were revealed. The goal of this trip is to show some exposures and the sequence of geological events determined by detailed mapping of the area, where rocks of STA 2, 3 and 5 occur.

Stop 5.9. Lake Verzhnee, 200 m to SW from the western lakeside (Figs. 5.1 and 5.12)

Exposures of amygdaloidal and homogeneous andesites overlain with a direct contact by quartz arenites. The contact is disintegrated, the andesites show signs of weathering documented by a positive Ce-anomaly in the case of a fractionated REE trend and a negative anomaly in the case of their non-fractionated distribution. The latter is a typomorphic character of tholeiitic-series andesites that constitute a large part of STA2.

Stop 5.10. Lake Verzhnee, 800 m to NW from the western lakeside (Figs. 5.1 and 5.12)

A series of exposures of the following rock sequence:

Amygdaloidal andesite-basalts and glomeroporphyric porphyrites of andesite-basalt composition (andesites 3) – a direct contact with quartz arenites with signs of hummocky cross-bedding – amphibolized clastic rocks. Visitors will see a gabbro diorite dyke that intersects quartz arenites in which recrystallized quartz veinlets are observed. The dyke was metamorphosed to epidote-amphibolite grade, but was not affected by earlier recrystallization processes. The lineation in the dyke agrees with the general lineation of the structure.

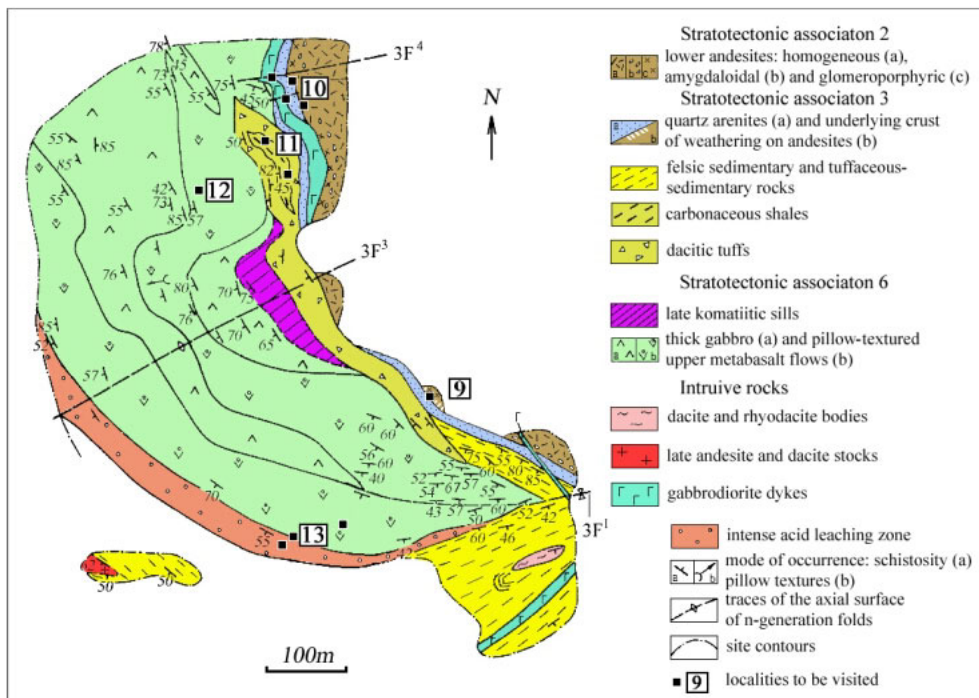


Fig. 5.12. Geological map of detailed area I, Khizovaara structure (Kozhevnikov, 1992).

Stop 5.11: Lake Verzhnee, 950 m to NW from western lakeside (Figs. 5.1 and 5.12)

Some exposures of gently sloping carbon-rich (4-8%) shales contain a cryptocrystalline form of graphite, a lower-temperature modification of carbon. These rocks carry abnormal quantities of Zn, Au and Cu. As the percentage of carbon decreases considerably (0.7-3%) and passes into a higher-temperature modification, hypocrySTALLINE graphite, in steep near-N-S

multiple foliation zones, the concentrations of all trace elements are observed to decline. In the intermediate zone both forms of carbon coexist.

Stop 5.12: Lake Verzhnee, 1100 m to W from western lakeside (Figs. 5.1 and 5.12)

A rhyodacite dyke, less than 1 m thick, will be shown in exposed pillow tholeiitic basalts of STA6. The dyke is dated at 2706 ± 7 Ma. Furthermore, visitors will see a thick (over 100 m) flow. Its lower, thickest part is composed of gabbro-amphibolite that passes upwards into a finer-grained variety. The top of the flow is clearly pillow-textured. The mafic STA6 is made up of tholeiitic basalts, indistinguishable geochemically from the above tholeiitic basalts of STA1 (Table 5.1), which is also reflected in REE distribution and the spidergrams (Fig. 5.7). This, together with structural and other geological data, shows that STA6 has an allochthonous nature and it is cogenetic with mafic rocks of STA1.

Stop 5.13: Lake Verzhnee, 500 m to W from western lakeside (Figs. 5.1 and 5.12)

A pillow basalt unit, in which thin flows consist of two members. Its lower, more massive portion is formed of homogeneous medium-grained rocks consisting of hornblende, plagioclase (40% An) and opaque minerals. The flow top exhibits pillow textures. The pillows are commonly flat, the long to short axis ratio in sections normal to lineation being 4-7. Chill zones consist of monomineral hornblende, and their core has quartz-filled gas vesicles are observed. Evolving along some zones are chlorite, carbonate, cummingtonite and garnet. When approaching a thick shear-zone at the contact zone of the mafic unit in some outcrops, the degree of deformation of the pillows increases gradually, accompanied by metasomatic transformation of flow tops. There the rock acquires andesitic-basaltic to andesitic composition. In the most intense alteration zone, the rocks are altered to quartz-kyanite-staurolite-garnet rock in which only the chill zones of the pillows, formed of amphibole, persist as shadows.

Mesoarchean lake Keret greenstone complex, Belomorian province

A.I. Slabunov, Institute of Geology, Karelian Research Centre, RAS (Petrozavodsk)

The purpose of the field trip is to show Mesoarchean (2.88-2.82 Ga) highly metamorphosed volcanogenic and sedimentary rocks in the Keret greenstone structure of the North Karelian greenstone belt. **The Keret structure** (Fig. 5.13) is part of the North Karelian greenstone belt (NKGSB). It is made up of two different-aged greenstone complexes (Slabunov, 2001): the 2.88-2.83 Ga Lake Keret complex and the 2.8–2.78 Ga Khizovaara complex. The latter has already been shown earlier to the group in the Khizovaara structure.

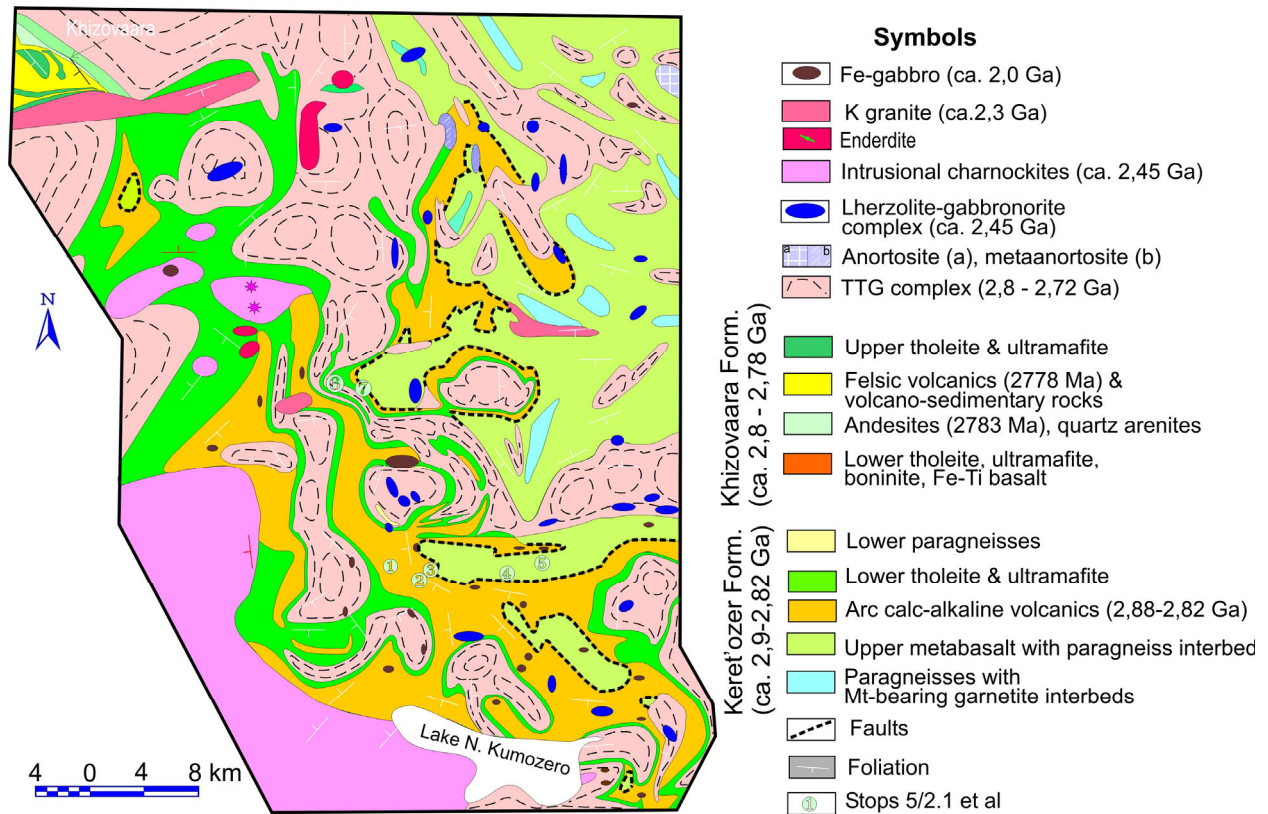


Fig. 5.13. Geological map of the northern Keret greenstone belt (Slabunov, 2005)

The Lake Keret complex consists of three mappable STA (or suites): Verkhneye Kumozero, Khat-tomozero and Maiozero (Slabunov, 1990), formed of komatiitic-tholeiitic, differentiated andesitic-basaltic-andesitic-rhyolitic and andesitic-basaltic-basaltic rock associations.

Komatiitic-tholeiitic association. It is strongly dominated by metabasalts. They belong chiefly to sodic-series tholeiites. In binary diagrams of MgO – oxides the figurative points of their compositions form a trend similar to the Fennerian trend (Slabunov, 1993). Their REE content (Table 5.13, analyses 1, 2) is 8-14 times that of chondrite, and the REE distribution of most rocks shows a nondifferentiated pattern with a small Eu-minimum, but some of the samples are considerably depleted in LREE. Metabasalts typically have no Nb- and Ti-anomalies but display a negative Th-anomaly. Consequently, they are correlatable with oceanic plateau basalts.

The HREE content of the best-preserved komatiitic-series rocks of this association is three times and the LREE content 10 times that of chondrite; the Eu-minimum is indistinct (Table 5.13, an 3). Rocks that have such a composition could have been formed in a mantle plume upon melting of an undepleted garnet-free mantle substrate at a depth of 75–120 km with subsequent fractionation of (mainly) olivine. Enrichment of komatiites in LREE is presumably due to the compositional characteristics of the mantle source (Vrevsky, 2000).

The komatiitic-tholeiitic rock association of the greenstone complex was formed most probably in an oceanic environment under the influence of a mantle plume.

Table 5.6. Chemical composition of Mesoarchean rocks from the Lake Keret greenstone complex

	1	2	3	4	5	6	7	8	9	10	11
<i>Sample</i>	<i>450-2</i>	<i>450-10</i>	<i>416-5</i>	<i>455-1</i>	<i>329-6</i>	<i>329-7</i>	<i>311-9</i>	<i>883-4</i>	<i>8A-1</i>	<i>989-1</i>	<i>12</i>
SiO ₂	48.80	48.80	47.96	64.20	56.40	53.10	46.60	53.56	70.13	71.10	62.28
TiO ₂	0.98	1.04	0.30	0.41	0.74	1.11	1.03	0.70	0.48	0.25	0.48
Al ₂ O ₃	15.14	15.77	6.32	16.27	16.07	16.70	14.51	14.23	15.96	14.53	15.68
Fe ₂ O ₃	2.93	2.16	4.66	1.90	3.71	9.45*	3.49	1.80	0.77	0.86	1.13
FeO	11.38	11.15	7.22	2.87	4.49		12.33	7.11	1.88	2.01	4.02
MnO	0.14	0.19	0.26	0.08	0.16	0.23	0.52	0.12	0.02	0.03	0.10
MgO	7.05	6.96	29.03	2.77	4.14	4.32	7.06	8.06	1.12	0.90	3.73
CaO	8.54	9.45	4.07	4.35	8.14	9.88	11.43	9.81	3.41	3.08	5.19
Na ₂ O	2.81	2.25	0.11	4.67	3.76	3.67	1.04	2.25	4.88	4.79	4.53
K ₂ O	0.28	0.23	0.02	1.50	0.98	0.76	0.23	0.61	0.98	1.53	1.33
P ₂ O ₅	0.10	0.17	0.06	-	-	0.34	-	-	0.36	-	0.35
H ₂ O	-	0.01	-	0.11	0.03	-	0.04	0.10	0.18	0.39	0.20
CO ₂	0.07	0.07	-								
loi	1.58	1.68	-	0.87	1.01	0.50	1.95	1.21	0.42	0.26	0.97
sum				100	99.63	100.06					
Cr	286	293	1800	170	143	112	230	400	73	-	102
Ni	68	89	850	46	30	28	100	80	11	-	53
Co	57	54	130	22	37	22	32	42	6	-	12
V	416	309	82	60	206	225	340	230	69	-	85
Cu	-	-	83	-	-	33	100	76	30	-	9
Zn				-	-	104	-		45	-	72
Sn				-	-	1.08	-		0.49	-	1.16
Mo				-	-	3.28	-		1.01	-	0.74
Rb	5	3	1	45	15	6	6	2	35	56	30
Cs				2.8	2.8	-				-	1.88
Ba	30	-	-	450	366	159	60	90	343	-	507
Sr	53	72	134	800	630	579	50	270	533	-	465
Ga				-	-	22	-		12	-	23
Li				16	7	-				-	25.50
Ta				-	-	0.43	-		0.27	-	0.19
Nb	-	-	5.0	-	4.0	4.5	-	-	4.0	-	4.7
Hf				-	-	2.94	-		3.58	-	1.91
Zr	43	47	38	104	101	120	49	65	104	-	91
Y	20	20	12	24	18	21	21	18	5	-	7
Th				-	3.00	2.88	-	-	3.26	-	2.92
U				-	-	0.72	-	-	0.55	-	0.15
La	1.80	4.60	3.90	26.00	25.00	34.60	3.50	-	14.96	12.00	15.90
Ce	5.40	8.80	8.60	52.00	54.00	73.10	6.30	-	25.20	24.00	30.80
Pr				-	-	10.60	-	-	2.99	-	3.25
Nd	5.00	-	-	-	-	43.80	-	-	10.01	-	15.40
Sm	1.80	2.40	1.50	4.10	6.00	8.47	2.30	-	1.36	2.10	2.35
Eu	0.51	0.61	0.41	0.90	1.30	2.44	0.44	-	0.98	0.42	0.88
Gd				-	-	6.43	-		0.69	-	2.32
Tb	0.55	0.51	0.27	0.41	1.00	0.87	0.54		0.18	0.20	0.30
Dy				-	-	3.80	-		0.69	-	1.79
Ho				-	-	0.73	-		0.07	-	0.21
Er				-	-	2.26	-		0.69	-	0.77
Tm				-	-	0.29	-		0.12	-	0.12
Yb	2.20	2.10	0.80	0.90	1.40	2.08	2.00		0.26	0.27	0.72
Lu	0.35	0.34	0.11	0.13	0.26	0.28	0.29		0.05	0.04	0.04

1, 2 – metabasalts, Verkhneye Kuzozero STA; 3 – metakomatiite; 4-6 – Khatomozero STA; 4 - neck-facies meta-dacite; 5-6 - tuffic facies of metaandesite-dacite; 7-9 - Maiozero STA 7 - metabasalt, 8 andesitic basalt; 9 – meta-sediment; 10-11 – TTG association

The differentiated andesitic-basaltic-andesitic-rhyolitic association is most common in the belt. It is referred to as the Khattomozero STA. As the U-Pb age of zircon from metatuffs of andesite composition is 2877 ± 45 Ma and that of neck-facies metadacite 2829 ± 30 Ma (Bibikova et al., 19996), the age of the association is 2.88–2.83 Ga. As volcanics often retain relics of agglomeratic, banded textures (Fig. 5.14), the rocks are reliably identified as tuffs. Furthermore, lava and neck facies are occasionally encountered. On petrochemical classification figurative composition points (Table 5.6) are chiefly in the potassic-sodic- and sodic-series calc-alkaline, intermediate- to felsic volcanic field. Andesites and dacites dominate.

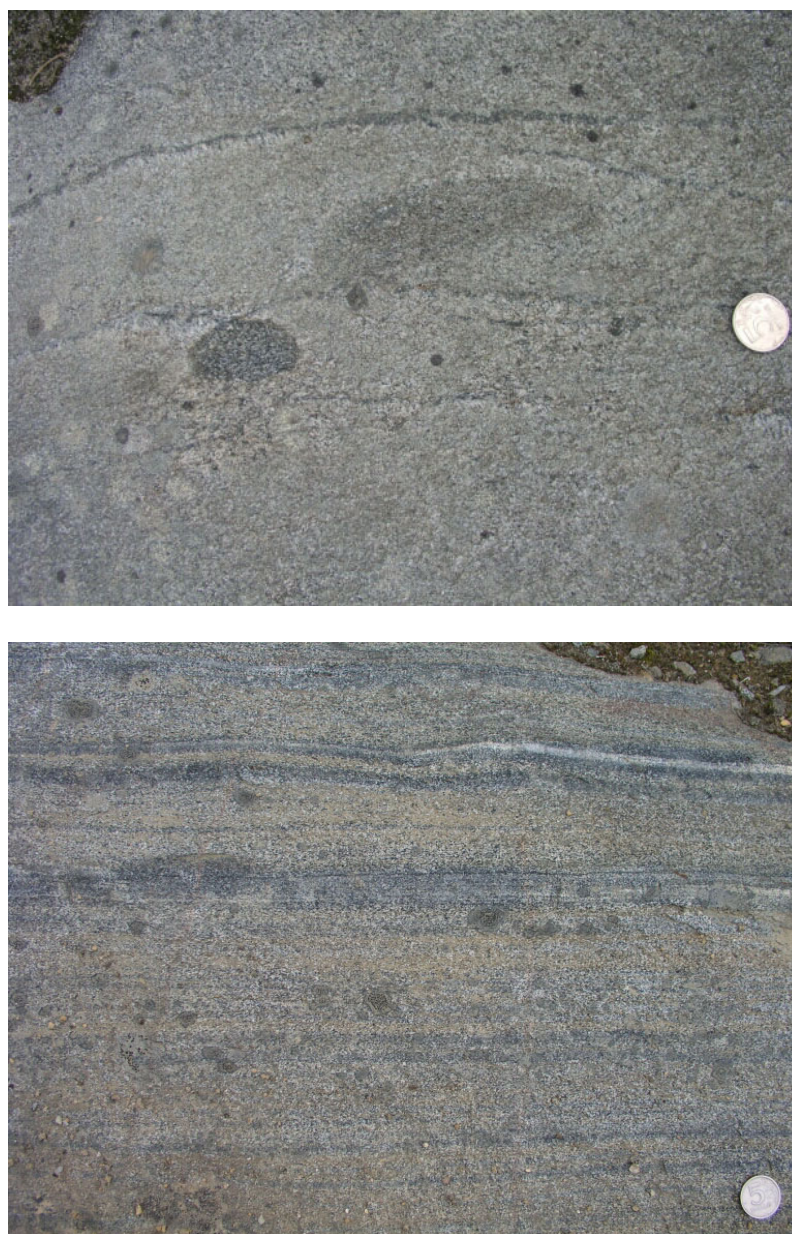


Fig. 5.14. Neck (a) and tuffic facies (b) of metaandesite-dacite of Khattomozero STA

The REE distribution spectrum for the rocks of the association discussed is highly differentiated $(La/Yb)_N \approx 10-30$; the percentages of LREE are 50–100 times, those of intermediate REE 12–30 times and those of HREE 6-8 times those of chondrite for andesite-basalts and andesites and about 4 times for dacites. Eu-minimum is indistinct. The distribution patterns of the normalized rare element

content of the rocks of the associations described and typical modern island-arc volcanics are fairly similar, including the presence of Nb-minimum.

The isotopic composition of Nd in the metaandesite of the association discussed ($\epsilon_{\text{Nd}}(2.85 \text{ Ga}) = +2.8$; $t_{\text{DM}} = 2800 \text{ Ma}$) suggests a juvenile nature of the volcanics and the absence of contamination by older crustal matter. Compositional correlation of Khattomozero volcanics with intermediate to felsic volcanics from modern subduction systems shows that they are most similar to calc-alkaline rocks from well-developed island-arcs.

The *andesite-basaltic-basaltic association* and metagraywacke and less common metamorphosed Fe-quartzite interbeds therein form the Maiozero STA (Fig. 5.15 a, b). The metavolcanics (amphibolites) of the unit are classified petrochemically as dominantly sodic- and potassic-sodic-series tholeiites (Table 5.6). At the same time, calc-alkaline-series andesite-basalts play a significant role in this association. Identified in the STA are ultrabasic rock bodies.



Fig. 5.15 a, b Amphibolites with garnet-diopside-epidote-plagioclase rock layers are poor relict of pillow-basalts (a), metagraywacke (b) of Maiozero STA.

Basaltoids of such a composition could have been generated by crystallization differentiation of moderately MgO-rich basalt melts in magmatic chambers at different depths. One chamber was located at a relatively shallow depth, and the other at a depth of at least 22 km (Slabunov, 1990). The REE content of the metabasalts is 8–20 times that of chondrite, and their REE distribution displays a nondifferentiated pattern, but with a well-defined Eu-minimum and relatively high percentages of Sm, Eu and Tb.

To cast light on the geodynamic setting in which the volcanics were formed, the composition of associated metasediments was analysed. Paragneiss horizons are mapped among the basaltoid of the Maiozero association (Slabunov, 1993; 2006). As they have not retained relics of primary sedimentary structures and their sedimentary textures are indistinct, a genetic classification of sedimentary rocks is not applicable to them, but a petrochemical classification can be applied (Neyelov, 1980; Pettijohn et al., 1973).

In the classification diagram $\lg(\text{SiO}_2/\text{Al}_2\text{O}_3) - \lg(\text{Na}_2\text{O}/\text{K}_2\text{O})$ (Pettijohn et al., 1973), the figurative points of paragneiss composition (Table 5/2.1) are plotted in the graywacke field. Calculations show that they could have been formed by mixing of the material that came from the source area and contained clasts corresponding in composition to basalts (ca. 50% of the mixture), felsic volcanics (45%) and komatiites (up to 5%).

The position of the figurative points of Maiozero metasediment (graywacke) composition in the discrimination diagrams of Th–Co–Zr, La–Th–Sc, Th–Sc–Zr and Th–La (Bhatia, 1983; Bhatia, Crook, 1986) corresponds mainly to the sedimentary rock fields formed in oceanic island-arc (less commonly continental island-arc) environments. Available data on the composition of Maiozero STA rocks, which includes volcanics of the andesite-basaltic-basaltic association and graywackes, thus show that it was formed in the frontal part of a volcanic island arc probably almost simultaneously with the differentiated andesite-basaltic-andesitic-rhyolitic association.

Rocks of the Keret greenstone structure were metamorphosed chiefly to epidote-amphibolite to amphibolite grade at pressures of 5-6 kbar.

Stop 5.14. Lake Zimneye (Fig. 5.13)

Exposures of amphibolites of the Upper Kumozero STA. The lower part of the STA unit is dominated by epidote and diopside amphibolites and the upper part by garnet amphibolites with biotite and less common chlorite and carbonate. Varieties with hornblende porphyroblasts are occasionally encountered. Table 5.6 (analyses nos. 1-7) shows the chemical composition of typical amphibolites from this unit.

Stop 5.15. Lake Severnoe Zhattamozero, western part (Fig. 5.13)

A group of exposures, composed of banded (epidote-biotite)-amphibole schists in which relics of agglomeratic texture are encountered. Varieties with relics of banded texture are common. These are overlain by amphibolites of the Maiozero STA. The contact between the STA's is tectonic.

Stop 5.16. Lake Severnoe Zhattamozero, NW part (Fig. 5.13)

Epidote-amphibole-biotite schists (metadacites) of the Khattomozero STA. Metadacites (for chemical analysis, see Table 5.6, no.5) are represented by grey, homogeneous, medium-

grained rocks with small scarce amphibolite and schist xenoliths. The schists clearly show lineation after amphibole. Zircons from these rocks were used for U-Pb dating of volcanism. The age of the zircons is 2829 ± 30 Ma (Bibikova et al., 19996).

Stop 5.17. River Verzhneye Kumozerka (Fig. 5.13)

Exposures of Maiozero STA paragneisses. A paragneiss (metagraywacke) horizon is traced in amphibolites throughout the entire Maiozero structure (Fig. 5.13). Paragneiss is represented by (kyanite-muscovite)-garnet gneiss with relics of primary sedimentary structure. The chemical composition of these metasediments is shown in Table 5.6 (analysis no. 9). Occurring in them is a sill-like amphibolite body with large garnet porphyroblasts. The amphibolites correspond in composition to Fe-rich basic rock.

Stop 5.18. Lake Chelozero (Fig. 5.13)

Amphibolites of the Maiozero STA are represented here by (epidote-diopside)-garnet varieties. They typically show a medium-grained, often porphyroblastic structure and a banded texture. The latter has developed by metamorphic alteration and deformation of pillow basalts. There are many lens-shaped garnet-diopside-epidote-plagioclase rock bodies among the amphibolites.

Stop 5.19. Pervoe Nogtevo Lake area (Fig. 5.13)

In the hinge zone of the Lake Nogtevo structure banded medium-grained amphibolites of the Upper Kumozero STA are in contact with the gneissose granites of the TTG-complex. The granite-gneisses of the TTG-complex vary in composition from quartz diorites to trondhjemitites (Table 5.6, analyses nos. 10, 11). Zircons from the quartz diorites are dated at 2803 ± 13 Ma, and their model Sm-Nd age is 2.9 Ga (Bibikova et al., 19996). It is the oldest constituent of the complex.

Stop 5.20. Leshevo Lake area (Fig. 5.13)

A series of exposures of grey (garnet-epidote)-biotite-amphibole schists (metatuffs) that vary in composition from andesite-basalt to andesite (Table 5.6, analyses nos. 5-6) and dacite. Horizons with relics of an agglomeratic texture were reported. The age of zircons from the agglomeratic tuffs of andesite composition is 2877 ± 45 Ma (Bibikova et al., 19996). Epidote-enriched lenticular aggregates are common. Amphibolization zones that cut banding are encountered.

Day 6, Saturday 2.8. 2008

Drive from Kalevala to Kostomuksha (ca. 100 km). TTG association, sanukitoids, granulites of the West Karelian terrain, Archean oceanic plateau and the island arc-type Kostomuksha greenstone belt with economic BIF-deposits.

Kostomuksha area

A.V. Samsonov¹ and A.A. Shchipansky²

¹ Institute of Ore Geology, Petrography, Mineralogy and Geochemistry (IGEM), RAS (Moscow), ² Geological Institute (GIN), RAS (Moscow)

The purpose of the Day 6 is to show Archean volcanic-sedimentary rocks of the Kostomuksha greenstone belt and granitoids of the TTG association, high-Mg granitoids (sanukitoids), lamprophyres and low-pressure granulites of the eastern West Karelian terrain of the Karelian craton.

Introduction

The Neoproterozoic Karelian craton, across which the group will drive, consists of the Central Karelian and West Karelian terrains (Slabunov et al., 2006). The Kostomuksha greenstone belt and associated syn- and post-tectonic granitoids are in the eastern part of the latter, near its eastern boundary (Fig. 6.1). The West Karelian terrain also includes low-pressure granulites of the Voknavolok block.

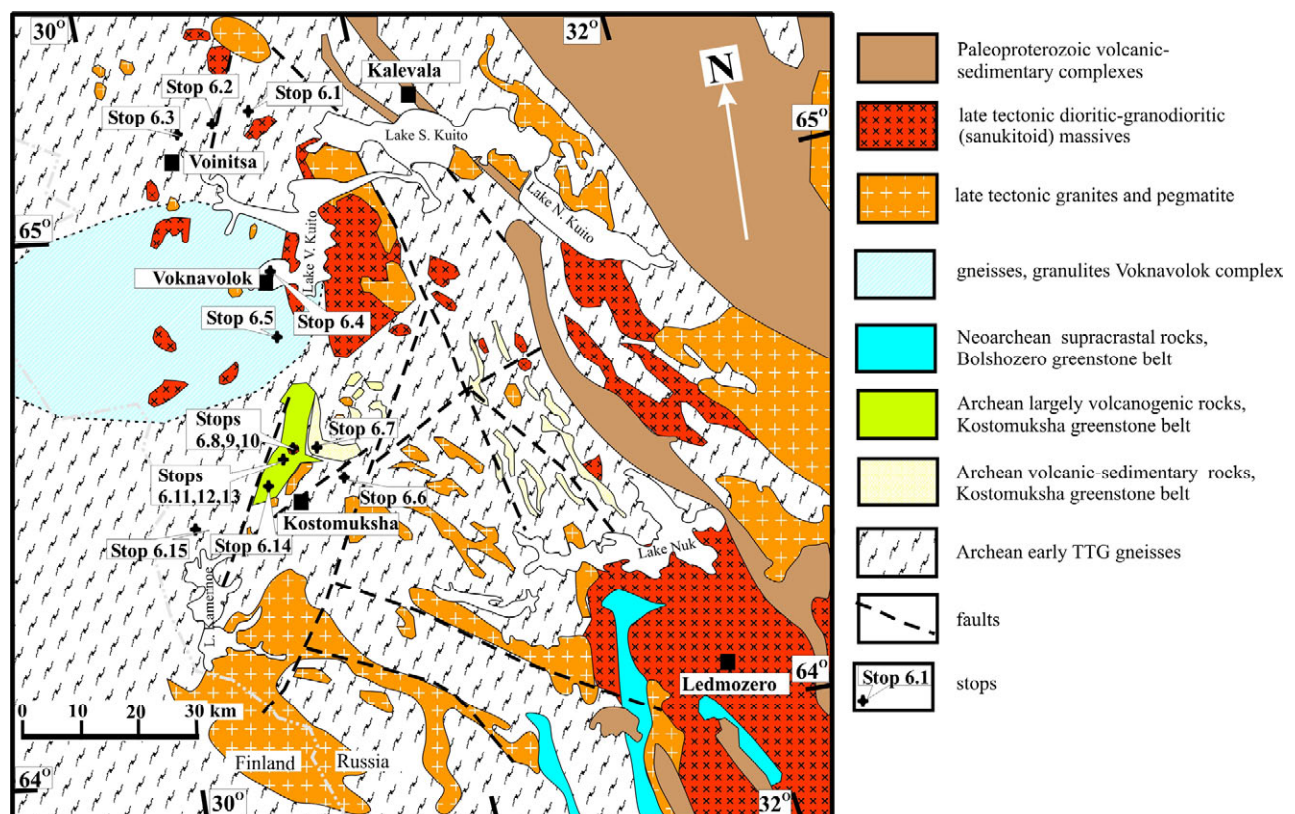


Fig. 6.1. Scheme showing the geological structure of the central Karelian craton, Kostomuksha-Kalevala area (Bibikova et al., 2005; Kostinen et al., 2001; Samsonov et al., 2001).

Volcanic-sedimentary rocks of the Kostomuksha structure

The Kostomuksha greenstone belt is the largest fragment of supracrustal rocks in the region. It includes two large lithostratigraphic units (series) (Fig. 6.2): 1) the largely volcanogenic Kontokki series and 2) the volcanic-sedimentary Gimoly series (Rayevskaya et al., 1992). Geologists are not unanimous about the relationship between rocks of these series (see be-

low). Metavolcanics of the Kontokki series make up the western flank of the structure and comprise an early basaltic-komatiitic association and a later dacitic-rhyolitic association.

Volcanics of a basalt-komatiite association build up the western part of the structure. Their structural pattern (Rayevskaya et al., 1992; Kozhevnikov, 2000, Kozhevnikov et al., 2006) and isotopic-geochemical characteristics (Lobach-Zhuchenko et al., 2000; Puchtel et al., 1997, 1998, 2001) are well understood. The association is dominated by tholeiitic metavolcanics altered to feldspathic-amphibole and epidote-feldspathic-amphibole schists with scarce thin magnetite-bearing schist and quartzite horizons. In spite of metamorphic alterations, primary volcanogenic textures are well-preserved in the metavolcanics throughout the unit. Pillow metalava is widespread (Stops 6.11 and 6.12), whereas massive, variolitic varieties and hyaloclastite horizons are less common. Sills of fine- to medium-grained gabbro, comagmatic with tholeiitic lava, are also quite common in the Kontokki series, and are considered as an integral part of its column (Fig. 6.3). Komatiites seem to make up not more than 20% of the total volume of volcanics in the association (Puchtel et al., 1997). Komatiites form both differentiated lava flows and undifferentiated sills composed of of peridotite. Pillow varieties of komatiitic lava are occasionally encountered. Thin horizons of komatiitic ash and lapilli tuffs in the Kontokki series are scarce (Stop 6.10; Gorkovets & Rayevskaya, 1983). Members of komatiitic lava flows, totalling up to 200 m in thickness, are occasionally encountered among associated tholeiites and gabbroid sills. Individual differentiated komatiitic lava flows vary in thickness from 0.5 to 6 m. Most lava flows display a classical textural differentiated pattern. Their top is marked by autobreccia, underlain by a chilled spinifex structure zone, and the base consists of cumulate olivine porphyrites that contain up to 39%wt. MgO. Although primary magmatic minerals are not preserved in Kostomuksha komatiites, their metamorphic replacement was pseudomorphic. Therefore, textural pattern shows clearly whether one or another part of a flow belongs to its chilled portion or to the cumulate bottom zone. It should be noted that metamorphism of komatiites did not have a marked effect on the behaviour of most major and minor elements, whose distribution shows the primary magmatic pattern (Puchtel et al., 1998). This, in turn, enables us to reliably constrain the petrogenetic conditions under which komatiitic volcanism was generated.

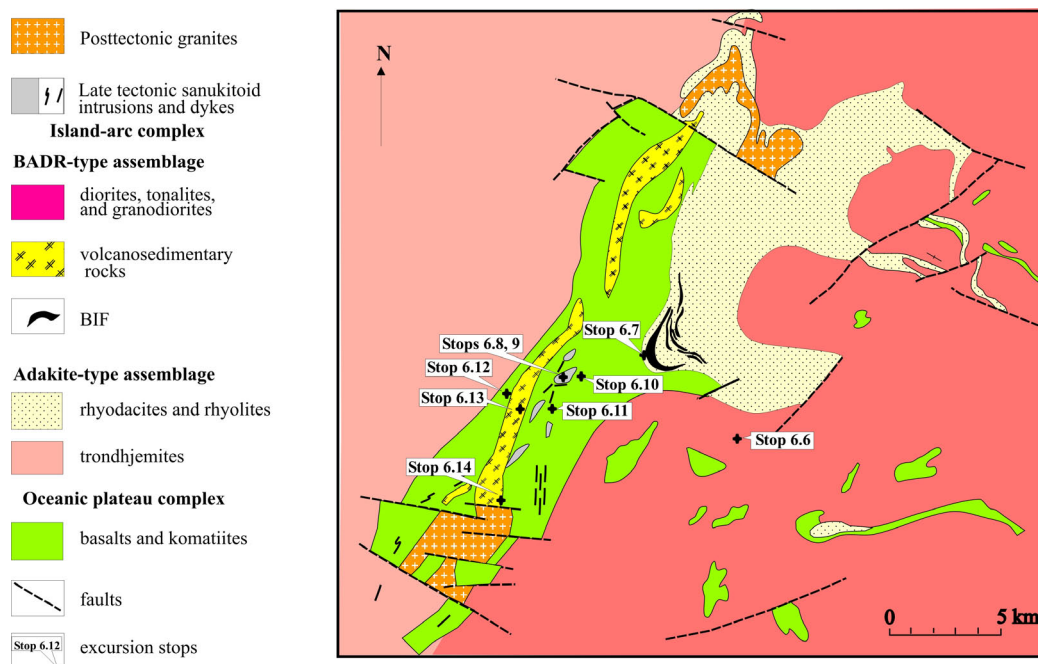


Fig. 6.2. Map of the Kostomuksha greenstone belt and its TTG-rim (Puchtel et al., 1998, with supplements).

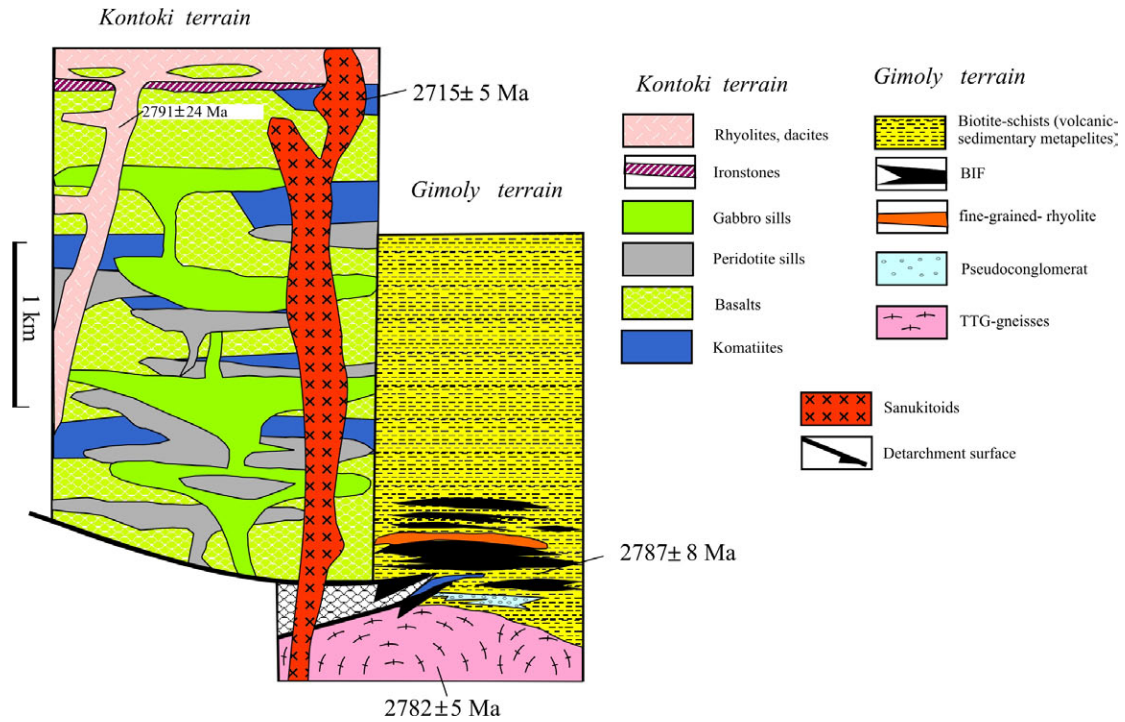


Fig. 6.3. Generalized tectono-stratigraphic scheme of the Kostomuksha greenstone structure showing a relationship between the Kontokki and Gimoly terrains. (Puchtel et al., 1998 with supplements from Shchipansky, 2005).

Volcanics of a komatiite-tholeiite association in Sm-Nd isochrone coordinates are approximated by a linear relationship the slope of which agrees with an age of 2843 ± 39 Ma, $\epsilon_{\text{Nd}} = +2.8 \pm 0.2$. Similar age values were obtained by isochrone determination for bulk samples of basalts and komatiites, using the Pb-Pb method (2813 ± 78 Ma, $\lambda_1 = 8.77 \pm 0.02$) (Puchtel et al., 1998) and the Re-Os method (2795 ± 40 Ma, $^{187}\text{Os}/^{188}\text{Os} = 0.1117 \pm 0.0011$) (Puchtel et al., 2001) and from silicic volcanics from an oceanic plateau section in the Kostomuksha belt are dated at 2791.7 ± 6.1 Ma (Kozhevnikov et al., 2006).

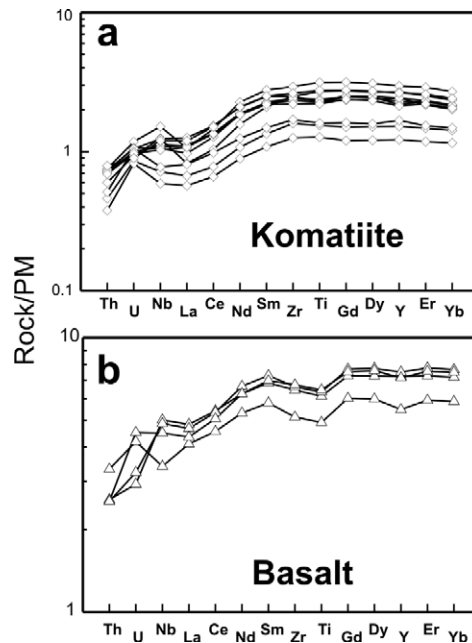


Fig. 6.4. Normalized (Hofmann et al., 1988) rare-element distribution in basalts (a) and komatiites (b) of a tholeiitic association, Kostomuksha structure (Puchtel et al., 1998).

Kostomuksha komatiites are classified petrogeochemically (Table 6.1) as Al- depleted komatiites ($Al/Ti = 17.0 \pm 0.6$). Their moderate depletion in HREE (Fig. 6.4) also shows that they are Al-depleted varieties. The spinifex-zone of the lava flow contains 26-29 %wt. MgO. An important diagnostic trait of the Kostomuksha komatiites is positive Nb anomalies (Fig. 6.4), an indicator character for volcanic-magmatic formations of oceanic plateaus. Similar anomalies are observed on spiderograms of tholeiitic metabasalts, associated with komatiites, emphasizing the genetic integrity of the mafic-ultramafic association of the Kontokki series (Fig. 6.4). The petrological study of the Kostomuksha komatiites shows that primary melts contained ~ 27 %wt. MgO, which agrees with a liquidus temperature of $1550 \pm 20^\circ C$ (Puchtel et al., 1998). Similar high melting temperatures are a distinctive character of mantle plumes. The melting of their head portions is believed to be responsible for the formation of komatiites (Arndt et al., 1997; Herzberg & O'Hara, 1998). The "Kontokki plume" was generated at a depth of over 400 km, because Al-depleted komatiites can only be formed if majoritic garnet is present as a restite phase. This, in turn, determines the depth at which partial melting is initiated (over 425 km) (Ohtani, 1990).

Table 6.1. Chemistry of basalts and komatiites from the Kostomuksha greenstone belt (Puchtel et al., 1998).

rocks	basalts			komatiites							
sample	91145	9436	9437	91157	9332	91155	91156	9479	9493	9496	94104
SiO ₂	47.2	49.8	49.4	45.9	45.4	45.1	45.6	44.6	44.7	45.0	45.3
TiO ₂	0.89	1.11	1.15	0.34	0.35	0.41	0.57	0.43	0.46	0.49	0.41
Al ₂ O ₃	14.5	16.0	15.9	5.93	6.44	7.01	9.47	7.31	7.91	7.89	7.12
Fe ₂ O ₃	14.1	13.4	13.3	11.3	10.5	14.1	14.0	13.0	13.2	13.8	12.3
MnO	0.19	0.20	0.20	0.16	0.17	0.16	0.18	0.17	0.17	0.18	0.18
MgO	8.37	6.46	6.83	31.0	30.3	27.2	22.1	27.8	26.4	25.4	27.9
CaO	13.4	10.8	11.1	5.28	6.66	5.93	7.60	6.55	6.98	7.12	6.77
Na ₂ O	0.95	1.86	1.80	0.01	0.02	0.02	0.40	0.01	0.09	0.01	0.01
K ₂ O	0.35	0.33	0.27	0.02	0.02	0.04	0.06	0.02	0.02	0.02	0.02
P ₂ O ₅	0.08	0.07	0.07	0.06	0.07	0.06	0.07	0.07	0.06	0.07	0.05
LOI	2.03	1.06	0.70	7.68	7.60	6.30	5.70	7.05	6.27	5.65	7.69
Cr	290	261	253	2902	2859	3812	3711	3083	3120	2968	2946
V	298	351	358	138	118	202	234	164	179	171	153
Co	52	61	61	100	104	113	110	103	104	99	98
Ni	145	129	120	1606	1609	1167	1007	1232	1244	1103	1378
Zr	50.0	62.7	64.4	19.4	19.9	24.5	28.5	23.6	24.4	24.3	22.6
Nb	2.10	3.10	3.01	-	0.768	0.937	0.654	-	0.762	0.693	-
Y	21.6	28.5	29.6	7.54	7.90	9.57	11.7	9.00	9.56	10.6	8.60
Sc	40.4	56.4	48.4	-	26.3	33.8	-	-	27.7	26.5	-
Rb	3.4	4.1	1.3	1.3	1.9	1.3	1.3	2.1	2.1	0.44	0.46
Sr	87.7	70.7	78.5	14.0	19.4	13.8	16.9	13.9	15.9	19.0	19.4
Th	0.270	0.209	0.206	-	-	0.0487	0.0613	0.0591	-	0.0599	0.0564
U	0.085	0.0594	0.0656	-	-	0.0190	0.0239	0.0216	-	0.0213	0.0199
Pb	1.76	4.73	4.79	-	0.285	0.299	-	-	0.298	0.295	-
La	2.52	2.97	2.87	0.466	0.488	0.505	0.650	0.596	0.635	0.772	0.676
Ce	7.30	8.68	8.57	1.58	1.64	1.66	2.33	2.04	2.09	2.46	2.13
Nd	6.33	7.44	7.92	1.76	1.83	1.87	2.70	2.21	2.27	2.48	2.19
Sm	2.24	2.65	2.82	0.723	0.759	0.811	1.072	0.876	0.913	0.963	0.858
Eu	0.756	0.923	0.986	0.239	0.249	0.270	0.353	0.216	0.307	0.416	0.313
Gd	3.09	3.73	3.95	1.04	1.08	1.21	1.62	1.27	1.36	1.40	1.27
Dy	3.82	4.63	4.94	1.27	1.33	1.51	1.97	1.56	1.66	1.71	1.57
Er	2.47	3.03	3.24	0.798	0.833	0.904	1.21	0.957	1.02	1.05	0.956
Yb	2.43	2.98	3.18	0.750	0.772	0.834	1.12	0.889	0.937	0.972	0.878
(La/Sm) _N	0.709	0.706	0.640	0.406	0.405	0.392	0.382	0.429	0.438	0.505	0.495
(Gd/Yb) _N	1.03	1.01	1.01	1.12	1.13	1.17	1.18	1.16	1.17	1.16	1.17

All the above isotopic-geochemical characteristics show that mafic and ultramafic volcanics of this association were formed from a depleted mantle source and rule out contamination of their parent melts by an old crustal substrate. This, together with abnormally high estimated temperatures, at which primary komatiitic melts were generated in the mantle source, and the geochemical similarity of these volcanics to modern oceanic plateau volcanics, suggest that the association was formed as the deep-seated mantle plume was rising. (Puchtel et al., 1997, 1998). A preserved fragment of the upper crustal levels of this oceanic plateau is represented by the Kontokki series of the Kostomuksha belt. Other fragments of the plateau are likely to occur as komatiite-bearing mafic-ultramafic associations in the Kuhmo-Suomussalmi and Tipasjärvi belts, eastern Finland.

Volcanics of a dacite-rhyolite association, identified as part of the Kontokki series, make up a long, narrow band in volcanics. The association is dominated by diatreme-facies eruptive breccia and tuff and tuffites of dacite-rhyolite composition (Stops 6.13 and 6.14) with thin carbonaceous shale and iron formation horizons. The concentration of both major and rare elements in the volcanics varies irregularly over a broad range, some of the rocks clearly showing the geochemical characteristics of adakites (Table 6.2, Fig. 6.5a). The geochemical pattern observed cannot be explained by either addition of an alien terrigenous-sedimentary component or the degree of postmagmatic or metamorphic alteration, because variations of the same type have been encountered in tuffs and subvolcanic rocks, but they could reflect compositionally different sources of melts. This assumption is favoured by substantial variations in ϵNd (-6.2/+1.7), suggesting that dacitic-rhyolitic melts were formed from at least two sources: 1) a mafic source with depleted isotopic-geochemical characteristics and 2) an old crustal source (Puchtel et al., 1998). U-Pb dating of zircons from several volcanic rock samples has given similar ages: 2793 ± 17 Ma (classical method) and 2791 ± 24 Ma (scarce grains on an ion-ion probe) (Bibikova et al., 2005).

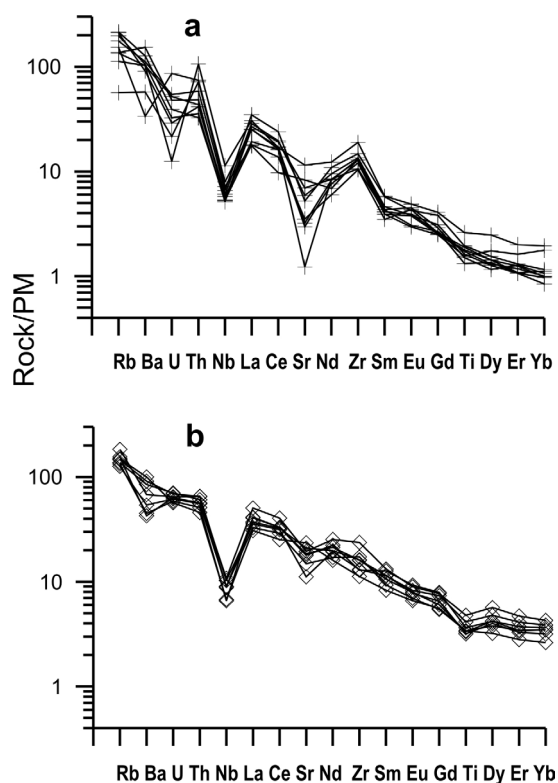


Fig. 6.5. Normalized (Hofmann et al., 1988) rare-element distribution for volcanic-sedimentary rocks of the Kostomuksha structure (Samsonov et al., 2005). a = dacite-rhyolite association of the Kontokki series; b = andesite-dacite-rhyolite (ADR) association of the Gimoly series.

The Gimoly series consists of volcanic-sedimentary rocks occurring in the eastern Kostomuksha structure, its lower, largely volcanogenic part being composed of iron formation of the Kostomuksha deposit (Stop 7). Here, tuffs of andesite-dacite-rhyodacite (ADR) composition, altered to fine-grained biotite (Bi)-schists, are interbedded with carbonaceous shales and iron formation. The abundance of chemogenic sediments has given rise to discussion of the terrigenous-sedimentary (Rayevskaya et al., 1992) or volcanic-sedimentary (Chernov, 1964) genesis of the protoliths of Bi-schists. Our data point to the volcanogenic nature of these rocks. Their zircon is represented by a morphologically homogeneous population dominated by elongate-prismatic crystals and has no traces of a mechanical effect, showing transportation of the material over a long distance. The volcanic origin of the protoliths of Bi-schists is also favoured by geochemical data. They correspond in composition to andesites, dacites and rhyodacites (55-69% mass. SiO₂) with regular variations in the percentages of major and trace elements, low concentrations and the K-Na specificity of alkalis, moderate REE concentrations with enriched spectra of light and poorly fractionated spectra of heavy lanthanoids and high levels of Yb and Y, and well-defined negative Sr, Eu, Ti and Nb anomalies (Table 2, Fig. 6.5b). Bi-schists are typically rich in Fe, Cr and Ni. This could be due to addition of a component of MgO-rich rocks similar to Kontokki-series tholeiitic volcanics – evidence in favour of the tuffaceous-sedimentary nature of the protoliths of these rocks. Based on U-Pb isotopic dating, the age of zircons from tuff of dacite composition is estimated at 2787±8 Ma. Sm-Nd isotopic-geochemical characteristics of dacitic tuffs ($\epsilon_{Nd}=+1.2/+1.5$) suggest the leading role of a depleted mantle source in the petrogenesis of these rocks (Bibikova et al., 2005).

Table 6.2. Chemistry of intermediate and felsic volcanics from the Kontokki and Gimoly series, Kostomuksha structure (Samsonov et al., 2004).

rocks	rhyolite tuffs		subvolcanic rhyolite				tuffs and tuffites		
sample	91147	136/93	13/97	138/93	22A/97	25/97	10/01	7/97	37-3/01
Stops	6.13	6.13	6.14	6.13	6.14	6.14	6.6	6.6	6.6
SiO ₂	72.20	79.14	69.43	71.20	72.68	66.98	60.39	64.64	68.47
TiO ₂	0.42	0.28	0.27	0.47	0.31	0.34	0.75	0.67	0.61
Al ₂ O ₃	16.00	12.19	12.09	16.39	12.57	13.05	16.28	16.44	15.04
Fe ₂ O ₃	1.38	1.61	3.31	1.51	3.17	3.40	12.06	6.99	6.50
MnO	0.11	0.11	0.16	0.12	0.14	0.17	0.14	0.14	0.12
MgO	1.01	0.33	2.42	0.56	1.26	2.34	3.65	3.29	2.04
CaO	2.37	1.77	4.51	2.91	1.53	4.23	2.36	3.21	1.96
Na ₂ O	3.40	3.14	0.74	4.08	1.57	0.29	1.84	2.70	2.92
K ₂ O	2.61	1.36	6.96	2.61	6.69	9.11	2.38	1.77	2.21
P ₂ O ₅	0.13	0.07	0.10	0.14	0.08	0.09	0.14	0.15	0.12
loi	1.72	1.04	0.57	0.64	0.59	0.74	1.39	1.40	0.69
Sc	5.01	3.38	4.13	6.58	4.89	3.75	21.99	14.10	15.61
V	40.3	12.7	17.8	29.4	21.7		164.11	95.40	107.93
Cr	18.3	15.7	20.1	35.1	44.8	20.9	207	125	196
Co	3.18	8.29	4.79	2.9	4.32	3.9	29.76	21.00	24.24
Ni	7.8	12.9	12.2	13.9	23.9	13.5	131.75	81.40	87.83
Cu	8.08	19.6	12.6	15.5	12	13.4	46.52	19.10	48.40
Zn	36.2	20.5	35.3	38.5	25.1	43	77.10	70.30	83.61
Rb	58.9	30.2	73	60	113	106	98.24	71.00	83.22
Sr	195	151	127	209	54	22.3	203.11	325.00	269.95
Y	9.63	6.63	5.17	8.33	5.32	5.29	18.35	13.00	15.09
Zr	128	127	124	184	117	103	127.07	125.00	167.44
Nb	5.82	4.45	3.29	7.01	3.55	3.17	6.35	4.06	5.57
Cs	1.59	0.918	1.44	0.997	3.03	0.655	4.67	9.49	4.06
Ba	419	346	925	621	548	637	410.48	271.00	257.10

La	9.89	10.8	16.5	18.8	11.8	15.6	21.88	25.30	20.20
Ce	22.4	15.6	30.7	27.1	25.8	26.2	50.27	53.00	46.36
Pr	2.52	2.46	3.03	4.27	2.5	2.85	5.87	6.33	5.22
Nd	9.53	8.19	10	14.6	9.07	10.1	23.02	26.60	20.20
Sm	2.17	1.51	1.67	2.24	1.51	1.59	4.39	4.90	3.60
Eu	0.64	0.431	0.656	0.709	0.548	0.571	1.20	1.35	1.01
Gd	1.8	1.28	1.49	2.09	1.3	1.35	3.78	4.06	2.79
Tb	0.29	0.185	0.169	0.277	0.142	0.178	0.54	0.57	0.42
Dy	1.67	1.11	0.741	1.58	0.832	0.907	3.04	2.67	2.42
Ho	0.36	0.208	0.154	0.3	0.152	0.186	0.65	0.54	0.54
Er	0.86	0.675	0.53	0.833	0.492	0.52	1.71	1.42	1.44
Tm	0.14	0.101	0.058	0.111	0.068	0.0649	0.25	0.21	0.22
Yb	0.95	0.732	0.441	0.807	0.415	0.411	1.60	1.44	1.44
Lu	0.14	0.11	0.048	0.099	0.06	0.0506	0.24	0.20	0.22
Hf	3.31	3	2.85	4.5	2.56	2.57	3.35	3.25	4.35
Ta	1.05	0.355	0.292	0.476	0.279	0.284	0.43	0.27	0.57
Pb	11.7	5.77	11.2	5.5	7.52	6.07	10.80	12.90	13.63
Th	7.47	5.84	3.92	8.63	3.37	2.9	5.31	4.15	4.57
U	1.89	0.438	0.971	0.253	0.589	0.659	1.32	1.19	1.29
(La/Yb)_N	7.0	10.0	25.3	15.7	19.2	713.5	9.3	11.9	9.5
(La/Sm)_N	2.9	4.5	6.2	5.3	4.9	4.4	3.1	3.3	3.5
(Gd/Yb)_N	1.5	1.4	2.7	2.1	2.5	25.6	1.9	2.3	1.6
Eu/Eu*	1.0	0.9	1.3	1.0	1.2	6.2	0.9	0.9	1.0

Correlation of the units of the Kontokki and Gimoly series is the subject of animated discussion fuelled by the complexity of unambiguous interpretation of the primary nature of the “conglomerates” that separate them (Fig. 6.6). Some authors assume that the units correlate stratigraphically with a conglomerate horizon (Fig. 6.6a) at the base of the later Gimoly series (Rayevskaya et al., 1992; Lobach-Zhuchenko et al., 2000). Another point of view, shared by the authors of the present Field Guide, is that the series are in tectonic overthrust contact (Puchtel et al., 1997, 1998; Kozhevnikov, 2000). In this case, the “conglomerate” horizon (Stop 6.7) is considered to be a cluster of boudin-structured, possibly synkinematic felsic dykes restricted to the tectonic zone (Fig. 6.6b).

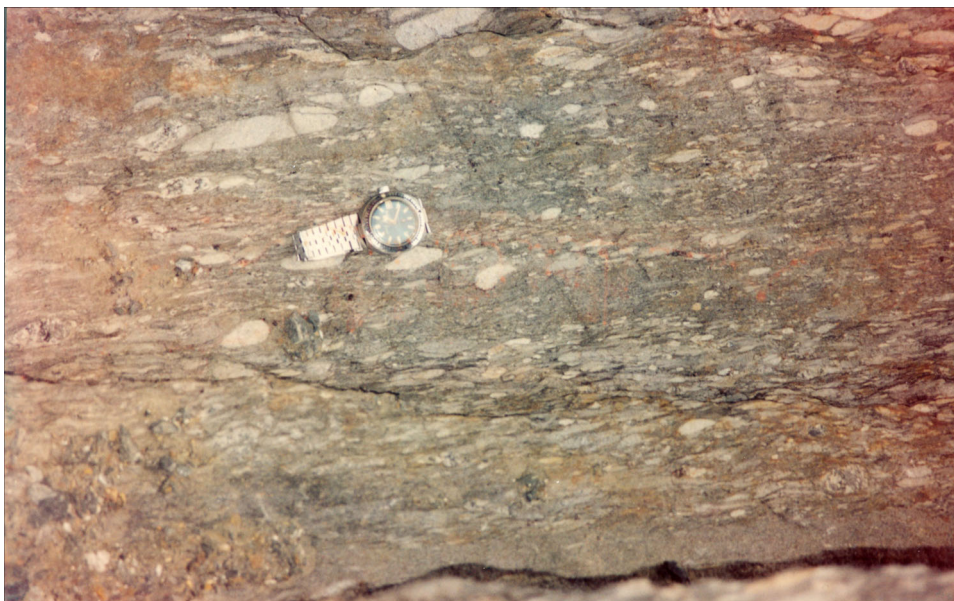




Fig. 6.6. Mixed rock in the contact zone between Kontokki and Gimoly volcanics, consisting of lens-shaped fragments of felsites of rhyolite composition in an andesitic-dacitic matrix. The rock is either highly deformed conglomerates (a) or as boudin-structured dykes (b).

Syntectonic TTG granitoids that make up a large part of the West Karelian terrain differ in structure and composition in its western and eastern parts, thus providing more evidence in favour of the asymmetry of the Kostomuksha greenstone belt (Fig. 6.1).

TTG granitoids, occurring on the western margin of the Kostomuksha structure, have practically no supracrustal rock inclusions and are homogeneous in composition (Stop 6.15). Predominant here are alumina-rich trondhjemites with geochemical characteristics typical of adakitic series: highly fractionated REE spectra, small percentages of heavy lanthanoids and Y, poorly defined Sr, Eu and Ti anomalies and distinct, strongly negative Nb anomalies (Table 6.3, Fig. 6.7a). Zircon from these granitoids is structurally homogeneous, no trapped zircon component has been encountered, and the U-Pb isotopic age is 2747 ± 17 Ma (Bibikova et al., 2005). The radiogenic isotopic composition of Nd ($\epsilon_{Nd}(T)$ +2.4 to +1.8) of the trondhjemites on the western margin points to a mafic source of their parent melts that could form upon melting of basalts in equilibrium with Cpx(40%)+Gar(30%)+Pl(20%)+Hbl(10%) restite.

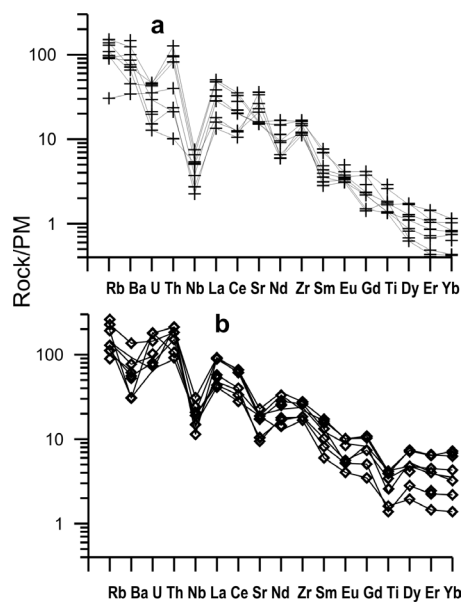


Fig. 6.7. Normalized (Hofmann et al., 1988) rare-element distribution for TTG granitoids from the western (a) and eastern (b) rims of the Kostomuksha structure (Samsonov et al., 2005).

Table 6.3. Chemistry of TTG granitoids of the Kostomuksha area (Samsomov et al., 2004).

rocks	trondhjemite			tonalite	trondhjemite	tonalite	pegmatite
	5/97	3/01	5-1/01	10/97	54/01	56/01	58/01
stops	6.15			6.6	6.6	6.6	6.6
SiO ₂	69.50	70.91	70.51	66.40	69.28	64.55	72.73
TiO ₂	0.47	0.32	0.25	0.62	0.42	0.53	0.15
Al ₂ O ₃	15.80	15.86	16.71	15.90	16.36	16.18	16.16
Fe ₂ O ₃	3.18	2.68	1.78	4.56	3.61	5.82	1.22
MnO	0.13	0.12	0.12	0.14	0.13	0.16	0.11
MgO	1.16	0.69	0.63	1.57	1.05	2.22	0.26
CaO	3.75	3.38	3.05	4.59	3.68	5.16	2.24
Na ₂ O	3.74	4.82	4.89	3.62	4.01	3.80	4.16
K ₂ O	1.57	1.12	1.97	1.70	1.34	1.40	2.90
P ₂ O ₅	0.10	0.11	0.09	0.17	0.13	0.17	0.07
loi	0.60	0.32	0.44	0.60	0.53	0.40	0.58
Sc	4.26	3.60	3.20	8.09	11.93	32.66	1.12
V		35.36	23.52		40.95	77.40	11.97
Cr	20.70	33.85	39.50	20.80	29.51	82.38	28.93
Co	6.83	5.52	4.23	8.39	6.16	14.42	1.86
Ni	17.10	24.08	27.51	11.90	19.07	40.04	18.52
Cu	2.19	3.47	2.54	5.02	9.44	24.08	2.64
Zn	50.10	49.99	34.71	74.00	60.26	87.27	27.40
Rb	73.70	51.93	49.41	103.00	69.09	47.89	73.92
Sr	282.00	279.60	653.18	189.00	316.91	313.33	363.98
Y	5.26	5.59	4.02	17.80	18.24	14.64	4.92
Zr	162.00	148.06	108.33	179.00	253.47	122.25	102.78
Nb	4.04	3.32	1.69	11.80	7.04	7.04	5.54
Cs	2.49	2.94	1.49	8.66	2.41	2.08	3.87
Ba	432.00	274.20	606.66	184.00	187.27	317.57	683.32
La	29.30	19.84	8.24	26.70	54.58	18.83	3.66
Ce	52.70	32.51	16.83	53.60	98.84	43.53	8.23
Pr	5.31	3.40	1.86	5.64	10.14	4.52	0.85
Nd	17.50	11.36	7.09	20.10	33.43	17.28	3.35
Sm	2.68	1.68	1.37	3.94	5.12	3.57	0.78
Eu	0.60	0.55	0.45	0.82	0.77	0.96	0.47
Gd	2.12	1.21	1.12	3.79	4.40	3.27	0.76
Tb	0.25	0.16	0.15	0.60	0.65	0.47	0.11
Dy	1.07	0.82	0.70	3.04	3.39	2.65	0.65
Ho	0.20	0.16	0.14	0.63	0.67	0.54	0.14
Er	0.60	0.43	0.36	1.87	1.68	1.32	0.40
Tm	0.07	0.07	0.05	0.26	0.23	0.18	0.07
Yb	0.48	0.42	0.33	1.78	1.34	1.10	0.45
Lu	0.06	0.07	0.05	0.23	0.19	0.18	0.08
Hf	4.08	3.53	3.18	4.18	6.78	3.10	3.23
Ta	0.20	0.30	0.15	1.59	0.46	0.34	0.82
Pb	6.52	10.63	12.56	11.40	13.67	13.10	18.05
Th	7.65	6.65	1.72	8.64	17.26	5.68	3.08
U	0.94	0.87	0.60	3.67	1.31	1.51	1.58
(La/Yb) _N	41.5	31.6	16.8	10.1	27.5	11.5	5.5
(La/Sm) _N	6.9	7.5	3.8	4.3	6.7	3.3	3.0
(Gd/Yb) _N	3.6	2.3	2.7	1.7	2.7	2.4	1.4
Eu/Eu*	0.8	1.2	1.1	0.6	0.5	0.9	1.9

TTG granitoids, occurring on the eastern margin of the Kostomuksha structure (Stop 6.6), exhibit a clearly domal structural plan view and contain numerous inclusions of supracrustal rocks comparable in composition to Kontokki and Gimoly rocks: they vary in composition from diorites to granodiorites (tonalitic varieties prevail), display LREE-enriched spectra and poorly fractionated HREE spectra, high percentages of Yb and Y and negative Sr, Eu, Ti and Nb anomalies (Table 6.3, Fig. 6.76) and are similar in geochemical characteristics to Gimoly dacite tuffs. Mineralogical and U-Pb isotopic studies have shown that magmatic zircon from tonalites, dated at 2782 ± 5 Ma, contain the cores of older trapped zircon dated at 2797 ± 4 Ma (Bibikova et al., 2005). The presence of the trapped zircon component suggests that previous felsic rocks contributed to the generation of TTG at the eastern boundary of the Kostomuksha structure. This assumption is also supported by near-zero $\epsilon_{\text{Nd}}(T)$ values in these granitoids.

TTG granitoids in the Voinitsa domain of the West Karelian terrain, like on the Kostomuksha structure margin, are represented by two geochemical types (Samsonov et al., 2001).

In the western part of the domain, west of the Town of Voinitsa, TTG granitoids are compositionally homogeneous, leucocratic, medium- to coarse-grained, highly gneissose and locally migmatized (Stop 6.3). Compositionally, they form a compact group and correspond to Al-rich trondhjemites with the geochemical characteristics of adakites, like those for TTG granitoids from the western margin of the Kostomuksha structure (Table 6.4, Fig. 6.8a). The U-Pb isotopic age of the zircon is 2788 ± 12 Ma (Bibikova et al., 2005).

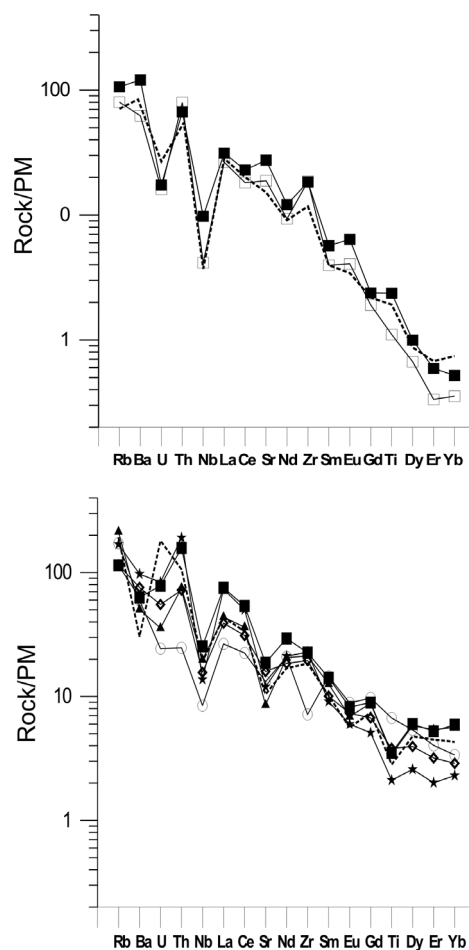


Fig. 6.8. Normalized rare-element distribution for TTG granitoids from the western (a) and eastern (b) Voinitsa domain (Samsonov et al., 2001).

Table 6.4. Chemistry of TTG granitoids and lamprophyres in the Voinitsa domain (Samsonov et al., 2001).

rocks	amphibolites		dorite	tonalite	trondhjemite		lamprophyres		migmatite	
nn	38-1/00	44-1/00	38-2/00	38-3/00	36-1/00	37-1/00	38-4/00	37-2/00	39-4/00	36-2/00
stops	6.1	6.1	6.1	6.1	6.3	6.2	6.1	6.2	6.2	6.3
SiO ₂	48.3	51.0	57.8	66.4	73.7	70.3	75.3	68.3	60.1	72.9
TiO ₂	1.13	1.01	0.82	0.76	0.25	0.35	0.13	0.94	1.35	0.20
Al ₂ O ₃	17.5	13.4	19.0	15.5	15.0	15.9	14.2	15.6	16.4	15.8
Fe ₂ O ₃	12.61	10.89	7.23	5.48	1.82	2.61	0.89	3.39	7.64	1.31
MnO	0.18	0.19	0.16	0.14	0.11	0.12	0.11	0.12	0.14	0.11
MgO	6.13	10.12	2.85	1.67	0.58	1.28	0.22	1.34	2.18	0.36
CaO	8.74	8.65	5.91	4.24	2.89	3.73	2.02	2.69	4.13	3.04
Na ₂ O	3.05	2.25	3.84	3.76	4.15	4.18	3.34	4.03	3.72	3.95
K ₂ O	2.05	2.22	2.09	1.81	1.40	1.47	3.82	3.34	3.76	2.32
P ₂ O ₅	0.34	0.24	0.26	0.19	0.09	0.10	0.01	0.31	0.57	0.09
LOI	0.72	0.85	0.87	0.74	0.47	0.72	0.68	0.77	1.08	1.02
Sc		42.55		12.58	3.97				15.18	
V		375.23		64.59	16.93				125.75	
Cr		275		54.09	30.81				62.17	
Co		54.38		15.32	5.11				17.97	
Ni		174.81		27.47	19.24				25.79	
Cu		11.23		16.34	10.74				14.95	
Zn		179.56		100.67	47.66				140.84	
Rb		112.85		74.72	52.33				214.66	
Sr		291.72		414.81	417.27				747.84	
Y		25.25		32.25	3.28				30.91	
Zr		84.88		267.20	219.73				803.22	
Nb		6.35		19.12	3.12				32.66	
Cs		2.33		1.13	1.20				2.87	
Ba		438.04		465.39	459.51				1423.83	
La		19.88		56.39	19.83				174.73	
Ce		43.79		105.05	35.40				321.41	
Pr		6.45		11.22	3.83				32.89	
Nd		30.25		42.67	13.53				121.89	
Sm		6.83		6.67	1.87				19.01	
Eu		1.58		1.46	0.72				3.29	
Gd		6.07		5.58	1.19				12.61	
Tb		0.78		0.86	0.16				1.52	
Dy		4.18		4.65	0.52				6.35	
Ho		0.83		1.04	0.08				1.02	
Er		2.05		2.66	0.17				2.45	
Tm		0.27		0.42	0.02				0.29	
Yb		1.70		2.99	0.18				1.97	
Lu		0.27		0.41	0.03				0.28	
Hf		2.95		6.54	5.50				17.09	
Ta		0.73		1.78	0.22				2.04	
Pb		6.81		13.17	9.22				14.23	
Th		2.45		15.68	7.89				19.98	
U		0.60		1.94	0.40				1.27	
(La/Yb) _N		7.88		12.72	74.66				59.95	
(La/Sm) _N		1.83		5.32	6.69				5.79	
(Gd/Yb) _N		2.88		1.51	5.36				5.18	
Eu/Eu*		0.75		0.73	1.48				0.65	

Widespread in the eastern part of the domain are mineralogical and geochemical counterparts of TTG-granitoids from the eastern margin of the Kostomuksha structure (Stop 6.1). Here, TTG granitoids are also structurally heterogeneous and contain numerous inclusions of fine-grained biotite plagiogneisses and amphibolites interpreted tentatively as xenoliths of volcanic rocks. The granitoids vary in chemical composition from diorites and tonalites to granodiorites (57-72%wt. SiO₂) and are geochemical analogues of the TTG granitoids at the eastern boundary of the Kostomuksha structure (Table 6.4, Fig. 6.8b).

The contact of two geochemical types of TTG granitoids has not been directly observed, but available data suggest that it is tectonic. Our assumption is also supported by the fact that the two geochemical types of granitoids are spatially isolated. In their contact zone, thin lamprophyre veins (Stop 6.2), whose intrusion was presumably controlled by a weakened tectonic zone, occur in highly migmatized gneisses with adakitic characteristics. Considering that the age of the lamprophyres in the Voinitsa domain is 2694±10 Ma (Bibikova et al., 2005), the authors assume that the tectonic overlapping of these different geochemical types of TTG did not occur more recently.

The above evidence for the mineralogical and isotopic-geochemical asymmetry of the TTG-greenstone complexes in the Kostomuksha are cannot be explained using the riftogenic model (Rayevskaya et al., 1992; Lobach-Zhuchenko et al., 2000). To interpret the contrasting geochemical and isotopic characteristics of mafic and felsic volcanics in the western part of the structure (Kontokki series), a tectonic model was proposed, in which mafic metavolcanics represent the upper crustal levels of an oceanic plateau obducted on the edge of the old continent (Gimoly series), and felsic melts were generated upon obduction by melting of the continental crust (Puchtel et al., 1998). The new data are reliable enough to improve the model and to assume that the Kostomuksha structure was formed in an active continental margin environment, the oceanic plate being subducted from west to east (Samsonov et al., 2001; Samsonov et al., 2005). The oceanic plateau, formed in an intraoceanic setting, was shifted close to the continental block on the oceanic crust that plunged under the old continent from west to east. As a result, the top of the oceanic plateau, comparable in thickness to the continental crust, was torn off and thrown away to the continental margin. At the same time, subduction of the oceanic crust under the continental block was responsible for the mineralogical and isotopic-geochemical zonation of magmatic associations observed for the Kostomuksha structure. On the subduction front, direct melting of the oceanic plate generated adakitic melts (TTG at the western boundary). Mixing of the melts with the crustal substrate melting products could provide initial melts for the dacitic-rhyolitic unit in the western band of the structure. In the rear subduction zone, dehydration of the oceanic plate triggered the fluid reworking of the mantle wedge, its enrichment in lithophile and light rare-earth elements and partial melting with generation of initial melts for Gimoly volcanics (and volcanogenic sources of their transport) and for TTG at the eastern boundary of the Kostomuksha structure. A similar tectonic model for the formation of the Kostomuksha structure has been proposed by Kozhevnikov (2000, 2006).

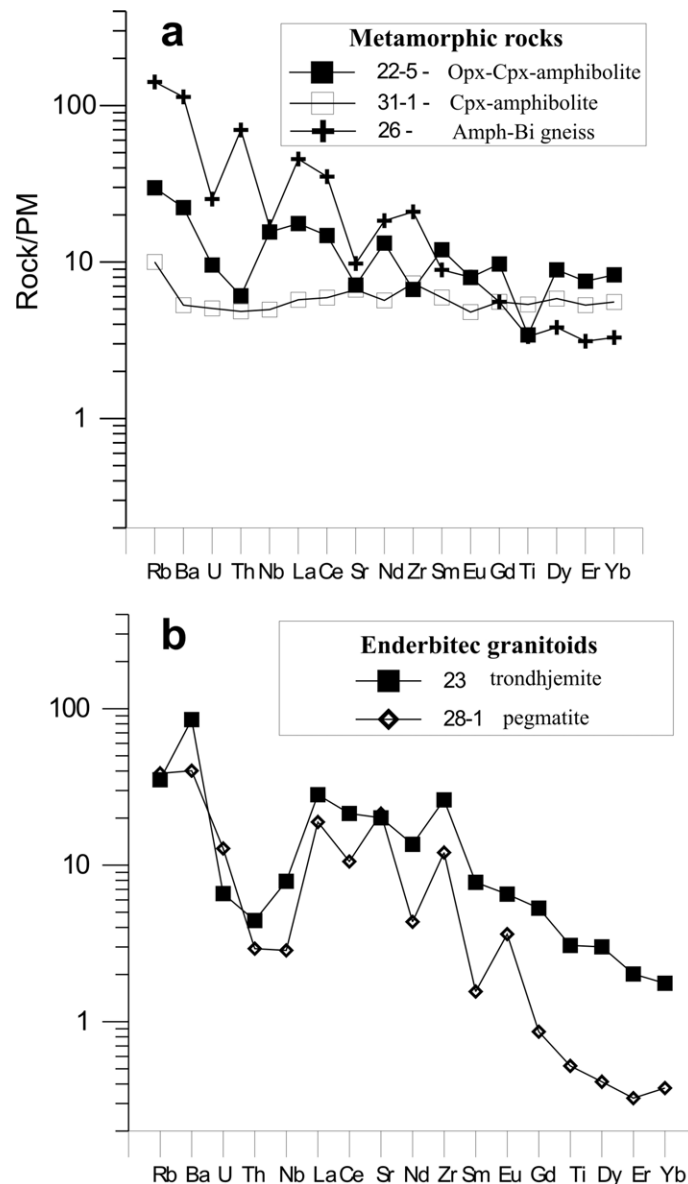


Fig. 6.9. Normalized (Hofmann et al., 1988) rare-element distribution for rocks of the Voknavolok complex (Samsonov et al., 2001).

Granulites of the Voknavolok block occur between the Kostomuksha structure and the Voinitsa domain (Fig. 6.1). The complex is indicated in geophysical fields by intense linear, NE-trending magnetic anomalies and by a strong positive gravity anomaly, the contour of which is the block boundary on different geologic maps. The geological-structural and age position of the Voknavolok complex in the structure of the West Karelian terrain, the genesis of the protoliths of its rock constituents and the directivity of their metamorphic alterations are the subject of debate. Sviridenko (1974) interprets pyroxene-bearing metamorphogenic parageneses in Voknavolok rocks as relics of a large granulitic block, the oldest unit in the region. Other authors (Kozhevnikov, 1982, 2000) argue that pyroxene-bearing parageneses were formed at the prograde stage of metamorphism, simultaneous with the Neoproterozoic (Reboly) phase of F2-folding (Kozhevnikov, 2000). Kozhevnikov's argument has been supported by our studies (Samsonov et al., 2001). The typical and most abundant rocks of the Voknavolok block are dark enderbite-like granitoids that contain inequidimensional gneiss and amphibolite inclusions (Stop 6.4). The inclusions are similar in geochemical characteristics to rocks of the Kostomuksha structure and the TTG granitoids occurring on its eastern margin (Fig. 6.9a). Dark enderbite-like granitoids, migmatites and pegmatites that form the image of the

Voknavolok complex were generated 2745 ± 4 Ma ago (Bibikova et al., 2005), as shown by U-Pb isotopic dating of zircons. The rocks correspond in composition to Al-rich tonalites and trondhjemites with an invariably high Na₂O/K₂O ratio and a low percentage of alkalis (Table 6.5) and differ greatly in geochemical characteristics from other groups of TTG gneisses and granitoids of the West Karelian block. For example, leucotonalite has a low REE content and an average REE fractionation, which suggests generation of its parent melt upon partial melting of a metabasic source in equilibrium with plagioclase+ amphibole+pyroxene (\pm up to 5% garnet) restite, i.e. at a depth of 30-40 km, the water content of the melt being not less than 5-7%. The high fluid content of the melts, initial for granitoids, is corroborated by the abundance of migmatite and pegmatite veins conjugated with granitoids. A distinctive geochemical characteristic of granitoids and pegmatites of the Voknavolok block is their distinct impoverishment in U and Th (Fig. 6.9b). This is typical of granulitic complexes, and could be due to the removal of these elements by CO₂-enriched fluid. The study of the density characteristics of the most abundant gneisses and granitoids of the Voknavolok complex has not revealed any anomalous values. This suggests a deep source of a positive gravity anomaly, the contour of which could then be much larger than the real distribution area of Voknavolok rocks on the surface. Mineral parageneses in metabasic rocks of the Voknavolok block were formed at pressures of 1.8 – 4.1 kbar and temperatures of $677 \pm 36^\circ\text{C}$ (Samsonov et al., 2001). The P-T parameters obtained disagree with the environment of formation of normal granulites and suggest that Voknavolok rocks have been metamorphosed at low pressures and high temperatures. Such metamorphic alterations were probably triggered by a local thermal plume (Samsonov et al., 2001).

High-MgO granitoids (sanukitoids), widespread in the Central Karelian terrain, are also well-known in the West Karelian terrain, where they are less abundant. One characteristic example of these granitoids here is the Taloveis massif (Samsonov et al., 2004) that intruded Kostomuksha mafic volcanics 2715 ± 5 Ma ago (Fig. 6.2). It is a small (ca. 0.5x1 km) poly-phase massif that displays a concentric-zonal structure and a homodromous phase intrusion sequence (Fig. 6.10). Early diorites make up a narrow (less than 50 m) rim along the massif periphery and occur as xenoliths among the most abundant granodiorites in the internal part of the massif. Porphyreous structures suggest that the massif was generated at a hypabyssal level. Representative analyses of granitoids are shown in Table 6. As SiO₂ concentration rises from 55 to 70 %mass., the percentages of TiO₂, Al₂O₃, Fe₂O₃, MgO, CaO and P₂O₅ in granitoids decrease, their Mg content (mg#) declines from 0.55 to 0.47), the percentages of V, Co, Sc, Y, heavy, intermediate and, to a lesser extent, light lanthanoids decrease, those of Nb, U, Th, Pb and Ba increase, and the degree of REE fractionation ($L_{\text{a}_N}/Y_{\text{b}_N}$) also increases from 20 to 35. For Zr and trace elements, such as Li, Rb and Cs, concentrations are observed to rise in diorites and decrease in granodiorites. On spider-diagrams, diorites and granodiorites display similar multi-element spectra with marked negative с резкими Nb anomalies and minor Ti anomalies; negative Zr anomalies are observed in diorites but are not encountered in granodiorites (Fig. 6.11a). Variations in the composition of sanukitoids are probably associated with the crystallization differentiation of hornblende, plagioclase and clinopyroxene in dioritic melts (55 to 63% mass. SiO₂) and a change in the composition of cumulus association to plagioclase + hornblende + biotite upon transition to granodioritic magma (66-68% mass. SiO₂). The primary melts of the sanukitoid series studied presumably represent the compositions of Mg-richest (mg#=0.55-0.61, MgO=5.5-7.1 %wt.) diorites from the Taloveis massif

Table 6.5. Chemistry of rocks from the Voknavolok block.

rocks	Cpx-amphibolites		enderbite-like granitoids		pegmatite	Opx-Cpx amphibolites	Bi-Amph gneiss
nn	31-1/00	31-2/00	22-1/00	23/00	22-4/00	22-5/00	22-3/00
Stops	6.4	6.4	6.5	6.5	6.5	6.5	6.5
SiO ₂	49.2	50.7	71.0	68.0	60.4	50.8	62.4
TiO ₂	0.99	1.00	0.31	0.60	0.60	0.70	0.92
Al ₂ O ₃	14.6	15.2	16.4	15.9	17.6	8.8	16.5
Fe ₂ O ₃	12.95	12.86	1.80	4.24	10.20	12.90	5.30
MnO	0.21	0.18	0.11	0.12	0.12	0.23	0.13
MgO	6.06	5.87	1.12	1.45	0.73	12.83	3.49
CaO	14.01	11.94	3.51	4.83	3.50	11.62	5.79
Na ₂ O	1.56	1.85	4.29	3.79	5.58	1.20	3.92
K ₂ O	0.17	0.20	1.33	0.86	1.10	0.76	1.33
P ₂ O ₅	0.22	0.18	0.13	0.14	0.09	0.13	0.26
loi	0.58	0.7	0.34	0.31	0.3	1.28	0.62
Sc	53.78			10.52		28.23	
V	371.69			56.83		172.36	
Cr	331			40.44		1816	
Co	66.64			13.15		62.91	
Ni	187.48			38.09		499.07	
Cu	122.78			7.65		10.91	
Zn	112.37			74.04		194.15	
Rb	6.53			22.92		19.43	
Sr	147.84			445.91		158.24	
Y	30.82			14.04		44.07	
Zr	86.53			309.74		79.14	
Nb	3.73			5.93		11.71	
Cs	0.18			0.10		0.22	
Ba	39.08			628.92		164.22	
La	4.29			21.08		13.18	
Ce	11.55			41.77		28.81	
Pr	1.66			5.35		4.45	
Nd	8.24			19.71		19.14	
Sm	2.80			3.66		5.64	
Eu	0.85			1.16		1.41	
Gd	3.48			3.32		6.07	
Tb	0.60			0.45		0.99	
Dy	4.54			2.34		6.92	
Ho	1.02			0.45		1.47	
Er	2.69			1.02		3.82	
Tm	0.43			0.14		0.64	
Yb	2.80			0.89		4.18	
Lu	0.43			0.11		0.59	
Hf	2.25			6.65		2.46	
Ta	0.97			0.24		0.65	
Pb	1.44			4.83		2.41	
Th	0.48			0.44		0.60	
U	0.13			0.16		0.24	
(La/Yb) _N	1.03			16.02		2.13	
(La/Sm) _N	0.97			3.63		1.47	
(Gd/Yb) _N	1.00			3.02		1.17	
Eu/Eu*	0.83			1.02		0.74	

and diorite dykes enriched in Cr (52-299 $\mu\text{kg/g}$), Ni (33-62 $\mu\text{kg/g}$) and simultaneously in many lithophile elements, including Ba (680-860 $\mu\text{kg/g}$), Sr (314-870 $\mu\text{kg/g}$) and light REE (La from 26 to 41 $\mu\text{kg/g}$). Such characteristics are best explained by the formation of these rocks upon partial melting of a primitive mantle source subjected to intense metasomatic reworking by felsic melts with the characteristics of earlier (2.8 Ga) syntectonic TTG granitoids rimming the Kostomuksha belt. Such a reworking of the mantle could be connected with a subduction stage in the tectonic evolution of the area discussed upon formation of TTG and greenstone complexes ca. 2.8 Ga ago (Larionova et al., 2007).

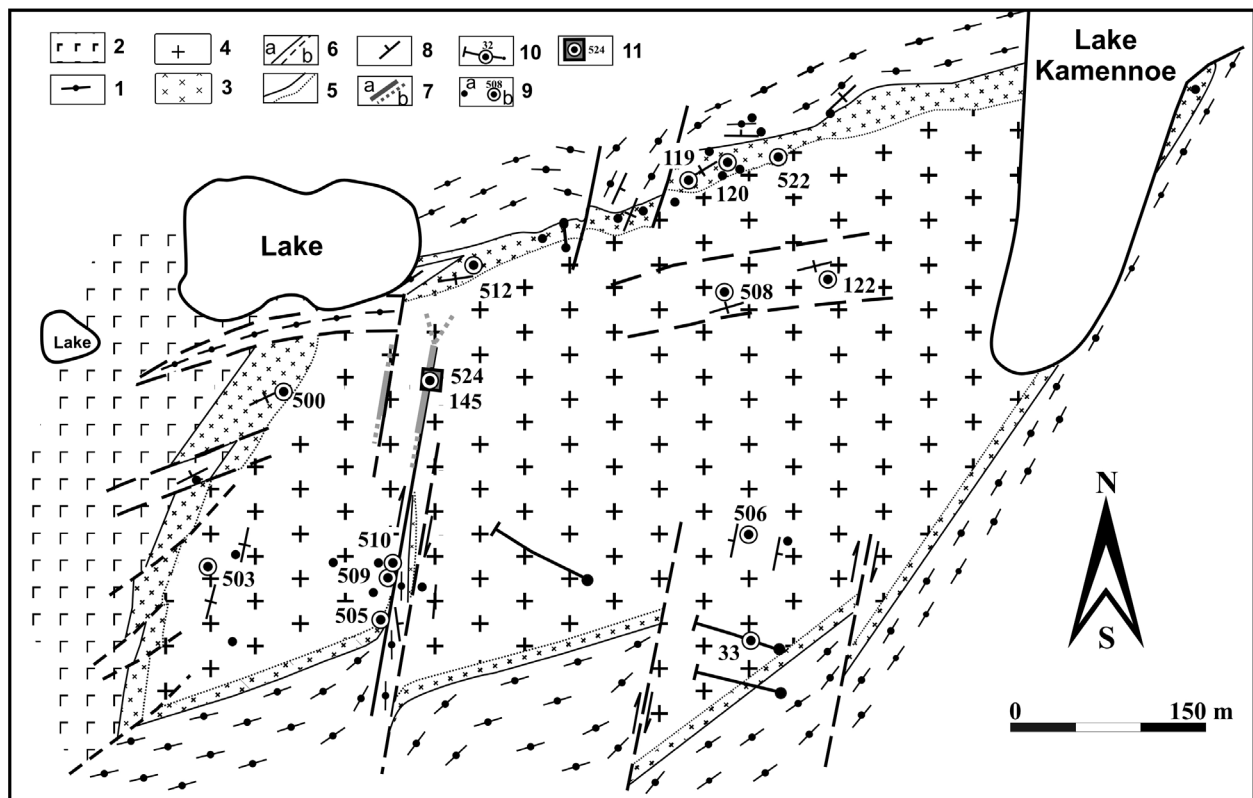


Fig. 6.10. Geological map of the Taloveis massif (After Larionov et al., 2004)

1 = komatiites; 2 = metagabbro and metabasalts; 3 = diorites; 4 = granodiorites; 5 = geologic boundaries of the massif (A) and its phases (B); b = traced (A) and assumed (B) faults; 7 = auriferous quartz veins; 8 = mode of occurrence of rock schistosity; 9-11 = geologic observation and sampling sites: 9 = from natural exposures and ditches: (A) = geochemical samples, (B) = Rb-Sr dating points; 10 = from drill core; 11 = from a prospecting hole.

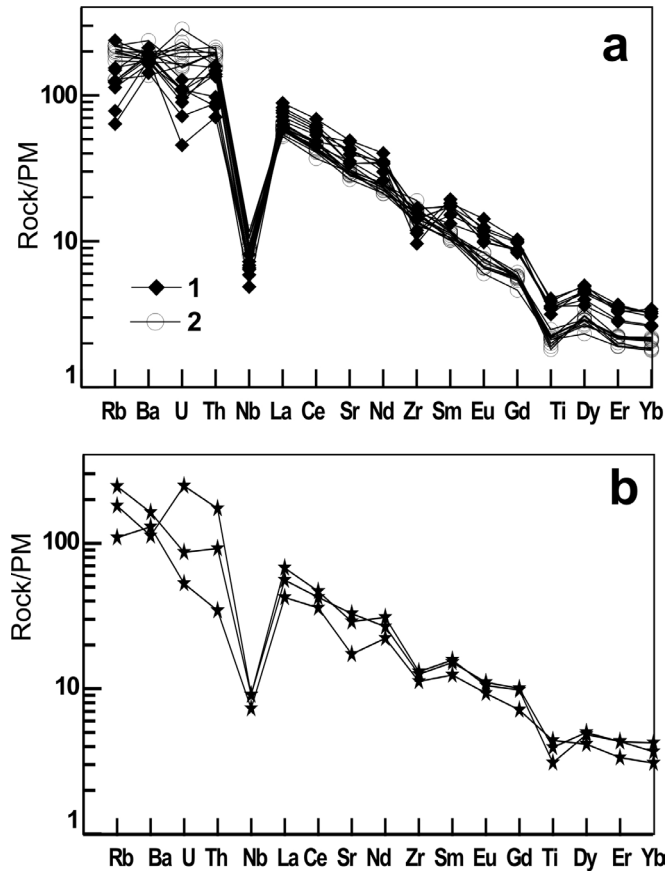


Fig. 6.11. Primitive mantle-normalized (Hofmann et al., 1988) rare-element distribution for sanukitoids and diorite dykes in Kostomuksha metavolcanics (Samsonov et al., 2004) (a) = diorites (1) and granodiorites (2) from the Taloveis massif; (b) = diorite dykes in Kostomuksha metavolcanics.

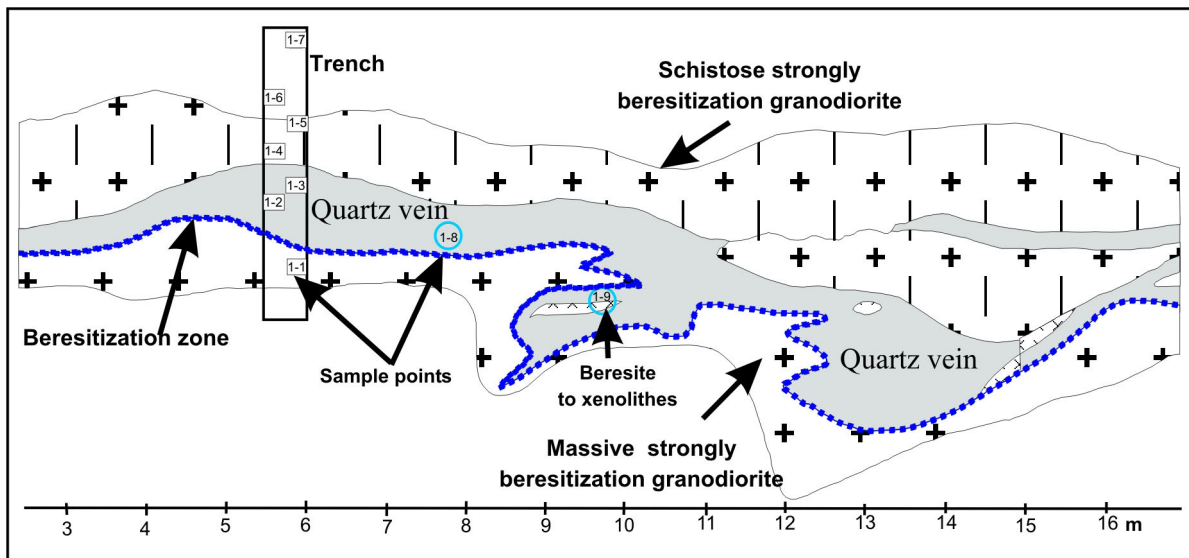


Fig. 6.12. A diorite dyke which cross-cuts the metamorphic banding of Kontokki host felsic metavolcanics and was broken by numerous strike-slip faults in a brittle-ductile deformation environment presumably in Paleoproterozoic time. The southern Kostomuksha structure, Stop 6.14.

The Taloveis massif hosts gold mineralization. It is restricted to quartz veins filling a system of N-S-trending faults that extend across the entire massif (Fig. 6.10) and are part of a regional Paleoproterozoic shear-zone (Volodichev et al., 2002). It seems that the same brittle-ductile deformations break the diorite dykes that cut felsic volcanics in the southern Kostomuksha structure (Fig. 6.12). The initiation of faults and the formation of quartz veins were accompanied by metasomatic alteration of host granitoids. Near the veins, granodiorites are altered to quartz-carbonate-muscovitic metasomatic rocks (beresites) that give way farther away to beresitization aureoles and propylitic-type quartz-feldspathic-biotitic metasomatic rocks. The diorites near the ore zones have suffered quartz-albite-amphibole metasomatism. The age of mineralization is estimated at ca.1720 Ma by the Rb-Sr (Larionova et al., 2004) and Sm-Nd (Vlasov et al., 2007) isochrone methods from mineral fractions of ore zones and near-ore metasomatic rocks. The structure of a gold-quartz ore vein is shown in Figure 6.13.



Fig. 6.13. Geological structure of an auriferous quartz vein in the Taloveis massif with geochemical sampling points (Larionova, 2005).

Stop 6.1. Korpiozero (Fig. 6.1)

Exposure in a roadcut on the Kalevala-Voinitsy highway. TTG granitoids of the eastern Voinitsa domain. The granitoids are structurally heterogeneous and contain numerous inclusions of fine-grained biotite plagiogneisses and amphibolites interpreted tentatively as volcanogenic rock xenoliths. The compositions of the granitoids are shown in Table 6.4, no. 38/1, 2, 3, 4 and in Fig. 6.8b, Samsonov et al., 2001).

Stop 6.2. River Voinitsa, lower stream (Fig. 6.1)

Exposure on the Kalevala-Voinitsy highway. Dykes of lamprophyres in migmatized TTG granitoids of the Voinitsa domain. The age of the lamprophyres within the Voinits domain is estimated at 2694 ± 10 Ma (Bibikova et al., 2005). For compositional characteristics, see Table 6.4, no. 37/1, 2 and 39/4 for comparison, Samsonov et al., 2001. The dykes are assumed to occur in a tectonic contact zone between two geochemical types of TTG granitoids.

Stop 6.3. River Kurzhma, lower stream (Fig.6.1)

Roadcut on the Kalevala-Voinitsy highway, near a bridge across the River Voinitsa. TTG granitoids of the western Voinitsa block that show the geochemical characteristics of adakites. For compositional characteristics, see Table 6.4, no. 36/1, 2; Fig. 6.8a.

Stop 6.4. Voknavolok, roadcut on the Voinitsy-Voknavolok road (Fig. 6.1).

A large remnant of pyroxene-bearing amphibolites in the Voknavolok block, similar in geochemical characteristics to Kostomuksha metabasalts. For the composition of the amphibolites, see Table 6.5, no. 31/1, 2; Fig. 6.9a, Samsonov et al., 2001.

Stop 6.5. Lake Rinojrvi, roadcut on the Voknavolok-Kostomuksha road (Fig.6.1).

Small remnants of bipyroxene amphibolites in Voknavolok enderbite-like granitoids. Based on U-Pb isotopic dating of zircons from the granitoids, the age of the granulites is estimated at 2745 ± 4 Ma (Bibikova et al., 2005). For the compositions of the rocks, see Table 6.5, nos. 22/1, 3, 4, 5 and no. 23, Fig. 6.9a, b, Samsonov et al., 2001).

Stop 6.6. Kostomuksha, northern end of town (Figs. 1 and 2).

Exposure in a drainage ditch around the tailings dump of the Kostomuksha Mining Concentration Plant. TTG granitoids rimming the Kostomuksha structure on the east. They host numerous inclusions of supracrustal rocks, comparable in composition to Kontokki and Gimoly rocks of the Kostomuksha belt. The granitoids vary in composition from diorites to granodiorites, tonalitic varieties being predominant (Table 6.3, nos. 10/97, 54/01, 56/01 and 58/01; Fig. 6.7 a, Samsonov et al., 2005).

Stop 6.7. Kostomuksha (Figs. 6.1, 2, 6).

View of the Kostomuksha iron deposit from the observation site of the Central open-pit mine (Fig. 6.14). Exposures of volcanic-sedimentary rocks (Gimoly series). Here, tuffs of andesite-dacite-rhyodacite composition, metamorphosed to fine-grained biotite (Bi)-schists, are interbedded with carbonaceous shales and iron formation. The lower, largely volcanogenic part is dominated by iron formation. A “conglomerate” horizon in an andesitic-dacitic matrix (Fig. 6.6, a, b) and metatuffs of andesite-dacite composition interbedded with carbonaceous shales and iron formation. For the composition of the metatuffs, see Table 6.2, nos. 7/97, 10/01 and 37-3/01; Fig. 5 б, Samsonov et al., 2005)



Fig. 6.14. View of the Kostomuksha iron deposit from the observation site of the Central open-pit mine

Stop 6.8. Lake Kamennoe-2 (Figs. 6.1, 2 and 8)

Group of natural outcrops and prospecting trenches in the internal part of the Kostomuksha structure. Located in Kontokki komatiites and gabbroids is the Taloveis sanukitoid massif, ca. 0.5 by 1 km in area, which exhibits a polyphase concentric-zonal structure and a sequence of intrusion from diorites and quartz diorites to granodiorites and trondhjemites. Early diorites make up a narrow (less than 50 m) rim along the massif periphery and are encountered as xenoliths in the internal part of the massif among predominant granodiorites. Porphyry structures suggest that the massif was generated on a hypabyssal level. The massif is dated at 2715 ± 5 Ma. For the composition of the granitoids, see Table 6.6, no. 118/A, F, G, 119, 509 and 510 and Fig. 6.11 a; Samsonov et al., 2004).

Stop 6.9 Taloveis (Figs. 6.1, 2, 8 and 12).

Internal part of the Kostomuksha structure. Mesothermal gold mineralization in Taloveis sanukitoids. It is confined to quartz veins (Fig. 6.12) conjugated with a system of N-S-trending faults that extend across the entire massif. Faulting and the formation of the quartz veins were accompanied by beresitization of host granitoids.

Stop 6.10. Lake Kamennoe-2 (Figs. 1 and 2).

Kontokki metavolcanics represented by differentiated komatiitic lava flows with thin horizons formed by komatiitic ash and lapilli tuffs. For the composition of the komatiites, see Table 6.1, nos. 91157, 9332, 91155 and 91156; Fig. 6.4 a (Puchtel et al., 1998).

Stop 6.11. Lake Kamennoe-2 (Figs.6.1 and 2). Slightly deformed pillow lava of Kontokki tholeiitic basalts (Rayevskaya et al., 1992).

Stop 6.12. Lake Figurnoe (Figs. 6.1 and 2). Deformed pillow and massive lava of Kontokki tholeiitic basalts (Rayevskaya et al., 1992). For the composition of the metabasalts, see Table 1, nos. 91145, 9436 and 9437; Fig. 4b, Puchtel et al., 1998.

Stop 6.13. Lake Domashneye (Figs. 6.1 and 2). Volcanics of a dacite-rhyolite association, Kontokki series. The association is dominated by diatreme-facies eruptive breccia and tuffs and tuffites, composed of dacite and rhyolite, within horizons of carbonaceous shales and iron formation (Rayevskaya et al., 1992). For compositions, see Table 6.2, nos. 136/93, 138/93 and 91147; Fig. 6.5a.

Stop 6.14. Lake Domashneye (Figs. 6.1, 2 and 10). Volcanics of a dacite-rhyolite association, Kontokki series. Diatreme-facies eruptive breccia and tuffs consisting of dacites and rhyolites. Diorite dykes (comagmatic with sanukitoids) that cross-cut the metamorphic banding of felsic tuffs are sheared. For the composition of the felsic volcanics, see Table 6.2, nos. 13/97, 22A/97 and 22B/97; Fig. 6.5a. For the composition of the diorite dykes, see Table 6.6, nos. 518-3 and 2/97, in Fig. 6.11 b (Samsonov et al., 2004)

Stop 6.15. Lutta (Figs. 6.1, 2 and 10). Roadcut on the Kostomuksha-state border highway, south-west of the Kostomuksha greenstone structure. Homogeneous, poorly gneissose TTG granitoids with the geochemical characteristics of adakites (Table 6.3, no. 5/97; Fig. 6.7 a, Samsonov et al., 2005).

Day 7, Sunday 3.8. 2008

Wake up at 7:00, breakfast. Kuhmo greenstone belt geology: tectonostratigraphy and tectonic setting, sanukitoids, komatiite-tholeiite successions, felsic volcanics. Drive to Nurmes where overnight at Bomba spa (<http://www.nnc.fi/bomba/eng/index.htm>).

Kuhmo greenstone belt

Tapio Halkoaho, Asko Käpyaho, Asko Kontinen, Petri Peltonen
Geological Survey of Finland

The Kuhmo greenstone belt forms the central part of the c. 220-km-long Suomussalmi-Kuhmo-Tipasjärvi greenstone belt in eastern Finland (Fig. 7.1). The supracrustal succession in the Kuhmo belt starts with rhyolitic-dacitic lavas and pyroclastics whose basement and original thickness is unknown. A single U-Pb zircon TIMS analysis available for Kuhmo felsic volcanics yielded an age of 2798 ± 15 Ma (Hyppönen, 1983). A pegmatoidal sample from a layered mafic sill within the Kuhmo mafic-ultramafic sequence yielded a TIMS U-Pb zircon age of 2790 ± 18 Ma (Luukkonen, 1988).

The felsic volcanics are overlain by an up to one km thick sequence of tholeiitic pillow lavas and hyaloclastites, with sporadic Algoma-type BIF-layers and hydrothermal Mg-Fe

precipitates in the middle part of the sequence. These were followed by komatiites (total thickness ~ 500 m), komatiitic basalts (~ 300 m), interlayered high-Cr basalts (~ 250 m) and komatiites, Cr-basalts (~ 250 m) and finally pyroclastic intermediate-mafic volcanics (Papunen et al., 1999).

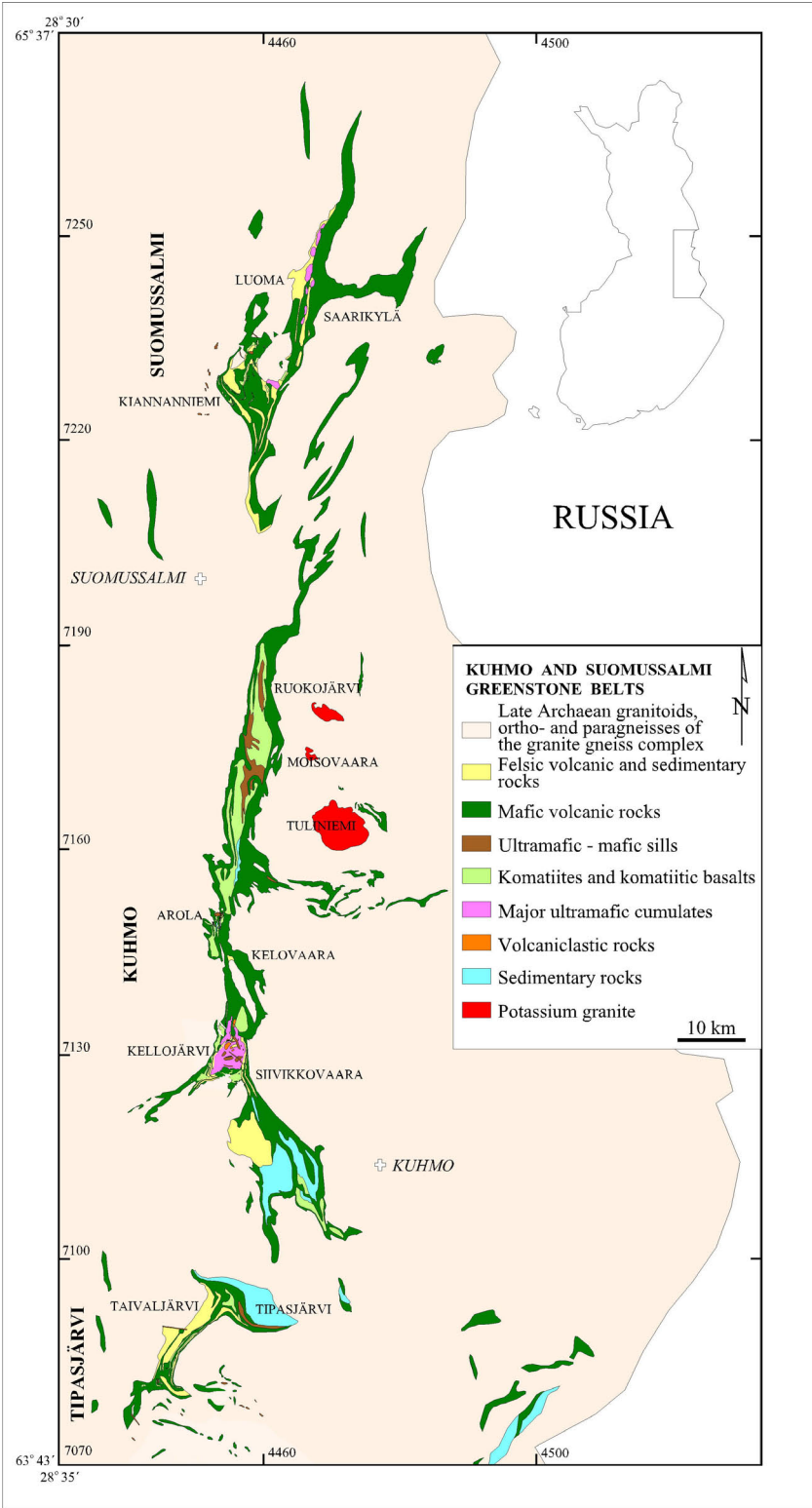


Fig. 7.1. Generalized geological map of the Kuhmo greenstone belt. Updated from the maps of Luukkonen (1991) and Taipale et al. (1993).

The komatiite volcanology has been studied in detail by Papunen et al. (1999) in the key area near Pahakangas. The komatiite sequence starts with a 1-2 m thick komatiite–BIF hybrid rock (metamorphosed to pyroxenite) that is overlain by three fractionated komatiite flows, with orthocumulate layers at their base and platy spinifex and random-spinifex zones at their tops. A detailed map of the key outcrop can be found in Halkoaho and Pietikäinen (1999). These lowermost fractionated flows are overlain by 13 less fractionated flows, characterised by flow top breccias and pillow lavas. Stratigraphically further upwards, komatiites and komatiitic basalts first erupted contemporaneously, later giving way to a ca 300m thick pile of variolitic or pillow textured komatiitic basalts. Lenses of olivine meso- and adcumulates (metamorphosed to serpentinite) are interpreted as lava pathways and are the main nickel exploration targets in the area. The Kellojärvi layered ultramafic complex is also believed to have crystallised from a komatiitic magma, either representing a lava lake (Tulenheimo, 1999) or a layered intrusion coeval with the komatiite sequence. The original stratigraphic thickness of the Kellojärvi complex was 300–500 meters and its areal extent is ca. 10 x 15 km.

The Kuhmo greenstone belt is bounded by Archean migmatitic tonalitic orthogneisses, migmatites of sedimentary origin, and TTG, sanukitoid, and granite plutons. Recently, an increasing number of high-precision U-Pb zircon ages have become available for these rocks (e.g. Käpyaho et al., 2006), providing important constraints on the mutual relationship between the greenstone belts and their surroundings. Although several previous studies have suggested that the Kuhmo greenstone succession was deposited on older continental crust (Martin et al., 1984; Luukkonen, 1992; Papunen et al., 1999), this is not supported by the more recent age data. With the exception of one mesosome sample ~ 30 km east of the Kuhmo greenstone belt (2843±18 Ma; "Lylyvaara"; Luukkonen, 1985), all samples yield crystallisation ages younger than the greenstone belt volcanics. Furthermore, Käpyaho et al. (2006) – based on an extensive Sm-Nd isotope study of the plutonic rocks in the Kuhmo area – concluded that the rocks represent relatively juvenile material without a major input of significantly older crust.

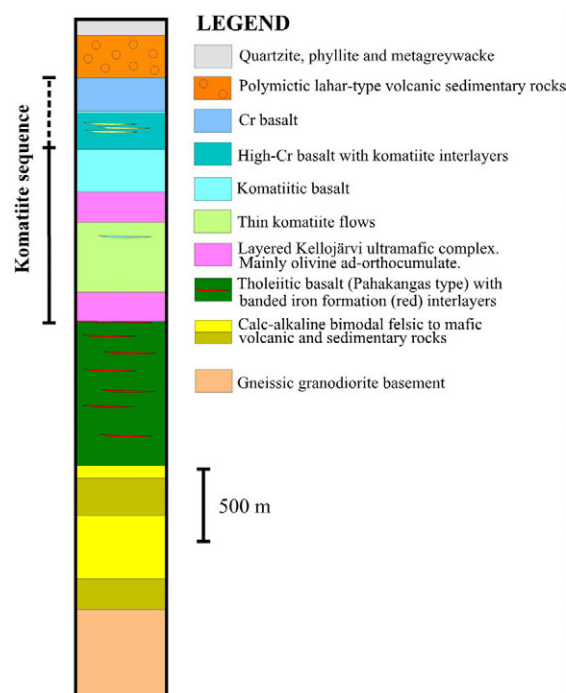


Fig. 7.2. Generalized stratigraphic column of the Kuhmo greenstone belt in the Siivikkovaara area, Kuhmo (modified after Halkoaho et al. 1997).

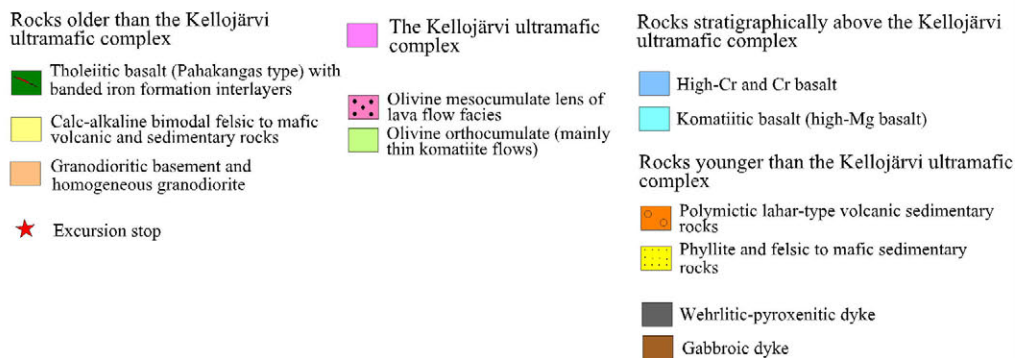
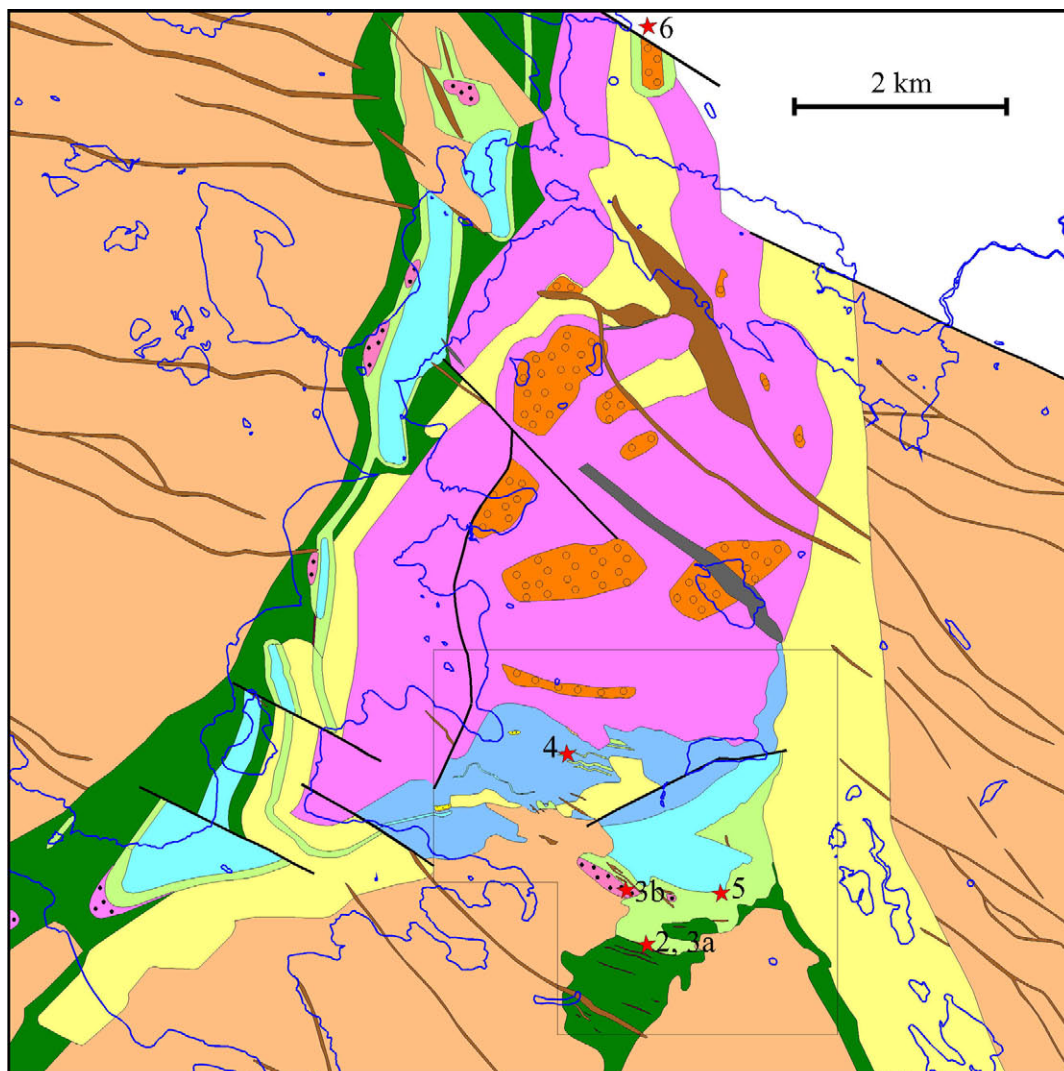
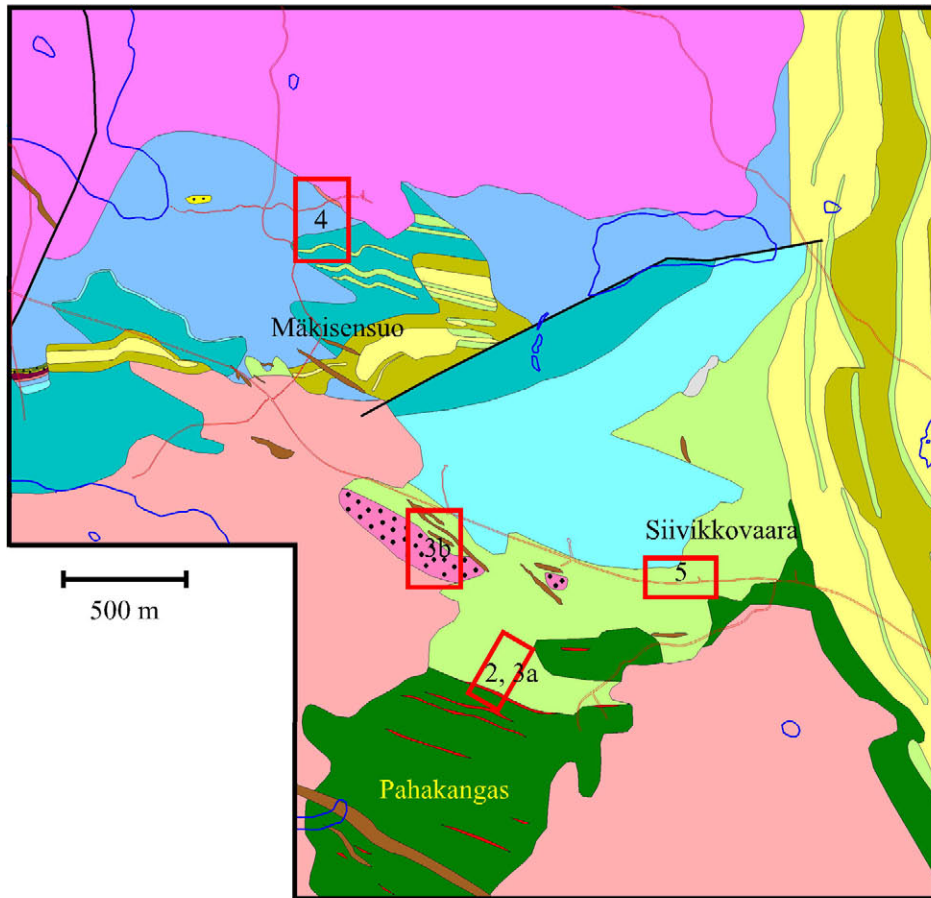


Fig. 7.3. Geological map of the Kellojärvi-Siivikkovaara area, Kuhmo. The Siivikkovaara area mapped in detail in Fig. 7.4. is delineated.



T. Halkoaho 1998

Rocks older than the komatiitic sequence

- Tholeiitic basalt (Pahakangas type) with thin banded iron formation interlayers
- Calc-alkaline bimodal felsic to mafic volcanic and sedimentary rocks

Rocks of the komatiitic sequence

- Cr basalt
- High-Cr basalt
- Komatiitic basalt
- Olivine orthocumulate (mainly thin komatiite flows)
- Olivine mesocumulate lens of lava flow facies
- The Kellojärvi ultramafic complex

Rocks younger than the komatiitic sequence

- Phyllite and felsic to mafic sedimentary rocks
- Homogeneous granodiorite or granodioritic dyke
- Pyroxenitic dyke
- Gabbroic dyke

- Major fault
- Excursion stop
- Road

Figure 7.4. Geological map of the Siivikkovaara area (modified after Halkoaho et al. 1996) and field trip stops.



Fig. 7.5. Dacitic lava at Katerma, Stop 7.1. (photo: P. Peltonen).



Fig. 7.6. Trench from the lowermost (Pahankangas) tholeiitic basalts to the lowermost thin komatiite lava flows; komatiitic orthocumulates and mesocumulates; platy, random, stringy beef spinifex-textures; pillow lavas and komatiitic flow top and bottom breccias + rhyolite fragments in komatiite flow.

Stop 7.1.

Lowermost stratigraphic unit dacitic lavas and volcanoclastic rocks at Katerma, conventional U-Pb zircon age 2789±15 Ma, or Juurikkajärvi felsic volcanic/agglomerate/volcanic conglomerate at same stratigraphic position (7144161, 4457232).

Stop 7.2. Trench from lowermost tholeiitic basalts to the lowermost thin komatiite lava flows; komatiitic orthocumulates and mesocumulates

Stratigraphically lowermost unit in the examination trench (Figs. 7.6.) is the porphyritic tholeiitic Pahakangas basalt, which is overlain by a 5-10 m thick sulfidic banded iron formation (it is not exposed in this trench but in an outcrop, 70 m to west and in another trench, 80 m to east; Fig. 7.7.). The lowermost rock type of the komatiitic sequence is narrow (1-2 m thick) tremolite rock, so-called "hybrid" rock, which has been assumed to form from a mixture of banded iron formation and komatiite lava (this is only exposed in the other trench about 80 m to east). Between the tremolite rock and about 20 m thick komatiite olivine orthomesocumulate is a 3-4 m thick plagioclase (quartz) porphyre which has been interpreted as a younger dyke because its stratigraphic position varies. The upper part of the first komatiite lava flow shows komatiitic textures from bottom to top: a narrow aligned hopper olivine layer (B1), about 4 m thick platy olivine pyroxene spinifex (A3) and about 2 m thick random spinifex layer (A2). The first komatiite lava flow is overlain by a 2-3 metres thick orthocumulate layer which contain up to 60 narrow (2-10 cm) spinifex "layers" or schlierens. There is two opinions how these narrow spinifex schlierens have formed: 1) they represent cracks which have been filled by a new komatiite melt or 2) they are levée banks of a komatiite lava river. In the westernmost outcrop in Fig. 7.8 this orthocumulate layer has totally eroded away the random spinifex layer of the first komatiite lava flow. The thickness of the third lava flow is about 2 m and it contains a 0.5 m thick orthocumulate, a 1 m thick platy spinifex and a 0.5 m thick random spinifex layer. Flow bottom or top breccias has not been found from these lowermost, altogether 30 m thick, komatiite lava flows. Above this stratigraphic level has not been found any spinifex textures even the rest of this trench (about 150 m) contains 13 individual lava flows. Four of these polyhedral jointing textured flows contain flow top breccia and one flow is a pillow lava.



Fig. 7.7. Tholeiitic pillow basalts at Pahakangas with banded oxide and sulfide facies iron formation (BIF) interlayers. (Photo: P. Peltonen).



Fig. 7.8. Komatiitic orthocumulate layer eroded by the random spinifex layer. Photo: T. Halkoaho

Stop 7.3. Archean komatiite lava river

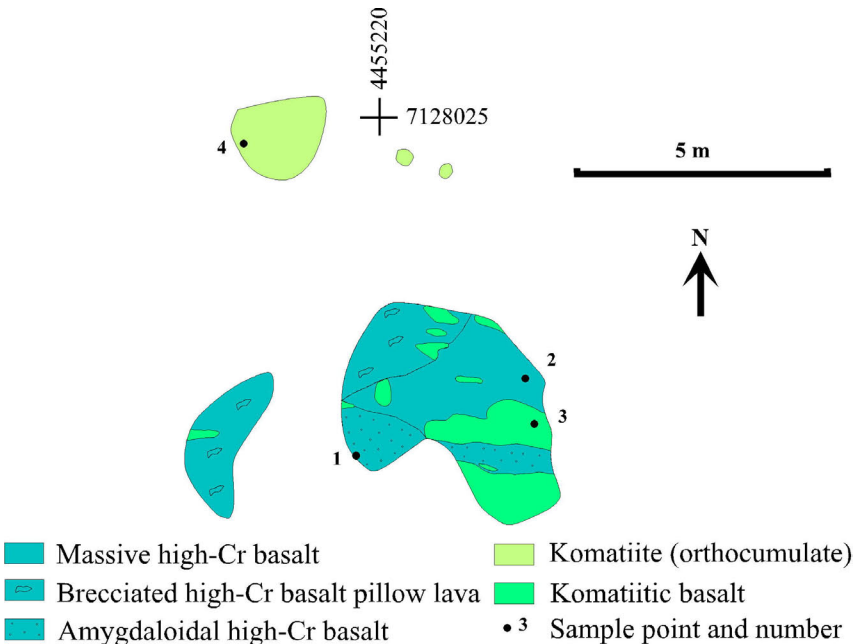
About 400 m northwest from the traverse of Fig. is a small serpentinite lens which has been interpreted to represent cumulates of an ancient komatiite lava river. The small serpentinite (originally mainly olivine) is about 600 m long and 100 to 150 m thick. According to ground magnetic measurements, drillings and outcrops it has been divided into two parts. Between those two about 50 m thick olivine mesocumulates is 10 m thick less magnetized tremolite rock layer. The lower part of this layer contains roundish granodioritic "boulders" which diameters vary between 0.2 to 3 m. Around of these boulder is a narrow (0.1-0.2 m thick) chlorite schist "crust". The tremolite rock layer might represent a pause in a lava flow. During this pause boulders dropped from surrounding granodioritic basement walls to the surface of the lower part cumulates. Then a thin komatiite lava layer (now tremolite rock layer) covered and melted those boulders and soon after that volume of the komatiite eruption increased and upper part of the small serpentinite lens formed. In Fig 10 the westernmost outcrop contains about 0.5 m thick chlorite magnetite dyke which have in both sides about 1 m thick alteration rim. The mineralogy of the vein itself is chlorite (clinochlore) and magnetite with minor amount of clinozoisite. About 200 m to northwest, stratigraphically about 70 m above the small serpentinite lens is a pyroclastic looking komatiite-komatiitic basalt outcrop which is intersected by a younger 1-20 m thick gabbro.

Stop 7.4. High-Cr basalts

These outcrops represent a chemically extraordinary type of basalt, so-called high-Cr basalt (Cr content varies between 1300-4500 ppm), with thin komatiite interflows (Fig. 7.9). Similar Cr contents in basalt has been described earlier only from lunar basalts (Huebner et al. 1976, Roeder and Reynolds 1991 and Basaltic Volcanism Study Project 1981) and basaltic meteorites (Huebner et al. 1976 and Basaltic Volcanism Study Project 1981). Stratigraphically this unit is above the komatiitic basalt unit. The outcrop is quite heterogeneous and contains a massive, a

brecciated pillow lava and an amygdaloidal high-Cr basalt with komatiitic basalt "fragments". About 5 m to north from the main outcrop is an outcrop of 10 m thick komatiite interlayer. Note that the Cr concentrations of the high-Cr basalts is even higher than the Cr concentrations in the komatiitic basalt fragments.

About 130 m to east is a large high-Cr basalt outcrop, which contains well preserved pillow lava texture. The komatiitic interflow is found on the northern side of the outcrop. About 150 m to north in a northern side of a dune ridge is few small outcrops of the medium-Cr basalt pillow lava. The next outcrops, about 100 m to northeast, belong to the Kellojärvi ultramafic complex. The ultramafic (serpentinite) outcrop is originally an olivine ad-mesocumulate. Some hundred metres to the north ultramafic outcrops contain also some pyroxenite cumulates.



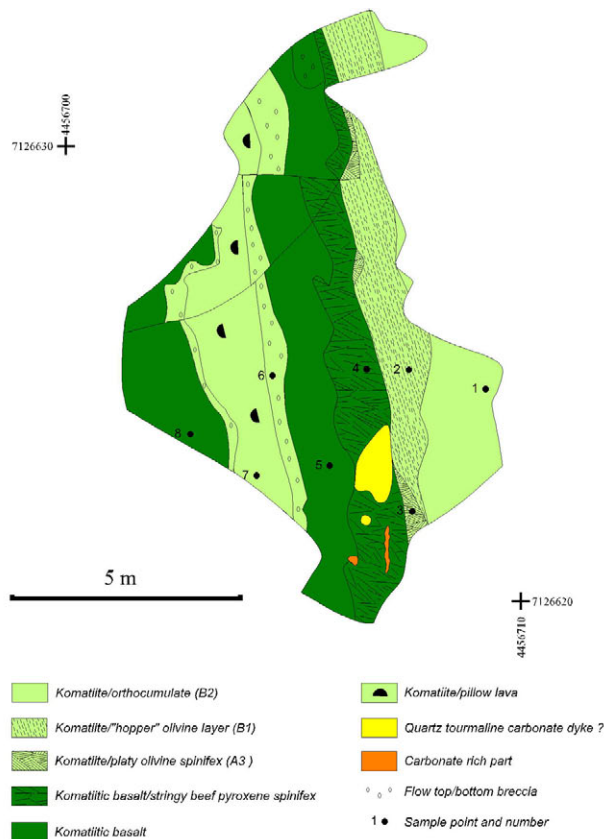
	1	2	3	4
SiO ₂ %	52.2	53.6	50.0	48.4
TiO ₂	0.61	0.71	0.45	0.34
Al ₂ O ₃	12.9	13.5	10.2	8.09
FeO	12.5	10.8	11.0	10.4
MnO	0.26	0.24	0.25	0.18
MgO	6.68	7.19	14.8	23.4
CaO	11.9	10.6	11.6	8.82
Na ₂ O	2.33	2.69	1.16	<0.01
K ₂ O	0.25	0.19	0.25	0.01
P ₂ O ₅	0.05	0.05	0.04	0.03
Cr ppm	2162	2443	1567	3038
Ni	310	260	540	810
S	30	<300	<300	970
V	259	279	194	143
Al/Ti	18.7	16.9	20.0	21.2
mg#	51.4	56.9	72.8	81.7

$$mg\# = 100 * (MgO/40.3) / ((MgO/40.3) + 0.9 * (FeO/71.85))$$

Figure 7.9. The detail map from the exceptionally Cr-rich (high-Cr basalt) basalt with komatiite interflow, the northern side of the Mäkisensuo area (modified after Halkoaho et al. 1996).

Stop 7.5. Penecontemporaneous eruption of komatiites and komatiitic basalts

Twentyfive metres to the south from the Näätäniemi road there is an excellent example of the situation where komatiites and komatiitic basalts erupted penecontemporally in the same area. The outcrop (Fig. 7.10) contains five individual lava flows: two komatiites and three komatiitic basalts. The first lava flow on the east side of the outcrop is komatiite, which lower part is massive olivine orthocumulate, the middle part is hopper-like komatiite and the uppermost part is platy olivine spinifex, which is almost totally eroded leaving only few remnants. Above this komatiite flow is a stringy beef spinifex textured komatiitic basalt bed, which is overlain by a massive komatiitic basalt lava flow. Above this layer is a komatiite pillow lava with flow bottom and top breccias. This is overlain again by a massive komatiitic basalt lava bed.



	1	2	3	4	5	6	7	8
SiO ₂ %	50.9	46.8	43.6	51.6	50.6	47.6	47.4	45.8
TiO ₂	0.33	0.42	0.54	0.57	0.57	0.53	0.47	0.72
Al ₂ O ₃	7.63	9.70	12.2	11.7	11.7	9.52	9.61	13.0
FeO	10.5	11.5	14.0	11.0	10.8	11.3	11.1	14.7
MnO	0.13	0.19	0.23	0.19	0.19	0.22	0.22	0.23
MgO	27.4	23.1	22.0	14.4	15.7	21.7	21.7	14.6
CaO	2.46	7.80	6.99	7.31	7.51	8.51	8.78	9.41
Na ₂ O	0.01	0.09	0.15	2.96	2.65	0.28	0.31	1.20
K ₂ O	<0.01	0.02	0.02	0.07	0.05	0.03	0.04	0.10
Cr ppm	3517	1936	1574	903	1389	2381	1888	1067
Ni	1320	790	600	320	460	860	780	350
V	141	175	224	233	210	174	184	264
Al/Ti	20.1	20.6	19.9	18.2	18.1	15.7	18.0	15.9
mg#	83.9	79.9	75.7	72.1	74.1	79.2	79.4	66.3

$$\text{mg\#} = 100 * (\text{MgO}/40.3) / ((\text{MgO}/40.3) + 0.9 * (\text{FeO}_{\text{tot}}/71.85))$$

Fig.7.10. The detail map from the outcrop which present penecontemporaneous eruption of komatiites and komatiitic basalts (modified after Halkoaho et al. 1996).

Stop 7.6. Viitavaara tonalite

Coordinates: 7120740, 4445870

Introduction

Viitavaara tonalite is lying near the contact zone of the supracrustal rocks of the greenstone belt. The intrusion has an U-Pb age of 2785 ± 7 Ma determined by SIMS method (Käpyaho et al., 2006), and thus it may be coeval with the felsic volcanic rocks at Katerma within the greenstone belt reported by Hyppönen (1983). This tonalite differs from other adakite-like tonalites of the Archean bedrock in the Karelia as it may have originated above garnet stability field.

Description

Viitavaara tonalite is grayish, medium-grained and foliated biotite and amphibole containing tonalite. This tonalite locally has biotite-rich enclaves. The Si_2O content vary from 65.4 to 58.3 wt. % and trace element geochemical characteristics include relatively weakly fractionated REE pattern, with no or weak negative Eu anomalies (Käpyaho, 2006). The sample taken for age determination from this locality reveals initial ϵ_{Nd} value ca. +2, thus corresponding to depleted mantle of that age (Käpyaho et al., 2006).



Fig 7.11. Viitavaara-type tonalite. Coordinates: northing 7118 000, easting 4447 200. Photo by Kerstin Saalman.

Stop 7.7. Nurmes paragneiss and its tectonostratigraphic significance

Coordinates: 7109590, 4474970

Introduction

The Nurmes paragneisses form a c. 150 km long belt and they are a prominent component of the Archean bedrock in eastern Finland. The protoliths of the gneisses are plagioclase and biotite dominated turbiditic greywackes locally intercalated with amphibolites that correspond to oceanic tholeiites (Kontinen et al., 2007). The Nurmes paragneisses usually are migmatized, but in some outcrops primary sedimentary features, such as layering, obviously after bedding, are visible. The mesosomes often contain minor graphite that shows $\delta^{13}\text{C}$ values from c. -36 to -14, thus suggesting biogenic origin (Kontinen et al., 2007). The detrital zircons analysed by SHRIMP from mesosomes of the paragneisses yield U-Pb ages from c. 2.7 Ga to nearly 3.1 Ga, although most of the grains have ages between 2.7 Ga and 2.75 Ga (Fig. 7.12.) (Kontinen et al., 2007). The apparent similarity with detrital population of the Nurmes paragneisses and the metasedimentary rocks from Superior province, Canada, were considered to support the hypothesis that Karelia and Superior province are fragments of the same supercraton, called Superia (Kontinen et al., 2007).

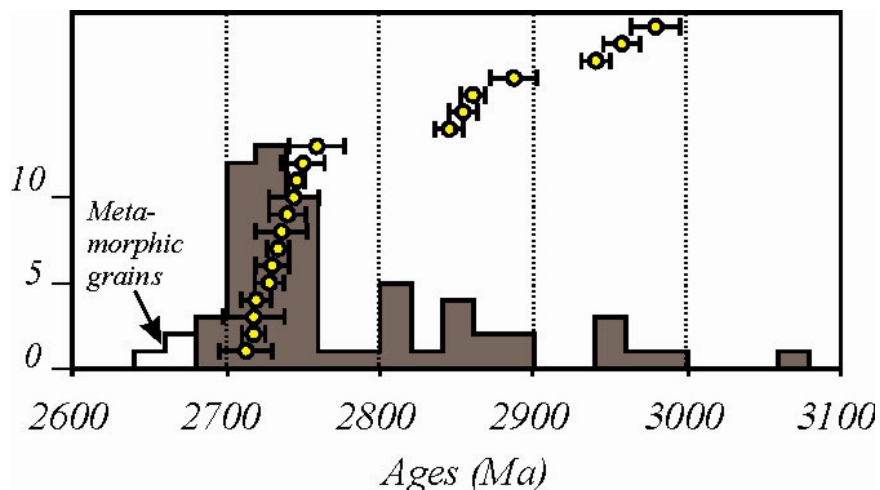


Fig. 7.12. Histogram showing ages from detrital zircons of Nurmes type paragneisses (brown) and metamorphic zircons (white). Histogram plot is compilation of three samples from geographically different parts of the Nurmes belt. Yellow circles show concordant and nearly concordant $^{207}\text{Pb}/^{206}\text{Pb}$ age data with 1σ error bars from this location (1-KUH-88). All data are from Kontinen et al. (2007).

Description

The Stop 7.8. outcrop shows an example of relatively weakly migmatized, layered, grayish-brownish coloured Nurmes-type paragneiss (Fig. 7.13). The mesosome layers mainly consist of quartz, biotite and plagioclase. Layering is relatively vertical and it shows open folding structures. Thin leucosome bands are light-colored and comprise mainly quartz and feldspar. Chemical composition of the mesosome material is typical of quartz-intermediate graywackes (cf. Kontinen et al., Table 5, sample 1-KUH-88). A distinctive feature is relatively high Ni (93 ppm) and Cr (206 ppm), a characteristic of Nurmes mesosomes and Archean greywacke sediments in general.

Age data from this locality reveal that c. 50% of the zircons have ages between 2.70 and 2.75 Ga (Kontinen et al., 2007), thus corresponding the other Nurmes-type paragneisses of the eastern Finland. On the basis of the zircon age, Sm-Nd isotope and trace-element geochemical

data Kontinen et al., (2007) speculated that the material for the paragneiss protholiths was dominantly derived from the plutonic rocks in the Ilomantsi belt. Deposition was considered to have occurred in a back-arc or intra-arc setting, just before the c. 2.70 Ga collisional accretion of the Kuhmo and Ilomantsi terrains (Kontinen et al., 2007).



Fig 7.13. Layered Nurmes-type paragneiss with thin leucosome bands.

Day 8, Monday 4.8. 2008

Archean granulites in the Iisalmi area, 2600 Ma Siilinjärvi carbonatite

Pentti Hölttä¹, Hannu Huhma¹, Irmeli Mänttari¹, Franziska Nehring² & Jorma Paavola¹

¹*Geological Survey of Finland*

²*Johannes Gutenberg-University Mainz, Institute of Geosciences*

Introduction

Rocks that were metamorphosed in medium pressure at mid-crustal or lower crustal levels are exposed as fault-bounded blocks in the Archean Iisalmi area, near the western boundary of the Karelian craton (Fig. 8.1). The Iisalmi granulite area represents Neoproterozoic terrane accretion where blocks that exhibit marked lithological, geochemical and age differences are juxtaposed with each other. The Jonsa block (Fig. 8.1) has younger zircon U-Pb (2.6-2.7 Ga) and Sm-Nd T_{DM} model ages (2.9-2.7 Ga) than other granulites (3.2-3.1 Ga), and also its lithology and geochemistry of mafic rocks differ from those in the other blocks (Hölttä, 1997; Mänttari & Hölttä, 2002). In all blocks the Sm-Nd garnet-whole rock ages are younger, ranging from 2.48-2.59 Ga, which evidently is the age of closure of the Sm-Nd system in these rocks (Hölttä et al, 2000).

Partial melting of compositionally basaltic and andesitic rocks produced garnet, plagioclase and pyroxene bearing restitic granulites at 9-11 kbar and 800-900°C. Peak conditions were followed by cooling and decompression to around 700°C and 7 kbar (Hölttä & Paavola, 2000; Nehring, 2007). Granulite facies metamorphism was simultaneous in all blocks. The clockwise PT path and medium pressure metamorphism indicate that the Varpaisjärvi granulites formed in collisional tectonic setting. Granulites underwent a second metamorphic event at lower pressure conditions, which seems to be connected with the semibrittle fracturing of the bedrock either during the emplacement of the Palaeoproterozoic dolerites at 2.3-2.1 Ga or during the Svecofennian orogeny at 1.89-1.88 Ga.

The excursion shows a lower crustal section of Mesoarchean and Neoarchean rocks from the highest pressure eclogitic granulites in the NW to a little bit lower pressure granulites in the SE.

Stop 8.1 . Kainuunmäki, eclogitic granulites

The petrography as well as the geochemical characteristics of granulites from the westernmost part of the Karelian craton have been described in detail by Paavola (1984), Hölttä (1997), Hölttä & Paavola (2000) and Nehring (2007). Granoblastic grt-cpx-pl-qtz±hbl assemblages are typical for the mafic granulites from the *Iisalmi-Sukeva* area (Fig. 1). They display steep fractionation trends on variation diagrams and exhibit a strong enrichment in CaO (8-16 wt.%). Trace element characteristics are LREE-depletion and enrichment in compatible elements similar as observed in tholeiitic basalts (Fig. 8.2 and 8.3a).

Peak metamorphic conditions in granulites were obtained from grt-cpx-pl-qtz assemblages indicating c. 9-11 kbar and 800-900°C, using the TWQ software of Berman (1988, 1991, 1990). Garnet-bearing mafic granulites normally have the mineral assemblage *hbl* (10-45%) - *cpx* (10-40%) - *opx* (5-10%) - *grt* (2-25%) - *pl* (25-50%) ± *qtz* (0-5%). In the northwestern exposures orthopyroxene is lacking, and also the highest metamorphic pressures and temperatures, c. 11 kbar and 900°C were obtained from mafic granulites in the area represented by Stop 8.1. This suggests a deeper crustal origin for the rocks in the northwestern part of the granulite area (Hölttä & Paavola, 2000). Granulites characteristically contain a high abundance of carbonic fluid inclusion (Nehring, 2007). Few of these carbonic inclusions record peak metamorphic conditions while most experienced resetting during Proterozoic overprint of the area. The overall abundance of carbonic fluid inclusions within granulites as well as the preservation of anhydrous mineral assemblages indicates that granulites formed in a dry environment.

In the exposure there are mafic granulite where dark mafic layers alternate with less mafic layers. Compositionally darker layers represent high-Mg tholeiitic basalts and lighter layers basalts in the Jensen's cation plot. Garnets and clinopyroxenes up to 1-2 cm are present. The mineral assemblage grt-cpx-pl-qtz without amphibole and orthopyroxene is common in the basaltic rocks. In Fig. 8.3 there is a pseudosection calculated using the Thermocalc 3.31 software (Holland & Powell, 1998 and references therein) that shows the stability fields for mineral assemblages of various variance for a composition analysed from Stop 1. According to the figure the grt-cpx-pl-qtz-assemblage is stable in pressures > 800°C and pressures > 11.5 kbars that fits well with the results calculated using the TWQ for this exposure (Hölttä & Paavola, 2000). However, because the jadeite content of clinopyroxene is not very high (Na₂O c. 0.5 wt%) and plagioclase is present the rock is not eclogite, and has probably never been because there are no relics of earlier omphacites.

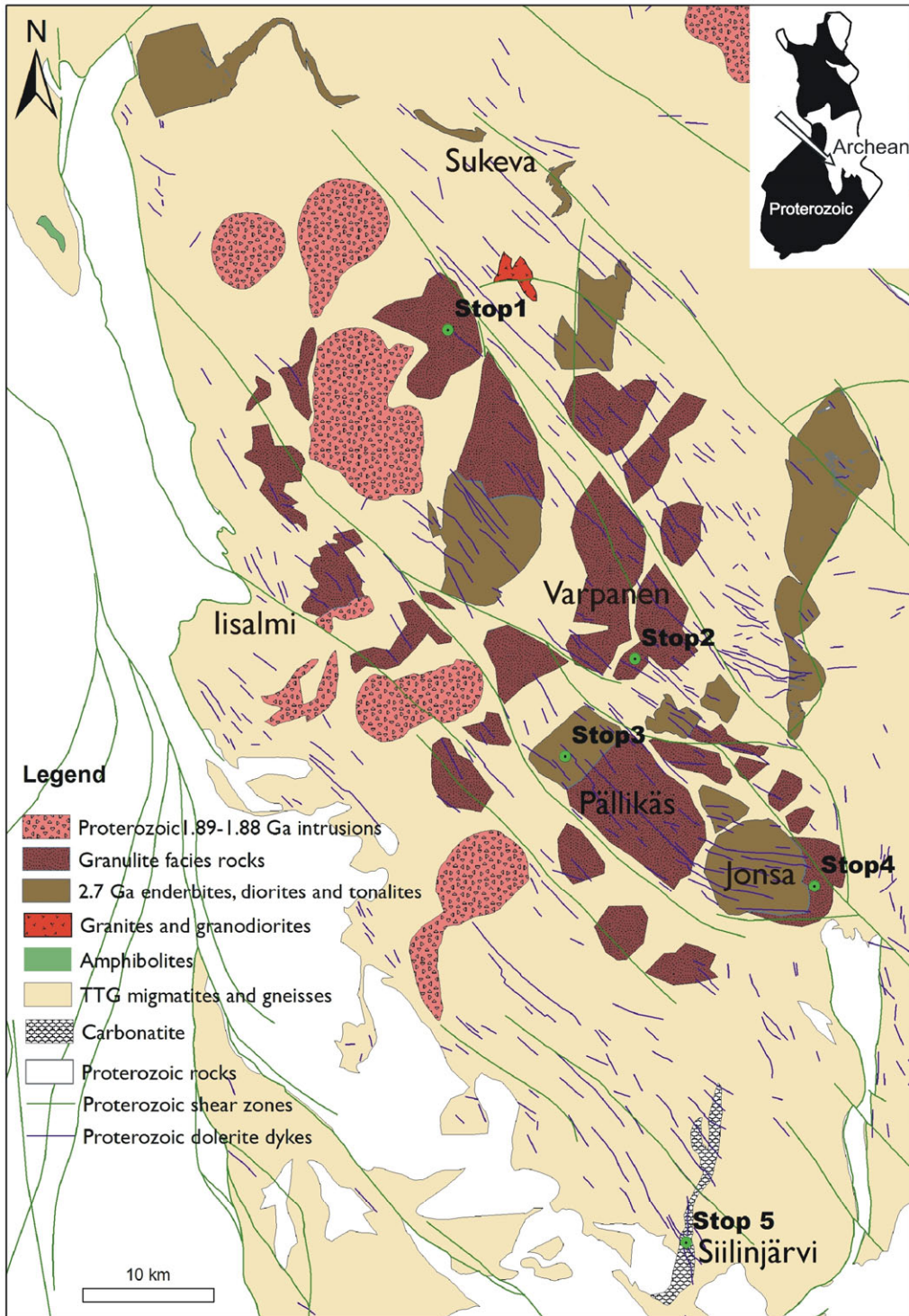


Fig. 8.1. A simplified geological map of the Iisalmi granulites showing the locations of the excursion stops. The arrow in the inset shows the location of the area in Finland.

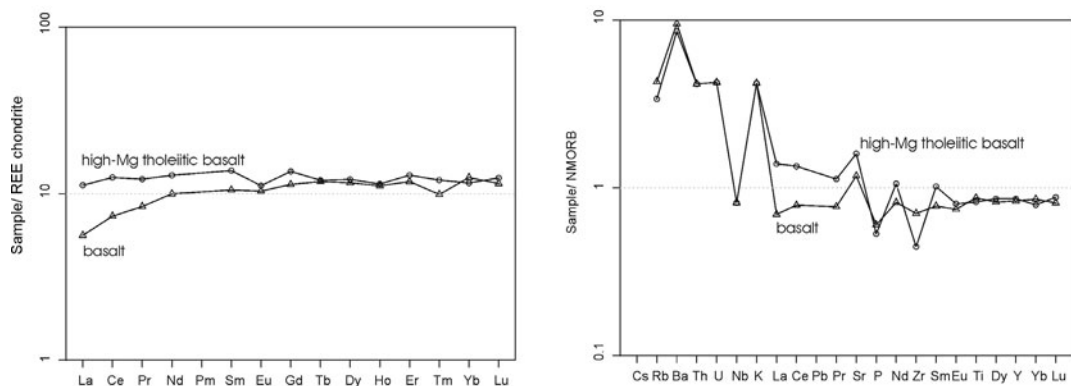


Fig. 8.2. Chondrite and NMORB normalised trace element patterns of mafic rocks in Stop 1.

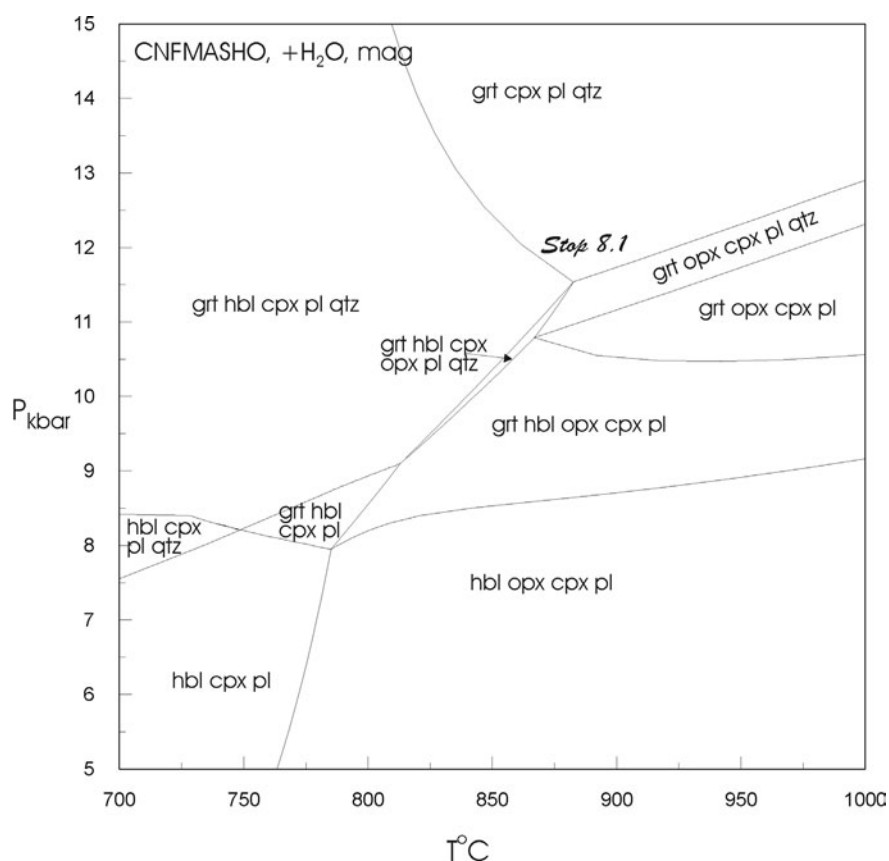


Fig. 8.3. A pseudosection calculated using the Thermocalc 3.31 for a whole rock composition analysed from grt-cpx-pl-qtz rock from Stop 8.1: SiO₂ 47.78, TiO₂ 1.09, Al₂O₃ 16.28, FeO 10.19, MnO 0.23, MgO 5.89, CaO 11.67, Na₂O 2.81 wt%.

Stop 8.2. Kumisevanmäki, intermediate and mafic 3.2-3.1 Ga granulites

Stop 8.2 is an example of mafic and intermediate granulites of the *Varpanen-Pallikäs* area. Intermediate granulites have lower CaO contents and low contents of compatible elements compared with mafic granulites. Their REE-patterns show LREE-enrichment (Fig. 8.3b).

Granulites from the *Varpanen-Pällikäs* area show compositional overlap with both groups. According to difference in mineralogy some samples are more similar to grt-cpx-pl granulites from the *Iisalmi-Sukeva* area, showing enrichment in CaO and characteristic steep fractionation trends, while others are intermediate in composition and resemble 2-pyroxene granulites from the *Jonsa* area. Both types may occur in a single outcrop and flat REE-patterns are restricted to more mafic, garnet-bearing layers (Fig. 8.3c). Field appearance and compositional differences within granulites from the *Jonsa* and *Varpanen-Pällikäs* areas suggest a pre-metamorphic layering of broadly andesitic rocks probably resembling volcanic successions.

On the concordia diagram zircon from the Kumisevanmäki intermediate granulite plots mostly on the age interval of 3.1-3.2 Ga (Fig. 8.4a). Only three analyses deviate from this main age group, two of them are c. 2.62-2.63 Ga and one 2.80 Ga. The minimum protolith age of the A1145 intermediate granulite is 3.2 Ga. The ages between 3.1-3.2 may indicate that the protolith underwent a high grade metamorphism already at ca. 3.2-3.1 Ga. Zircon from leucosome gives ages of ca. 3.2-3.0 and around 2.7 Ga (Fig. 8.4b). The older zircon grains are inherited from the mesosome and younger ages indicate leucosome crystallization after melting (Hölttä et al., 2000; Mänttari & Hölttä, 2002).

Granulites underwent a multi-stage metamorphic development from the Mesoarchean to the Paleoproterozoic. For the Kumisevanmäki the TWQ thermobarometry shows peak crystallization pressures of c. 9-10 kbar and temperatures of 840-930°C. Ferromagnesian phases in leucosomes are iron rich, giving slightly lower pressures than those in mesosomes, which suggests that decompression promoted melting. Peak conditions were followed by cooling and decompression to around 700°C and 7 kbar. Garnet broke down in the reaction $\text{grt} + \text{cpx} + \text{qtz} = \text{opx} + \text{pl}$ producing pseudomorphs after garnet. Mg-rich basaltic mafic granulites have small abundances of internal leucosomes, whereas in more Fe-rich intermediate compositions migmatization was more intense. Narrow quartz-plagioclase films are often present between pyroxenes, amphiboles and garnets representing remnants of melt that was expelled from the restitic granulites.

Another metamorphic event at lower pressure, c. 6-7 kbars and 600-700°C produced orthopyroxene-plagioclase and hornblende-plagioclase symplectites on garnet rims and fractures (Fig. 8.5), and opx-pl and cpx-pl symplectites on hornblende rims (Hölttä & Paavola, 2000). This seems to be connected with the semibrittle fracturing of the bedrock either during the emplacement of the Palaeoproterozoic dolerites at 2.3-2.1 Ga or during the Svecofennian orogeny at 1.89-1.88 Ga. Hydration connected with this event produced epidote filled fractures which are common in Stop 8.2.

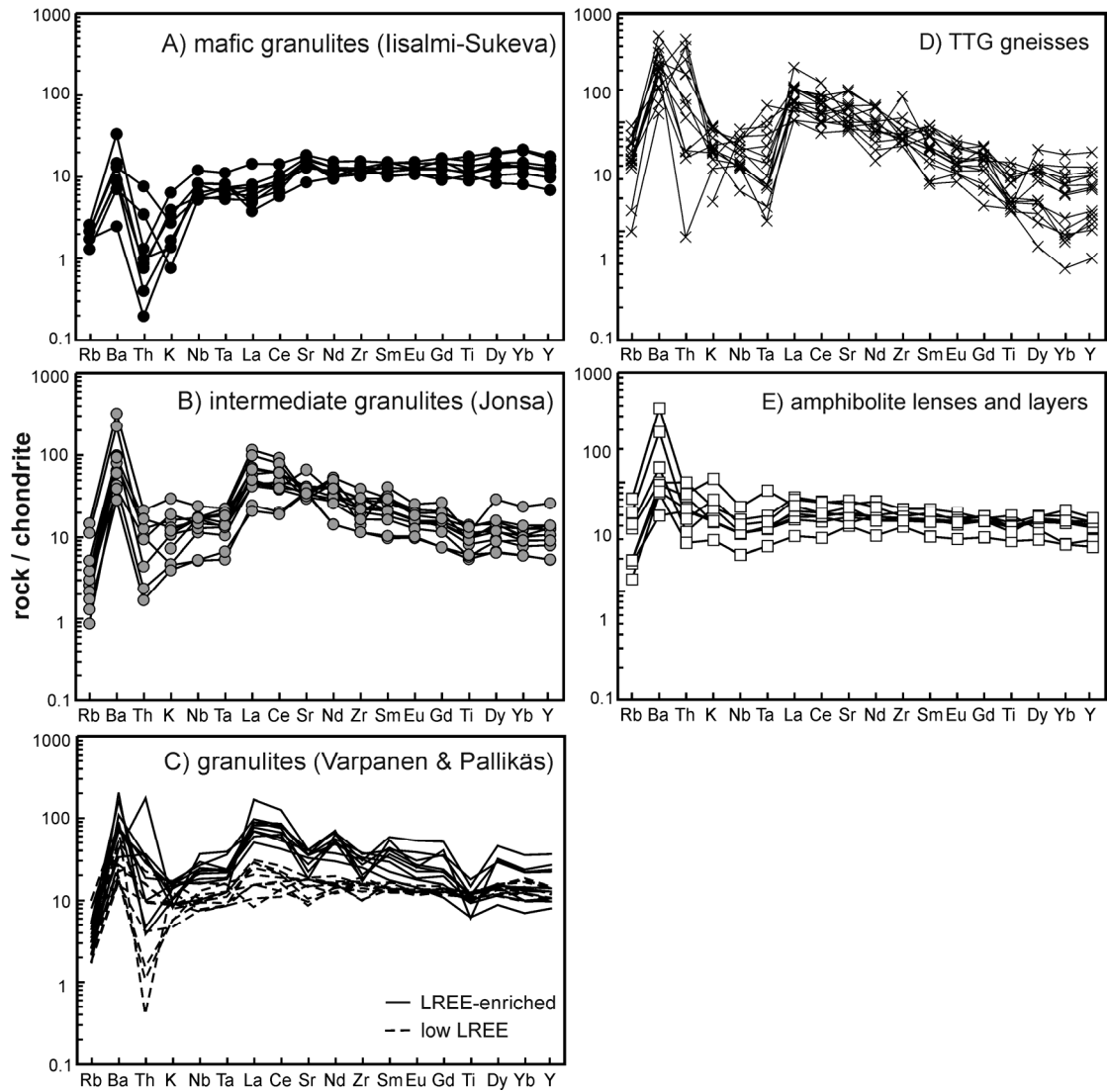


Fig. 8.3. Extended trace element diagrams for the mafic lithologies from the Iisalmi area.

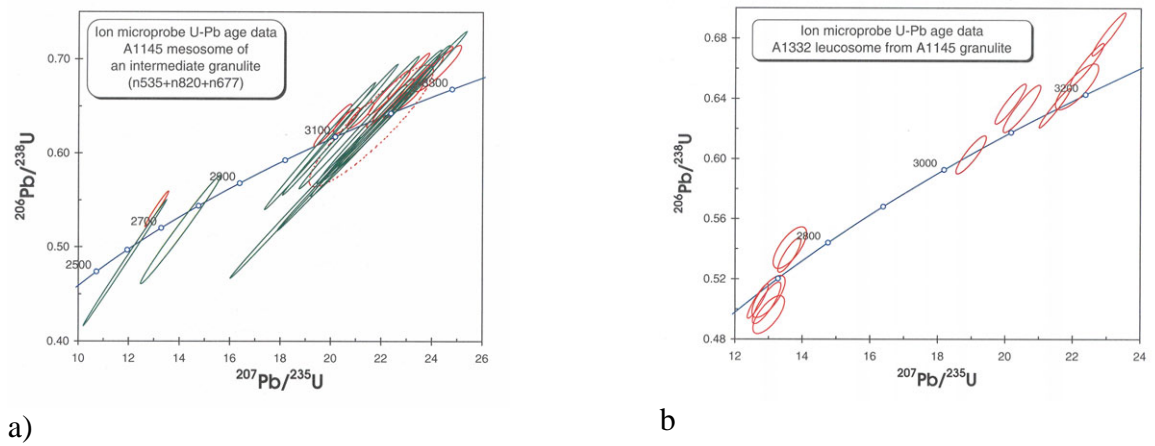


Figure 8.4. Nordsim ion microprobe concordia plots for zircon from the Kumisevanmäki mesosome (a) and leucosome of migmatitic granulite (b).

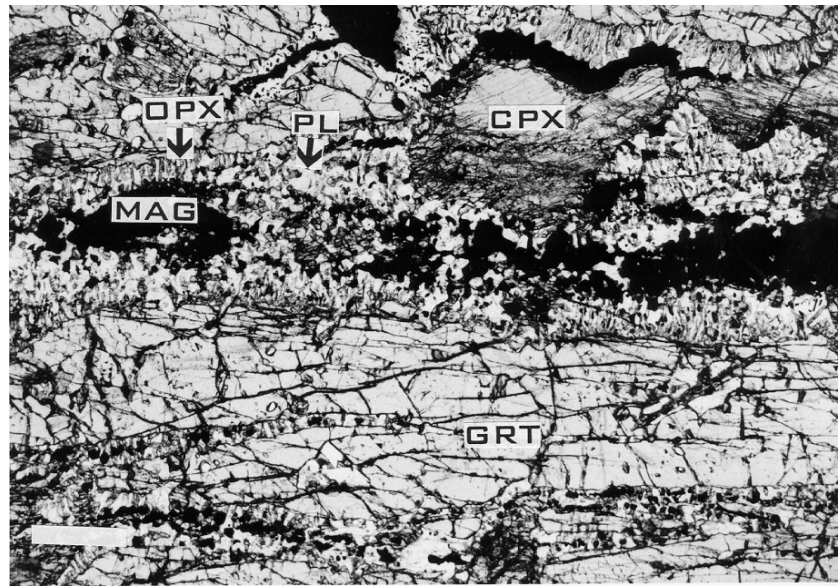


Figure 8.5. Orthopyroxene-plagioclase symplectites after garnet, Stop 8.2, Kumisevanmäki.

Stop 8.3. Lampiinsalmi, enderbite

The enderbites are medium-grained, weakly or moderately foliated rocks, with a typical dark brownish-green colour on fresh surfaces. They normally have gradational contacts with adjacent lithologies, although sharp contacts also occur. The mineral assemblage is opx-hbl-bt-pl-qtz-mag-ap (mineral abbreviations after Kretz, 1983), and the rock texture is hypidiomorphic. The enderbites contain rare anorthositic layers, only a few meters thick, with the assemblage pl-qtz-opx. Mafic xenoliths are also present, particularly near country rock contacts. Close to the shear zones orthopyroxene has been hydrated into hornblende and the dark colour of the enderbites commonly disappears.

The term enderbite is used here *sensu lato*, because most of the Varpaisjärvi enderbites correspond compositionally to hypersthene quartz diorites based on the classification of charnockitic rocks after Le Maitre (1989). However, there are also more siliceous enderbites which plot on the QAP diagram in the hypersthene tonalite (or enderbite) field. The enderbites are peraluminous, with Al_2O_3 contents of 17-19 wt.%. They have high Na_2O and P_2O_5 contents (c. 5 and 0.3 wt.%, respectively). Enderbite V contents vary generally from 110-180 ppm. They have 50-130 ppm Zn, 24-85 ppm Cr and 9-39 ppm Ni, and high Ba and Sr content, 320-1270 and 760-1050 ppm, respectively. Enderbites have fractionated and rather peculiar REE distributions where the LREE patterns from La to Nd are almost flat, La/Sm being 2.03-2.86 (Fig. 8.6; Hölttä, 1997).

The enderbites have two age populations, ca. 2.72-2.70 Ga and ca. 2.64 Ga (Fig. 8.7, Mänttari & Hölttä, 2002). The weighted average of the older concordant $^{207}\text{Pb}/^{206}\text{Pb}$ ages is 2.701 ± 0.04 Ga, which were measured from the magmatically zoned zircons. The younger ages from metamorphic overgrowths which crystallized during the granulite facies metamorphism.

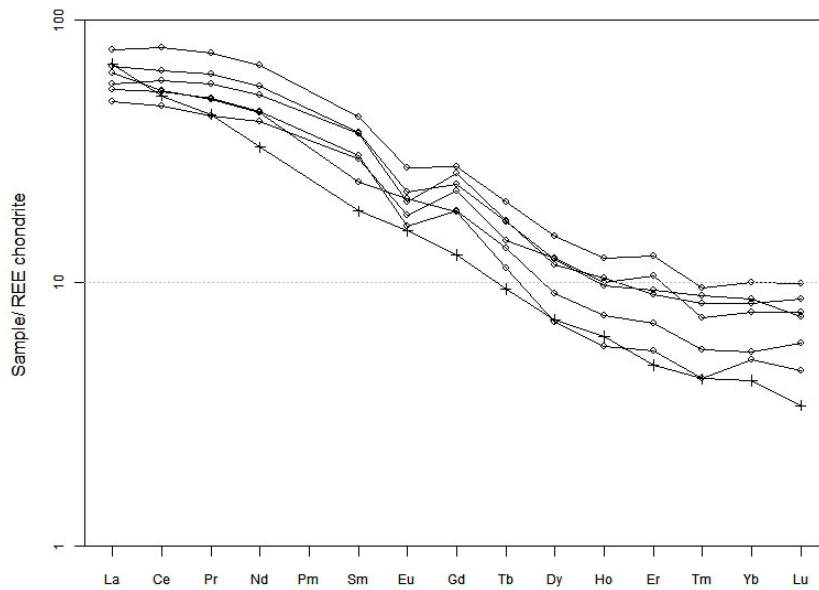


Fig. 8.6. Chondrite normalised REE patterns of the enderbites in Varpaisjärvi (diamonds) and in Voknavolok (crosses, data from Table 6.5).

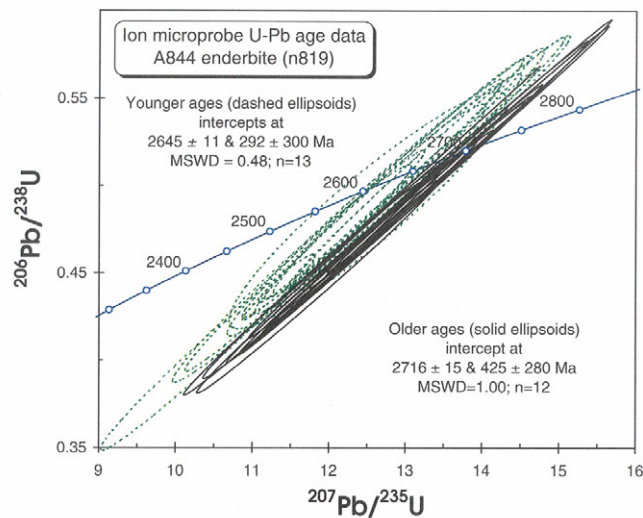


Fig. 8.7. Concordia plot for zircon from enderbite.

Igneous rocks of 2.7 Ga in age that share the geochemical features of the enderbites, although not pyroxene bearing, are found also elsewhere in the westernmost part of the Karelian craton. Compared with the Voknavolok enderbites the Iisalmi area enderbites are more mafic, they have less fractionated REE patterns (Fig. 8.6), higher P and Sr and lower U and Th contents (Fig. 8.8), the latter being evidently due to the granulite facies metamorphism that they underwent. Consequently, the present mineral assemblage in the Varpaisjärvi enderbites is rather metamorphic than magmatic.

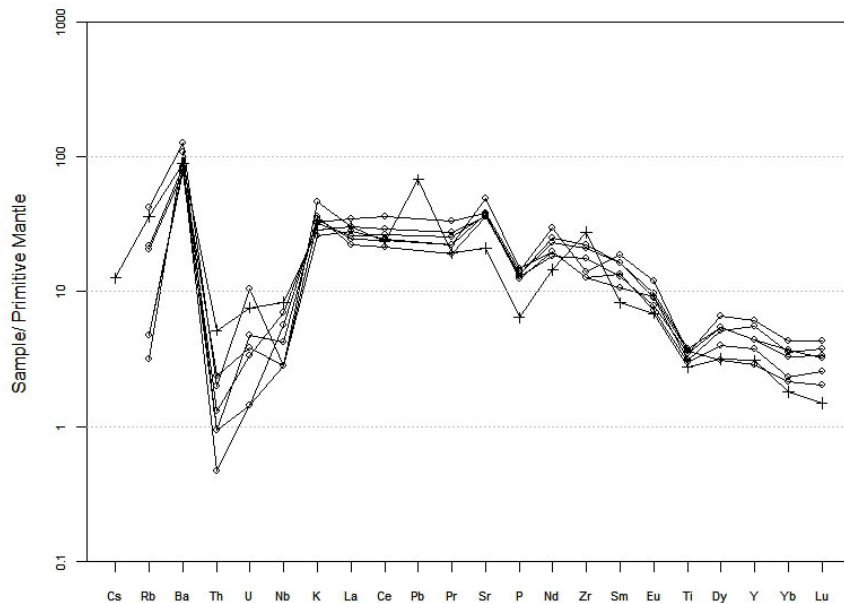


Fig. 8.8. PM normalized trace element patterns of the Varpaisjärvi enderbites (diamonds) and Voknavolok enderbite (crosses).

Stop 8.4. Jouhimäki, mafic granulites, Mg-Al granulites

In Stop 8.4 there are mafic garnet-clinopyroxene-orthopyroxene-hornblende granulites intercalated with Mg-Al granulites and quartz rocks. Prograde, granoblastic orthopyroxene is characteristic for mafic granulites from the *Jonsa* area. The *Jonsa* block Mg-rich garnet-free mafic granulites have the assemblage:

hbl (10-25%)-*cpx* (20-30%)-*pl* (50-60%)±*opx* (0-10%)±*qtz* (0-5%)

In migmatitic intermediate rocks the mineral assemblage of the mesosome is

hbl (10-40%)-*cpx* (5-20%)-*grt* (10-20%)-*pl* (30-40%)-*qtz* (10-30%)±*opx* (10-30%)

The composition of mafic granulites varies from basalt to andesite, their Ti/Zr ratio is below 100 and they have LREE enriched REE patterns. On multi-element plots these granulites resemble modern island-arc basalts due to negative Nb-Ta, Ti- and Zr-anomalies (Hölttä, 1997; Nehring, 2007).

Granulite samples from the *Jonsa* area have zircon with ages mostly between 2.7 and 2.6 Ga (Fig. 8.9). Apart from the onset of melting, the 2.73-2.70 Ga ages from the cores of prismatic zircon grains also give a minimum age for the protolith. The Sm-Nd model ages, 2.93 Ga from the mesosome of an intermediate migmatitic granulite and 2.76 Ga from its leucosome (Hölttä et al., 2000; Mänttari & Hölttä, 2002), are considered as maximum age for these rocks. The younger ages ca. 2.60-2.68 Ga from metamorphic zircons date the duration of the granulite facies metamorphism, which is considered to have lasted for c. 80 Ma.

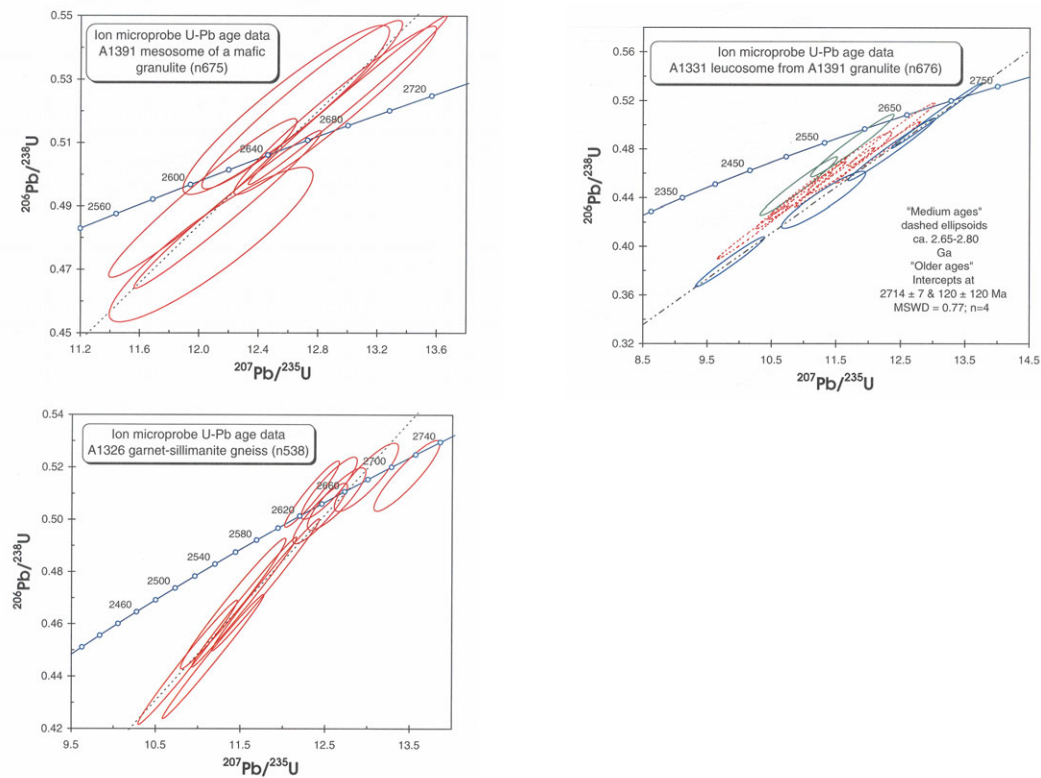


Fig. 8.9. Concordia plot for zircon from the Jonsa block granulites

Enclaves and pods of chemically altered, highly Mg- and Al-enriched rocks are found in the Jonsa area as interlayers in andesitic and basaltic granulites. The trace element geochemistry of the Mg-Al granulites indicate that they were altered from surrounding mafic rocks (Fig. 8.10). The Jonsa sapphirine-kornerupine rock occurs as boudinated, 0.5-4 m thick mafic layers in a light quartz-cordierite rock (Fig. 8.11). The outer parts of the layers have the mineral assemblages grt-crd-opx-oam-sil-qtz-rt, grt-crd-opx-sil-qtz-rt, grt-crd-sil-qtz-rt, opx-sil-crd-oam-qtz-rt, grt-crd-oam-sil-qtz-rt, grt-crd-oam-qtz-rt and oam-crd-qtz. The inner parts of the narrow, ca. 0.5 m layers have the mineral assemblages krn-oam-phl±cor±opx±rt, oam-crd-cor-sil-rt, opx-oam-sil-crd-rt and krn-oam-crd-sil-rt. The thickest, ca. 4 m layer has in its inner, quartz-free parts the mineral assemblages oam-cor-mag-phl-spr-rt-hoeg±spl±opx, oam-cor-mag-spr-krn-phl-rt-hoeg, oam-krn-spl, krn-oam-sil, krn-opx-crd-phl, oam-opx±sil and oam-sil-crd-grt-opx. The quartz rich light rock where the mafic layers are intercalated has the assemblage crd-qtz. Orthoamphibole, orthopyroxene, kornerupine and garnet are mostly centimetre-sized. Ferromagnesian minerals are mostly strongly retrogressed along rims and fractures, forming chlorite, talc, tiny needles of staurolite and kyanite and up to 1 mm andalusite. This was obviously caused by Proterozoic metamorphism which had a strong imprint in the Archean bedrock.

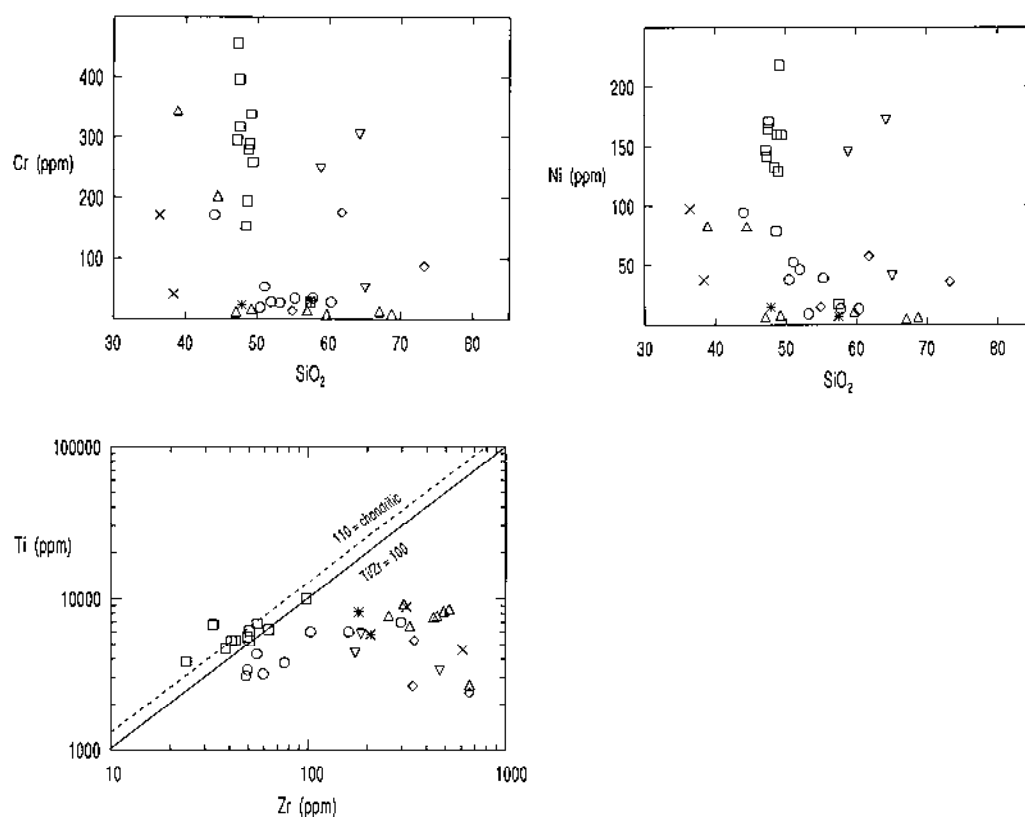


Figure 8.10. Trace element variations of mafic granulites and chemically altered rocks. The latter (diamonds, triangles, crosses) have similar Ni, Cr and Zr contents with mafic and intermediate granulites in the Jonsa block (circles). Ni and Cr are higher in mafic granulites in the Sukeva-Iisalmi and in the Varpanen-Pällikäs areas (squares) than in Jonsa.

The prominent feature in the Jonsa rocks are spectacular corona textures, in the mafic rock even multiple coronas. The spinel bearing parts have the most complicated corona textures (Fig. 8.12). Orthoamphibole is the major constituent of the rock, and orthoamphibole and spinel seem to have been the earliest phases. In the simplest case there is a corona of sapphirine between orthoamphibole and spinel. All sapphirines have not spinel inclusions but they are very common, suggesting that sapphirine was formed in a reaction where spinel was a reactant. In multiple coronas there are nested coronas of sapphirine-kornerupine, sapphirine-kornerupine-orthopyroxene and, in the most complicated case, sapphirine-kornerupine-orthopyroxene-phlogopite on spinel.

In the outermost parts of the mafic layers kornerupine and corundum are not found and quartz becomes abundant. Oam-grt-crd-qtz±sil is a common assemblage in these layers, in which case orthoamphibole, garnet and cordierite are often in textural equilibrium forming dihedral angles. Quartz is interstitial between other minerals. Sillimanite, when present, occurs only as inclusions in cordierite. Between orthopyroxene and sillimanite there is often a narrow corona which is formed of garnet, cordierite and quartz (Fig. 8.13). This texture indicates that garnet and cordierite were formed in the univariant FMAS reaction $opx + sil + qtz = grt + crd$ during either temperature increase or pressure decrease at c. 8.3 kbars and 820°C (Fig. 8.14).

Orthoamphibole analysed in the Al-Mg granulites is gedrite, (Fig. 8.13) (Leake, 1978), and are heterogeneous in composition. Gedrite analysed in sapphirine present microdomains, are more magnesian ($X_{Mg} = 0.73-0.76$), rich in Al_2O_3 (17.22-17.54wt.%), and Na_2O (1.67-1.69wt.%), but contain less SiO_2 (44.26-44.39wt.%), compared with the gedrite analysed in

sapphirine free, garnet present microdomains ($X_{Mg} = 0.70-0.73$, $Al_2O_3 = 14.69-16$ wt.%, $Na_2O = 1.24-1.40$ wt.%, and $SiO_2 = 44.65-46$ wt.%).

Sapphirine compositions are homogeneous, and intermediate between 7:9:3 and 2:2.1 in terms of $MgO:Al_2O_3:SiO_2$. Their content of Al_2O_3 ranges between 59.44 and 60.75wt.%, Fe_2O_3 ranges between 3.95 and 4.25 wt.% and Cr_2O_3 is negligible, and X_{Mg} ranges between 0.87-0.89.

Spinel inclusions in sapphirine are characterized by high ZnO (1.06-3.88 wt.%), and very low content of Cr_2O_3 (0-0.30wt.%) , X_{Mg} ranges between 0.48 and 0.52.

Garnet is mainly almandine-pyrope ($X_{Mg} = 0.26-0.58$), with low content of MnO and CaO 0.19-0.24wt.% and 0.22-0.41 wt.% respectively. They are characterized by a high depletion in Mg towards the fine fractures (Fig. 8.15).

Orthopyroxene the available analysis are made only on relics of primary orthopyroxene which are characterized by lower content of Al_2O_3 (8.30-8.60wt.%) compared with the primary orthopyroxene of most of Al-Mg granulite in the world. X_{Mg} varies between 0.73-0.77.

Cordierite are essentially unzoned, X_{Mg} ranges from 0.89-0.92 and the sum of oxides is significantly lower than 100%, suggesting the presence of volatiles.

Kornerupine do not show any regular zoning in their composition, X_{Mg} is ranging between 0.74 and 0.76, with $SiO_2 = 27.17 - 28.34$ wt.%, $Al_2O_3 = 44.65-46.13$ wt.%, with 0.90 wt.% of B_2O_3 .

Biotites are characterized by X_{Mg} ranging between 0.71 and 0.79, low content of TiO_2 (0.84-1.60wt.%), and very low content of F and Cl (<0.5 wt.%).

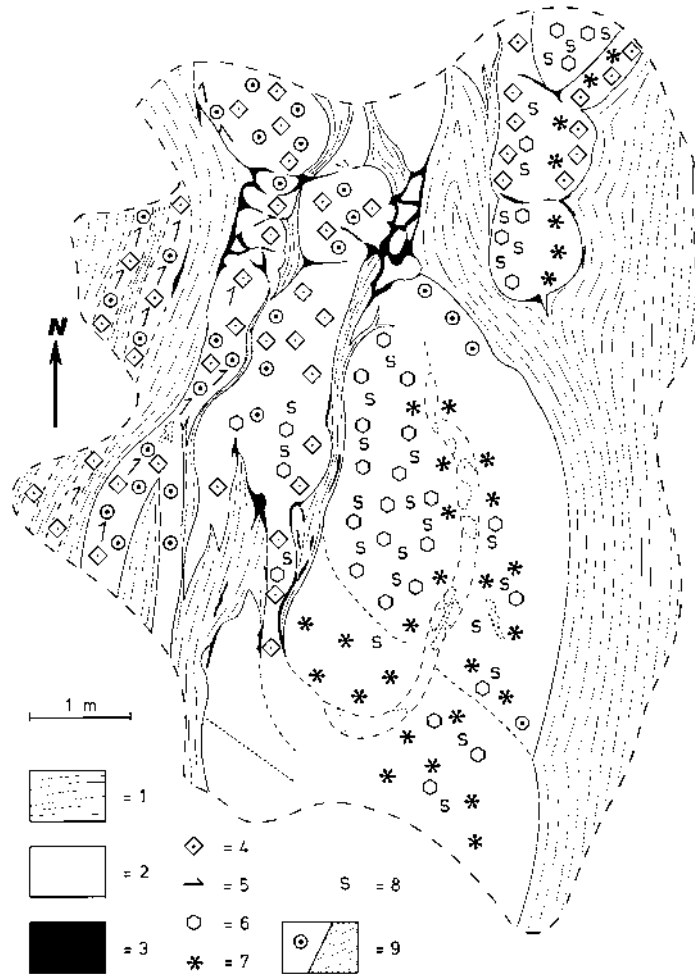


Fig. 8.11. A detail map of a part of the kornerupine rock layer in Stop 4. 1 = quartz-cordierite rock, 2 = orthoamphibole-kornerupine rock, 3 = vein quartz, 4 = orthopyroxene, 5 = sillimanite, 6 = corundum, 7 = kornerupine, 8 = sapphirine, 9 = garnet/nearly monomineralic garnet rock.

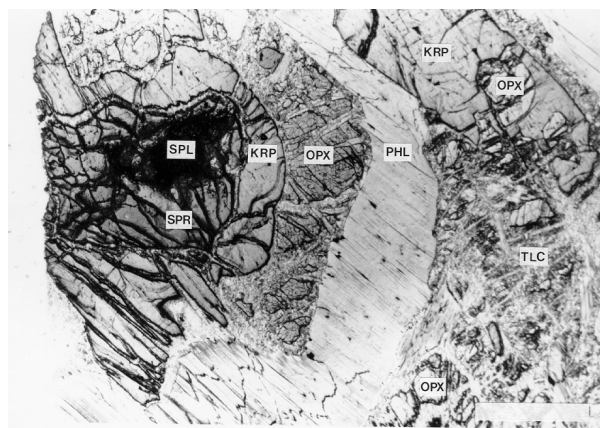


Figure 8.12. Corona textures in sapphirine-kornerupine rock.

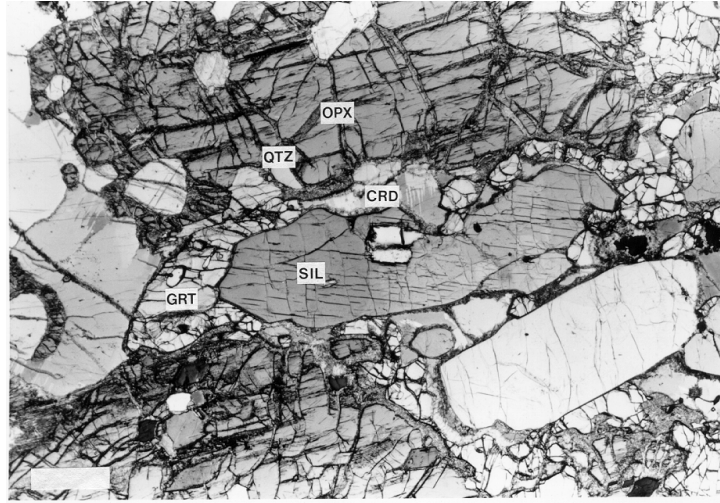


Fig. 8.13. Garnet and cordierite formed between orthopyroxene and sillimanite in the reaction $\text{opx} + \text{sil} + \text{qtz} = \text{grt} + \text{crd}$.

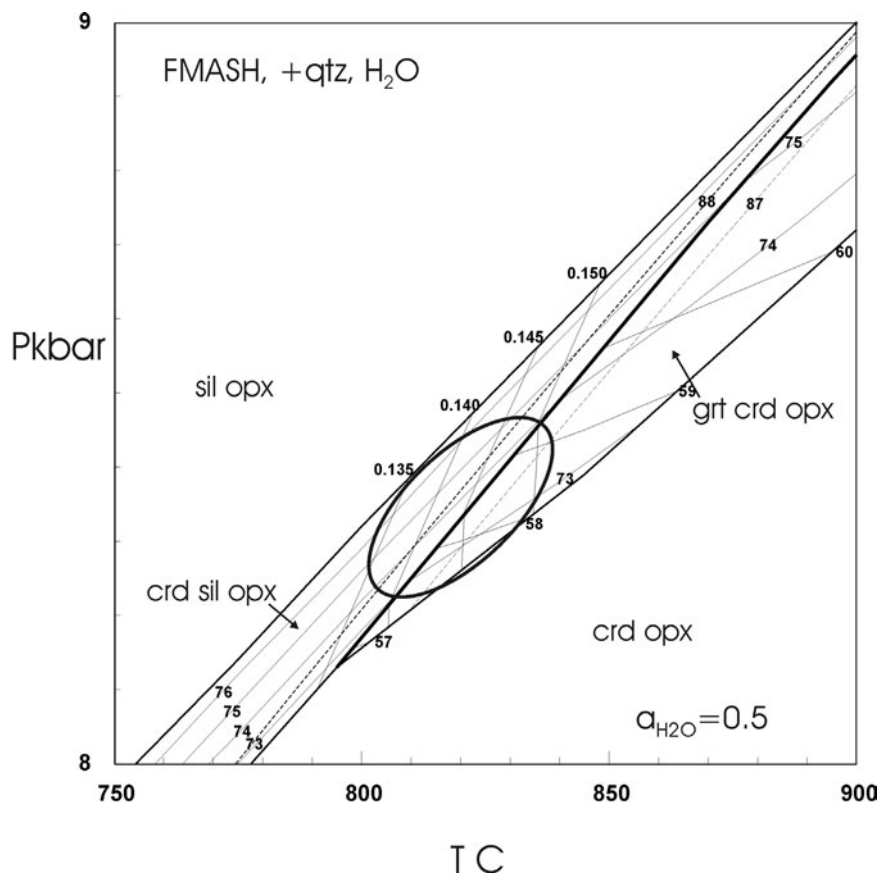


Fig. 8.14. A pseudosection calculated using the Thermocalc software for the opx-sil-grt-crd-qtz rock in Stop 4. Heavy line is for the univariant reaction $\text{opx} + \text{sil} + \text{qtz} = \text{grt} + \text{crd}$. Isopleths marked with numbers 57-60 are for the Mg numbers of garnet, isopleths with numbers 73-76 are for the Mg numbers of orthopyroxene, dashed line is for Mg_{88} isopleth of cordierite, and isopleths with numbers 0.135-0.150 are for X_{Al} in orthopyroxene. The ellipsoid shows the PT conditions indicated by analysed mineral compositions in the exposure.

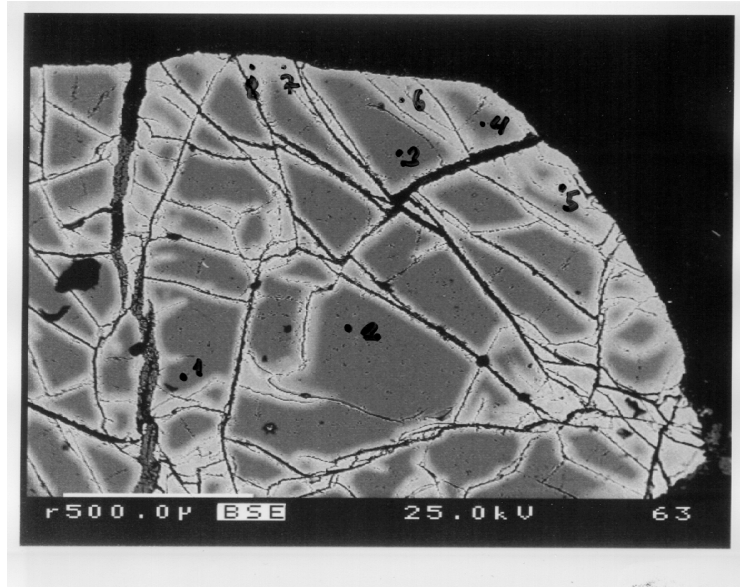


Fig. 8.15. A BSE image of garnet in Stop 8.4. Light areas near fractures are depleted in Mg.

Stop 8.5. Archean Siilinjärvi carbonatite

(text after O'Brien et al., 2005)

The Siilinjärvi carbonatite complex is located in Eastern Finland close to the city of Kuopio. It consists of a steeply dipping lenticular body roughly 16 km long with a maximum width of 1.5 km and a surface area of 14.7 km² intruded into granite gneiss bedrock. It was discovered in 1950 after samples of carbonatite were found by local mineral collectors; studies of these samples at GTK ultimately led to the body. Exploration drilling began in 1958 and continued along with laboratory and pilot plant work until 1979 when an open pit mine for phosphorus ore was commissioned. Present production at the Siilinjärvi mine is about 9.2 Mt of ore per year.

The carbonatite within the Siilinjärvi complex occurs as a central tabular 600-700 m wide body of calcite and dolomite-bearing phlogopite rocks surrounded by a fenite margin. Although not strictly zoned, cross-cutting relationships and xenoliths suggest that at least at the present level of exposure some of the syenites formed early, followed by a relatively carbonate-poor ultramafic magmatic pulse that created the majority of the phlogopite rocks, finally culminating in a carbonate-dominated pulse.

White-green medium-grained pure carbonatite formed during the carbonate-dominated pulse is relatively rare and in general true carbonatite (>50 modal % carbonates) is a relatively minor rock-type at Siilinjärvi. The vast majority of the central body is formed of phlogopite-rich rocks ranging from almost pure glimmerite (biotitite) via carbonate glimmerite to silicocarbonatites and finally to carbonatites. On top of this variability, blue-green richterite contents can be significant, forming up to 30% of the rocks in places. The phlogopite-rich nature of the Siilinjärvi intrusion becomes obvious from this diagram. Even though all varieties of the latter magmatic pulse contained sufficient phosphorus to crystallize apatite, apatite is nonetheless concentrated in the carbonate-rich rocks. As for the overall mode of the carbonatite-glimmerite portion of the complex, the mineralogical make-up of the average Siilinjärvi ore provides a good estimate comprising 65% phlogopite (including tetraferriphlogopite), 20% carbonates (with a 4:1 calcite:dolomite ratio), 5% richterite and 10% apatite (equivalent to 4% P₂O₅ in the whole rock). Other, relatively rare accessory minerals at Siilinjärvi include barite,

strontianite, monazite, pyrochlore, baddelyite, ilmenite, magnetite, pyrite, pyrrhotite and chalcopyrite.



Fig. 8.16. Carbonatite-glimmerite rock in the Siilinjärvi phosphate mine (photo: Petri Peltonen)

Fenites surrounding the carbonatite-biotitite central core developed as a result of sodium metasomatism of the surrounding granite gneiss country rocks. The main minerals in these fenites are microcline, amphibole and pyroxene but there exists a wide variety of syenite types including pyroxene, amphibole, carbonate, quartz, aplitic, and quartz-aegirine syenites. Compositions of the fluids that produced these fenites have been determined from fluid inclusions within magmatic zircon and apatite. Zircon crystals, which occur predominately in the amphibole-rich parts of the intrusion, contain two types of fluid inclusions trapped prior to emplacement of the carbonatites. Type 1 fluid is a $\text{H}_2\text{O}-\text{CO}_2$ mixture with low salinity (1-4 wt.% NaCl equivalent) whereas type 2 is moderate salinity (7-18 wt.% NaCl equivalent), alkali- and H_2O -rich, with type 1 surrounding rounded, presumably older zircon cores and type 2 surrounding type 1 inclusions. Apatite crystals contain only type 2 inclusions and this is consistent with the fact that apatite crystallized predominately after zircon, although rare minute apatite daughter crystals in some of the type 1 inclusions in zircon indicate initiation of apatite saturation at this stage. The development of H_2O - and alkali-rich late stage fluids was a consequence of crystallizing predominantly carbonate + apatite at this stage and supplied the high salinity, alkali-rich fluid that formed the fenite halo of the Siilinjärvi complex (Poutiainen, 1995). Ascent and hydrofracturing by the evolving H_2O -rich fluid may have facilitated the ascent of these ultramafic and carbonatite magmas along deep crustal shears, with attendant fenitization along the path.

A concordant zircon U-Pb age of 2609 ± 6 Ma shows that Siilinjärvi is one of the oldest carbonatites in the world.

Field trip ends to Kuopio 04.08 c. 5 pm. Drop-off to Kuopio railway station (Helsinki trains 17:20-22:00, 19:51-00:36) or Kuopio airport (Blue 1 Kuopio-Helsinki 17:55-18:45) and hotels.

References

- Anonymous, 1972: Ophiolites. *Geotimes* 17, 24-25.
- Arai, S., Matsukage, K., Isobe, E. & Vysotsky, S., 1997: Concentration of incompatible elements in oceanic mantle: Effect of melt/wall interaction in stagnant or failed melt conduits within peridotite. *Geochimica et Cosmochimica Acta* 61, 671-675.
- Arndt, N.T., Albaride, F. & Nisbet, E.G. 1997: Mafic and Ultramafic Magmatism. M. de Wit, L.D., Ashwal (eds). *Greenstone Belts, Oxford Monographs on Geology and Geophysics* 35, 233-254.
- Berman, R.G. 1991: Thermobarometry using multiequilibrium calculations: a new technique with petrologic applications. *Canadian Mineralogist* 29, 833-855.
- Berman, R.G. 1990: Mixing properties of Ca-Mg-Fe-Mn garnets. *The American Mineralogist* 75, 328-344.
- Berman, R.G. 1988: Internally-consistent thermodynamic data for stoichiometric minerals in the system Na₂O-K₂O-CaO-MgO-FeO-Fe₂O₃-Al₂O₃-SiO₂-TiO₂-H₂O-CO₂. *Journal of Petrology* 29, 445-522.
- Bibikova, E.V., Samsonov, A.V., Petrova, A. Yu. & Kirnozova, T. I. 2005: *Archean geochronology of Western Karelia, Stratigraphy and Geological Correlation*, 13 (5), 459-475
- Capaldi, G., Chiesa, S., Manetti, P., Orsi, G., Poli, G. 1987: Tertiary anorogenic granites of the western border of the Yemen Plateau. *Lithos* 20, 433-444.
- Chernov, V.M., 1964: *Stratigraphy and depositional environment of volcanogenic (leptitic) iron-cherty formations in Karelia. M.-L.*, 123 p.
- Chian, D., Louden, K.E., Minshull, T.A. & Whitmarsh, R.B., 1999: Deep structure of the continent transition in the southern Iberia Abyssal Plain from seismic refraction profiles: Ocean Drilling Program (Legs 149 and 173) transect. *Journal of Geophysical Research* 104, 7443-7462.
- Claesson, S., Bogdanova, S.V., Bibikova, E.V. & Gorbatshev, R. 2001: Isotopic evidence of Palaeoproterozoic accretion in the basement of the East European Craton. *Tectonophysics* 339, 1-18.
- Claesson, S., Huhma, H., Kinny, P.D. & Williams, I.S. 1993: Svecofennian detrital zircon ages - implications for the Precambrian evolution of the Baltic Shield. *Precambrian Research* 64 (1-4), 109-130.
- Coleman, R.G., DeBari, S. & Peterman, Z., 1992: A-type granite and the Red Sea opening. *Tectonophysics* 204, 27-40.
- Cornen, G., Girardeau, J. & Monnier, C. 1999: Basalts, underplated gabbros and pyroxenites record the rifting process of the West Iberian margin. *Mineralogy and Petrology* 67, 111-142.
- Dann, J.C., 1997: Pseudostratigraphy and origin of the Early Proterozoic Payson ophiolite, central Arizona. *Geological Society of America, Bulletin* 109, 347-365.
- Furnes, H., Banerjee, N.R., Muehlenbachs, K. & Kontinen, A., 2005. Preservation of biosignatures in metaglassy volcanic rocks from the Jormua ophiolite complex, Finland. *Precambrian Research* 136, 125-137.

- Gorkovets, V.Ya. & Rayevskaya, M.B. 1983: Ultramafic effusive rocks from the Kostomuksha Iron Ore Province// Magmatism and metallogeny of Karelian Precambrian rocks. Petrozavodsk.
- Halkoaho, T., Liimatainen, J., Papunen, H. & Välimaa, J. 1996: Komatiittiprojektin loppuraportti 1a. Unpublished report 1a of the Komatiite Project, University of Turku, 99 p.
- Halkoaho, T., Liimatainen, J., Papunen, H. & Välimaa, J. 1997: Cr-rich basalts in komatiitic volcanic association of the Archaean Kuhmo greenstone belt: evidence for reducing conditions during magma generation. In: *Papunen H (ed.) Mineral Deposits: Research and Exploration Where do They Meet? Balkema, Rotterdam*, pp.431-434.
- Hanski, E.J. 1980: Komatiitic and tholeiitic metavolcanics of the Kellojärvi group in the Siivikkovaara area of the Archaean Kuhmo greenstone belt, eastern Finland. *Bull. Geol. Soc. Fin.* 52,67-100.
- Hanski, E.J., 1997: The Nuttio serpentinite belt, central Lapland : an example of Paleoproterozoic ophiolitic mantle rocks in Finland. *Ofioliti* 22 (1), 35-46.
- Herzberg, C. & O'Hara, M.J, 1998: Phase equilibrium on the origin of basalts, picrites, and komatiites. *Earth-Sci. Rev.* 44, 39-79.
- Holland, T.J.B, & Powell, R. 1998: An internally-consistent thermodynamic dataset for phases of petrological interest. *Journal of Metamorphic Geology* 16, 309–344.
- Hölttä, P., 1997, Geochemical characteristics of granulite facies rocks in the Varpaisjärvi area, central Fennoscandian Shield. *Lithos*, 40, pp. 31-53.
- Hölttä P. & Paavola, J. 2000. P-T-t development of Archaean granulites in Varpaisjärvi, Central Finland, I: Effects of multiple metamorphism on the reaction history of mafic rocks. *Lithos*, 50, 97-120.
- Hölttä, P., Huhma, H., Mänttari, I. & Paavola, J. 2000: P-T-t development of Archaean granulites in Varpaisjärvi, Central Finland, II: Dating of high-grade metamorphism with the U-Pb and Sm-Nd methods. *Lithos* 50, 121-136.
- Huebner, J.S., Lipin, B.R. & Wiggins, L.B. 1976: Partitioning of chromium between silicate crystals and melts. *Proc. Lunar Sci. Conf.* 7,1195-1220.
- Hypönen, V. 1983: Kallioperäkarttojen selitykset, 4411 Ontojoki, 4412 Hiisijärvi ja 4413 Kuhmo. English summary: Pre-Quaternary rocks of the Ontojoki, Hiisijärvi, and Kuhmo map-sheet areas. *Explanation to the maps of Pre-Quaternary rocks, Sheets 4411, 4412 and 4413, 1:100 000. Geol. Surv. Finland.* 60 s.
- Hypönen, V. 1983: Ontojoki, Hiisijärvi and Kuhmo. *Explanation to the Geological map of Finland 1:100000, pre-Quaternary rocks, sheets 4411, 4412, 4413, Geological Survey of Finland, 60 p.* (in Finnish with English summary)
- Hytönen, K. & Hautala, T. 1985: Aegirine and riebeckite of the alkali gneiss of Pikkukallio in the Honkamäki-Otanmäki region, Finland. *Bulletin Geological Society of Finland* 57, 169-180.
- Ivanikov, V.V. & Philippov, N.B. 1997: Geochemical evidence for the geotectonic setting of early Proterozoic metabasalts in the Ladoga region (Russia). *COPENA Conference at NGU, Abstracts and Proceedings, NGU Report 97*, p. 131.
- Jagoutz, E., Palme, H., Baddhausen, H., Blum, K., Cendales, M., Dreibus, G., Spettel, B., Lorenz, V. & Wänke, H. 1979. The abundances of major, minor and trace elements in the earth's mantle as derived from primitive ultramafic nodules. *Proceedings of 10th Lunar Planetary Science Conference*, 2031-2050.
- Koistinen, T. J. 1981: Structural evolution of an early Proterozoic stratabound Cu-Co-Zn deposit, Outokumpu, Finland. *Transactions of the Royal Society of Edinburgh: Earth Sciences* 72 (2), 115-158.
- Koistinen, T., Stephens, M.B., Bogachev, V., Nordgulen, O., Wennerström, M. & Korhonen, J. 2001: Geological map of the Fennoscandian Shield, scale 1:2000000. *Geological Sur-*

- vey of Finland, Norway and Sweden and North-West Department of Natural Resources of Russia.
- Kontinen, A. & Peltonen, P. 1998: Excursion to the Jormua ophiolite complex. In: Hanski, E. & Vuollo, J. (eds.) *International ophiolite symposium and field excursion : generation and emplacement of ophiolites through time, August 10-15, 1998, Oulu, Finland. Abstracts, excursion guide. Geological Survey of Finland, Special Paper 26*, 69-89.
- Kontinen, A. & Sorjonen-Ward, P. 1991: Geochemistry of metagraywackes and metapelites from the Palaeoproterozoic Nuasjärvi Group, Kainuu schist belt and the Savo province, North Karelia: implications for provenance, lithostratigraphic correlation and depositional setting. In: Autio, S. (ed.) *Geological Survey of Finland, Current Research 1989-1990. Geological Survey of Finland. Special Paper 12*, 21-22
- Kontinen, A., 1987: An early Proterozoic ophiolite - the Jormua mafic-ultramafic complex, northeastern Finland. *Precambrian Research* 35, 313-341.
- Kontinen, A., Huhma, H. & Laajoki, K., 1995: Sm/Nd isotope data on the Central Puolanka Group, Kainuu schist belts, Finland; constraints for provenance and age of deposition. *The 22nd Nordic Geological Winter Meeting, Turku - Åbo, 8-11 January 1996. Abstracts*, p. 95.
- Kontinen, A., Käpyaho, A., Huhma, H., Karhu, J., Matukov, D. I., Larionov, A. & Sergeev, S.A., 2007: Nurmes paragneisses in eastern Finland, Karelian craton: Provenance, tectonic setting and implications for Neoproterozoic craton correlation. *Precambrian Research* 152 (3-4), 119-148.
- Kontinen, A., Paavola, J. & Lukkarinen, H., 1992: K-Ar ages of hornblende and biotite from Late Archaean rocks of eastern Finland - interpretation and discussion of tectonic implications. *Geological Survey of Finland Bulletin* 365, 1-31.
- Kozhevnikov, V. N., Berezhnaya, N. G. & Presnyakov, S. L. et al. 2006: Geochronology (SHRIMP-II) of zircon from Archean lithotectonic associations in the greenstone belts of the Karelian craton: implications for stratigraphic and geodynamic reconstructions, *Stratigraphy and Geological Correlation, Vol. 14. No 3*, pp. 240-259.
- Kozhevnikov, V.N. 2000: Archean greenstone belts of the Karelian Craton as accretionary orogens. *Karelian Science Centre, Petrozavodsk*, 223 p. [in Russian].
- Kozhevnikov, V.N. 1982: Environment of formation of structural-metamorphic parageneses in Precambrian complexes, 184 p.
- Käpyaho, A., 2006: Whole-rock geochemistry of some tonalite and high Mg/Fe gabbro, diorite, and granodiorite plutons (sanukitoid suites) in the Kuhmo district, eastern Finland. *Bulletin of the Geological Society of Finland* 78 (2), 121-141.
- Käpyaho, A., Mänttari, I. & Huhma, H., 2006: Growth of Archaean crust in the Kuhmo district, eastern Finland: U-Pb and Sm-Nd isotope constraints on plutonic rocks. *Precambrian Research* 146 (3-4), 95-119.
- Kärki, A. & Laajoki, K. 1995: An interlinked system of folds and ductile shear zones - late stage Svecokarelian deformation in the central Fennoscandian Shield, Finland. *Journal of Structural Geology* 17, 1233-1247.
- Laajoki, K., 1991: Stratigraphy of the northern end of the early Proterozoic (Karelian) Kainuu Schist Belt and associated gneiss complexes, Finland. *Geological Survey of Finland. Bulletin* 358. 105 p.
- Laajoki, K. 2005: Karelian supracrustal rocks. In: Lehtinen, M., Nurmi, P.A., Rämö, O.T. (eds.): *Precambrian Geology of Finland – Key to the Evolution of the Fennoscandian Shield. Elsevier B.V., Amsterdam*, pp. 279-342.
- Lahtinen, R., 2000: Archaean-Proterozoic transition: geochemistry, provenance and tectonic setting of metasedimentary rocks in central Fennoscandian Shield, Finland. *Precambrian Research* 104, 147-174.

- Lahtinen, R., Korja, A. & Nironen, M. 2005: Paleoproterozoic tectonic evolution. In: Lehtinen, M., Nurmi, P.A., Rämö, O.T. (Eds.), *Precambrian Geology of Finland – Key to the Evolution of the Fennoscandian Shield*. Elsevier B.V., Amsterdam, pp. 481-532.
- Larionova, Yu.O., Samsonov, A.V. & Nosova, A.A. 2004: The Rb–Sr geochronology and isotopic geochemistry of ore-hosting rocks and wall-rock metasomatites of the mesothermal Taloveis gold deposit, Western Karelia. *Transactions (Doklady) of the Russian Academy of Sciences/Earth Science Section*. Vol. 396. No. 4. pp. 525-528
- Larionova, Yu.O., Samsonov, A.V. & Shatagin, K.N. 2007: Sources of Archean sanukitoids (high-Mg subalkaline granitoids) in the Karelian craton: Sm-Nd and Rb-Sr isotopic-geochemical evidence. *Petrology*. Vol. 15. No. 6. pp. 530-550
- Larionova, Yu.O. 2005: Isotopic-geochemical characteristics of the Taloveis and Päkylä gold occurrences, Karelia. *Ms. Sc.thesis. Moscow, MGU*, 83 p.
- Leblanc, M. & Ceuleneer, G., 1992: Chromite crystallization in a multicellular flow: Evidence from a chromitite dike in the Oman ophiolite. *Lithos* 27, 231-257.
- Lemoine, M., Tricart, P. & Boillot, G. 1987: Ultramafic and gabbroic ocean floor of the Ligurian Tethys (Alps, Corsica, Apennines): In search of a genetic model. *Geology* 15, 622-625.
- Liipo, J., Vuollo, J., Nykänen, V., Piirainen, T., Pekkarinen, L. & Tuokko, I. 1995: Chromites from the early Proterozoic Outokumpu-Jormua ophiolite belt: a comparison with chromites from Mesozoic ophiolites. *Lithos* 36, 15-27.
- Lobach-Zhuchenko, S.B., Arestova, N.A., Mil'kevich, R.I., Levchenkov, O.A. & Sergeev, S.A. 2000. Stratigraphy of the Kostomuksha belt in Karelia (Upper Archean) as inferred from geochronological, geochemical and isotopic data. *Stratigraphy and Geological Correlation*, Vol. 8. No. 4, pp. 319-326.
- Lobach-Zhuchenko, S.B., Chekulaev, V.P., Arestova, N.A., Levskii, L.K. & Kovalenko, A.V. 2000: Archean terranes in Karelia: geological and isotopic–geochemical evidence. *Geotectonics, Moscow*, 34(6), 452- 466
- Luukkonen, E.J. 1991: Late Archaean and early Proterozoic structural evolution in the Kuhmo-Suomussalmi terrain, eastern Finland. Turun Yliopiston julkaisu. *Annales Universitatis Turkuensis. sarja-Ser. A. II. Biologica-Geographica-Geologica* 78.
- Mänttari, I. & Hölttä, P. 2002: U-Pb dating of zircons and monazites from Archean granulites in Varpaisjärvi, central Finland : evidence for multiple metamorphism and Neoproterozoic terrane accretion. *Precambrian Research*, 118, 101-131.
- McElduff, B. & Stumpfl, E.F. 1991: The chromitite deposits of the Troodos Complex, Cyprus - Evidence for the role of a fluid phase accompanying chromite formation. *Mineralium Deposita* 26, 307-318.
- Nehring, F., 2007: Partial melting within the lower crust – Constraints from bulk rock geochemical data and trace element mineral analyses of granulites and migmatites in Central Finland. PhD thesis, Johannes Gutenberg-University Mainz, Institute of Geosciences.
- Nicolas, A., 1989: *Structures of Ophiolites and Dynamics of Oceanic Lithosphere*. Dordrech,: Kluwer, 367 p.
- Nironen, M., 1997: The Svecofennian Orogen: a tectonic model. *Precambrian Research* 86, 21-44.
- O'Brien, H., Peltonen, P. & Vartiainen, H. 2005: Kimberlites, karbonatites, and alkaline rocks. In: Lehtinen, M., Nurmi, P.A. & Rämö, O.T. (eds.): *Precambrian of Finland – a Key to the Evolution of the Fennoscandian Shield*. Elsevier, Amsterdam, 616-646.
- Ohtani, E. 1990: Majorite fractionation and genesis of komatiites in the deep mantle. *Precambrian Research* 48, 195-202.

- Papunen, H. 1960: Havainnot Siivikkovaaran alueen kallioperästä Kuhmon pitäjän Viieksin kylässä. *Unpub. Master's thesis. Manuscript at the Department of Geology, University of Helsinki*, 56 pp. (in Finnish).
- Papunen, H., Kopperoinen, T. & Tuokko, I. 1989: The Taivaljärvi Ag-Zn deposit in the Archean greenstone belt, eastern Finland. *Economic Geology* 84, 1262-1276.
- Park, A.F., 1988: Nature of the early Proterozoic Outokumpu assemblage, eastern Finland. *Precambrian Research* 38, 131-146.
- Park, A.F. 1983: Nature, affinities and significance of metavolcanic rocks in the Outokumpu assemblage, eastern Finland. *Bulletin of Geological Society of Finland* 56, 25-52.
- Pearce J.A., Harris, N.B.W. & Tindle, A.G. 1984: Trace element discrimination diagrams for the tectonic interpretation of granitic rocks. *Journal of Petrology* 25, 956-983.
- Peltonen, P. 2005: Ophiolites. In: Lehtinen, M., Nurmi, P.A., Rämö, O.T. (Eds.), *Precambrian Geology of Finland – Key to the Evolution of the Fennoscandian Shield*. Elsevier B.V., Amsterdam, pp. 237-278.
- Peltonen, P. & Kontinen, A. 2004: The Jormua Ophiolite: a mafic-ultramafic complex from an ancient ocean – continent transition zone. In: Kusky, T.M. (ed.): *Precambrian Ophiolites and Related Rocks. Developments in Precambrian Geology vol 13 (K.C. Condie, Series Editor)*, Elsevier B.V., pp. 35-71.
- Peltonen, P. & Brügmann, G. 2006: Origin of layered continental mantle (Karelian craton, Finland): Geochemical and Re-Os isotope constraints. *Lithos* 89, 405-423.
- Peltonen, P., Kontinen, A. & Huhma, H. 1996: Petrology and geochemistry of metabasalts from the 1.95 Ga Jormua Ophiolite, northeastern Finland. *Journal of Petrology* 37 (6), 1359-1383.
- Peltonen, P., Kontinen, A. & Huhma, H. 1998: Petrogenesis of the mantle sequence of the Jormua ophiolite (Finland) : melt migration in the upper mantle during Palaeoproterozoic continental break-up. *Journal of Petrology* 39 (2), 297-329.
- Peltonen, P., Mänttari, I., Huhma, H. & Kontinen, A. 2003: Archean zircons from the mantle – the Jormua Ophiolite revisited. *Geology* 31(7), 645-648.
- Peltonen, P., Mänttari, I., Huhma, H. & Whitehouse, M.J. 2006: Multi-stage origin of the lower crust of the Karelian craton from 3.5 to 1.7 Ga based on isotopic ages of kimberlite-derived mafic granulite xenoliths. *Precambrian Research* 147, 107-123.
- Puchtel, I. S., Hofmann, A. W. & Mezger, K. et al. 1998: Oceanic plateau model for continental crustal growth in the Archaean: a case study from the Kostomuksha greenstone belt, NW Baltic Shield. *Earth and Planetary Science Letters* 155, 57-74.
- Puchtel, I.S., Brugmann, G.E. & Hofmann, A.W. 2001: ¹⁸⁷Os-enriched domain in an Archean mantle plume: evidence from 2.8 Ga komatiites of the Kostomuksha greenstone belt, NW Baltic Shield, *Earth and Planetary Science Letters* 186, 513-526.
- Puchtel, I.S., Hofmann, A.W., Jochum, K.P., Mezger, K., Shchipansky, A.A. & Samsonov, A.V. 1997: The Kostomuksha greenstone belt, N.W. Baltic Shield: Remnant of a late Archean oceanic plateau? *Terra Nova* 9, 87-90.
- Rampone, E. & Picardo, G.B. 2001: The ophiolite-oceanic lithosphere analogue: new insights from the northern Apennines (Italy). In: Dilek, Y., Moores, E.M., Elthon, D., Nicholas, A. (Eds.), *Ophiolites and Oceanic Crust: New Insights from Field Studies and Ocean Drilling Program. Geological Society of America Special Paper* 349, 21-34.
- Rayevskaya, M.B., Gor'kovets, V.Y., Svetova, A.I. & Volodichev, O.I. 1992: Precambrian stratigraphy of Karelia. In: Rybakov, S.I. & Stenar M.M. (eds) *Reference sections of Upper Archean deposits. Karelian Research Centre, Petrozavodsk*, 190 p. (in Russian).
- Rehtijärvi, P. & Saastamoinen, J. 1985: Tectonized actinolite-albite rocks from the Outokumpu district, Finland: field and geochemical evidence for mafic extrusive origin. *Bulletin of the Geological Society of Finland* 57 (1-2), 47-54.

- Samsonov, A. V., Bibikova, E. V., Larionova, Yu. O., Petrova, A. Yu. & Puchtel, I. S. 2004: Magnesian granitoids (sanukitoids) of the Kostomuksha area, Western Karelia: petrology, geochronology and tectonic environment of formation *Petrology* 12,437-468
- Samsonov, A.V., Berzin, R.G. & Zamozhnyaya, N.G. et al. 2001: Early Precambrian crust-forming processes in NW-Karelia, Baltic Shield: evidences from geological, petrological and deep seismic (4B profile) studies. In *Berzin, R.G., Lipilin, A.V., Minz, M.V. et al. (Eds.): Deep Structure and Crustal Evolution of the Eastern Fennoscandian Shield: Kem'Kalevala Reflection Profile: Karelian Sci. Centre RAS, Petrozavodsk*, pp. 109-143 [In Russian].
- Samsonov, A.V., Bogina, M.M., Bibikova, E.V. et al. 2005: The Relationship between adakitic, calc-alkaline volcanic rocks and TTGs: implications for the tectonic setting of Karelian greenstone belts, Baltic Shield, *Lithos* 79, 83–106.
- Scott, D.J., Helmstaedt, H. & Bickle, M.J. 1992: Purtunij Ophiolite, Cape Smith Belt, northern Quebec, Canada; a reconstructed section of early Proterozoic oceanic crust. *Geology* 20 (2), 173-176.
- Serri, G. 1981. The petrogeochemistry of ophiolite gabbroic complexes: a key for the classification of ophiolites into low-Ti and high-Ti types. *Earth and Planetary Science Letters* 52, 203-212.
- Sviridenko, L.P. 1974: *Early Precambrian metamorphism and granite formation in West Karelia*, 155 p.
- Säntti, J., Kontinen, A., Sorjonen-Ward, P., Johanson, B. & Pakkanen, L. 2006: Metamorphism and chromite in serpentized and carbonate-silica-altered peridotites of the Palaeoproterozoic Outokumpu-Jormua Ophiolite Belt, Eastern Finland. *International Geology Review* 48, 494-546.
- Taipale, K., Horneman, R. & Hyvärinen, T. 1993: Suomen geologinen kartta 1:100 000, kallio-peräkartta. Lehti 4322, Puukari. *Geological map of Finland 1:100 000, Pre-Quaternary rocks, sheet 4322, Puukari*.
- Talvitie, J. & Paarma, H. 1980: Precambrian basic magmatism and the Ti-Fe ore formation in central and northern Finland. *Geological Survey of Finland Bulletin* 307, 98-107.
- Tsuru, A., Walker, R. J., Kontinen, A., Peltonen, P. & Hanski, E. 2000: Re-Os isotopic systematics of the 1.95 Ga Jormua ophiolite complex, northeastern Finland. *Chemical Geology* 164 (1-2), 123-141.
- Tuisku, P. 1997: An introduction to Palaeoproterozoic (Svecofennian) regional metamorphism in Kainuu and Lapland, Finland. In: Evins, P., Laajoki, K. (Eds.), *Archaean and early Proterozoic (Karelian) evolution of the Kainuu-Peräpohja area, northern Finland. A guidebook for the Nordic research field seminar organized by the universities of Oslo, Oulu and Turku, June 2-10, 1997. Res Terrae, Ser. A, No 13*, 27-31.
- Whalen, J.B., Currie, K.L. & Chappell, B.W. 1987: A-type granites: geochemical characteristics, discrimination and petrogenesis. *Contributions to Mineralogy and Petrology* 95, 407-419.
- Vlasov, E.A., Baksheyev, I.A., Kushch, P.V., Korneva, I.V., Prokofyev, V.Yu., Gritsun, A.S. & Larionova, Yu.O. 2007: Mineralogy of metasomatic rocks and ores from the Taloveis deposit, West Karelia. *Proceedings of the 8th International Conference "New ideas in earth sciences". RGGRU, Moscow. 2007. Vol. 3*,76-79
- Volodichev, O.I., Kuzenko, T.I. & Kozlov, S.S. 2002: On the structural-metamorphic study of Kontokki Series volcanics from the Kostomuksha structure. *Geology and commercial minerals of Karelia. Issue 5. Petrozavodsk, KarRC RAS*, 15–26 [in Russian].
- Vuollo, J., Liipo, J., Nykänen, V., Piirainen, T., Pekkarinen, L., Tuokko, I. & Ekdahl, E. 1995: An early Proterozoic podiform chromitite in the Outokumpu Ophiolite Complex, Finland. *Economic Geology* 90, 445-452.